Discovery of NEK9 and Aurora A PROTACs Using a Proteomics-Based Screening Approach

William Thomas Darlow

Centre for Cancer Drug Discovery Cancer Therapeutics Unit

The Institute of Cancer Research

University of London

This thesis is submitted in partial fulfilment of the requirements for the degree of Doctor of Philosophy

September 2022

ICR The Institute of Cancer Research

Signed Declaration

I, William Thomas Darlow, confirm that the work presented in this thesis is my own. Where work has been performed by others, and where information has been derived from other sources, I confirm that this has been indicated in the thesis.

William Thomas Darlow

September 2022

Acknowledgements

Firstly, I would like to thank Swen and Ben for giving me the opportunity to carry out my PhD at The Institute of Cancer Research, and for the invaluable guidance I've received over the 4 years from you both.

I am certain I wouldn't be where I am today without the direction of Alice, Alfie and Danny. For this I am especially grateful and hope to always remain in touch with you all, that is if you aren't sick of me yet.

All past and present members of Medicinal Chemistry 4 deserve a special thanks from me, including: Matt, Owen, Ellen, Rosemary, Jack, Katie, Nick, Charlie, and Pasquale. All of you have made the past 4 years some of the best I could have asked for.

Thank you to everyone within the Cancer Therapeutics unit and Functional Proteomics teams who have helped me with various techniques over the course of my PhD. Especially, Jack O'Hanlon, Habib Bouguenina, Theo Roumeliotis, Fernando Sialana, Mark Stubbs, Olivier Pierrat, Meirion Richards, Joe Smith, Amin Mirza, Maggie Liu and John Caldwell.

I would like to thank my parents and sister for their continuous support throughout my education, enjoy trying to read this! A big thank you to my friends who have supported me whilst living in London, especially Jake and Luke, both of you have made living in the worst part of the country extremely enjoyable. And finally, a huge thank you to Demi. Whether its dealing with my mardy moods or sending videos of Lucy eating nana, you have stuck with me through it all. I know none of this would have been possible without any of you.

Abstract

Chemically induced degradation has emerged as a valuable tool in chemical biology and medicinal chemistry for both potential therapies, and to investigate protein function. Proteolysis targeting chimeras (PROTACs) are small molecules that can hijack E3 ligases, the protein complexes that catalyse ubiquitination, to direct proteasomal degradation of selected targets. Simultaneous binding of both the E3 ligase recruiting moiety and warhead to their respective targets induces ternary (E3-PROTAC-target) complex formation, allowing the E3 ligase to perform ubiquitination on non-native substrates. Subsequent polyubiquitination of the target protein signals for proteasome dependant degradation. Despite significant strides in PROTAC development, including multiple early phase clinical trials, currently only proteins with known binders can be targeted for degradation. We hypothesise that to improve the target landscape of PROTACs and increase the degradable proteome, we could implement a proteomics-based screen of promiscuous kinase focussed PROTACs.

An array of small molecular weight kinase binding PROTACs were synthesised and triaged through proteomics analysis, identifying selective NEK9 and Aurora kinase A (AURKA) hit degraders. Subsequent validation confirmed degradation of NEK9, however, through a neddylation and CRBN independent mechanism. Warhead alterations were explored to determine what component of the degrader conferred the unexpected degradation mechanism. A selective AURKA PROTAC was found to be active at low nM concentrations, affording robust reductions in protein levels over a 2-72 hour treatment. Warhead substitutions to previously published AURKA inhibitors in addition to truncation of the warhead afforded reduced degradation potency. Through the use of small molecular weight warheads, we highlight the ternary complex driven degradation of AURKA, and demonstrate that some PROTACs may not require high affinity warheads. Our approach has the potential to afford degraders of underexplored proteins and provide valuable chemical tools to elucidate protein function.

Abbreviations (Add more to this)

AR: Androgen receptor

AURKA: Aurora kinase A

AURKB: Aurora kinase B

BCL-xL: B-cell lymphoma-extra large

BRD4: Bromodomain-containing protein 4

CAND1: Cullin-associated NEDD8-dissociated protein 1

cIAP: Cellular inhibitor of apoptosis

CRBN: Cereblon

CUL: Cullin

DC_{50}: Half maximal degradation concentration

DCM: Dichloromethane

DIAD: Diisopropyl azodicarboxylate

DIPEA: *N*,*N*-Diisopropylethylamine

D_{max}: Maximal degradation percentage

DMF: Dimethylformamide

ER: Estrogen receptor

EtOAc: Ethyl acetate

GI_{50}: Concentration for 50% of maximal inhibition of cell proliferation

HECT: Homologous to the E6AP carboxyl terminus

HIF1-α: Hypoxia-inducible factor 1-alpha

HPLC: High performance liquid chromatography

HRMS: High-resolution mass spectrometry

IC_{50}: Half maximal inhibitory concentration

IMiD: Immunomodulatory imide drug

IAP: Inhibitor of apoptosis

K_d: Dissociation constant

LCMS:	Liquid-chromatography mass spectrometry
MetAP-2:	Methionine aminopeptidase 2
NMP:	*N*-methyl-2-pyrrolidone
PROTAC:	Proteolysis targeting chimera
PDB:	Protein data bank
PLK3:	Polo-like kinase 3
PTB:	Phosphotyrosine-binding
qRT-PCR:	Real-time quantitative polymerase chain reaction
RBR:	RING – between – RING
RBX1:	RING-box protein 1
RING:	Really interesting new gene
RIPK2:	Receptor-interacting serine/threonine-protein kinase 2
RNF4:	RING finger protein 4
RTK:	Receptor tyrosine kinase
SAR:	Structure activity relationships
SH2:	Src homology 2
SMAC:	Second mitochondria-derived activator of caspases
S_NAr:	Nucleophilic aromatic substitution
SRP:	Substrate recognition protein
THF:	Tetrahydrofuran
TFA:	Trifluoroacetic acid
TMT:	Tandem mass tag
TRIM24:	Tripartite motif-containing 24
VHL:	von Hippel-Lindau
WT:	Wildtype
XIAP:	X-linked inhibitor of apoptosis

Contents

Chapter 1: Introduction

1.1 PROTAC Mediated Degradation

Chemically induced degradation has emerged as a valuable tool in chemical biology and medicinal chemistry for both therapies, and to investigate protein function. Hijacking the cellular ubiquitination machinery accounts for the mode of action of most degraders, with some notable examples utilising the heat shock protein response and direct proteosome interactions.[1] Proteolysis targeting chimeras (PROTACs) are small molecules that can hijack E3 ligases, the protein complexes that catalyse ubiquitination, to direct proteasomal degradation of selected targets *in vitro* and *vivo*.[2]

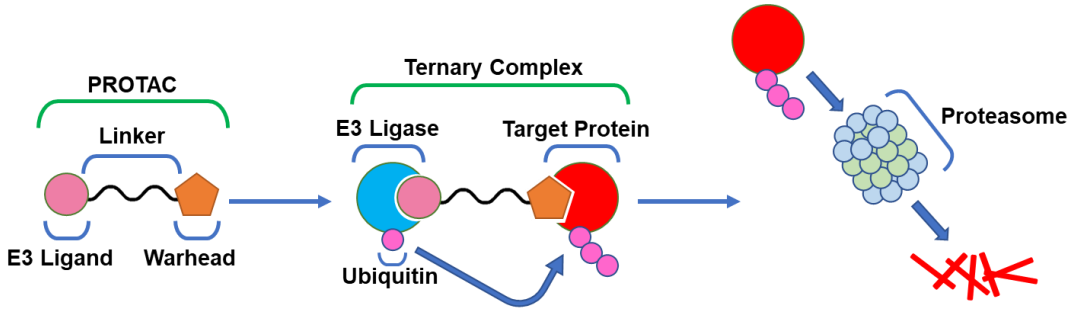

Figure 1.1 Illustration of the structure and function of PROTAC molecules. PROTACs facilitate the formation of a ternary complex, allowing the E3 ligase to ubiquitinate selected proteins.

PROTACs are bifunctional molecules containing three distinct units: the E3 ligase binder, linker, and warhead. Simultaneous binding of both the E3 ligase recruiting moiety and warhead to its respective target induces ternary (E3-PROTAC-target) complex formation, allowing the E3 ligase to perform ubiquitination on a non-native substrate (Figure 1.1). Polyubiquitination of target proteins results in proteasome dependant degradation of the target, liberating the degrader, giving rise to the catalytic nature of PROTACs.[3] Some inherent advantages to this modality over classical inhibition include: the use of sub stoichiometric quantities of drug, the ability to target non-functional domains, the complete removal of proteins from the cellular environment, and overcoming resistance mechanisms.[4]

1.2 Ubiquitin-Proteasome Degradation Pathway

1.2.1 Overview

The cell must regulate the equilibrium between protein synthesis and removal to maintain homeostasis. The most prevalent degradation mechanism in cells is through the ubiquitin-proteasome pathway, whereby E3 ligases mark proteins for degradation with a poly-ubiquitin tag that is subsequently recognised by the proteasome.[5] Ubiquitin is a small globular protein that tags available lysine residues on substrates, and can form poly-ubiquitin chains through further addition to one of 6 surface lysine residues (Figure 1.2). This pathway can affect many cellular processes including regulation of transcription, degradation of misfolded proteins, cell cycle progression, autophagy, development and differentiation, and modulation of the immune and inflammatory responses.[6] Although ubiquitination is often associated with degradation, differential linking of ubiquitin units in the poly-ubiquitin chain can signal for multiple other cellular processes highlighted in Figure 1.2.[7]

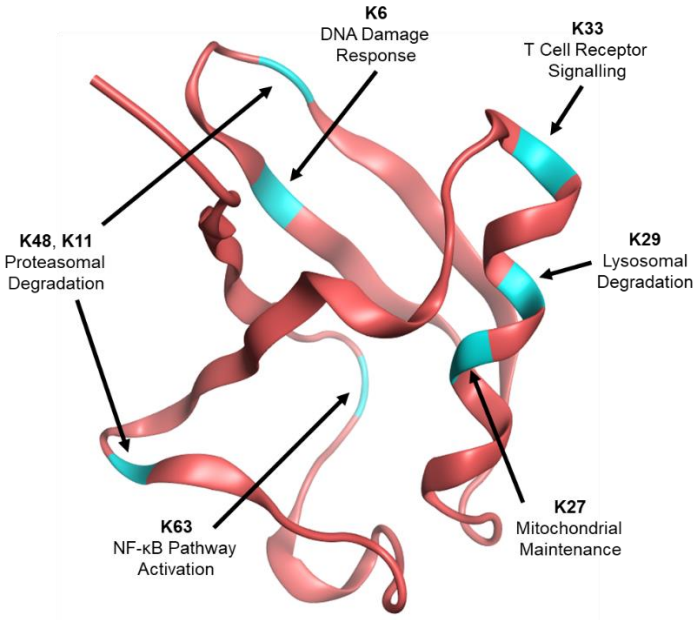

Figure 1.2 Crystal structure of ubiquitin, highlighting individual lysine residues and consequences of poly-ubiquitination on each (PDB: 1UBQ).[8]

1.2.2 Classes of E3 Ligase

E3 ligases catalyse the covalent linkage of ubiquitin to specific proteins in cells. E3 ligases belong to four classes: really interesting new gene (RING) (including multi-subunit RING E3), homologous to the E6AP carboxyl terminus (HECT), RING – between – RING (RBR) and U-box E3 ubiquitin ligases.[9] RING and U-box E3 ligases are distinct from the others as they transfer ubiquitin directly from an E2 enzyme to the target through their RING domain. The E2 protein initially

requires activation through an E1 ubiquitin conjugating enzyme, covalently attaching ubiquitin to the catalytic cysteine (Figure 1.3 A).

The most utilised E3 ligases in PROTAC design are von Hippel-Lindau (VHL) and Cereblon (CRBN), belonging to the multi-subunit RING family of E3 ligases. These E3s generally consist of a cullin (CUL)-RING-box protein 1 (RBX1) heterodimer and a substrate recognition protein (SRP). Human cells express seven different cullins including CUL1, 2, 3, 4a, 4b, 5 and 7, each having the ability to bind different SRPs which in turn recognise a variety of different proteins. The CRBN E3 ligase complex is formed of CRBN, DDB1, CUL4a/b, and RBX1, and is known to degrade several endogenous substrates such as MEIS2,[10] calcium-activated potassium channel subunit α-1,[11] glutamine synthetase,[12] and chloride channel protein 1.[13]

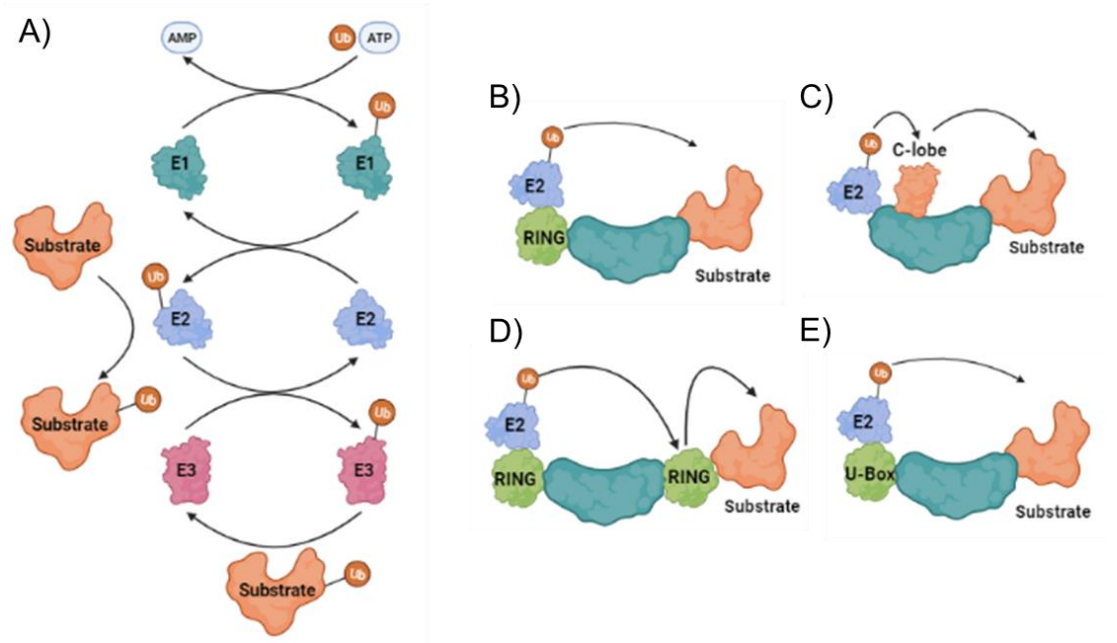

Figure 1.3 Representative structures of how E3 ligases are activated and function. A) Ubiquitin cascade that activates ubiquitin to be conjugated to substrates from either an E2 enzyme (RING and U-box e3 ligases) or an E3 enzyme (HECT and RBR E3 ligases). B) Ubiquitination with RING E3 ligases C) Ubiquitination with HECT E3 ligases D) Ubiquitination with RBR E3 ligases E) Ubiquitination with U-box E3 ligases.

HECT E3 ligases ubiquitinate substrates through an intermediate complex whereby the ubiquitin conjugates to the E3 ligase before transfer to the substrate. RBR E3 ligases are a hybrid between RING and HECT due to containing both a RING domain, but also forming the intermediate ubiquitin conjugate on the E3 ligase prior to transfer. U-box E3 ubiquitin ligases act in an

analogous way to RING E3 ligases with the RING domain replaced by a U-box domain (Figure 1.3 B-E).[14]

The most utilised E3 ligases in PROTAC design are RING E3 ligases: CRBN VHL, MDM2, and IAPs however, some less used ligases are DCAF15, DCAF16, RNF4, and βTrCP.[15–18] The recruitment of alternate E3 ligases is likely to become more important for the future of PROTAC design to potentially modulate off target effects and gain compartmental selectivity in the body due to differing expression levels.[19]

1.2.3 Regulation of multi-subunit RING E3 ligase activity

Neddylation is required to maintain an active cullin-based E3 ligase. Neddylation of cullins is achieved in an analogous way to ubiquitination. An E1-like enzyme (a heterodimer of APPBP1 and UBA3) transfers activated NEDD8 to an E2 enzyme known as UBC12. DCN1 then acts as a NEDD8 E3 ligase by interacting with UBC12 and cullins, allowing neddylation to occur.[20]

Neddylation of cullins activates the E3 ligases through blocking the binding site for CAND1 association, allowing complete assembly of the E3 complex (Figure 1.4). CAND1 is a scaffolding protein that can wrap around the CUL-RBX1 heterodimer before an adaptor protein has bound, therefore behaving as a negative regulator of cullin E3 ligase activity. CAND1 is unable to bind neddylated cullins due to the NEDD8 induced conformational change of the cullin C terminal domain.[21] CAND1 has been shown to facilitate the exchange of different SRPs on cullin E3 ligases through the formation of an unstable complex. As the unstable complex formation is reversible, it allows for the exchange of many different SRPs to degrade what the cell requires.[22]

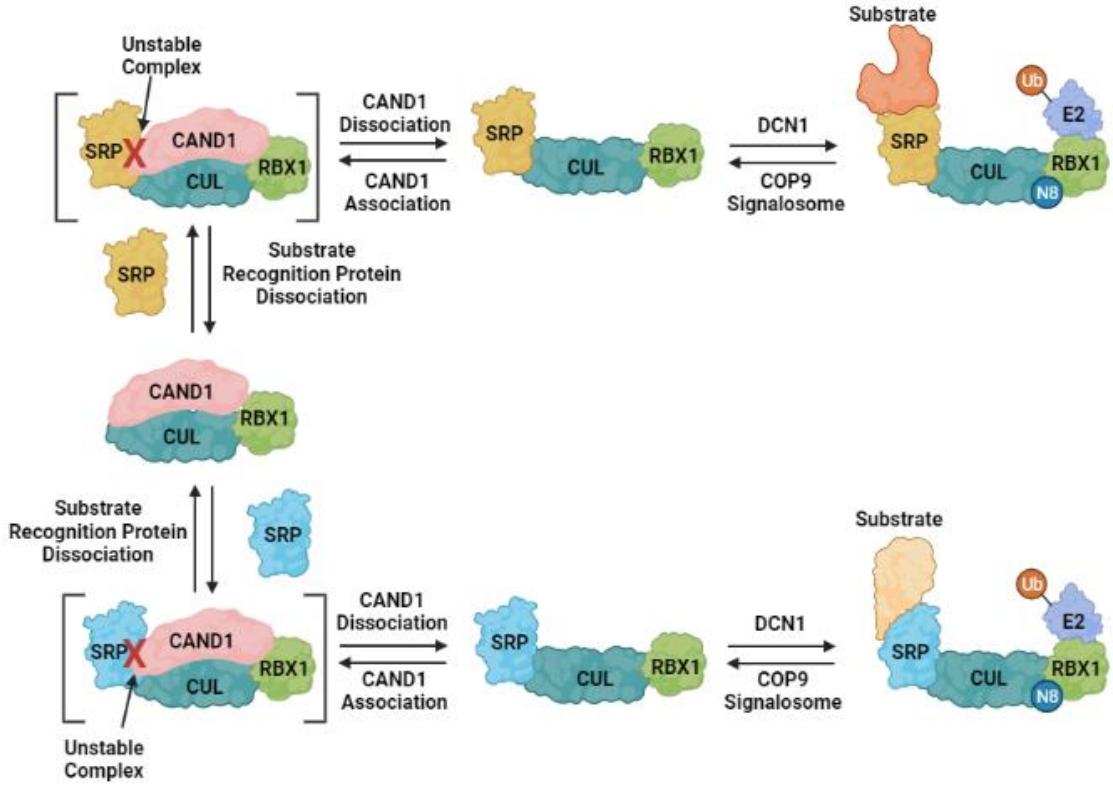

Figure 1.4 Illustration of how CAND1 and neddylation regulate substrate degradation. Different substrates are degraded through the swapping of SRP, mediated by an unstable complex with CAND1. CAND1 can only bind when CUL is not neddylated. High concentration of substrate will force the equilibrium to the active degrading complex.

When a cullin E3 ligase complex is formed a target protein and E2 ubiquitin conjugating enzyme are brought together in relatively close proximity (~50 Å) however, this distance is too far to allow ubiquitin conjugation. Conjugation of NEDD8 to the cullin is required to allow flexibility of its RING domain, and in turn, ubiquitination of the target protein. This process stops the interaction of RBX1 with the cullin winged-helix B sub domain, thereby allowing conformational flexibility of RBX1 (Figure 1.5).[21] Flexibility of RBX1 allows the E2 to span the 50 Å cleft and ubiquitinate a target protein.[23]

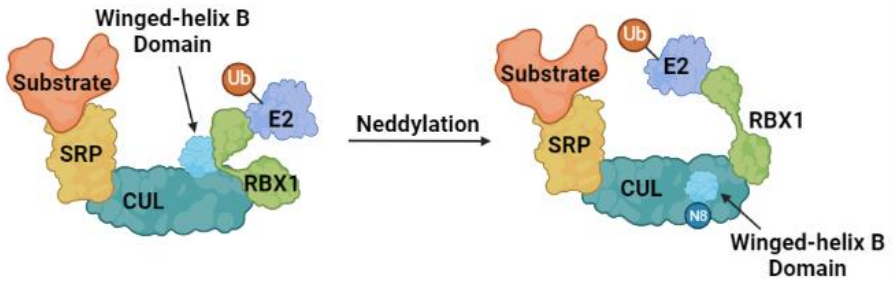

Figure 1.5 Illustration of how neddylation induces conformational change in the CUL C terminal domain as a result of NEDD8 interacting with the winged-helix B domain. This allows conformational flexibility of RBX1, reducing the distance between substrate and E2 enzyme.

The COP9 signalosome is a protein complex that can remove NEDD8, allowing CAND1 to bind, thereby rendering the E3 ligases inactive. Deneddylation cannot occur when substrate is attached to the SRP, therefore substrate presence keeps the E3 ligase in an active form. Isolation of purified neddylated CUL1 and COP9 signalosome demonstrated the lack of deneddylation in the presence of substrate.[24,25] This also occurs with the CUL4-DDB1 complex and is thought to happen on all cullin based E3s.[26]

Regulation of cullin complexes allows for the efficient degradation of built-up proteins. If a high concentration of substrate is present, then the relevant SRP cannot dissociate until the required amount of substrate is degraded. Substrate-bound cullins cannot be deneddylated, therefore cannot bind CAND1 to swap out SRP, resulting in a shifted equilibrium towards the required active ternary complex.

1.2.4 Proteasomal Degradation

When the target protein has been successfully ubiquitinated, it is recognised by the proteasome to be degraded. The 26S proteasome is a large protein complex formed of two smaller protein components, the 20S core particle and the 19S regulatory particle (Figure 1.6). The two subunits form a complex that can recognise and degrade ubiquitinated proteins into small 2-10 amino acid long peptides. Previously, it was thought that ubiquitination of proteins was sufficient in order to mark for degradation by the proteasome, it is now known that degradation is not only dependant on having ubiquitinated protein, but also a loosely folded region (ideally containing ~30 varied amino acids, little flexibility, and being relatively hydrophobic).[27,28]

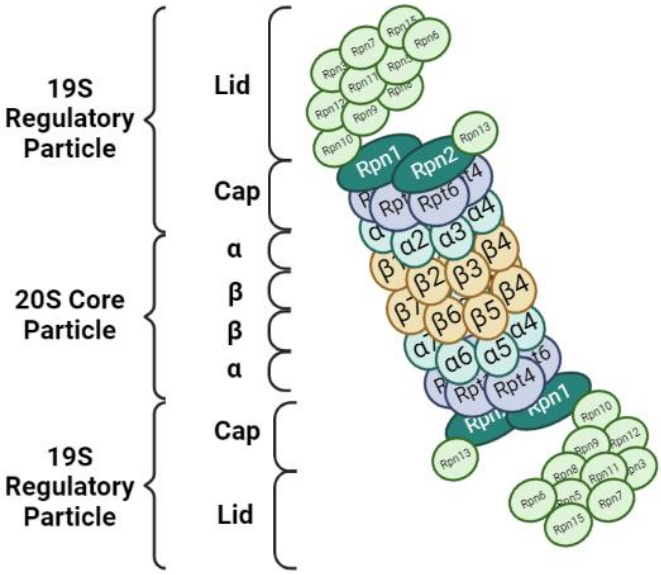

Figure 1.6 Structure of the 26S proteasome. The 19S regulatory particle recognises and removes ubiquitin before helping to form a loosely folded region of the protein and initiating the degradation process. The 20S core particle breaks proteins into smaller amino acid sequences at the β1, 2 and 5 subunits.

Ubiquitination is initially recognised by forming a reversible interaction with Rpn10[29] and Rpn13[30] on the 19S subunit. These proteins have specific domains for binding to conjugated ubiquitin and bind very weakly to free ubiquitin. Deletion of these subunits is non-lethal in budding and fission yeast unlike most other subunits of the proteasome, suggesting other ubiquitin recognition subunits exist on the 19S particle.[31] More recent studies have identified an additional ubiquitin binding subunit Rpn1[32] and Dss1,[33] which may account for this lack of lethality associated with Rpn10 and Rpn13 removal. It is not known whether these sites work in a cooperative fashion or if each are selective to a particular target. The step committing the protein to degradation requires ATP hydrolysis and the previously mentioned loosely folded region of the target protein.[34] After ubiquitinated protein is bound to the proteasome, deubiquitinating enzymes remove the ubiquitin chain, recycling the tag to be used again. Several of these enzymes exist including Rpn11,[35] Usp14,[36] and Uch37.[37] The protein is then pulled through the 20S gate, and peptide hydrolysis occurs at the β1, β2, and β5 subunits.

It is not always necessary to polyubiquitinate a target in order to cause its degradation by the proteasome, short lengths,[38] and even a single ubiquitin can lead to a proteins degradation.[39] It is likely that a lower number of ubiquitin tags could increase the chance of protein escaping degradation, as they can be removed by cytosolic or proteasome associated deubiquitinating enzymes.

1.3 Early PROTACs

1.3.1 Peptidic PROTACs

The first example of targeted protein degradation with a bifunctional molecule was developed by Sakamoto *et al.,* linking a phosphopeptide to ovacilin in an attempt to recruit the Skp1-CUL-F box ($SCF^{\beta\text{-}TRCP}$) E3 ligase to ubiquitinate MetAP-2.[40] Partial degradation was observed within 30 minutes of PROTAC addition to *Xenopus* egg extracts, confirming their hypothesis that ubiquitin-dependent proteolysis could be hijacked to degrade a selected protein. Whilst this proof of concept study showed PROTAC molecules could induce targeted degradation, the degrader suffered from low permeability, effectiveness in the low micromolar range, and in cell phosphatases could inactivate the E3 ligase ligand.[1] The androgen receptor (AR) and estrogen receptor (ER) were also degraded with the $SCF^{\beta\text{-}TRCP}$ recruiting phosphopeptide, and in these cases were dosed using micro injection technology.[18] Further improvements, mainly to the E3 ligase ligand, would be required for improved degradation and cellular activity.

Schneekloth *et al.* were amongst the first to utilise an amino acid peptidic fragment from HIF1α, a known substrate of von Hippel-Lindau (VHL) E3 ligase, modified with a poly-D-arg tag for permeability.[41,42] Conjugation to dihydrotestosterone allowed for the degradation of AR in HEK293 cells at a 25 μM treatment.[43] This and other HIF1α peptide fragments have been used to develop degraders for MetAP-2,[44] FKBP12,[43] aryl hydrocarbon receptor,[45] and ERα.[46]

Cyrus *et al.* discovered that linker attachment point can have a large impact on degradation through using estradiol and a VHL binding peptide to target ERα.[47] Estradiol has multiple synthetically tractable sites for derivatisation with a linker. It was found that one position of the ligand was best suited to degrade ERα more potently. The authors surmise this is a result of higher binary binding affinity towards ERα however, may also be due to better positioning of the VHL E3 ligase into a more productive conformation.

Peptidic E3 ligands were extremely useful proof of concept tools, showing the possibility of this technology, however further improvement to these was

required to increase permeability, and reduce metabolic liabilities. Small molecule E3 binders were soon utilised in PROTAC design to alleviate some of these issues.

1.3.2 PhosphoPROTACs

Tyrosine phosphorylation is an important post-translational modification and modulates the activity of many proteins and pathways. Phosphorylated receptor tyrosine kinases (RTK) can bind downstream targets with both Src homology 2 (SH2) and phosphotyrosine-binding (PTB) domains that further the signalling pathway.[48] Selectively targeting proteins for degradation that contain either PTB or SH2 domains may stop the RTK signalling cascade, nullifying overactive pathways, and have antiproliferative effects.

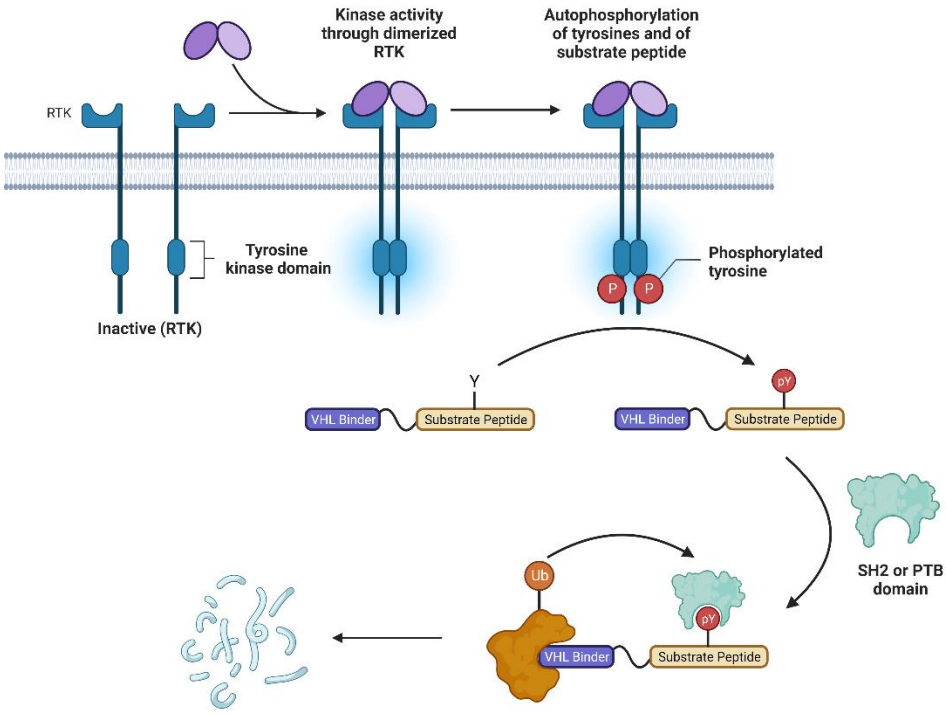

Figure 1.7 Illustration of RTK activation and activation of phosphoPROTACs leading to degradation of proteins with SH2 or PTB domains. Warhead peptides with the ability to be phosphorylated are used to bind to SH2 or PTB domain containing proteins, whilst being tethered to a VHL binding peptide..

PhosphoPROTACs are similar in structure to PROTACs, however contain an inactive peptidic sequence that requires phosphorylation by RTKs. Once phosphorylated, the peptidic sequence is active and can bind to SH2 and PTB domains causing degradation and stopping the RTK signalling cascade (Figure

1.7). The warhead sequences were based upon phosphorylation sites of both TrkA and ErbB2, using a VHL binding peptide with a poly-D-Arg tag for permeability. The TrkA-based phosphoPROTAC successfully targeted the downstream effector fibroblast growth factor receptor substrate 2α (FRS2α), reducing levels by 90% with 80 μM after 7 h. The ErbB3-based phosphoPROTAC only showed partial degradation of PI3K at over 40 μM. Both PROTACs showed subsequent downstream signalling effects, going on to be efficacious in a mouse xenograft model.

A phosphoPROTAC likely has low toxicity to normal cells since only activated RTK signalling pathways can afford degradation. In addition, phosphoPROTACs are less likely to cause commonly seen direct RTK mutations that would normally lead to resistance, as the phosphoPROTAC acts downstream of this. However, this does not exclude E3 ligase-based resistance mechanisms.[49] These molecules are far from ideal tools due to their poor permeability, potency, and likely metabolic instabilities.

1.4 Small molecule ligands in PROTACs

From 2008 onwards, the field of targeted degradation mostly moved away from peptidic ligands to small molecule E3 ligase recruiters. This development was aided by several key discoveries including: the molecular target for IMiDs being identified,[50] the optimisation of a VHL binding peptide,[51] and identification of MDM2 and IAP binding scaffolds.[52]

1.4.1 MDM2

Nutlin 3a (Figure 1.8) was discovered from a screen at Roche and found to displace recombinant P53 from MDM2 (IC_{50} 88 nM).[53] Knowing that MDM2 can ubiquitinate substrates through its RING domain, Smith *et al.* linked nutlin 3a to an AR ligand, decreasing levels after 7h at 10 μM in HeLa cells.[54] This was the first example of an all-small molecule PROTAC identifying MDM2 as a recruitable E3 ligase in PROTAC design. Further optimisation to the degraders would be required to optimise the degradation potency of the PROTACs.

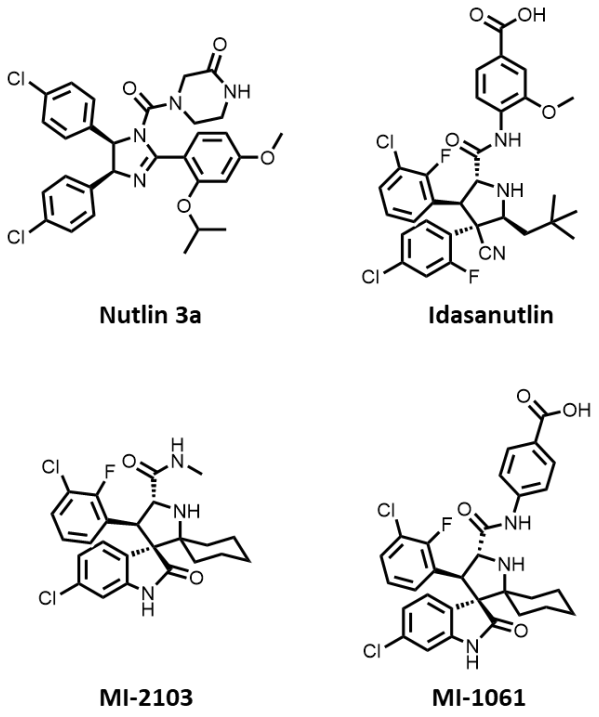

*Figure 1.8 Structure of the MDM2 inhibitors **nutlin 3a**, **RG7388** (**idasanutlin**), **MI-2103**, and **MI-1061** that have been used in PROTAC design. **Nutlin 3a** being utilised in the first all small molecule PROTAC degrader.*

Multiple MDM2 inhibitors have emerged as tools and potential therapies, including **nutlin 3a**, **RG7388** (**idasanutlin**), **MI-1061**, and **MI-2103** (Figure 1.8). All these molecules have been used as MDM2 recruiters in PROTACs, however there are many other MDM2 binders published that could offer improved binding affinity and alter physicochemical properties in PROTAC design.[52]

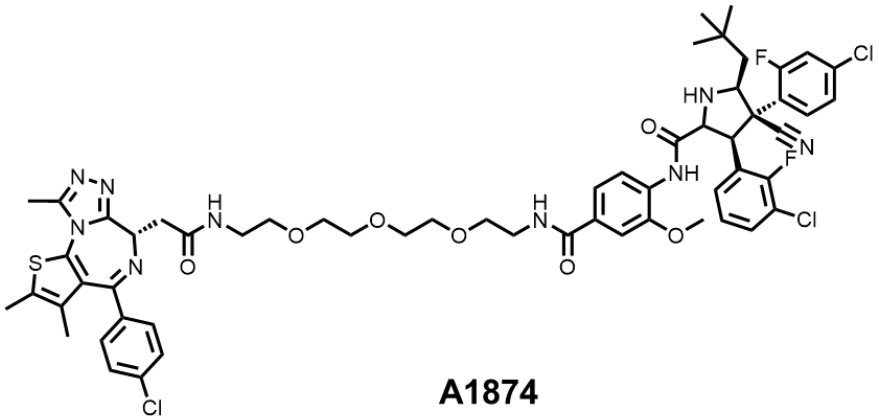

*Figure 1.9 Structure of **A1874**, a BRD4 degrader that along with BRD4 degradation maintained the ability to rescue P53 through the use of the MDM2 binding scaffold **nutlin 3a**. This afforded a PROTAC with increased efficacy due to the synergistic effects of P53 rescue and BRD4 degradation.*

An interesting feature found with a BRD4-MDM2 based degrader (**A1874**, Figure 1.9) was a synergistic antiproliferative effect of BRD4 degradation with P53 rescue. This showed advantages over the corresponding VHL based

PROTAC with similar BRD4 degradation potency, showing how synergistic antiproliferative effects can be achieved with the right choice of E3 ligase.[55] The synergy shown in this example has the potential to be utilised with other degraded targets, but also may be applicable to other E3 ligase recruiters, such as IMiDs if neo-substrate degradation is maintained.

As MDM2 is itself an attractive target due to its modulation of P53, multiple degraders have emerged utilising VHL or CRBN to remove MDM2 from cells. The first examples of MDM2 degraders utilised VHL and CRBN as E3 recruiters, all successfully degrading MDM2 in the nanomolar range however, the CRBN recruiter showed increased potency.[56] Whether MDM2 E3 ligase activity remains and can degrade CRBN was unanswered in this study, and would be interesting to see if this impacts the long-term effectiveness of the PROTAC.

1.4.2 VHL

HIF1α is a known substrate of VHL and is involved in hypoxic response. Under normoxic conditions, HIF1α is oxidised and the resulting hydroxyproline residue is recognised by VHL, ubiquitinating HIF1α, causing its subsequent degradation. Under hypoxic conditions, oxidation of this proline doesn't occur and HIF1α is free to act as a transcription factor for genes such as Epo, VEGF, Glut1, and transferrin.[51,57] Through chemical optimisation around the key hydroxyproline moiety found in the initial VHL binding peptides, a potent small molecule inhibitor of the HIF1α-VHL interaction was found (Figure 1.10). Through conjugation of inhibitors to one of two solvent exposed and chemically tractable sites on **VH298**, several effective PROTACs have been synthesised.

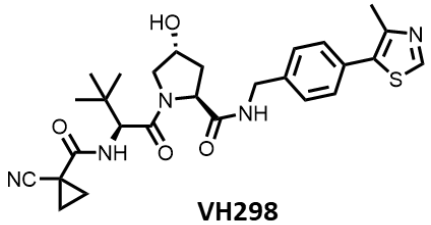

VH298

*Figure 1.10 Structure of **VH298**, an inhibitor of the HIF1α -VHL interaction found through the optimisation of a VHL binding peptide. This, through multiple linker attachment vectors is one of the most commonly utilised E3 recruiters used.*

The use of VHL PROTACs uncovered several key discoveries in the field of targeted degradation, including experimentally determining the sub stoichiometric nature of a RIPK2-based PROTAC.[3] Quantifying bands

corresponding to RIPK2 and its ubiquitinated equivalent identified that a single PROTAC molecule is capable of sub-stoichiometric degradation. Their data showed that one molecule of PROTAC can result in 3.4 times as many ubiquitin modified RIPK2 proteins. Although clearly catalytic, these measurements are likely a conservative estimate due to degradation occurring of polyubiquitinated RIPK2.

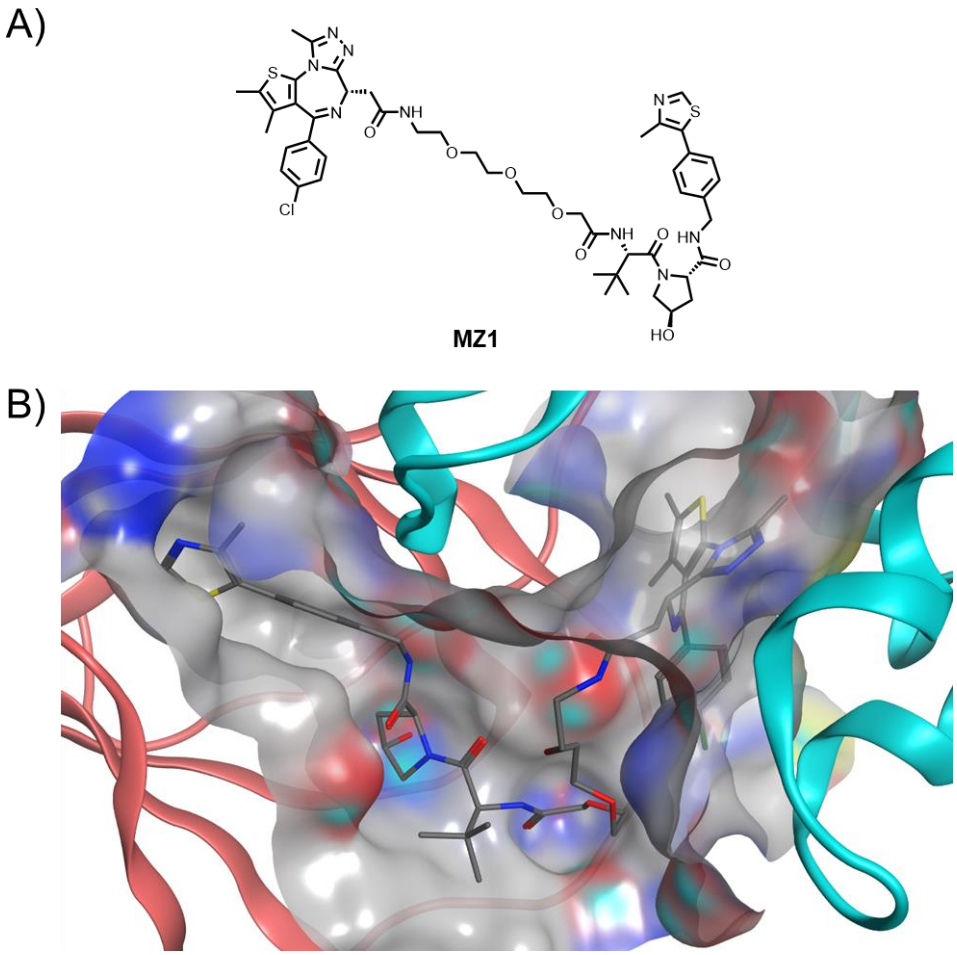

*Figure 1.11 A) Structure of **MZ1**, a BRD4 degrader. B) Ternary complex crystal structure of **MZ1** with $BRD4^{BD2}$ and VHL (PDB: 5t35). $BRD4^{BD2}$ in cyan and VHL in salmon highlighting the kinked linker conformation and large area of interaction formed within a ternary complex.*[58]

MZ1 is a degrader of BRD4 discovered through the attachment of JQ1, a BRD4 ligand, with a VHL E3 ligase binder through a flexible PEG linker.[59] Elucidation of the ternary complex crystal structure between VHL-MZ1-$BRD4^{BD2}$ was a large step in understanding the linker involvement in degradation systems (Figure 1.11 B).[58] The total surface area of contact between $BRD4^{BD2}$ and VHL was calculated to be 688 $Å^2$, showing the vast area of interactions possible that can lead to positive cooperativity of the ternary complex. In addition, MZ1 was shown to be folded into a bowl shape, with the linker forming interactions with

the BC loop of BRD4^{BD2} and an internal hydrogen bond with the JQ1 ligand. Solving of ternary complex structures could lead to a more structure guided approach in PROTAC design, as opposed to the trial-and-error linker optimisation done by most. However, it is important to note that the stable ternary complex observed in a crystal structure may not be the active productive ternary complex required for degradation.

Often highlighted is the potential of PROTACs to target the undruggable proteome, as it is not necessary to have an inhibitor only a binder of a target. Although degraders could conceptually target any domain with a ligand, functional or not, limited cases have been reported. One example of this is the TRIM24 bromodomain which, upon inhibition, elicits no phenotypic response. Gechijan *et al.* utilised PROTAC technology to degrade TRIM24 using a VHL binder.[60] This PROTAC showed activity in acute leukaemia, highlighting how other domains of proteins may need to be supressed in order to elicit the desired phenotypic effect. Identification of these non-functional and druggable sites is still a challenge and may benefit from a promiscuous PROTAC screening approach.

An extensive study by Burslem *et al.* showed, through the degradation of multiple RTKs, that degradation can have prolonged effects over inhibition.[61] A lapatinib-based EGFR degrader was utilised in cell proliferation assays, demonstrating improved cell antiproliferative potency against inhibition. Inhibition of EGFR can lead to kinome rewiring whereby alternate kinases take over the role of EGFR when it is inhibited, continuing the signalling cascade.[62] Despite decreasing upon initial suppression of ERK1/2, phosphorylation levels of Akt, c-Met, and HER3, levels returned close to basal levels after 24-48 h of treatment despite continued presence of the inhibitor. The degrader equivalent did not show this phenomenon and continued to elicit sustained suppression of downstream targets. This may be due to scaffolding roles of EGFR being present during inhibition, causing a feedback mechanism that cannot occur during degradation.

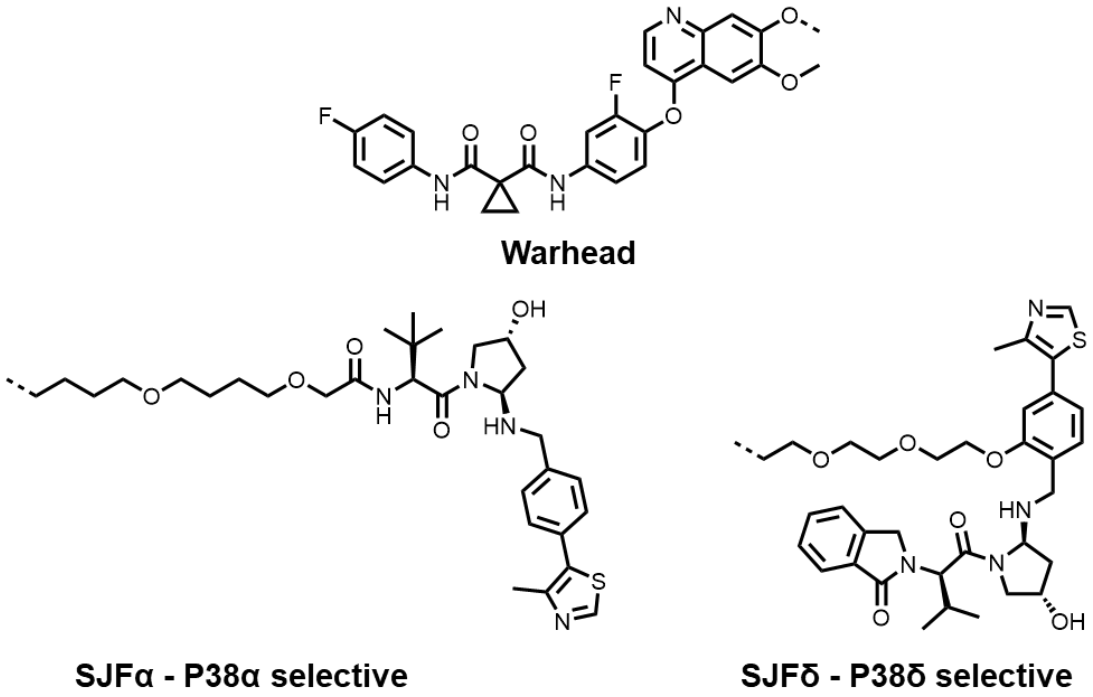

Figure 1.12 Structure of SJFα and δ, p38 isoform selective degraders. Through alternate attachment points and linkers isoform selective degraders were discovered, likely the result of stringent ternary complex constraints allowing for high levels of selectivity.

A study from Smith *et al.* describes the power of the ternary complex in inducing selective degradation of protein isoforms.[63] Through linker optimisation as well as alterations to the VHL ligand attachment point, selectivity was gained over p38α and δ isoforms, exemplifying the potential selectivity gains that can be achieved, likely through stringent ternary complex requirements (Figure 1.12).

Generally, it has been shown that there is a positive correlation between the strength of the ternary complex and degradation potency, although this does have exceptions.[64] One example by Han *et al.* showed that the ternary complex can drive degradation potency through the use of a truncated VHL ligand.[65] A key methyl thiazole was removed from a 25 nM VHL binding ligand, reducing VHL affinity to 9.9 μM. Linker re-optimisation resulted in a potent PROTAC against AR, likely attributed to a favourable ternary complex that can overcome the weakly binding ligand. As poorly binding ligands can still cause potent degradation of targets, this could give more scope for ligand optimisation of permeability, solubility, and metabolic issues as smaller molecular weight ligands may be utilised.

1.4.3 IAP

The inhibitor of apoptosis (IAP) family of proteins including cIAP1/2 (cellular inhibitor of apoptosis) and XIAP (X-linked inhibitor of apoptosis), are essential in controlling cell survival.[66] IAPs can promote activation of caspases-3/7/9, through binding of the IAPs BIR2/3 domain, leading to apoptosis of the cell. Along with their BIR domains, IAPs also contain a RING domain, necessary for E2 binding and subsequent ubiquitination of targets. The BIR domains of IAPs were initially drugged by peptides mimicking second mitochondria-derived activator of caspases (SMAC), disrupting the caspase-IAP interaction.

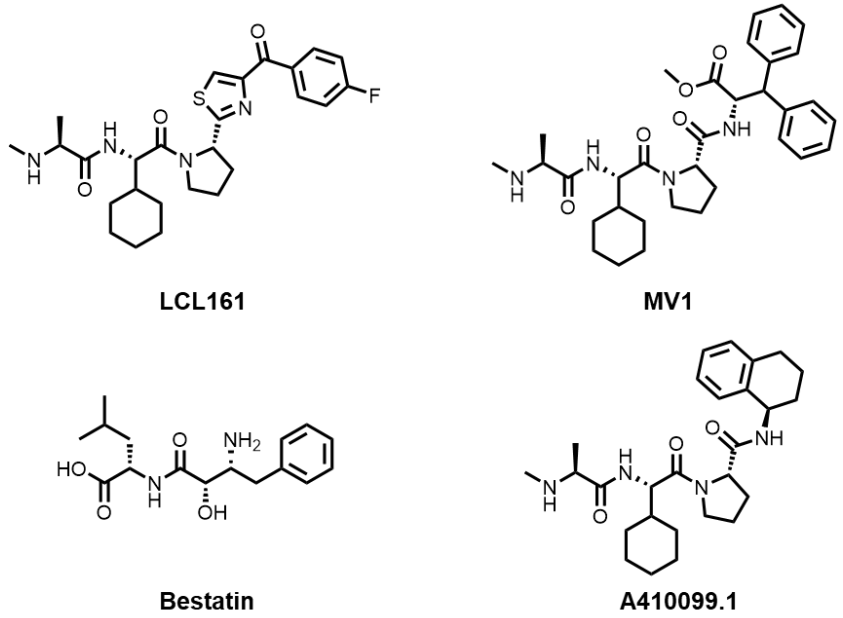

Figure 1.13 Structure of multiple IAP ligands used in PROTAC design.

The first use of IAPs in targeted degradation was achieved by Hashimoto *et al.* who targeted CRABPI and CRABPII.[67] The degrader consisted of bestatin (Figure 1.13) and all–*trans*–retinoic acid to bind to cIAP and CRABP respectively. This class of PROTACs were only effective in the micromolar range and induced auto-ubiquitination of cIAP, a consequence of the bestatin ligand.

A notable publication by Mares *et al.* utilising a IAP binding moiety showed the first PK/PD results from a RIPK2 selective degrader.[68] Their analysis showed that the PROTAC was active in rats at concentrations below the level of quantification, attributed to the slow resynthesis rate of RIPK2. This shows potential for PROTACs in the clinic with much smaller or less frequent doses than inhibitor molecules.

1.4.4 CRBN

IMiDs (Figure 1.14) are molecules that bind to the surface of CRBN, altering its structure, allowing the recruitment of non-native CRBN targets (neo-substrates). Of the neo-substrates recruited by IMiDs, all have a common structural beta hairpin loop which is recognised by CRBN, allowing for ubiquitin tagging. This molecular glue mode of action was uncovered by Ito *et al.*, using an immobilised IMiD that pulled down CRBN and DDB1.[50] These drugs are clinically used for the treatment of multiple myeloma, however recently have been used to hijack CRBN to degrade selected targets.

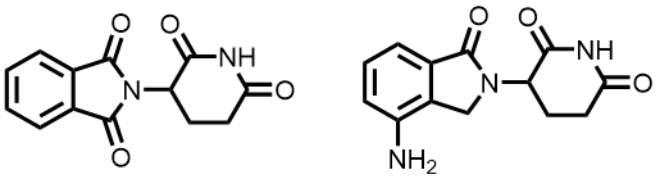

Thalidomide **Lenalidomide**

Figure 1.14 Structure of the two most utilised scaffolds in CRBN-based PROTACs. Both these approved drugs are currently used to treat multiple myeloma and were found to bind to the CRBN E3 ligase. They are amongst the most used E3 ligase binders in PROTAC design.

CRBN has been shown to be a more promiscuous E3 ligase and gives a broader number of proteins degraded relative to a VHL matched pair, although a comparison has not been made with either MDM2 or IAP recruiting degraders.[69,70] The promiscuity of CRBN based degraders can be attributed to the E3 complex and how the cullin is able to freely rotate around DDB1 ~150˚, thereby allowing for a larger ubiquitinating area.[71]

One potential pitfall with CRBN recruiting PROTACs is the IMiD ligand itself. These molecules can maintain the molecular glue activity upon PROTAC conversion however, slight linker modifications can tune out IMiD targets from the degradation profile.[72] Although off-target activity is not typically desirable, one could imagine a potential synergistic effect when degrading a protein relevant to multiple myeloma, similar to the previous example with P53 rescue in MDM2-based PROTACs.

Although PROTACs have been shown to overcome resistance mechanisms of the target protein, resistance can still occur and often involves the E3 ligase itself.[49] Stable genetic changes were observed effecting the E3 ligase

components as opposed to mutations in the protein target. Resistance to the BET targeting CRBN-based PROTAC was revealed to be due to deletion of 12 million base pairs corresponding to the CRBN gene. Cells were resensitised to the PROTAC through overexpression of CRBN. Similarly, the VHL equivalent PROTAC incurred resistance due to multiple genetic alterations of the CUL2 locus that were again rescued by overexpression of CUL2. Interestingly the VHL resistant cell line was still sensitive to CRBN treatments and *vice versa*. This highlights the need for an expansion of E3 ligases used in PROTAC design, potentially using essential complexes that cannot be genetically deleted.[19]

The differing tissue expression of E3 ligases could offer compartmental selectivity, reducing both on and off-target toxicity. To date only one example of this is published using CRBN to alleviate thrombocytopenia toxicity seen during BCL-xL treatments.[73] Western blotting confirmed the level of CRBN expression in platelet cells was low, and hence their degrader showed minimal platelet toxicity as a result, highlighting another potential benefit for PROTAC conversion of drug molecules.

PROTACs are often formed of 2 small molecule ligands, individually obeying ‘rule of 5’ chemical space however, when these are joined through a linker the resulting PROTAC tends to have poor physicochemical properties. The poor physicochemical properties associated with PROTACs was highlighted with a BCL6-CRBN degrader showing poor permeability. It was found that the PROTACs permeability decreased 400-fold relative to the parent warhead, highlighting the impact addition of an E3 ligase ligand and linker can have on a molecules properties.[74] Measuring the permeability of PROTACs has been found to be challenging due to poor recovery in PAMPA assays.[75] It was suggested that a Caco-2 assay would likely be better to explore permeability, however in-cell target engagement assays could also be used as a surrogate.[76] To date several PROTACs have shown *in vivo* activity despite the innate solubility and permeability issues, potentially due to the PROTACs catalytic nature, mitigating the lack of cellular concentrations.

Efflux has been shown to have drastic effects on the potency of PROTACs. Either inhibition of PGP, or knockdown with shRNA showed increased degradation and inhibition of cell growth with ALK or PTK2 degraders.[77,78] Efflux

is therefore an important factor to consider during PROTAC design due to the dramatic effects it can have on degradation.

1.5 Activatable PROTACs

1.5.1 CLIPTACs

In an effort to mitigate the poor property space of PROTACs, Lebraud *et al.* utilised in-cell Click chemistry to degrade BRD4 and ERK1/2.[79] Through an inverse electron demand Diels-Alder reaction of a tetrazine and *trans*-cyclo-octene, cellular degradation of both targets was observed (Figure 1.15). Although no permeability measurements were taken, degradation was not seen with pre-formed CLIPTAC and required sequential addition of tetrazine and *trans*-cyclo-octene. This study provides a strategy for the design of potentially brain penetrant PROTACs, an area which may be challenging using traditional PROTAC design.

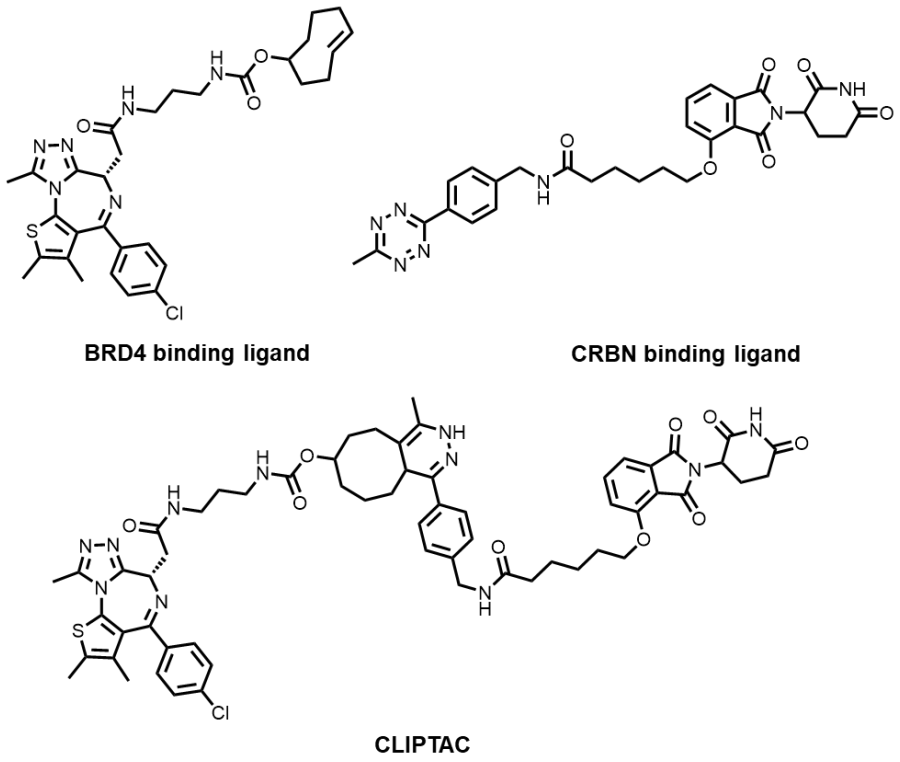

Figure 1.15 Structures of a BRD4 targeting CLIPTAC formed from a CRBN binding tetrazine and trans-cyclo-octene containing BRD4 ligand. Through in-cell Click chemistry, overcoming the poor cell permeability of the intact molecule, the CLIPTAC was able to degrade BRD4.

1.5.2 Light activated PROTACs

Light activation of PROTACs has been achieved in two manners, first by inactivation of the E3 or target ligand with a photo-cleavable group, second

through a diazo group that can be switched between active and inactive forms. The former was first introduced through the use of a nitroveratryloxycarbonyl (**NVOC**) moiety, a functionality that can be cleaved upon exposure to UV light (λ = 365 nm).[80] The obvious position for attachment of the **NVOC** group on CRBN and VHL binders are the key Glutarimide NH and hydroxy proline moieties respectively, as modifications to these are often used as negative controls in PROTAC validation experiments.[10,81] **NVOC** photo-caged PROTACs have been used to degrade targets such as BRD4, ALK, and BTK.[82] Similarly, 6-nitropiperonyloxymethyl (**NPOM**, requiring λ = 402 nm), diethylaminocoumarin (**DEACM**, requiring λ = 365 nm), and 4,5-dimethoxy-2-nitrobenzyl (**DMNB**, requiring λ = 365 nm) have been used for the photo induced degradation of BRD4 and ERRα.[80,83,84]

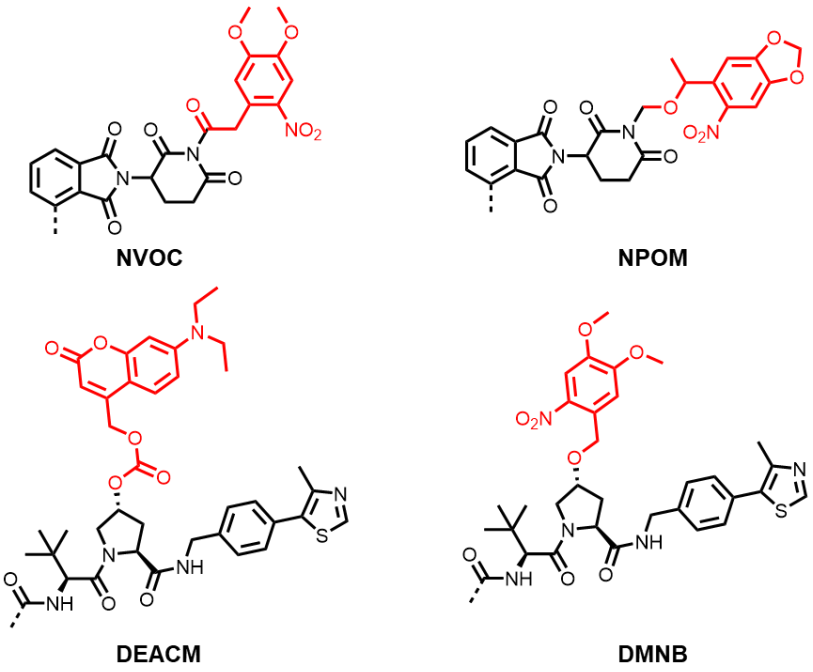

Figure 1.16 Structure of photo-cleavable groups (red) attached to E3 ligase ligands (black) rendering them unable to bind and therefore degrade the respective targets.

Photo-switchable PROTACs offer the ability to reversibly modulate PROTAC activity through isomerisation of key functionalities, often contained in the linker. As ternary complexes often have stringent linker requirements, drastic conformational change is likely to have a large impact on degradation. All three examples of photo-switchable PROTACs contain diazo derivatives that can be switched to their active or inactive forms through exposure to different wavelengths of light. These systems have been used to degrade BRD4,

FKBP12, BCR-ABL and ABL.[85,86] The controlled activation of PROTACs is a very promising approach, however, is subject to several limitations including DNA damage during exposure to UV light, UV penetration, and an increased molecular weight of the PROTAC.

1.6 PROTAC Development Approaches

Often PROTACs are designed with a particular target in mind, one with a known potent and selective warhead. Although this approach tends to afford potent degraders, it may not be necessary due to cooperativity arising from ternary complex effects. The vast area of interaction formed within the ternary complex has the potential to drive potency of degradation, overcoming weaker binding warheads.[65] The large surface can also impart significant amounts of selectivity over the parent warhead and is dependant of the E3 ligase utilised.[70]

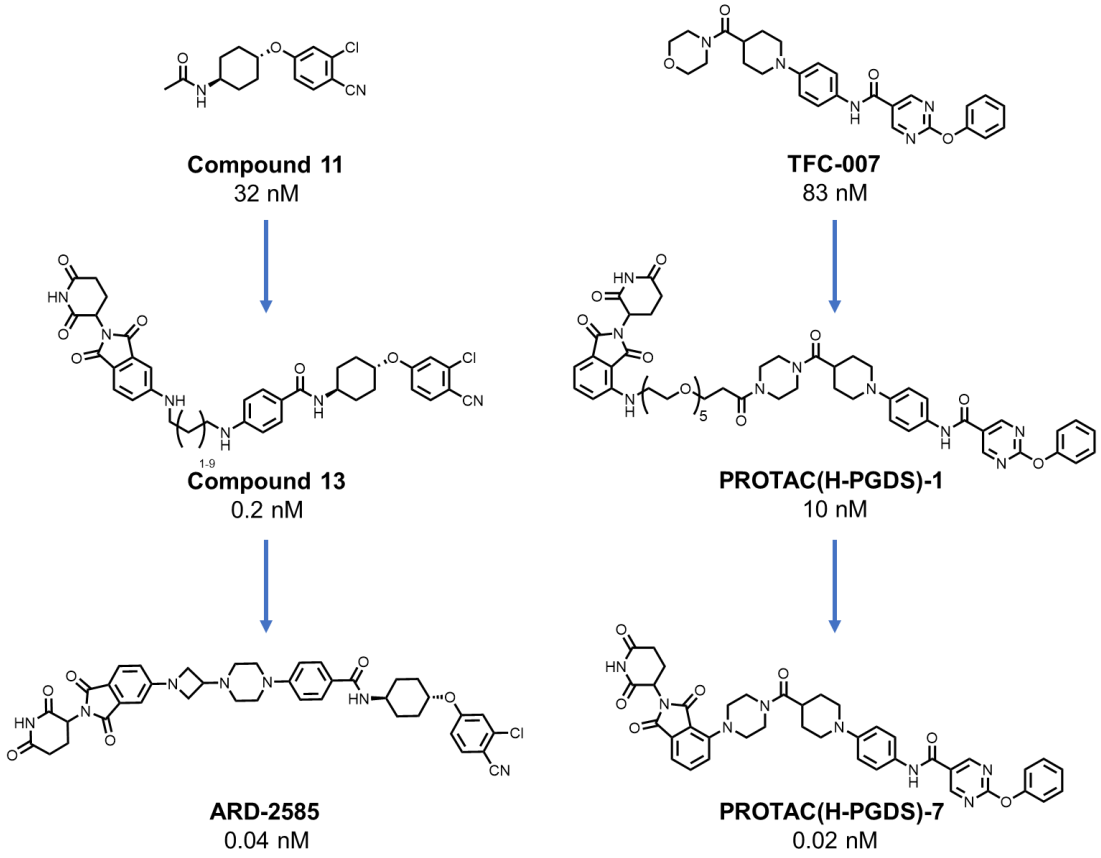

Figure 1.17 Development of two PROTACs targeting AR (left) and hematopoietic prostaglandin D synthase (right) through linker modifications. The linker is the main section of degraders that is optimised, likely due to the highly optimised warheads and E3 ligase ligands used.[87–90]

The linker region of PROTACs if often the most explored when optimising for potent degradation. This is likely a result of the highly optimised binders of E3 ligases and targets used, with simple, synthetically tractable PEG or alkyl linkers

utilised in the first instance. Commonly, rigidity and polarity are added to the linker, aiming to lock the degrader in its active conformation and improving solubility. Highlighted in Figure 1.17 is two examples of linker optimisation on separate target classes where rigidity significantly affected degrader potency and likely improved solubility.[87–90] In both examples a known solvent exposed area of the warhead was conjugated to multiple linker lengths, either PEG or alkyl based. From this, an ideal linker length range is discovered, and was further optimised through the addition of rigid rings into the linker.

An in-depth publication by Donovan *et al.* discovered degraders of ~200 kinases through screening numerous highly elaborated promiscuous kinase binding scaffolds.[76] Validation of multiple PROTAC principles on a large scale was seen, including the lack of correlation between target engagement with degrader potency, and the fact that formation of a stable ternary complex does not predict degradation efficacy. In addition, some kinases were seen to have a high propensity for degradation including Aurora kinase A. This screen was predicted to afford tractable degrader starting points for chemical optimisation however, a recent example attempting to improve selectivity of one PROTAC screening hit afforded a degrader that maintained off-target activity, suggesting this may be a challenging parameter to optimise when starting with a highly promiscuous degrader.[91]

1.7 Proteomic Methods Applied to PROTACs

Proteomics has been used in the context of PROTAC design as early as 2015 with the aim of confirming selectivity of degradation,[92] but more recently to probe how ternary complex formation effects degradation through use of promiscuous warheads.[70,76] Proteomics is an extremely powerful technique to identify upwards of several thousand proteins through a bottom-up or ‘shotgun’ approach. This approach relies on the breaking down of in-tact proteins into peptides using a tryptic digest. Trypsin breaks down proteins in a highly selective manner, at the C-termini of arginine or lysine residues, ideal for proteomic analysis as peptides tend to have a high intensity mass ion.[93] Despite the highly powerful analysis proteomics can provide, a lot of information can be lost through the tryptic digest yielding over half of all peptides having >6 amino acids, being too small to be identified. Subsequent fractionation (HPLC

separation and combination of fractions) allows for enhanced depth during proteomics analysis and ensures highly abundant peptides are less likely to overwhelm the mass spectrum. This does increase the cost of machine running as more samples need to be run, and is why fractions are often combined, reducing depth of the proteomics while reducing costs.

As protein concentration does not necessarily correlate with mass spectrum signals, in order to compare separate samples we are required to multiplex, using either TMT labels or a SILAC approach.[94] The SILAC approach is lower throughput than TMT labelling as commonly only two samples can be ran simultaneously, being ‘heavy’ and ‘light’, although up to 5 differing samples can be made. The samples are modified using media enriched with heavy isotopes of arginine or lysine during cell culture.[95] TMT labels over recent years have improved the throughput of proteomics, now allowing for up to 18 samples to be ran simultaneously, deconvoluting at the MS2 stage of proteomic analysis. This has enabled the high throughput analysis of degraders and has uncovered multiple important milestones that has enabled degrader discovery.[96]

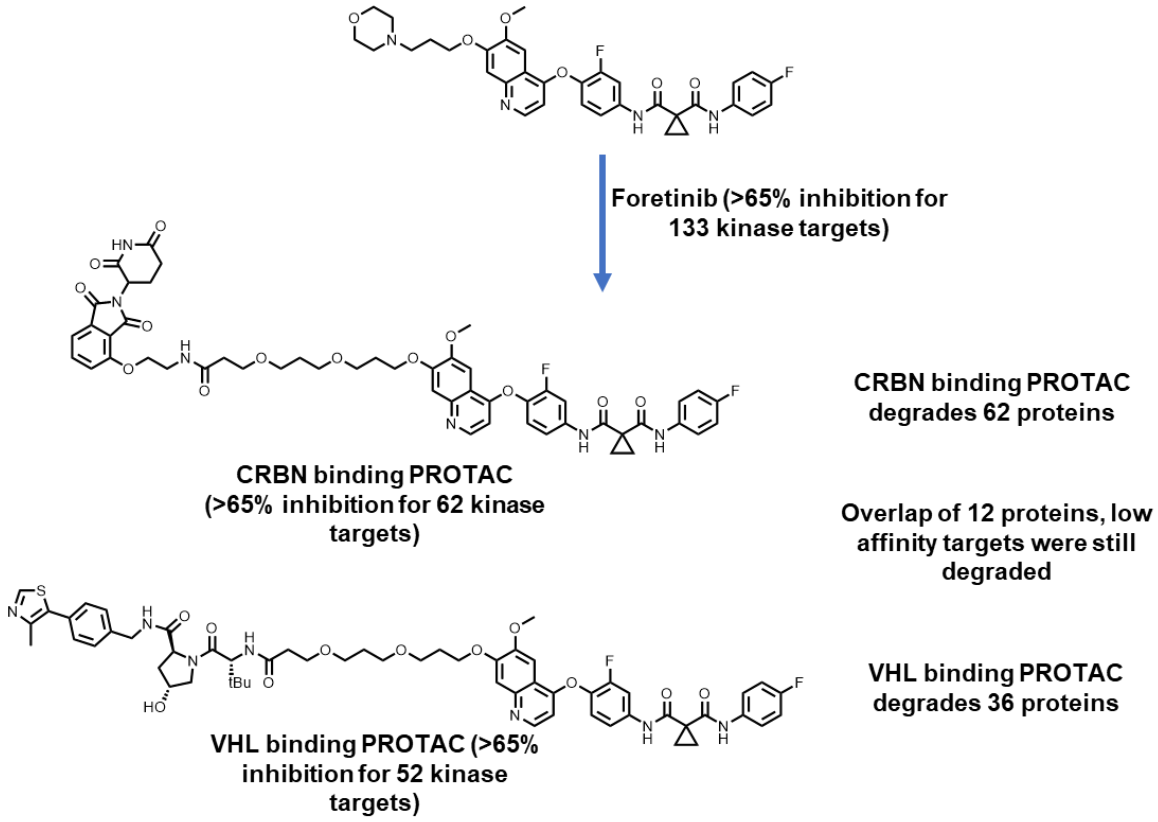

Figure 1.18 Bondeson et al. utilised a promiscuous kinase degrader to query the degradation profile utilising proteomics analysis. PROTACs were found to be significantly more selective than the parent inhibitor, whilst having differential selectivity through use of alternate E3 ligase recruiting ligands.

The first use of proteomics analysis highlighted the degradation profile of two PROTACs containing different E3 ligase binders but the same highly promiscuous warhead (Figure 1.18). The study highlighted the drastic selectivity increase observed with degradation as opposed to inhibition, attributing this to ternary complex effects. Increasing the selectivity of parent warheads has been a feature seen in further examples,[63,97] highlighting the power of ternary complex formation and widens the scope of available ligands that can be utilised for selective degradation.

Further use of proteomics came from a large scale study by Donovan *et al.*[76] providing evidence that: target engagement and ternary complex formation does not predict degradation, degradation is cell line dependant, alternate E3 ligases utilisation changes the degradation profile and IMiD off targets can be tuned with linker modifications. The authors also claim this study provides excellent starting points for kinase degrader discovery, however the only effort to utilise an unselective degrader from this data set resulted in a maintained lack of

selectivity.[91] We believe this approach could be improved through the use of weaker affinity ligands, relying on productive ternary complex formation to degrade targets.

1.8 Project Aims

Despite all the developments in the field of PROTAC mediated degradation over the last 21 years, there are multiple key areas that still need to be addressed, namely drugging the undruggable proteome, and the large molecular weight space PROTACs occupy. We hypothesise that we can uncover orphan proteins of interest and maintain favourable physicochemical space through screening low molecular weight PROTACs in proteomics, exploiting favourable ternary complex formation to afford hit PROTACs that can be further optimised for improved potency. In doing so, this work will highlight the lack of requirement for highly elaborated and optimised warheads, providing further options for PROTAC optimisation.

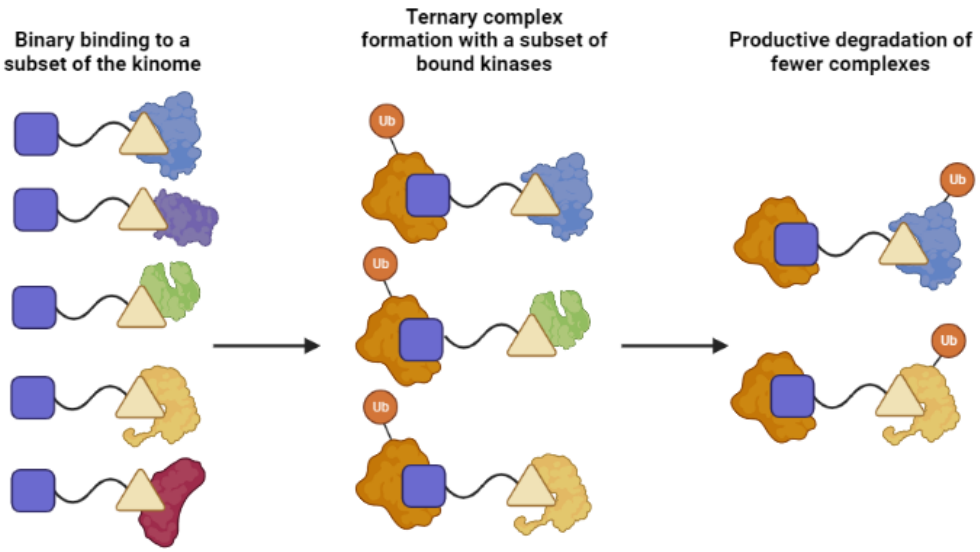

Figure 1.19 With a promiscuous kinase binder ternary complex formation of only a subset of bound kinases is expected due to strict ternary complex requirements and a subset of ternary complexes will likely form productive ternary complexes and will be able to degrade the bound kinase. A screen of small promiscuous PROTACs will likely afford degradation of a small number of hit proteins than is bound.

For this proof of concept screen, targeting kinases would offer an opportunity to bind a large range of the family with a simple hinge binding motif, whilst having the potential to degrade undrugged and unannotated proteins. With this target class in mind, we believe we will be able to achieve modest levels of binding potency using low, near fragment sized warheads, whilst affording degradation upon incorporation into a PROTAC (Figure 1.19). As the warheads will be much

smaller than what is commonly used, warhead optimisation can be undertaken, an area often less researched in PROTAC design, but will still allow for the classical linker optimisation if required.

For the screen itself, an in-house validated global proteomics platform will be utilised and followed up with Western blot validations of hit proteins.[96] Through careful design of our library, we believe SAR will be visible in the proteomics, giving confidence in the results, and options on how to optimise the degraders further. Upon validation of hit protein targets, optimisation will be attempted involving both warhead and linker changes, giving the opportunity to improve potency.

Chapter 2: PROTAC Library Design and Proteomics Screening

2.1 Library Design

To validate a PROTAC screening approach, a suitable warhead scaffold must be selected that is appropriate for incorporation into a PROTAC. As a proof of concept, we aimed to target kinases due to the ability to bind many through the use of a variety of hinge binding scaffolds (Figure 2.1).[98] In addition, although kinases are amongst some of the more highly studied drug targets, the family contains 168 members that fall within the 'dark kinome', encompassing underexplored and unannotated proteins, highlighting a need to discover tool compounds for these targets.[99] As PROTACs tend to occupy chemical space beyond 'rule of 5' guidelines, it is important to mitigate any potential physicochemical property liabilities that could lead to poor solubility or permeability. For this reason, we aimed to utilise a warhead scaffold with a low molecular weight and low number of hydrogen bond donors and acceptors. Having favourable physicochemical properties with the hit PROTACs would yield better starting points for medicinal chemistry optimisation.

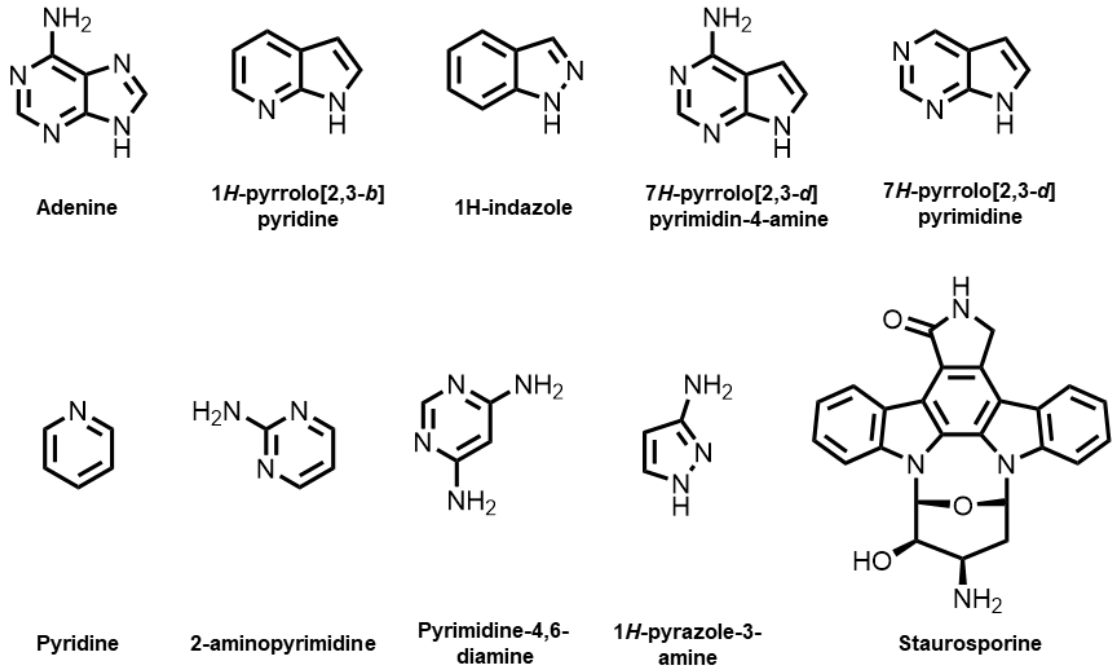

Figure 2.1 Common hinge binding scaffolds from the crystal structure database at Pfhizer. Any of these scaffolds could have been selected for our proof of concept screen and could give highly varied degradation profiles.[98]

The PROTACs in the screen were based on the 2-aminopyrimidine containing compound **BOS-172722**, an MPS1 ligand developed in our group currently in phase 1 clinical trials (Figure 2.2).[100] This particular scaffold was selected as the warhead, which early in its discovery demonstrated a range of off target activity across the kinome.[101] In addition to promiscuity, the scaffold had favourable physicochemical properties, including few hydrogen bond donors and a low PSA which was appealing to facilitate better cell permeation of the final PROTAC molecules. The scaffold had also been extensively explored in our group with known structural information along with knowledge of the chemistry.

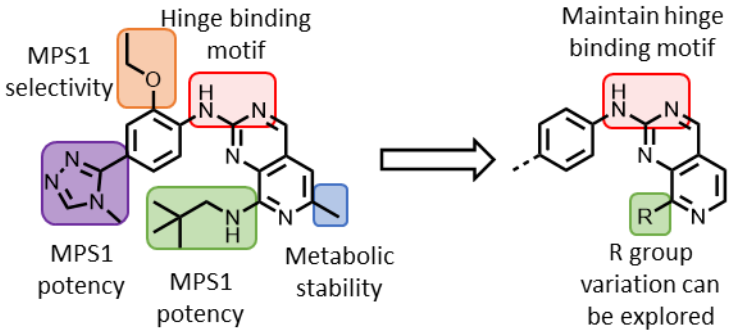

*Figure 2.2 Structure of **BOS-172722** and how it was truncated to a core hinge binding unit. Truncation should lead to a poorly selective kinase binder that will also not be significantly potent to any kinase. A highly cooperative ternary complex should mitigate the lack of binary kinase affinity whilst increasing selectivity.*

Truncating **BOS-172722** to the core pyridopyrimidine component will likely result in weaker binding to kinases. However, we believe productive ternary complex formation may still occur and achieving potent degradation will still be possible. High levels of degradation with low affinity ligands has been seen previously and can likely be attributed to a highly productive ternary complex with potentially high levels of cooperativity.[65,70] With a small warhead, weak binding to a variety of kinases may be expected, but potent degradation would be expected in only a subset of bound proteins after PROTAC conversion. A selectivity gain is commonly seen with PROTACs and occurs due to the stringent ternary complex requirements for productive degradation imposed by the E3 ligase.[70]

Removal of the ethoxy functionality from the phenyl ring can recover the absence of selectivity we required for this set of molecules, as this group is essential for selective MPS1 binding. We also sought to remove the triazole functionality and instead, use this position as a vector for linker attachment.

BOS172722 contains a pyridyl-methyl substituent to confer metabolic stability, a property we are not concerned with in this early stage PROTAC discovery therefore, this was removed.[100] Finally, we believed we could use different amine substituents to replace the original neopentylamine, in order to explore potential chemical space around the warhead. The groups we chose to explore were varied sizes and included a dimethyl amine, azetidine and morpholine.

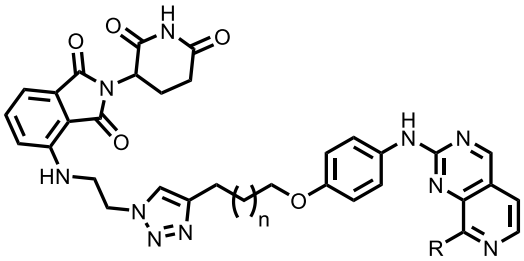

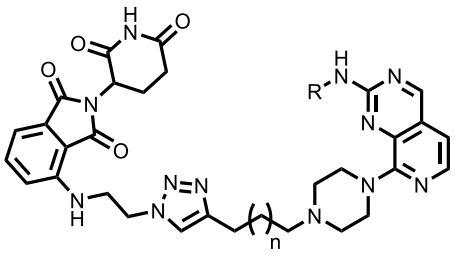

	R group	Linker length (n)
1		1
2		3
3		5
4		1
5		3
6		5
7	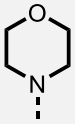	1
8		3
9		5

	R group	Linker length (n)
10	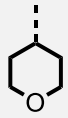	1
11		3
12		5
13	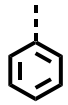	1
14		3
15		5

Figure 2.3 Structure of the two sections of our library with alternate exit vectors towards the E3 ligase binder. The pyrimidine linker library should bind kinases that have a similar solvent exposed channel to MPS1 whilst the pyridine linked library may bind alternate kinases.

	1	***9***	***11***	***15***
Molecular weight/gmol^{-1}	689.72	759.81	750.85	770.88
tPSA	189.46	198.69	192.7	183.47
cLogD	3.6	4.1	2.6	5.1
HBD/HBA	3/14	3/15	3/15	3/14

*Table 2.1 Predicted properties of 4 reprasentitive library compounds to be screened in proteomics (**1**, **9**, **11**, and **15**), cLogD calculated in MOKA. Values highlight the favourable physicochemical space the library of degraders occupy, being similar in cLogD and HBD count to small molecule drugs.*

As the warhead scaffold is low molecular weight, has favourable physicochemical properties (Table 2.1), and has the potential to bind outside

the kinome therefore, it is important to explore multiple exit vectors that may be solvent exposed in other target classes (Figure 2.3). An alternate linkage library was also synthesised to expand the number of bound proteins potentially targeted by the scaffold and maximise hits in the screen. This involved changing the linker vector from the hinge binding position to the pyridine position (Figure 2.3). The change allowed us to explore SAR around the hinge binder, altering both saturation and polarity of the R group.

Of the common sets of E3 ligase ligands, a CRBN binder was selected due to their favourable physicochemical properties, often higher promiscuity,[1,70] and chemical amenability (Figure 2.3). Utilisation of the $CUL4^{CRBN}$ E3 ligase has been hypothesised to be more promiscuous due to the increased flexibility of the CUL4 scaffolding unit, leading to a more accommodating ternary complex with a larger range of conformations that can be adopted over other E3 ligases.[2] As we wanted to maximise the number of hit proteins, we chose to use a CRBN binder.

Linker length and composition plays an important role in PROTAC design and is likely to have a large effect on the degradation profile of the array of degraders. We believe the use of 3 linker lengths differing by two CH_2 units will maximise the number of hits through differential linker preferences of ternary complexes (Figure 2.3). A triazole moiety will aid in the synthesis of these large molecules through the use of highly robust Click chemistry, while not increasing the number of hydrogen bond donors in the final PROTAC molecules.

If hit targets are identified using this library, each area of the PROTAC could be optimised for increased potency, selectivity and improved physicochemical properties. Due to the near-fragment sized warhead, potency could be gained through increased binding affinity to the degraded target. Achieving this with the pyridopyrimidine scaffold may be possible through exploration of substituents in the synthetically tractable positions used for linker attachment. The linker unit is often explored for optimisation and could be both rigidified and made basic to improve both conformational rigidity and solubility. Finally, alternate positions of attachment to the CRBN binder are available, in addition to using other more potent binders could afford improved degradation.

2.2 Proteomics Screening

To uncover the degradation profile of the library of compounds, we opted for a global proteomics platform. Although pull down methods exist to increase the number of kinases observed,[2,102] we chose to run global proteomics in order to observe any degradation of other families of proteins, including IMiD-based off targets as degradation of neo-substrates can be maintained after PROTAC conversion.[2] The use of Tandem Mass Tag (TMT) labels (Figure 2.4) in our analysis allows for the multiplexing of samples, lowers the cost of machine running, and facilitates direct quantitative comparison of compounds. The TMT label contains 3 distinct parts, an amine reactive group, balance, and reporter. Both the reporter and balance are differentially isotopically labelled in order to identify samples in the mass spectrum. As an isotopic label is added to the reporter region, an isotopic label is removed from the balance, overall affording two different compounds with the same total molecular weight. Current technology allows for 18 different labels. The TMT reagent can identify each individual treatment condition in the mixed sample through the unique isotope pattern of the reporter region.[94] The balance portion of the reagent can also be used as a validation tool in the mass spectrum analysis as this is also specifically isotopically labelled like the reporter ion.

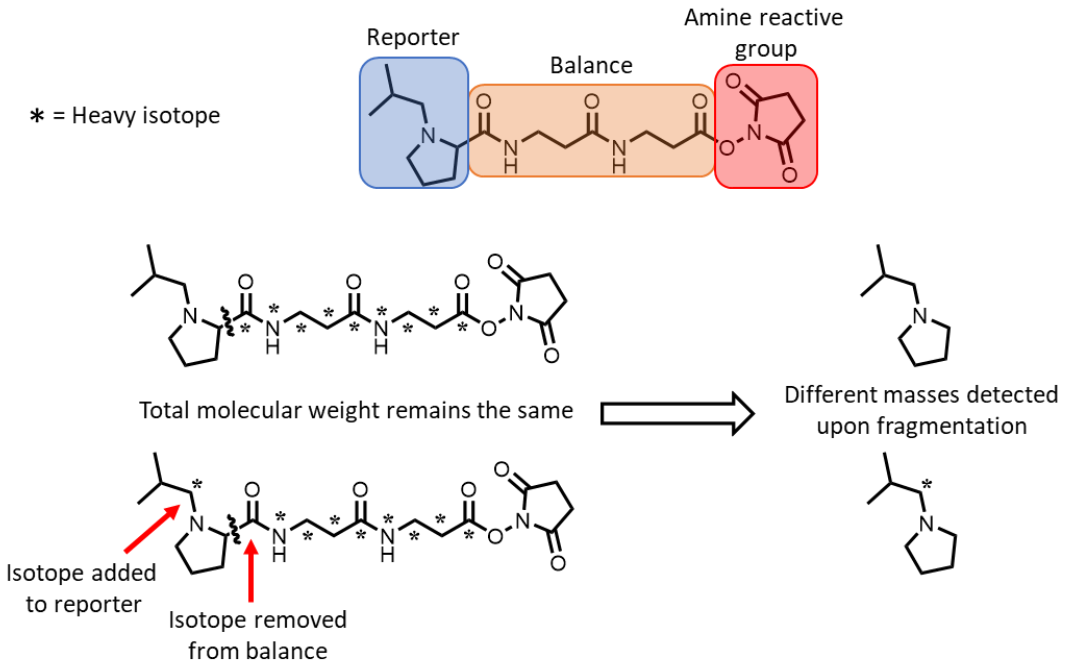

*Figure 2.4 Structure and example of how TMT labels work. TMT labels contain 3 distinct areas, the reporter, balance, and amine reactive group. The amine reactive group reactive group covalently attaches to peptides while both the balance and reporter regions are isotopically labelled (denoted by *). Overall, the mass of labelled peptides remains constant and upon fragmentation the different reporter isotopes are observed.*

Preparing the proteomics samples requires treatment of cells at a specific concentration and time point. For our analysis we chose HCT116 cells as it is well annotated in Professor Choudhary's in house proteomics team.[103] A concentration of 1 μM at a 6 h timepoint was selected to give the highest chance of discovering a degraded target with potentially poorly efficient PROTACs, whilst avoiding the risk of identifying downstream target perturbations. Treated cell pellets were digested and labelled with the 11 plex or 16 plex Tandem mass tag reagents then combined (Figure 2.5).

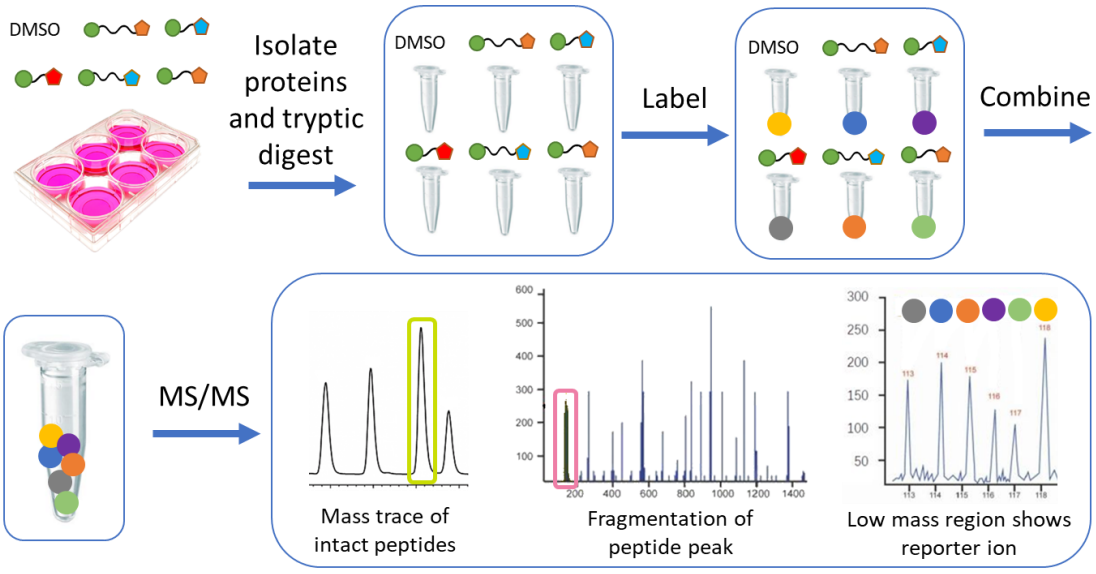

Figure 2.5 Workflow of the proteomics screen, utilising multiplexed TMT labelling. Cells are treated with degrader and cellular proteins are digested into peptides following TMT labelling. TMT labels are combined and fractionated before running through a mass spectrometer. Individually treated samples can be identified through the unique isotope from the TMT label.

Once the differentially labelled peptides are combined, these must go through a HPLC purification process separating labelled peptides based on lipophilicity. Multiple fractions containing a subset of the total peptides in the proteome are afforded from this purification. If the original sample was passed through the mass spectrometer only highly abundant proteins would be detected therefore, separation allows for more peptides to be discovered. This process is called fractionation and the more fractions that are taken the more of the proteome is observed, leading to a deeper proteomic analysis. We chose to do a shallower proteomic analysis due to the lowered machine time and cost, achieved through combination of HPLC fractions.

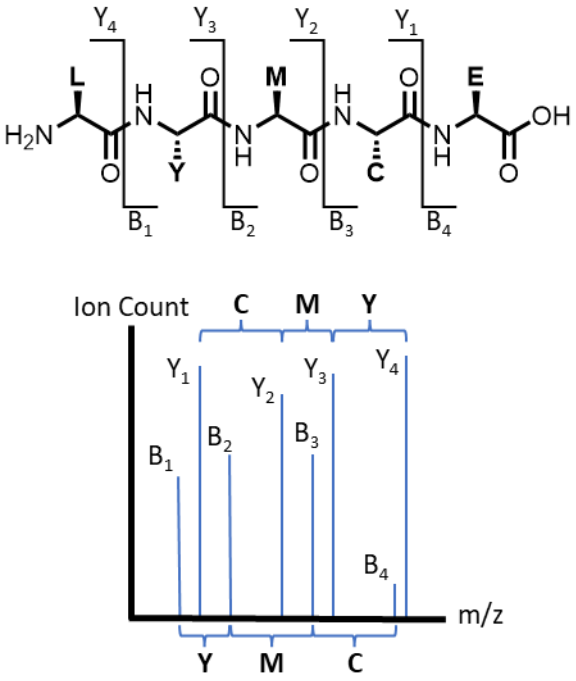

*Figure 2.6 Example peptide and how the MS2 fragmentation pattern can identify the sequence. Example peptide (containing amino acids **LYMCE**) will be fragmented at amide bonds and all potential mass ions of the fragmented peptide will be seen. Through identification of B and Y ions and the difference between subsequent B and Y ions, the peptide sequence can be identified.*

Once intact peptide masses have been identified, further fragmentation occurs breaking apart individual amide bonds allowing for the sequencing of each amino acid through evaluation of the differences in ion peaks (Figure 2.6). Conventionally, ions containing the N terminus are labelled as B ions and containing the C terminus are Y ions.

We used both 11plex and 16 plex TMT labelling systems to screen the array of degraders relative to a DMSO control. We also used dBET1 as a positive control and observed the expected degradation of BRD2 and BRD4.[92] Often proteomics screening samples are run in triplicate, however, we believed we could do duplicate experiments as the compounds are matched pairs and we didn't expect significant amounts of variation in degradation profiles. Duplicates have also been shown to be satisfactory in prior proteomic screens.[96] We intended to validate any non-IMiD related hit proteins in an orthogonal assay so deemed it acceptable to run the proteomics in duplicate only. Volcano plots shown are from the combined results of both the 11plex and 16plex runs.

Two significant kinase hits were identified (-log10(p-value) >2, log2FC <-0.35) from the proteomics screening of all 14 compounds, Aurora kinase A (AURKA) and NEK9. Independent SAR emerged for each kinase based on linker length

requirements and were only degraded by the phenyl-linked library (**1**-**9**). NEK9 was only degraded by the n=3 linkers (**2**, **5**, **8**) with flat SAR observed between amine substituents (Table 2.2). AURKA was degraded by two of the three longer linker lengths (n=5) containing morpholine and dimethylamine substituents (**3**, **9**, Table 2.2). The azetidine substituted compound, **6**, showed no degradation of AURKA. However, as the result was found to be non-significant, the possibility that **6** does degrade Aurora A cannot be excluded, but would require further validation. Unfortunately, the piperazine linked library (**11**-**15**) only revealed 2 significant targets, both being zinc finger containing proteins ZBTB21 and ZFP91 (Figure 2.7). As ZFP91 depletion is commonly seen in degrader and IMiD treatments, we decided to focus our later validation efforts on AURKA and NEK9.[70] The SAR of ZFP91 degradation of all library compounds was difficult to interpret from the proteomics, as in each case the degradation was close to the cut off used (<-0.35) and would require validation using western blotting. ZBTB21 is a Zinc finger and BTB containing protein and was degraded using only **12**.

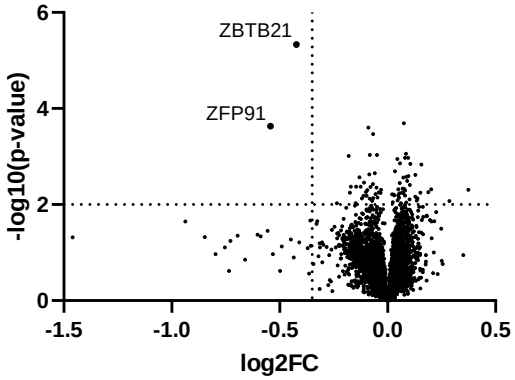

*Figure 2.7 Volcano plot of **12** after a 6 h treatment at 1 μM in HCT116 cells, highlighting the degradation of only ZFP91 and ZBTB21, likely IMiD off-targets.*

Despite the use of a heavily truncated warhead, surprisingly selective degradation was observed with only loss of one protein seen for most PROTACs. With such a small warhead we believed more proteins could have been degraded, but these results demonstrate how these may be excellent starting points for medicinal chemistry optimisation.

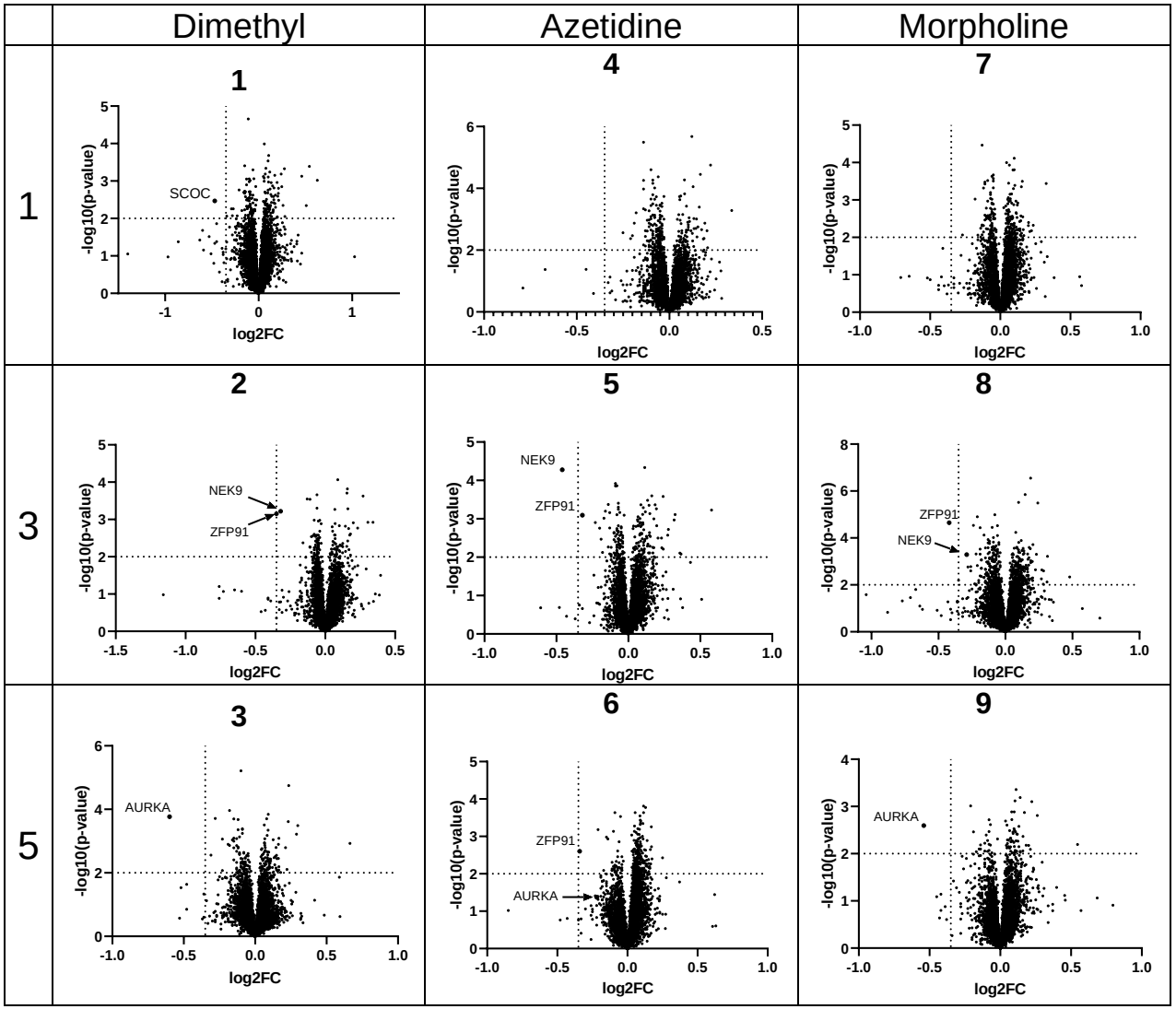

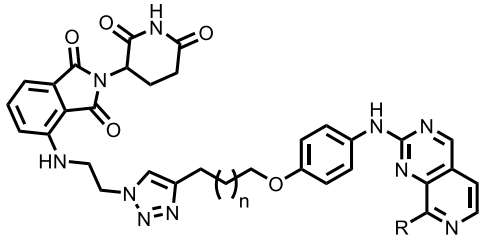

	R group	*Linker length (n)*
1		1
2		3
3		5
4	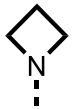	1
5		3
6		5
7	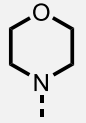	1
8		3
9		5

*Table 2.2 Volcano plots of **1**-**9** after a 6 h treatment at 1 μM in HCT116 cells, highlighting degradation of AURKA, NEK9, ZFP91 and SCOC with differential linker selectivity.*

2.3 Library Synthesis

The route to make the pyridopyrimidine kinase ligand is well established in our group and is amenable to modification on two areas of the ring (Scheme 2.1).[104] The commercially available bromo-pyrimidine (**16**) is reacted with a vinyl boronic ester under Suzuki conditions, forming the alkene **17**. Amide formation with ammonia followed by a cyclisation with catalytic acid gave rise to the pyridone **18**. Chlorination with phosphorus oxychloride yielded the key intermediate **19**, which can react with various amines affording **20**-**22**. To give the handle for linker functionalisation, oxidation of the sulfides **20**-**22** was carried out using OXONE, yielding the sulfones **23**-**25**.

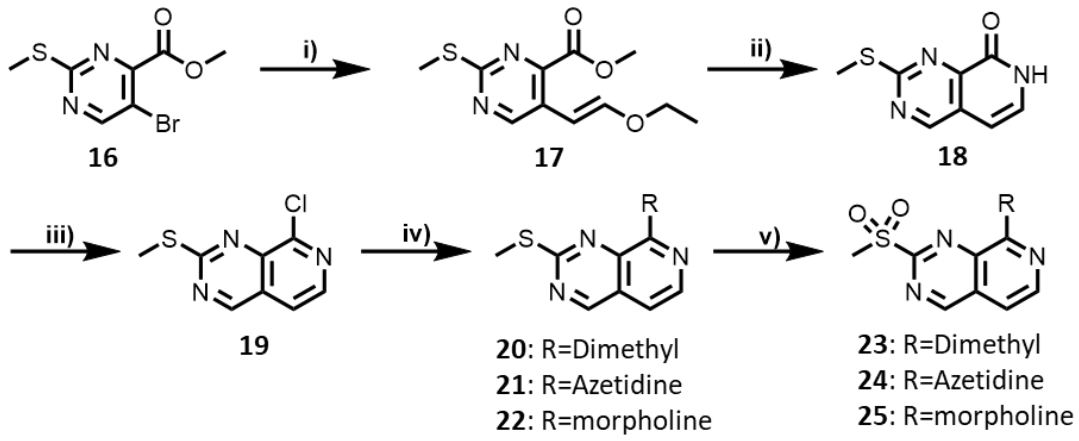

Scheme 2.1 Route to make key warhead intermediates. Reagents and conditions: i) $Pd(dppf)Cl_2$, (E)-2-(2-ethoxyvinyl)-4,4,5,5-tetramethyl-1,3,2-dioxaborolane, THF, aq 2 M $NaHCO_3$, 80 ˚C, 38%. ii) 7 M Ammonia in methanol, 60 ˚C, then p-TsOH, toluene, 80 ˚C, 59%. iii) $POCl_3$, 80 ˚C, 40%. iv) amine, DIPEA, NMP, 120 ˚C, 80-92%. v) OXONE, water, methanol, rt, 24-63%.

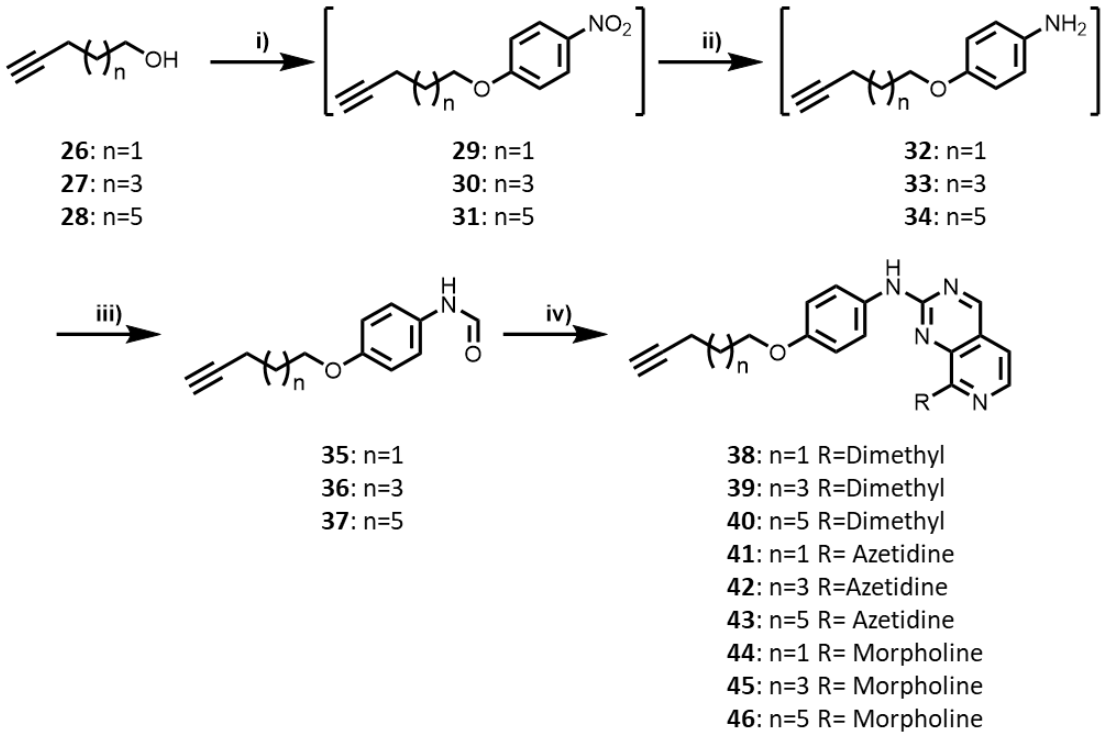

*Scheme 2.2 Phenyl linked linker synthesis and attachment to the warhead. Reagents and conditions: i) DIAD, PPh_3, p-nitrophenol, THF, rt. ii) Iron, NH_4Cl, water, methanol, 80 ˚C. iii) formic acid, 80 ˚C 12-49%. iv) NaH, THF, **23-25**, 0 ˚C, 35-61%*

To synthesise the library a Click chemistry platform was utilised, requiring a CRBN ligand functionalised with an azide and an alkyne handle on the warhead. Different lengths of alkyne linkers were successfully synthesised with the correct functionality to undergo the Click reaction (Scheme 2.2). To achieve this, the alcohol starting materials **26**-**28** were treated with *p*-nitrophenol in a Mitsunobu reaction to give the nitro compounds **29**-**31**. Iron-based reduction of the nitro groups in **29**-**31** resulted in the anilines **32**-**34**, which were subsequently formylated to yield **35**-**37**. The penultimate step in the synthesis of the degraders requires deprotonation of the formamide with sodium hydride in order to react with the sulfones **23**-**25**. This route gave all 9 alkynes (**38**-**46**) ready for a Click reaction with an azide.

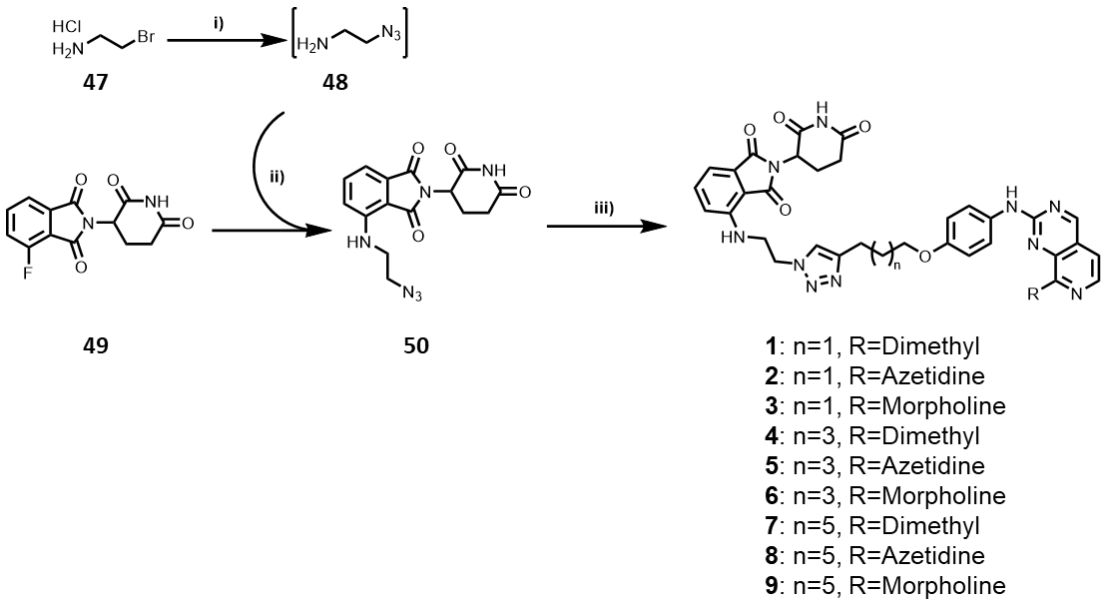

Scheme 2.3 Azide functionalised CRBN ligand synthesis and Click reaction. Reagents and conditions: i) NaN_3, DMSO, 80 ˚C ii) 14, DIPEA, 80 ˚C, 34%. iii) ***38-46****, sodium ascorbate, $CuSO_4$, THF, water, rt, 21-44%*

To synthesise the CRBN binder **50**, sodium azide was reacted with the bromo-amine **47** affording the azide **48** *in situ*. **48** was immediately reacted with the fluoro compound **49** to afford the desired azide **50**, ready to Click onto the alkyne functionalised warheads (**38**-**46**) (Scheme 2.3). The Click reaction of the 9 alkynes (**38**-**46**) with **50** in the presence of sodium ascorbate and copper sulfate, was successful and produced the first small library of 9 compounds **1**-**9**.

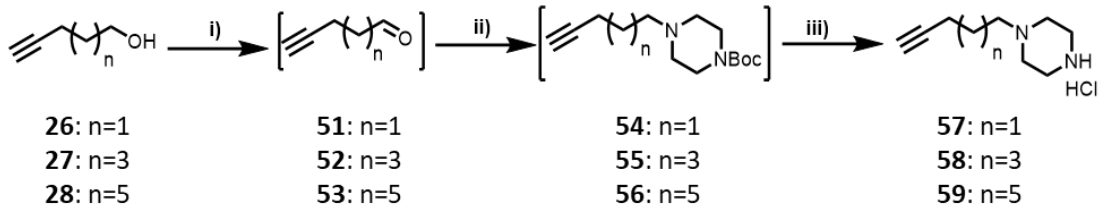

Scheme 2.4 Synthesis of piperazine-based linkers. Reagents and conditions: i) $(COCl)_2$, DMSO, NEt_3, DCM, -78 ˚C. ii) tert-butyl piperazine-1-carboxylate, $NaB(OAc)_3H$, DCM, rt. iii) 4 M HCl in dioxane, DCM, rt, 37-72%,

To synthesise the alternate piperazine linked library, we set out to make the piperazine-alkyne linkers required to utilise the validated click chemistry route shown previously (Scheme 2.3). The first step of the synthesis is a Swern oxidation on the same three alkyne starting materials previously used (**26**-**28**), giving the required aldehyde functionality for a reductive amination with mono-Boc protected piperazine (Scheme 2.4). Boc deprotection of **54**-**56** yields the linkers (**57**-**59**) ready to be reacted with **19**.

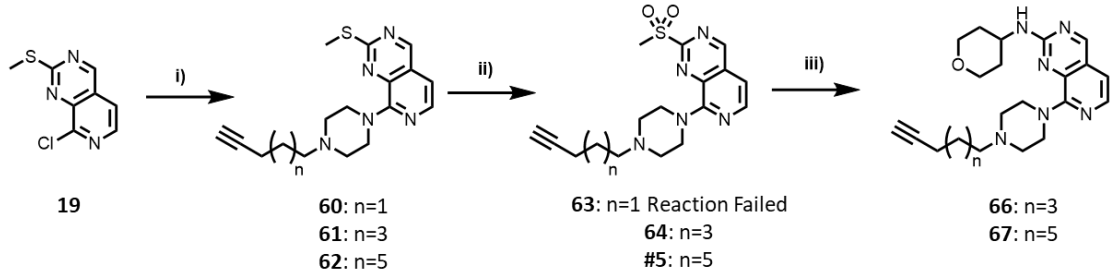

*Scheme 2.5 Synthesis of alkynes **66**-**67**. Reagents and conditions: i) **57-59**, DIPEA, NMP, 120 ˚C, quantitative. ii) OXONE™, methanol, water. iii) 4-aminotetrahydropyran, DIPEA, NMP, 102 ˚C, 34-97%.*

Despite previous success reacting with the chloride **19** to append R groups and oxidising the sulfide, inconsistencies were observed involving dealkylation of the piperazine linkers (Figure 2.8). Initially we were successful in making three sulfides **60**-**62** requiring oxidation and subsequent S_NAr reaction (Scheme 2.5).

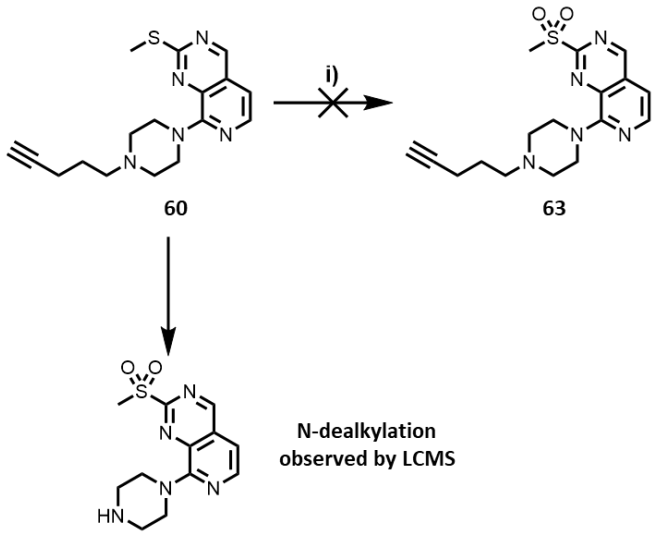

*Figure 2.8 Failed reaction of **60** where dealkylation of the piperazine was observed by LCMS. Reagents and conditions: i) OXONE™, methanol, water.*

Only two of the three THP containing alkynes (**63**-**65**) were synthesised due to dealkylation of the n=1 piperazine **63** during the subsequent oxidation. The two accessed alkynes were reacted under the same Click chemistry conditions as previously used (Scheme 2.3), affording two of the desired piperazine linker library (Scheme 2.7).

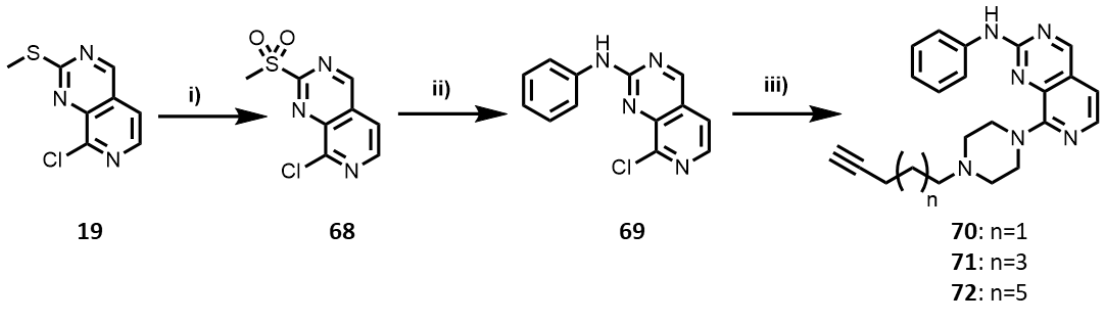

*Scheme 2.6 Synthesis of alkynes **70**-**72**. reagents and conditions: i) OXONE™, methanol, water, 57% ii) N-phenylformamide, NaH, THF, 0 ˚C, quantitative. iii) DIPEA, NMP, 120 ˚C, 24-55%.*

Upon repeating the chloro S_NAr to access more starting material, dealkylation was observed with all linker lengths (**60**-**62**). A change in synthetic route was required in order to access more starting material and was achieved through swapping the order of reactions. The sulfone oxidation and substitution were performed prior to piperazine addition, affording a common intermediate to be appended to varying linker lengths (**69**). Upon reaction with the piperazine linker the alkynes (**70**-**72**) were subjected to Click conditions, affording the three desired PROTACs (**13**-**15**). Unfortunately, this route cannot be used to synthesise the remaining THP containing PROTAC **10** as amines reacts preferentially on the chloro position of **19**.

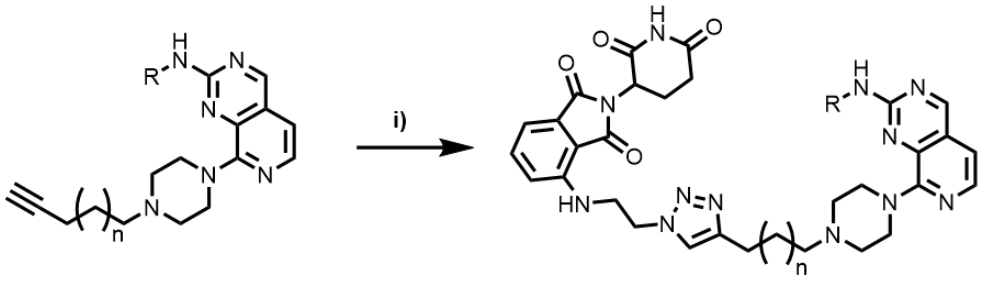

*Scheme 2.7 Click reaction to form the 5 piperazine-linked library compounds. Reagents and conditions: i) **50**, sodium ascorbate, $CuSO_4$, THF, water, rt, 13-61%.*

2.4 Conclusions and Future Work

To summarise, we truncated an existing kinase binding molecule to a core hinge binding unit and modified it from two exit vectors with a linker. We also modified the warhead with R groups to observe SAR based on scaffold changes. Overall, we maintained favourable physicochemical properties through having an overall

low molecular weight, in addition to a low hydrogen bond donor and acceptor count. The use of a truncated warhead will likely bind to multiple kinases, and through ternary complex constraints afford selective degraders. We chose to hijack the CRBN E3 ligase, mainly due to its increased promiscuity when compared with other E3 ligases. This would allow for a wider range of the bound targets to be degraded, increasing the hit rate of the PROTACs. We also explored multiple linker lengths to degrade a wider variety of targets while containing a triazole moiety for synthetic tractability.

The 14 PROTACs were triaged through a proteomics screen identifying two tractable kinase targets to validate in an orthogonal assay. The selectivity of the degraders was striking considering the likely promiscuity of the warheads used, and is likely a result of selective ternary complex formation. The piperazine linked library (**11**-**15**) only afforded two hits (ZFP91 and ZBTB21), neither of which will be followed up on as they are possibly IMiD off targets. Flat SAR was observed when altering the R group, however, only n=3 linkers (**2**, **5**, **8**) degraded NEK9 and two of the three n=5 linkers (**3**, **6**, **9**) degraded AURKA. The linker length is extremely important in forming productive ternary complexes and is likely why such steep SAR is observed.

In contrast to Donovan *et al* who screened more structurally elaborated promiscuous compounds, we have achieved selective degradation through the use of small warheads with the ability to start medicinal chemistry optimisation for improved potency.[76] The selectivity achieved is likely due to our compounds only having weak binding affinity to kinases and relying on productive ternary complexes in order to degrade targets, highlighting the need to explore multiple linker lengths.

The results highlight that near fragment sized warheads can confer observable degradation in a proteomics screen and paves the way for fulfilling the promise of targeting the undruggable proteome with PROTACs. The hit compounds now require validation, most common of methods being Western blotting. Although other methods can determine degradation quantitatively, Western blotting requires little optimisation. If confirmed, optimisation can be done on any part of the hit compounds due to their simplicity. The use of more elaborated warheads with increased binding affinity could increase binding potency and therefore

improve degradation. Similarly, as there are several known binders of CRBN with improved binding affinity, this could also be changed to improve the potency of degradation. Finally, as we are using simple alkyl linkers, this area could be rigidified and made basic, this may lock the PROTAC in its active conformation while improving solubility.

Chapter 3: Validation and Optimisation of NEK9 PROTACs

3.1 NEK9 Introduction

NEK9 is a member of the 'dark kinome', defined as the one-third of kinases that are understudied and for which no selective tool compounds exist.[105] Despite the lack of selective chemical probes for NEK9, biological tools have elucidated multiple disease-relevant roles that warrant further exploration. NEK9 is known to be involved in the separation of centrosomes during mitosis. Upon activation from both CDK1 and Plk1, NEK9 can phosphorylate NEK6/7. Eg5 is then phosphorylated on two sites by NEK6/7 and CDK1, allowing a pool of protein to accumulate around the centrosome, bind microtubules, and separate the centrosomes (Figure 3.1).[106] siRNA knockout studies also indicate NEK9 has a role in the proliferation of multiple p53 mutant cell lines however, selective chemical tools are not available to validate this.[107] Identification of a NEK9 degrader could validate these findings and indicate if NEK9 is a potential therapeutic target.

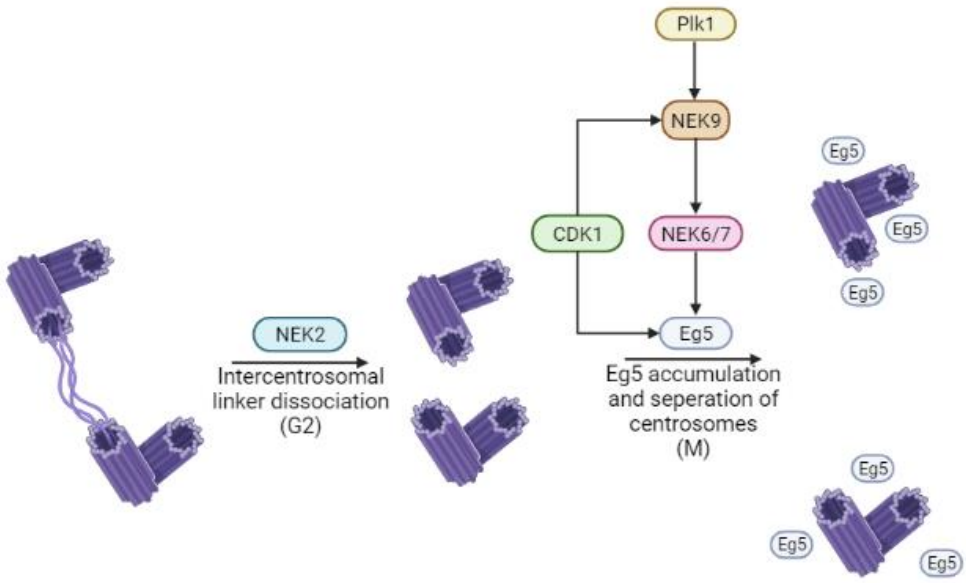

Figure 3.1 NEK9 involvement in centrosomal separation. NEK9 and PLK1 activate NEK6 and NEK7 allowing for phosphorylation of EG5. EG5 then localises around the centrosomes and can bind microtubules to separate them and allow mitosis to occur.

To date, the only known binders of NEK9 are compounds with off-target kinase activity, no selective inhibitors exist. Recently a promiscuous degrader screen

identified multiple non-selective degraders of NEK9 through the use of promiscuous kinase inhibitor warheads, one of which was **DB-0614** (Table 3.1).[76] Upon further interrogation of **DB-0614**, including linker and E3 ligase ligand changes, no improvement in the selectivity of degradation against the initial 9 off target kinases was seen.[91] Selectivity optimisation may be a challenge with PROTACs as many factors can affect if a protein will get degraded. The use of a warhead with reduced binding affinity to kinases may infer more selective degraders due to the increased importance of an efficient and productive ternary complex as opposed to warhead affinity. **DB-0614** has excellent physicochemical properties considering its molecular weight and indeed would be an excellent NEK9 degrader starting point for optimisation if not for the poor selectivity (Table 3.1). Utilisation of a smaller sized warhead, as in this report, could allow for optimisation of the warhead, an area often excluded due to the use of larger, potent, and more selective inhibitors, introducing another area to introduce selectivity of the PROTAC.

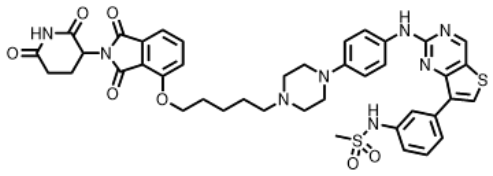

DB-0614

Molecular weight/gmol^{-1}	822.96
tPSA	183.24 Å^2
cLogD	3.6
HBD/HBA	3/13

*Table 3.1 Structure and calculated properties for **DB-0614**. tPSA, and cLogD were calculated using MOKA, showing the favourable chemical space this PROTAC occupies, likely due to the pKa of the sulfonamide and piperazine.*[108]

3.2 NEK9 Hit Validation

To uncover any SAR in our library and validate the accuracy of the proteomics Western blotting was used to determine NEK9 protein levels upon compound treatment. The library compounds (**1**-**9**) were treated under identical conditions as the proteomics (HCT116 cells, 6 h, 1 μM). Degradation of NEK9 was observed for PROTACs containing the n=3 linker length (**2**, **5**, **8**, Figure 3.2 A) confirming the screening result. Figure 3.2 A showed linker lengths of n=1 (**1**, **4**, **7**) and 5 (**3**, **6, 9**) do not degrade NEK9, as expected, validating the initial SAR

from proteomics. Despite the differently sized R groups used, it had no impact on degradation selectivity, suggesting there may be room to optimise the warhead from this synthetically amenable position. Moving forward, the morpholine n=3 compound (**8**) was selected for further studies as we had the largest amount of this compound.

Maximal PROTAC mediated degradation (D_{max}) is time dependant and it is therefore important to test degraders at multiple time points. Our results show improved degradation upon longer treatments, with recovery of degradation after 72 h (Figure 3.2 B). In order to validate the mechanism of action of the PROTACs, a methylated control (**73**) was synthesised in order to abrogate the key glutarimide N-H interaction with CRBN.[10] As expected, the methylated negative control compound showed no degradation of NEK9 (Figure 3.2 C) leading us to believe the mechanism is CRBN mediated. Methylation of the IMiD has the potential to change the physicochemical properties of the molecules due to the loss in a hydrogen bond donor. A HPLC solubility assay was completed (performed by Jack O'Hanlon), showing poor solubility for the degrader **8** (1.8 μM) with no solubility being observed for the methylated control **73**, potentially explaining why no degradation was seen with **73**.

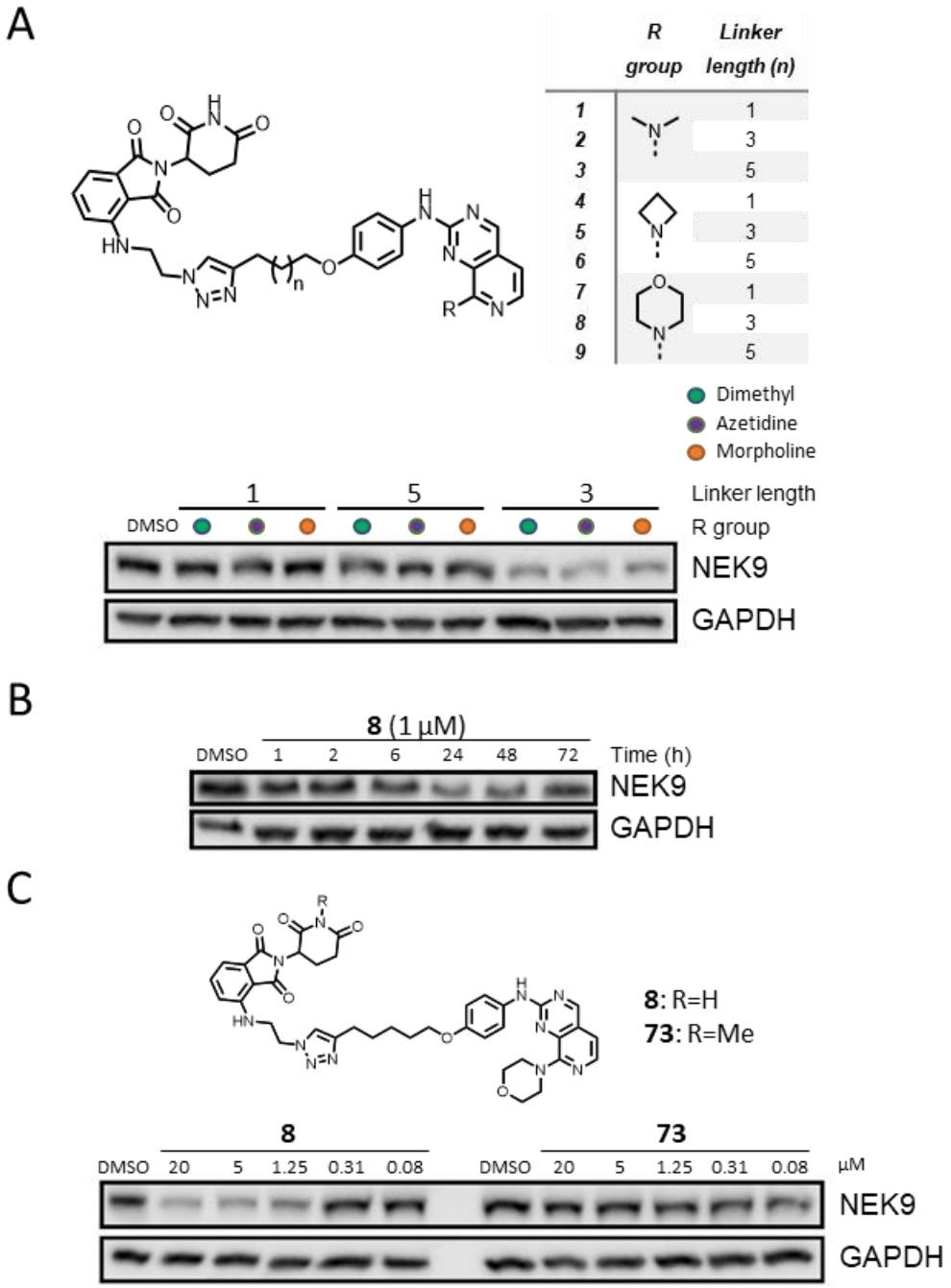

*Figure 3.2 A) Structure of screened compounds (**1**-**9**) and the selectivity of NEK9 degradation after a 6 h treatment in HCT116 cells.at 1 µM. Selectivity was consistent with proteomics and NEK9 was only degraded with the n=3 compounds. B) Time course experiment with 1 uM of **8** in HCT116 cells. Time dependance was observed with an improved D_{max} at longer time points. C) Dose response of **8** and negative CRBN binding control **73** after a 6 h treatment in HCT116 cells. Degradation seems to be in the low µM range and dependant on binding to CRBN.*

To further probe the mechanism of action of these degraders we preincubated cells before treatment with inhibitors of the proteasome (**MG132**, **bortezomib**), NEDD8 activating enzyme (**MLN4924**), the E1 inhibitor **MLN7243**, and the respective warheads of both ends of the PROTAC (**pomalidomide** and a reported NEK9 binder **CYC-116**), all of which should rescue degradation of a

PROTAC mediated process (Figure 3.3 A). Interestingly, the neddylation inhibitor **MLN4924** and pomalidomide did not rescue degradation (Figure 3.3 B). Neddylation is a process which activates cullin-based E3 ligases of which CRBN is a member,[109] indicating a lack of CRBN dependence. This is a direct contradiction to the loss of degradation seen with **73** (Figure 3.2 D) and requires further interrogation to determine the degradation mechanism. The lack of rescue with pomalidomide is also peculiar, given the degradation can be rescued with **73**.

8 is therefore a validated degrader of NEK9 however, the mechanism of degradation is not through the canonical PROTAC mediated process. As the process is still proteasomal, ubiquitination is likely to be occurring and therefore requires further interrogation to determine how this is possible. Further to this, identification of SAR of the mechanism could give insight into the mode of action of the degraders and improve degradation of an underexplored kinase.

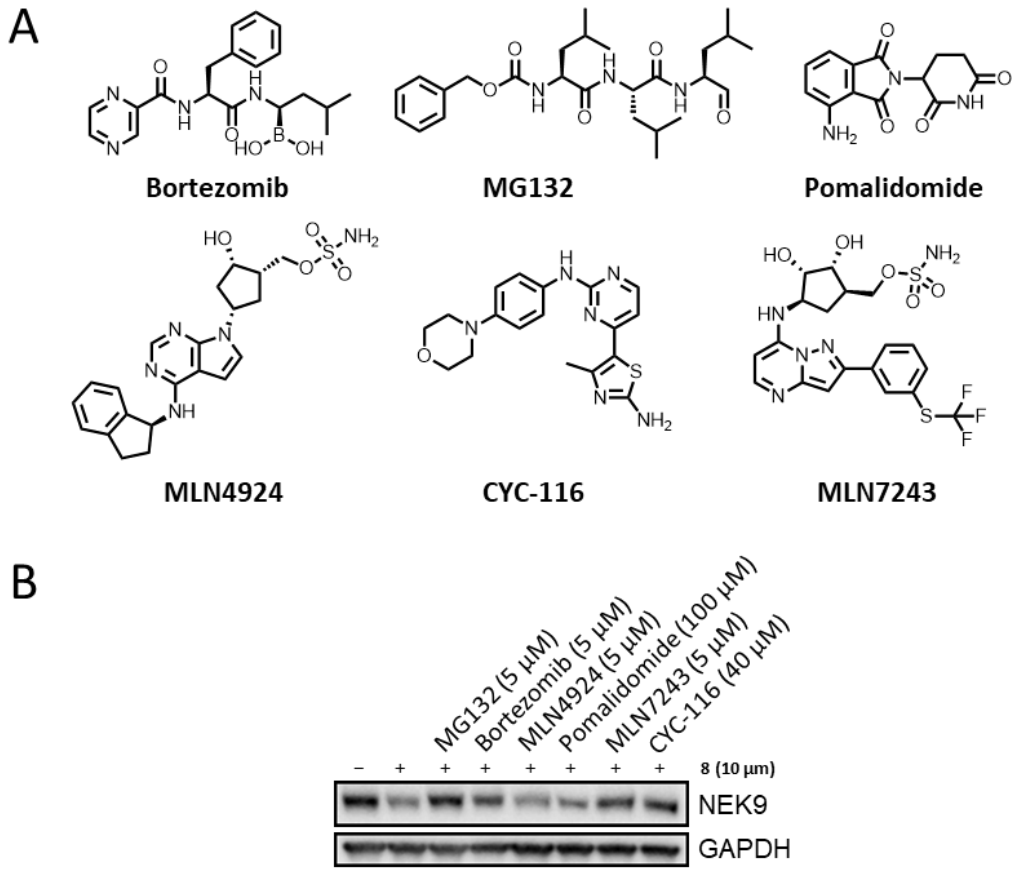

Figure 3.3 A) Structure of compounds used to out compete degradation of NEK9. ***Bortezomib*** *and* ***MG132*** *are proteasome inhibitors,* ***pomalidomide*** *binds to CRBN,* ***MLN4924*** *inhibits neddylation,* ***CYC-116*** *inhibits NEK9 (unselectively) and* ***MLN7243*** *inhibits E1 ubiquitin transfer. B) NEK9 degradation rescue experiment with 10 μM of* ***8*** *after a 6 h treatment in HCT116 cells. Rescue was seen with both proteasome inhibitors, E1 inhibition and NEK9 inhibition. No rescue was seen with neddylation inhibition and CRBN inhibition.*

3.3 NEK9 SAR Exploration

3.3.1 Linker Modifications

Initial PROTAC linker design commonly relies on a trial and error approach, whereby a variety of flexible linker lengths are synthesised and tested without structural information as guidance.[110] Our proteomics screening approach aims to yield degraders with an appropriate linker length for specific ternary complexes, thereby bypassing the trial and error stage of degrader development, allowing for immediate optimisation of linker composition for the hit protein. Linker length initially plays a key role in the development of degraders due to its impact on ternary complex formation, selectivity, and degradation potency and, when optimised, can actually form interactions within the ternary complex pocket.[58,111] A loss in degrader potency could result from linker lengths too long, causing steric clashes within the ternary complex, or too

short, where both binding sites of the ternary complex cannot be engaged simultaneously (Figure 3.4). Additionally, the linker must tolerate the productive conformation of degradation, potentially requiring longer linker lengths than expected (Figure 3.4).[112] Linker length preference is dependent on each member of the ternary complex, therefore, a direct swap of the recruited E3 ligase for a particular target would require further linker optimisation.

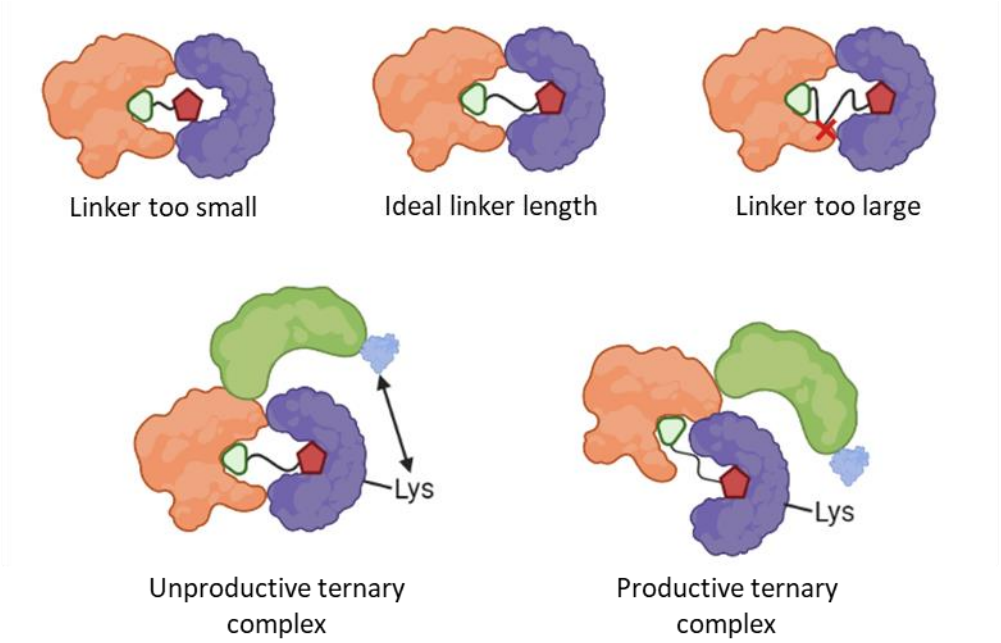

Figure 3.4 Representation of linker length effects on ternary complex formation. Linkers are required to be long enough to engage both targets whilst being short enough to not disrupt ternary complex formation. Longer linker lengths may be required to facilitate the productive ternary complex formation.

Before probing the lack of neddylation dependence further, we intended to see if the linker length was ideal for NEK9 degradation. In order to have a larger variety of linker lengths tested in proteomics, we did not initially test the intermediate linker lengths n=2 and 4. The corresponding morpholine analogues were synthesised in the same manner as the screened library (**1-9**) and tested in Western blotting (**74**, **75**). A preference for **8** was seen containing the originally tested n=3 linker length from the proteomics screen (Figure 3.5). The n=2 linker length (**74**) showed slight degradation however, no loss in NEK9 levels was seen with treatment of the n=4 linker length (**75**). The steep linker length SAR observed highlights the advantage of a proteomics screening approach as little to no trial and error is now required for ideal linker length determination.

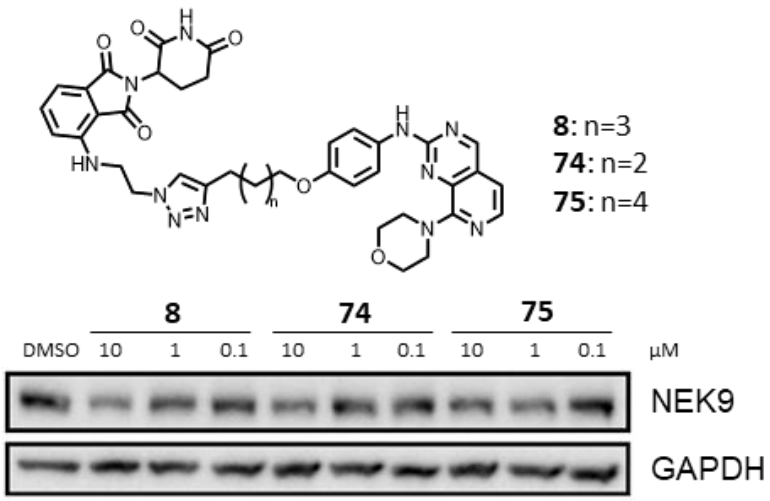

*Figure 3.5 Dose response of n=2, 3, and 4 linker lengths after a 6 h treatment in HCT116 cells. the screening hit **8** degrades NEK9 with an improved D_{max} relative to the n=2 and 4 linker lengths.*

Adding rigid groups in the linker region of a PROTAC can have a large impact on potency and physicochemical properties, through both the addition of basic centres,[113] and reduction in conformational flexibility, potentially fixing the PROTAC in an active conformation.[114] The linkers in the screened library contain a rigid triazole moiety, however, we do not know if the current position along the alkyl chain is ideal for degradation potency. To determine if other triazole positions are tolerated, or provide improved degradation, we synthesised derivatives with the same total linker length whilst moving the triazole down the alkyl chain (**76-78**, Figure 3.6). A preference for the original linker composition (**8**) was seen with no degradation for any of the synthesised analogues. The drop off in potency may be explained through a preference of conformational restriction on the linker close to the IMiD region of the degrader, or a lost hydrogen bond within the ternary complex pocket when moving the triazole.

Despite multiple linker changes, **8** remained the compound with the best, although modest, degradation. Little linker change toleration was seen, and only the n=2 linker length (**74**) showed some degradation. This is unusual as PROTACs tend to have a larger tolerance for linker changes. The linker of **8** will be maintained through further SAR exploration to identify what structural changes to the warhead can be tolerated.

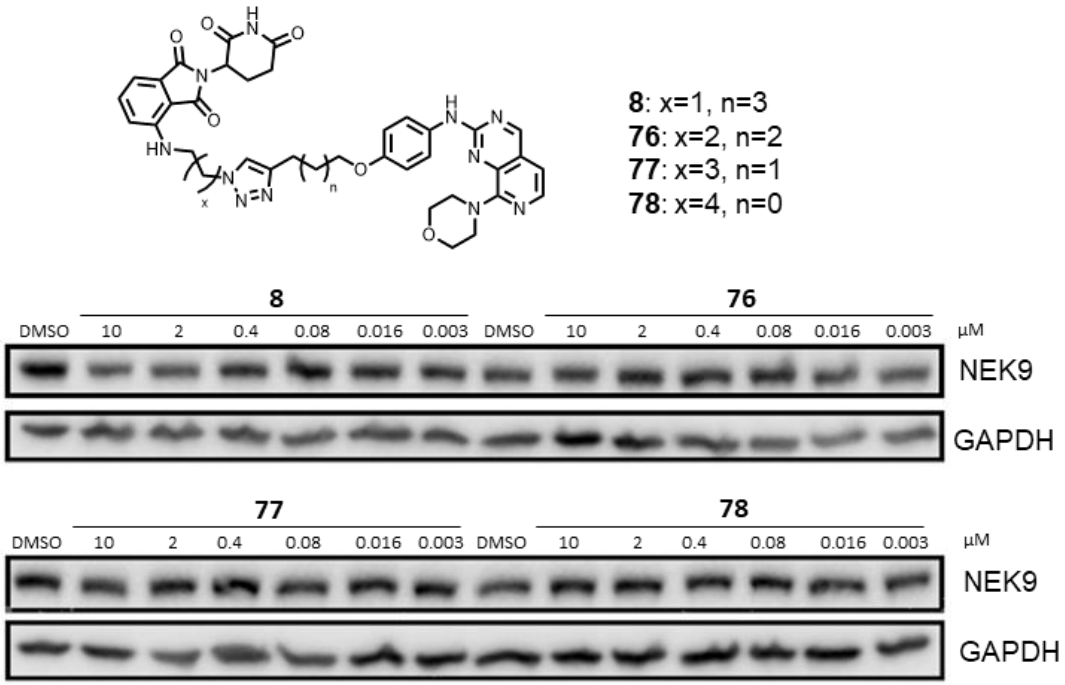

*Figure 3.6 Dose response of **8, 76**-**78**, moving the triazole along the alkyl linker after a 6 h treatment in HCT116 cells. No degradation was observed with and of the triazole position movements suggesting its importance in the degradation of NEK9.*

3.3.2 Warhead Modifications

Warhead optimisation is often underexplored, with no published examples exploring SAR, likely a result of the highly optimised inhibitors utilised. It has been reported that weakly potent E3 ligase and target protein binders can still confer potent levels of degradation, as highly efficient and stable ternary complex can still be formed.[65,70]

A screen of PROTACs with multiple linker lengths is likely to afford the near-ideal linker lengths for particular targets, leaving other areas of the PROTAC to be optimised. As the small molecular weight warhead is likely to be only modestly potent towards the target, this could be readily optimised to improve degrader potency. In the first instance the warhead could be switched for a more potent binder, assuming the binding mode and linker exit vector remain constant.

The published NEK9 degrader **DB-0614** is a potent NEK9 PROTAC therefore, we sought to determine if the mechanism of action was also seemingly independent of neddylation. **DB-0614** was synthesised and NEK9 degradation was determined. In contrast to the hit degrader **8**, **DB-0614** showed the expected dependencies of a PROTAC as rescue experiments showed a

dependence on the proteasome, neddylation and CRBN binding (Figure 3.7). In contrast to the hit degrader **8**, **DB-0614** showed the expected dependencies of a PROTAC. To further explore this, we aimed to determine if a specific component of the hit PROTAC **8** was causing the modified mechanism of degradation.

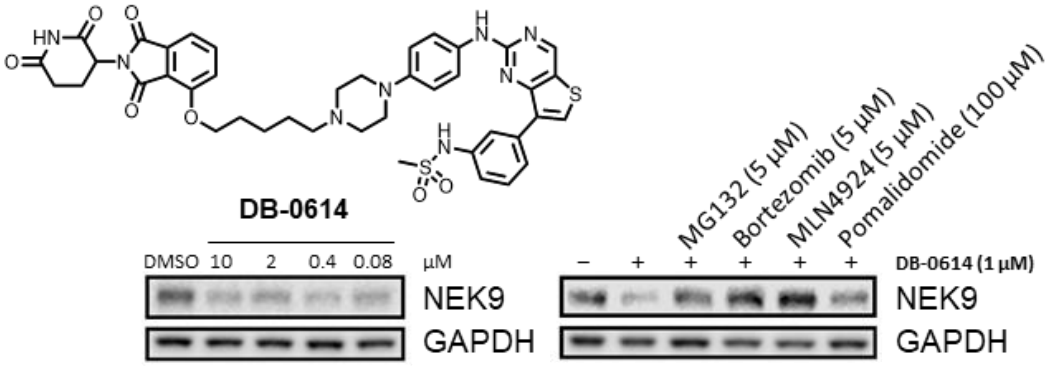

*Figure 3.7 Dose response and rescue experiment with **DB-0614** after a 6 h treatment in HCT116 cells. **DB-0614** showed high levels of degradation but not full loss in NEK9 levels. Degradation was dependant on the proteasome, neddylation, E1 inhibition and CRBN binding.*

Swapping the warheads of **DB-0614** and **8** may elucidate if the linker or warhead segment of the degrader is responsible for the altered mechanism (compounds **79** and **80**). We believed this would be possible due to the warheads containing a similar amino pyrimidine hinge binding moiety, what we expected would lead to a similar exit vector for the linker. The expected degradation of **8** and **DB-0614** was observed however, only degradation using the warhead of **DB-0614** and linker of **8** (**80**) was seen (Figure 3.8 A). The degradation of **80** utilising the **DB-0614** NEK9 binder was slightly improved compared to the screened compound (**8**) at 1 µM. The mechanism of action of **80** was determined through a rescue experiment (Figure 3.8B), indicating the lack in neddylation dependence is driven by the presence of the linker-CRBN binder combination found in **8** and **80**. The lack of degradation seen for **79** may be due to the warhead being too weakly potent to cause degradation utilising the linker-CRBN binder combination of **DB-0614**. The binding affinity of the parent warhead of **DB-0614** was found to be 150 nM using the DiscoverX KINOMEscan™ technology, this is significantly more potent than the hit degrader **8** (7.9 µM) and may have resulted in the increased potency. The KINOMEscan™ assay is based on the use of beads with an immobilised kinase ligand which is outcompeted by a test compound. The DNA-tagged kinase that is outcompeted

off the bead by the test compound then undergoes qPCR to determine amount of kinase displaced. With the slightly improved degradation seen with **80** we wanted to determine if this could be optimised through the use of other binders of NEK9, and if the neddylation independent mechanism of degradation was maintained through the use of other warheads.

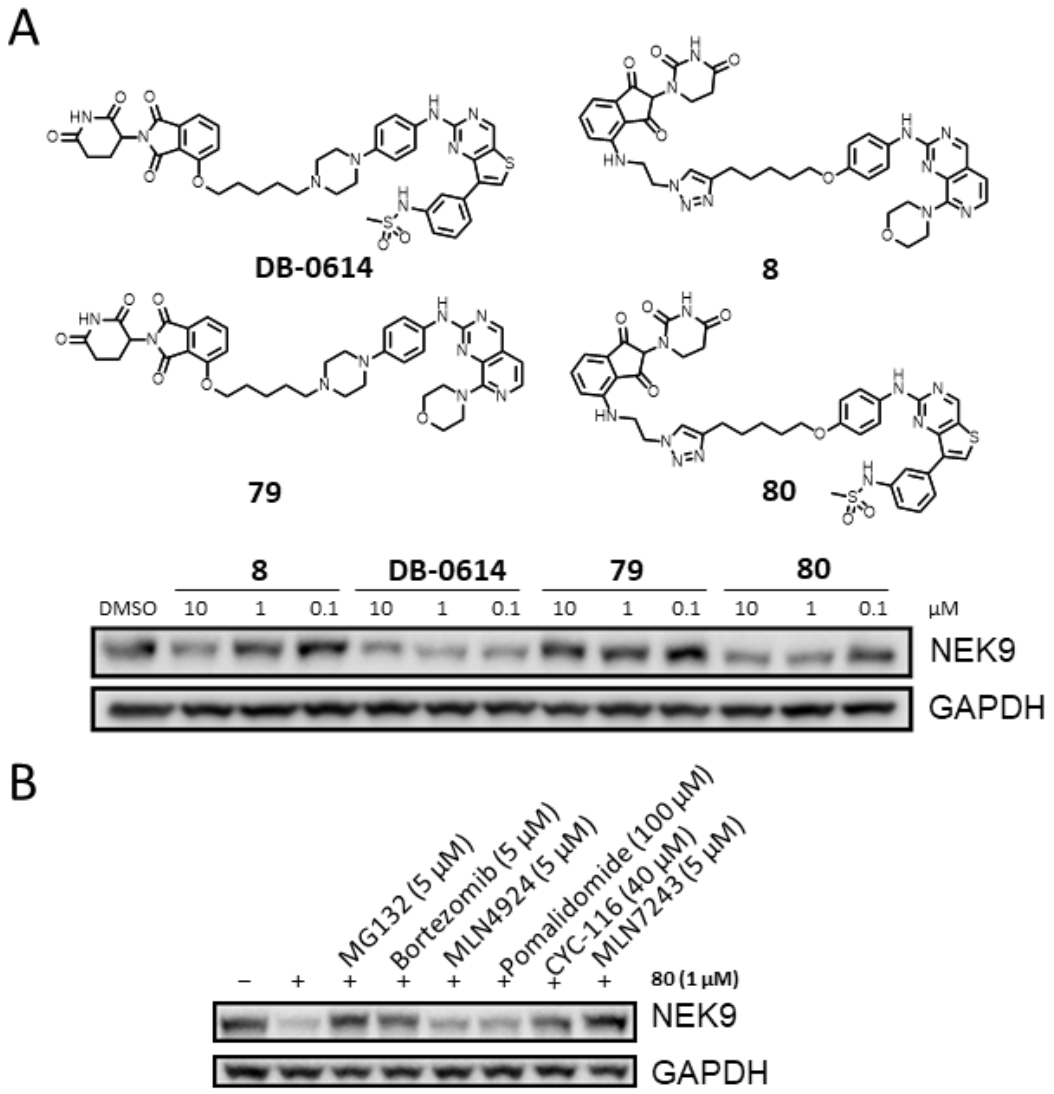

*Figure 3.8 A) Structure of PROTACs **DB-0614**, **8**, **79** and **80**, PROTACs **79** and **80** are hybrids of **DB-0614** and **8**. Compounds are being used to identify which section of the degrader is causing the alternate degradation mechanism of NEK9. Dose response of each compound was performed at a 6 h time point in HCT116 cells. Degradation of **80** highlights the linker and E3 ligase binder causing the change in mechanism of degradation. B) NEK9 degradation rescue experiment with 1 μM of **80** after a 6 h treatment in HCT116 cells. Western blot is consistent with the altered degradation pathway seen with compound **8**.*

We explored binders of NEK9 using the ChEMBL database and identified ligands with potent off target affinity against NEK9 (Figure 3.9 A).[115] Two candidates were selected with similar amino-pyrimidine kinase binding scaffolds as we hypothesised that this moiety would bind in a similar position to the

original warhead, providing the same exit vector to a linker (Figure 3.9 A). A known kinase binding scaffold, able to pull-down NEK9 in a kinobead platform, was also selected to be attached to the linker-E3 ligase ligand combination of **8** (**82**). The synthesis of the compounds **81-83** utilised Click chemistry as previously described for the original library **1-9** (Chapter 2.3). Of the appended kinase ligands, **83** showed improved degradation compared with **8**, with almost complete removal of NEK9 after 6 h (Figure 3.9 B). Unexpectedly, **81** and **82** showed no degradation after 6 h, even though the warhead of **81** has been previously shown to potently bind to NEK9, and both can bind to CRBN (1.57 μM and 3.55 μM for **81** and **82** respectively).[115]

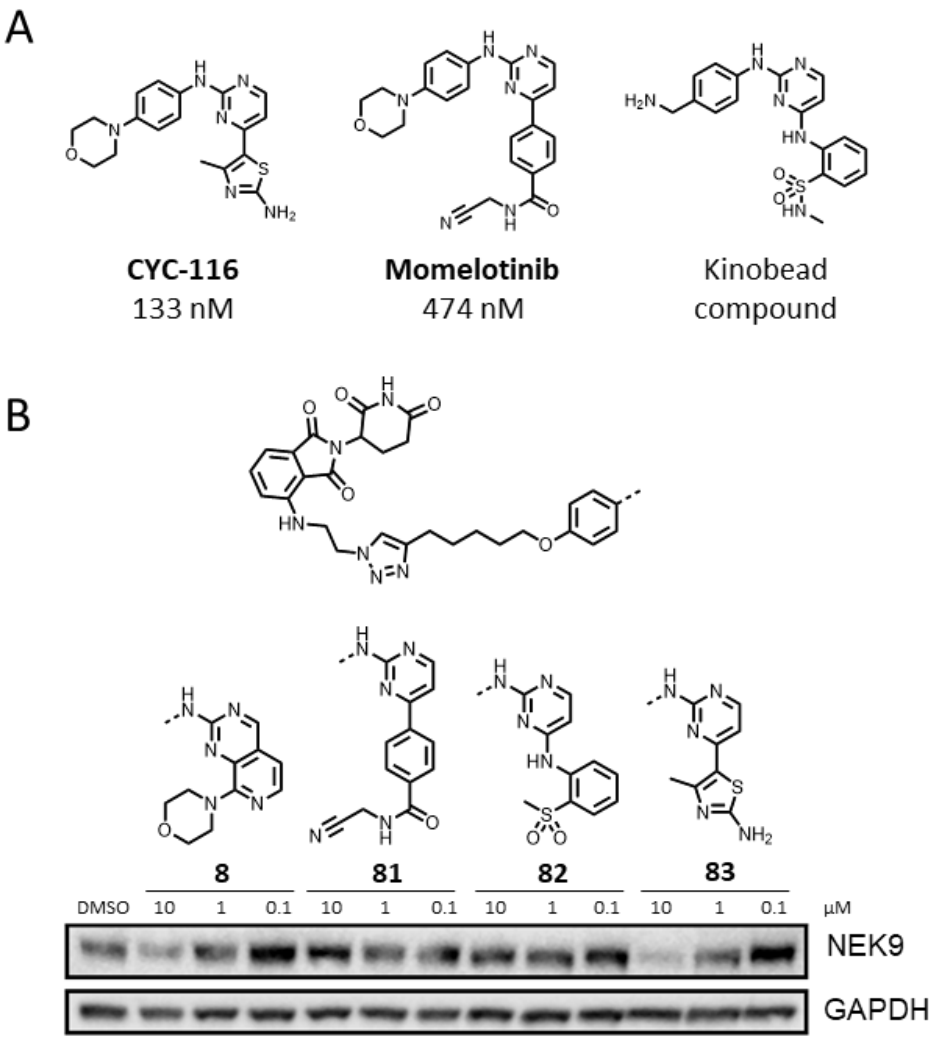

*Figure 3.9 A) Structure of 3 NEK9 binders used as a warhead replacement, **CYC-116** and **momelotinib** have potencies published from a kinobead screen.[115] Warheads used to identify if other binders of NEK9 could show the similar degradation pathway as **8** and **80**, being independent of neddylation. B) Warhead replacement dose response Western blot where HCT116 cells were treated with compound for 6 h. showing near full degradation of NEK9 with **83** at potencies consistent with **8** and **80**.*

83 also showed fast onset of degradation at 2 h with a 1 μM treatment (Figure 3.10). Testing of this compound in the DiscoverX KINOMEscan™ assay showed a K_D of 1.1 μM, ~7 fold more potent than the hit degrader **8** however, significantly lower than what was previously reported.[115] The disparity in binding affinities may be due to inaccuracies in the previously published result, as only a 3-point dose response was completed, or a result of the significantly different assay conditions. The triazole containing degrader **83** was ideal to further probe the mechanism of NEK9 degradation due to its near complete removal of NEK9. Significantly improved degradation potencies were not observed upon changing to more potent warheads, suggesting that other areas of these PROTACs should be optimised.

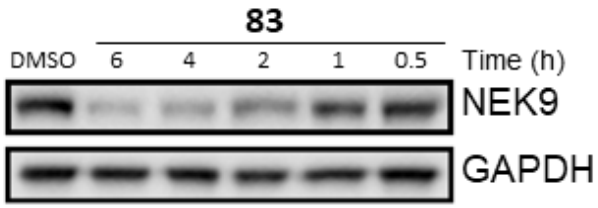

*Figure 3.10 Time course experiment with 1 uM of **83** in HCT116 cells. Blot highlights a faster degradation (2 h) with **83** than was seen with compound **8** (24 h).*

Methylation of **83** also showed rescue of degradation, similar to **73**, again suggesting a CRBN dependent mechanism (Figure 3.11 A). The solubility of **83** and **84** was 1.5 μM and 1 μM respectively, therefore is not expected to have a significant impact on the degradation. The same dependencies were showed by **8** were observed in the rescue experiments with **83** (Figure 3.11 B) suggesting the degradation goes through the same non-neddylation dependant mechanism, contrary to the methylation result. To interrogate the seemingly non-CRBN dependence of degradation further, $CRBN^{-/-}$ HEK293T cells (developed and validated by Habib Bouguenina) were treated with the NEK9 degrader **83** and MLN4924 (Figure 3.11 C). Strikingly, degradation of NEK9 was observed in both the wild type and CRBN knockout cell lines. The results suggest CRBN is not required for the degradation of NEK9. Whether CRBN contributes to the overall degradation of NEK9 and only in the presence of neddylation inhibition or CRBN knockout a forced change in the degradation mechanism occurs is unclear and would require further investigation. The expected CRBN dependence of the published degrader **DB-0614** was also confirmed in the CRBN knockout cell line, highlighting the non-canonical

degradation of **8** mediated NEK9 degradation is not a common feature with NEK9 degradation (Figure 3.11 D).

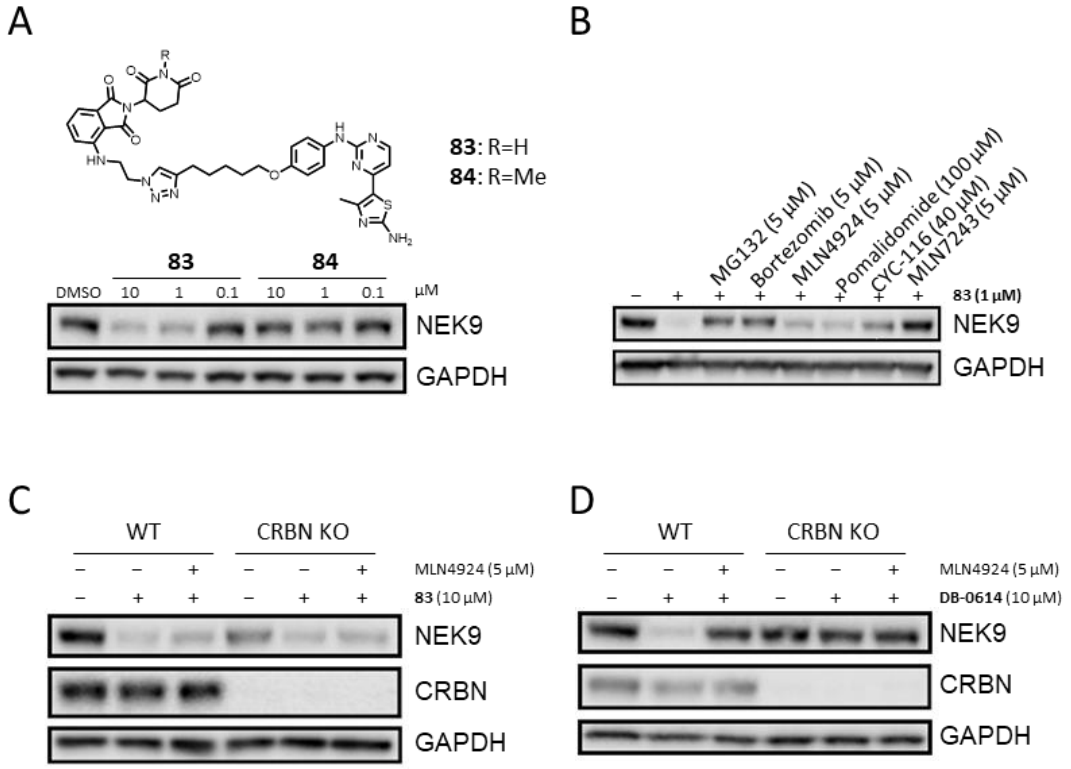

*Figure 3.11 A) Dose response of **83** and its methylated analogue **84** that should not bind CRBN and therefore degrade NEK9, treated for 6 h in HCT116 cells. No degradation was seen with **83**, contradicting the lack of dependence on neddylation and CRBN. B) Rescue experiment treated for 6 h in HCT116 cells. Highlighting a similar profile to **8** and **80** with no dependence on neddylation or CRBN binding. C) Rescue experiment of **83** treated in wild-type and knockout HEK293T cells. Degradation was seen in CRBN knockout cells which should not happen with CRBN recruiting degraders. D) Rescue experiment of **DB-0614** treated in wild-type and knockout HEK293T cells. Highlighting that the degradation mechanism is different between **83** and **DB-0614** as **DB-0614** degrades in a CRBN dependant manner.*

Concerned the loss in NEK9 could be the result of a change in mRNA levels, a TaqMan assay was performed. The TaqMan assay utilises a fluorescent probe that selectively binds to a single stranded DNA of interest. The probe's fluorescence is normally quenched when bound to its complementary DNA strand, however, when PCR is performed Taq polymerase (due to its 5' exonuclease activity) destroys the DNA linkage of the Taq probe. The fluorophore is therefore free from the quenching moiety and can emit a signal (Figure 3.12 A). The resulting NEK9 mRNA levels were unaffected by compound treatment (Figure 3.12 B). As the results show no change in NEK9 mRNA levels, it suggests depletion is a protein level event however, this does not rule out downstream protein effects causing NEK9 degradation.

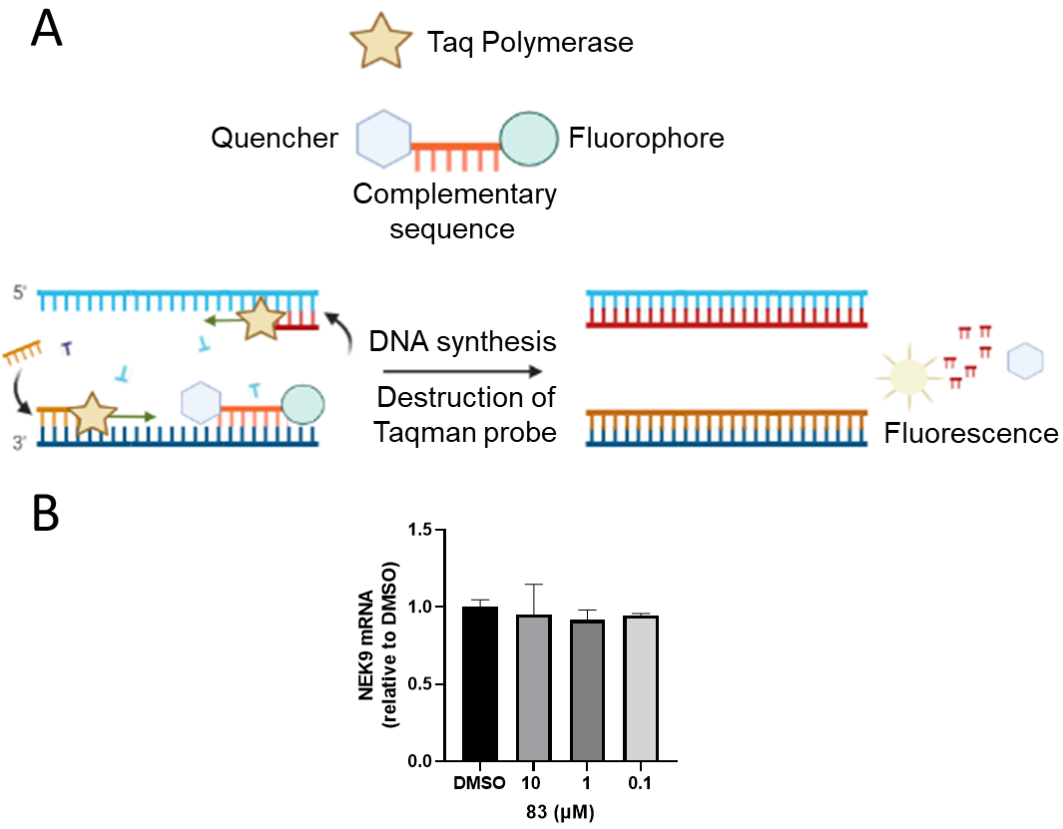

*Figure 3.12 A) Representation of how a TaqMan assay works and the structure of a TaqMan probe. As DNA synthesis occurs of the target gene the Taqman probe is destroyed, allowing the fluorophore to emit a signal. B) TaqMan assay result showing NEK9 mRNA levels after treatment with **83** in HCT116 cells for 6 h. No effects on mRNA levels were seen highlighting the degradation of NEK9 with **83** is not influencing DNA expression.*

Thus far we have confirmed degradation goes through a proteasome dependant but neddylation independent mechanism whilst leaving NEK9 mRNA levels unaffected. As degradation goes *via* the proteasome, it is likely ubiquitin is still conjugated to NEK9 therefore, a ubiquitin pull-down experiment was performed to confirm this. NEK9-Ub was observed in both the compound treatment (**83**) and in the compound cotreatment with bortezomib, indicating compound treatment induces ubiquitination of NEK9 (Figure 3.13). The fact NEK9-Ub was not observed in the proteasome inhibitor sample suggests NEK9 is not naturally turned over *via* the proteasome during the timeframe of the experiment. E1 inhibition supresses NEK9 ubiquitination, as to be expected when inhibiting the first stage of the ubiquitin activation process. As NEK9-Ub is observed, it suggests a direct ubiquitination event on NEK9 whereby the ubiquitin must be conjugated through an E3 ligase and subsequently degraded *via* the proteasome.

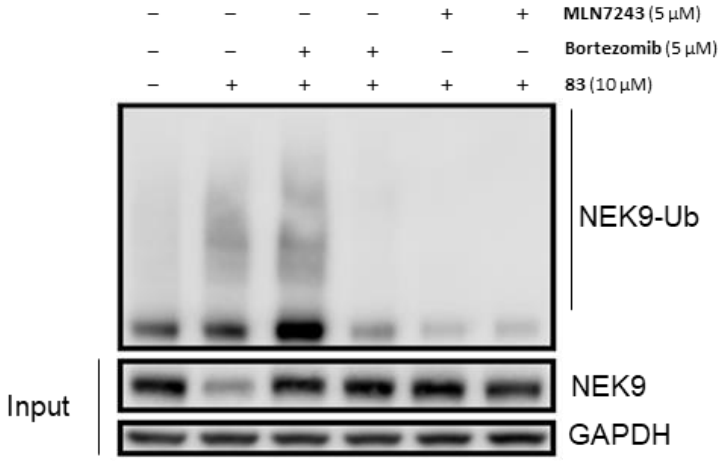

*Figure 3.13 Ubiquitin pull-down experiment using **83** in HCT116 cells after a 6 h treatment. Ubiquitinated NEK9 is seen in both degrader treatment, and with a proteasome inhibitor co-treatment. This shows that NEK9 is indeed being ubiquitinated, induced by treatment with **83**. As expected no ubiquitination was seen with E1 inhibitor present.*

3.4 NEK9 Degrader Synthesis

3.4.1 IMiD Methylated Control Compounds

The methylated control compounds (**73** and **84**) were synthesised following Scheme 3.1 and Scheme 3.2. S_NAr Reaction of **85** afforded azide **86** which allows for Click chemistry (analogous to Chapter 2.3) to be performed with the corresponding alkynes**.** The click reaction finally afforded both negative control compounds **73** and **84**.

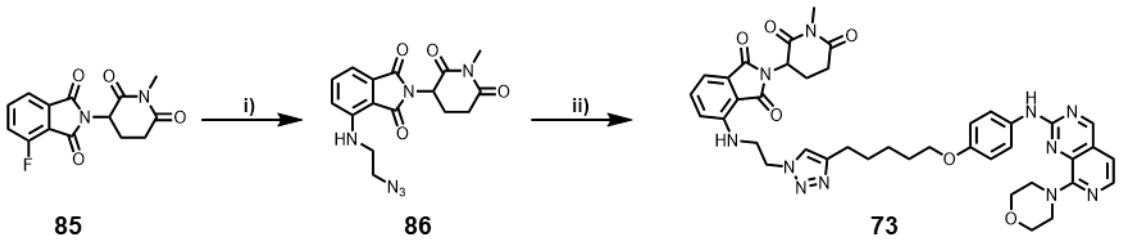

*Scheme 3.1 Synthesis of **73**, a methylated control compound, having reduced CRBN binding. Reagents and Conditions: i) NaN_3, 2-Bromoethylamine hydrobromide, DMSO, 75 ˚C then **85**, DIPEA, 75 ˚C, 11%. ii) **86**, $CuSO_4$, Sodium ascorbate, THF, water, rt, overnight, 39%.*

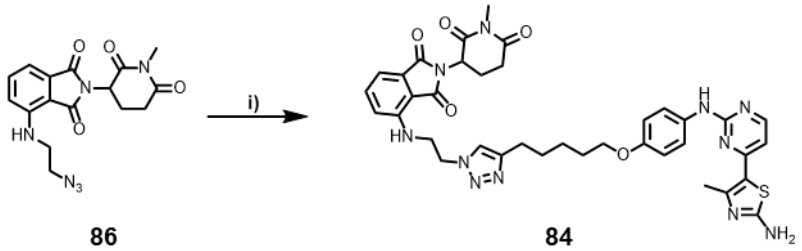

*Scheme 3.2 Synthesis of **84**, a methylated control compound, having reduced CRBN binding. Reagents and Conditions: i) **86**, $CuSO_4$, Sodium ascorbate, THF, water, rt, overnight, 10%.*

3.4.2 Modified Linker Synthesis

The n=2 and 4 linker length PROTACs (**74** and **75**) were synthesised through the same route as the screened library compounds (Chapter 2.3). Although different alkyne alcohol starting materials were used, the same purification issues with triphenylphosphine oxide were encountered during the Mitsunobu reaction and had to be carried forward crude.

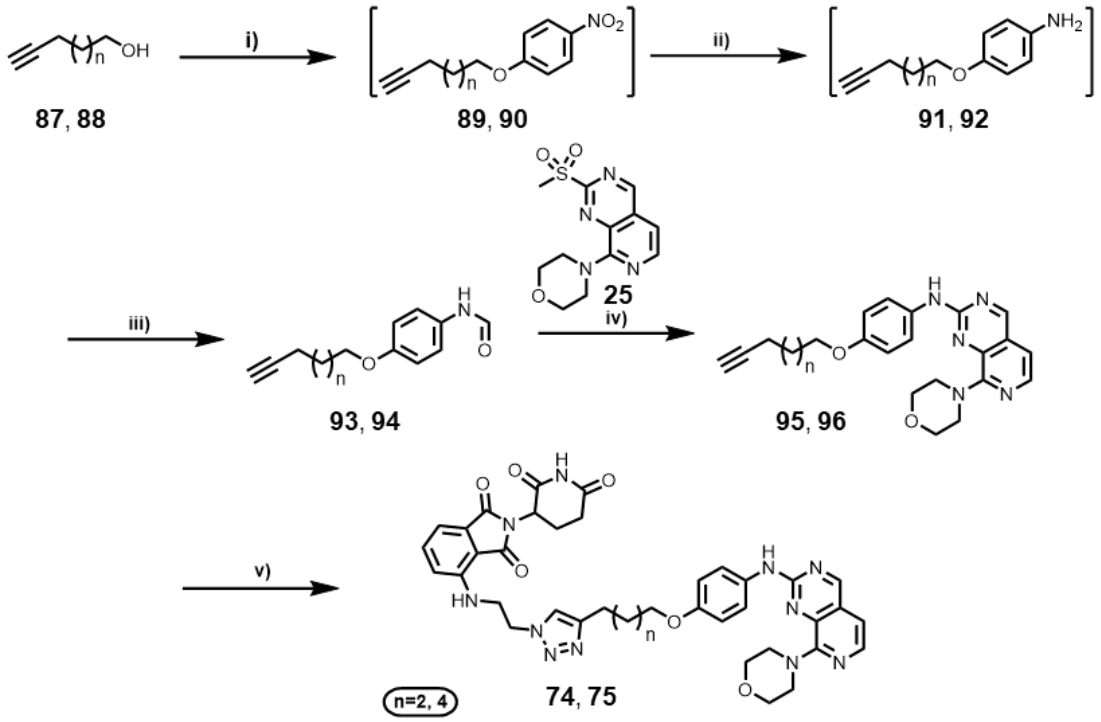

*Scheme 3.3 Synthesis of **74** and **75**, PROTACs with linker lengths not tested using proteomics. Reagents and Conditions: i) PPh_3, p-nitrophenol, DIAD, THF 2 h. ii) Iron, NH_4Cl, ethanol, water, 80˚C, 3 h. iii) Formic acid, 80 ˚C, 18 h n=2 29% n=4 52%. iv) NaH, THF, 0˚C, overnight. v) **50**, $CuSO_4$, Sodium ascorbate, THF, water, rt, overnight, n=2 17%, n=4 26%.*

The compounds with differing triazole positions to **8** (**76**-**78)** were synthesised following a similar process as in Chapter 2.3, however, two azides required an alternate synthetic route (Scheme 3.4, Scheme 3.6). Bromo-amines with longer alkyl chain length were not commercially available, therefore, an alternate strategy was utilised involving the use of an azide-transfer reagent (**110**).[116] The use of **110** was published recently and employed on IMiD derivatives, however the overall yields for this route were significantly lower than the previous azide synthesis strategy (Chapter 2.3). For the synthesis of **78**, the corresponding alkyne **104** needed to be synthesised (analogously to Chapter 2.3). Initially the fluoro-IMiD **49** is reacted under S_NAr conditions to afford the Boc-protected amines **105** and **106** that are subsequently deprotected and reacted with **110**,

affording the azides **111**, and **112**. The click reactions with **44** and **104** afforded the corresponding degraders with varied triazole positions (**74** and **75**).

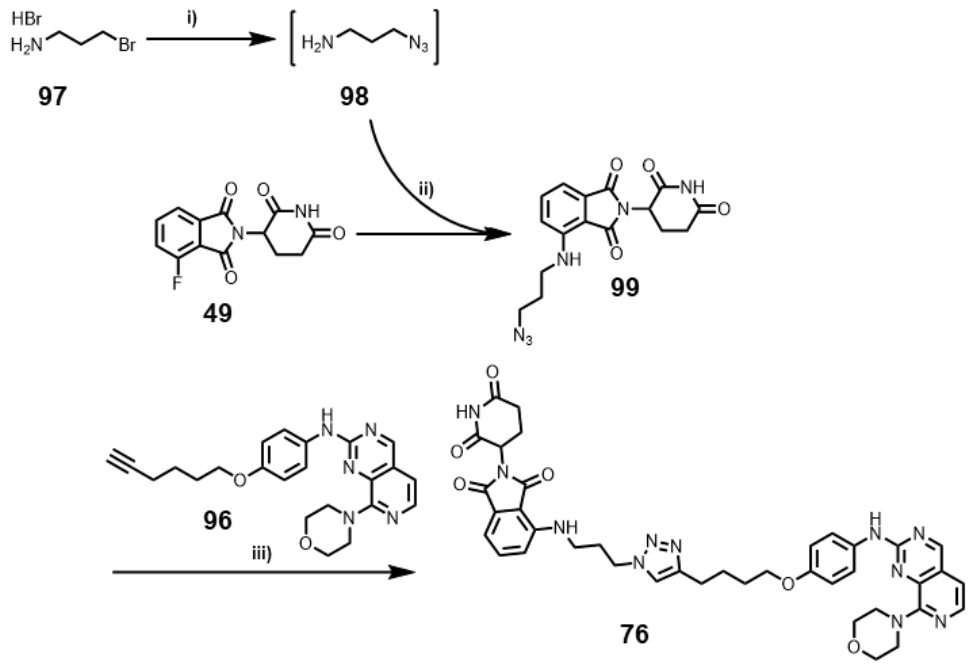

*Scheme 3.4 Synthesis of **76**, altering the position of the triazole. Reagents and Conditions: i) NaN_3, DMSO, 75 ˚C. ii) DIPEA, 75 ˚C, 44%. iii) $CuSO_4$, Sodium ascorbate, THF, water, rt, overnight, 42%.*

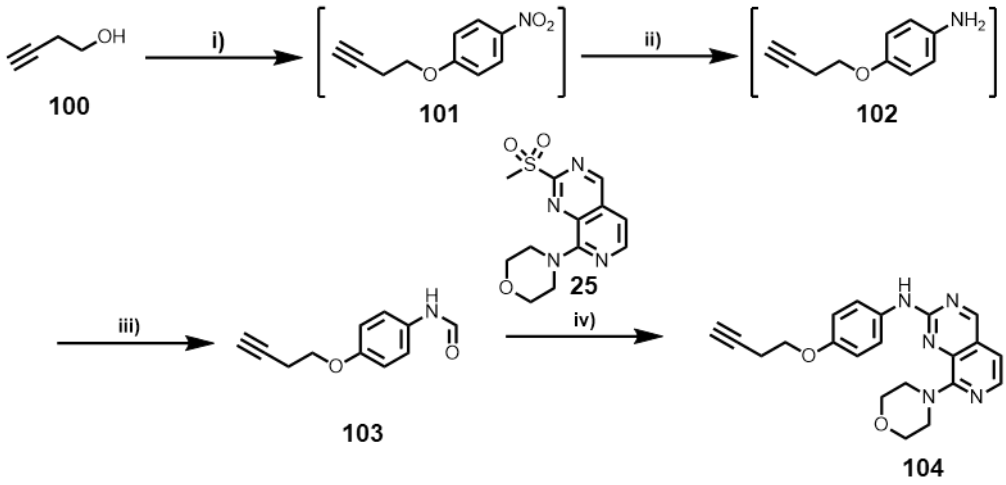

*Scheme 3.5 Synthesis of **104** required for synthesis of **77.** Reagents and conditions: i) PPh_3, p-nitrophenol, DIAD, THF 2 h. ii) Iron, NH_4Cl, ethanol, water, 80˚C, 3 h. iii) Formic acid, 80 ˚C, 18 h n=2 29% n=4 83%. iv) NaH, THF, 0˚C, overnight, 32%.*

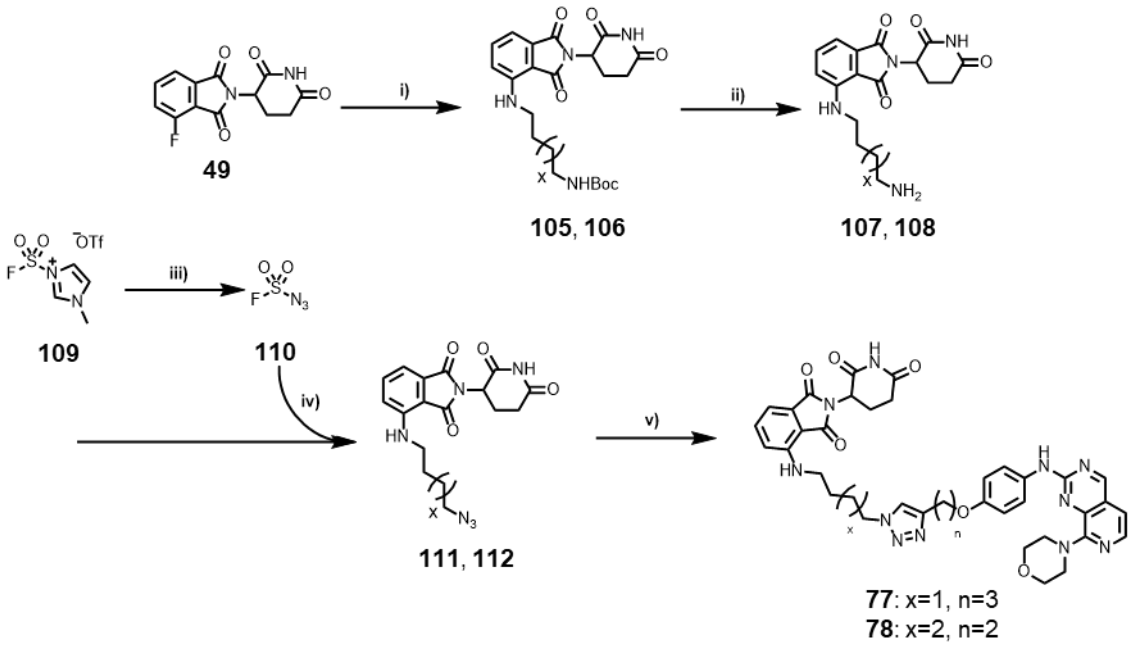

*Scheme 3.6 Synthesis of **77** and **78**, altering the position of the triazole utilising an azide transfer reagent. Reagents and Conditions: i) Appropriate Boc protected amine, DIPEA, DMSO, 75 ˚C, overnight. ii) HCl in dioxane, DCM, x=1 100%, x=2 86%. iii) NaN_3, MTBE, MeCN, 0˚C. iv) DMF x=1 43%, x=2 75%. v) **44** and **104**, $CuSO_4$, Sodium ascorbate, THF, water, rt, overnight, x=1 29%, x=2 43%.*

3.4.3 Synthesis of Warhead Modified Degraders

DB-0614 was synthesised as previously reported, and modified to incorporate the warhead and linker of **8** (Scheme 3.7-Scheme 3.9).[76] Synthesis of a tosylated IMiD derivative (**114**) was required in order to displace with the nucleophilic piperazine moiety of the warheads **119** and **122** (Scheme 3.7).[76] **114** was synthesised through the double tosylation of pentane-1,5-diol followed by displacement with 4-hydroxy thalidomide.

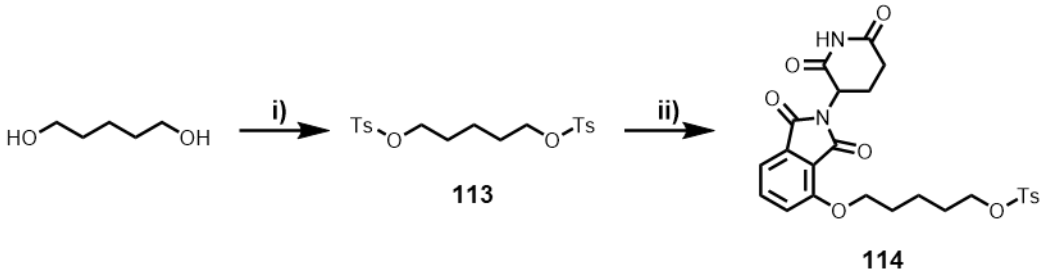

*Scheme 3.7 Synthesis of the IMiD intermediate **114**. Reagents and Conditions: i) Pyridine, p-toluene-sulfonyl-chloride, 0˚C, 2 h, 81%. ii) 4-hydroxy thalidomide. DIPEA, DMF, 80˚C 3 h, 60%.*

The commercially available starting material **115** was iodinated with *N*-iodosuccinimide affording **116**. **116** was then subjected to Suzuki conditions affording the common intermediate **117**.[76] **117** was treated under Buchwald-Hartwig conditions affording intermediates **118** and **120**, **118** requiring acidic

Boc deprotection. Tosyl displacement of **114** with the piperazine moiety of **119** afforded **DB-0614 (**Scheme 3.8). Similarly to **DB-0614**, **79** was synthesised utilising Buchwald-Hartwig chemistry to append the Boc protected piperazine which was deprotected and subjected to S_N2 conditions with **114** to yield **79** (Scheme 3.9). Analogous to chemistry in Chapter 2.3, **120** was subjected to Click conditions, affording the PROTAC **80** (Scheme 3.10).

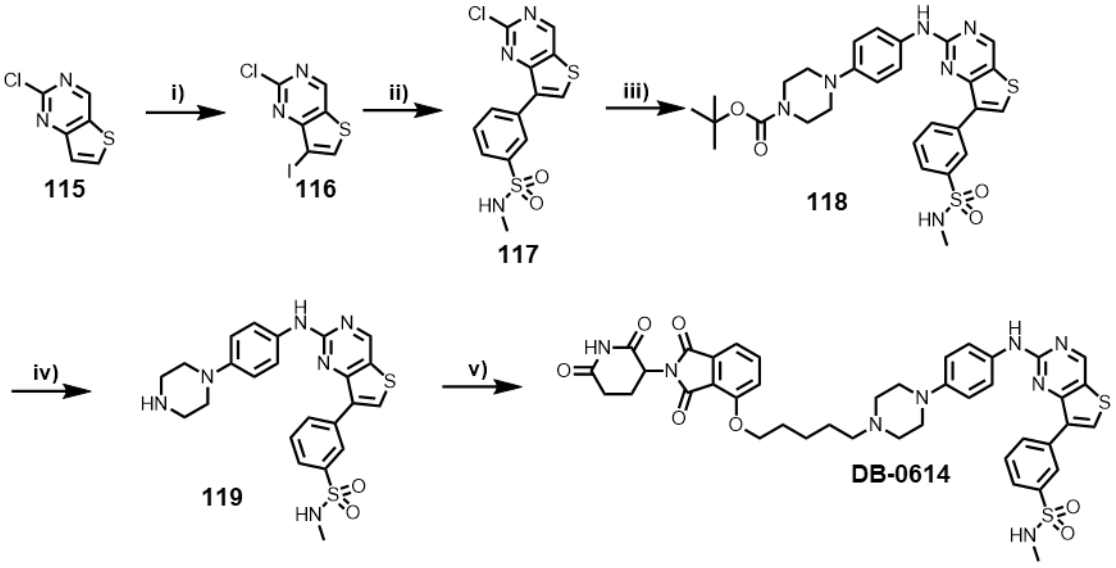

*Scheme 3.8 Synthesis of **DB-0614**. Reagents and Conditions: i) AcOH, N-iodosuccinimide, 80 ˚C overnight, 33%. ii) [3-(methanesulfonamido)phenyl] boronic acid, 1,4 dioxane, K_2CO_3, water, Pd(dppf)Cl·DCM, 90 ˚C, 6 h, 31%. iii) XPhos, Cs_2CO_3, DMF, $Pd(DBA)_3$, 90 ˚C, 30 min. iv) DCM, HCl in dioxane, 2 h, 58%. v) **114**, DIPEA, DMF, 60˚C, overnight, 17%.*

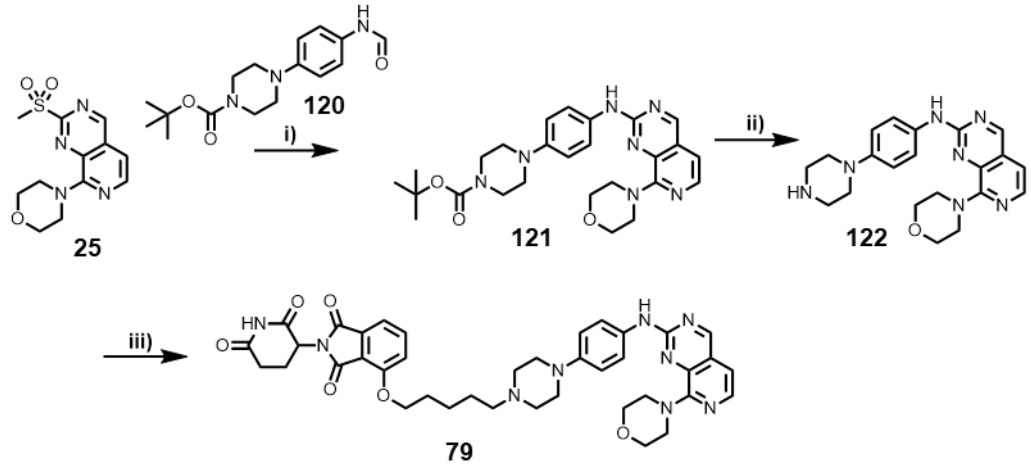

*Scheme 3.9 Synthesis of **79** comprised of the warhead of **8** and the linker-E3 ligase binder of **DB-0614.** Reagents and conditions: i) NaH, THF, 0˚C, overnight. ii) DCM, HCl in dioxane, 1 h rt, 27%. iii) **50**, DIPEA DMF, 60 ˚C, overnight, 39%.*

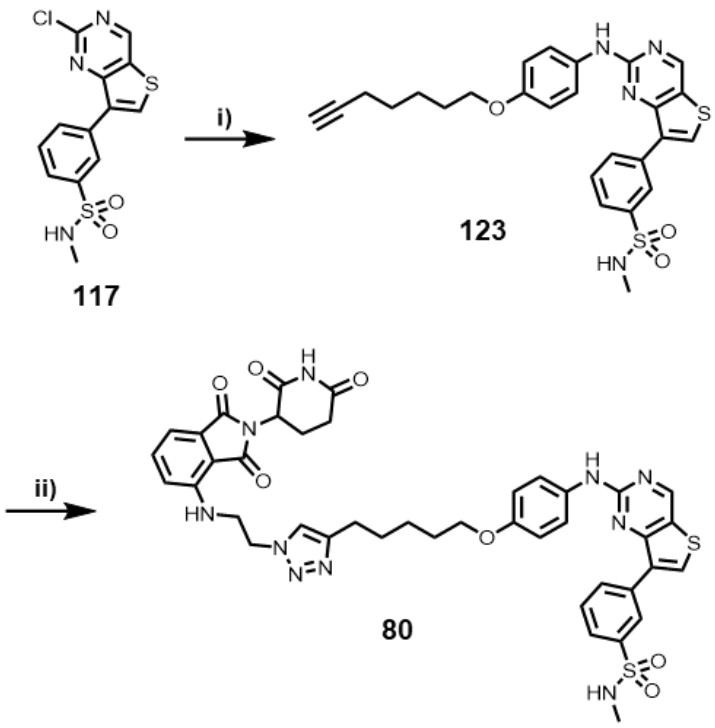

*Scheme 3.10 Synthesis of **80** comprised of the linker-E3 binder of **DB-0614** and the warhead of **DB-0614.** Reagents and conditions: i) Xphos, Cs_2CO_3, DMF, $Pd_2(dba)_3$, 90 ˚C, 30 min, 39%. ii) **50**, $CuSO_4$, Sodium ascorbate, THF, water, rt, overnight, 36%.*

To make **81** requires synthesis of the core pyrimide from a guanidine **124**. **124** was synthesised from the corresponding aniline **33** (Chapter 2.3), using cyanamide (Scheme 3.11). Utilising the commercially available starting material **125**, treatment with DMF-DMA affords the correct functionality to undergo the pyrimidine formation.[117] The ester of **127** is hydrolysed and subsequently reacted under amide coupling conditions to afford alkyne **129**. The alkyne is reacted under Click conditions affording **81**.

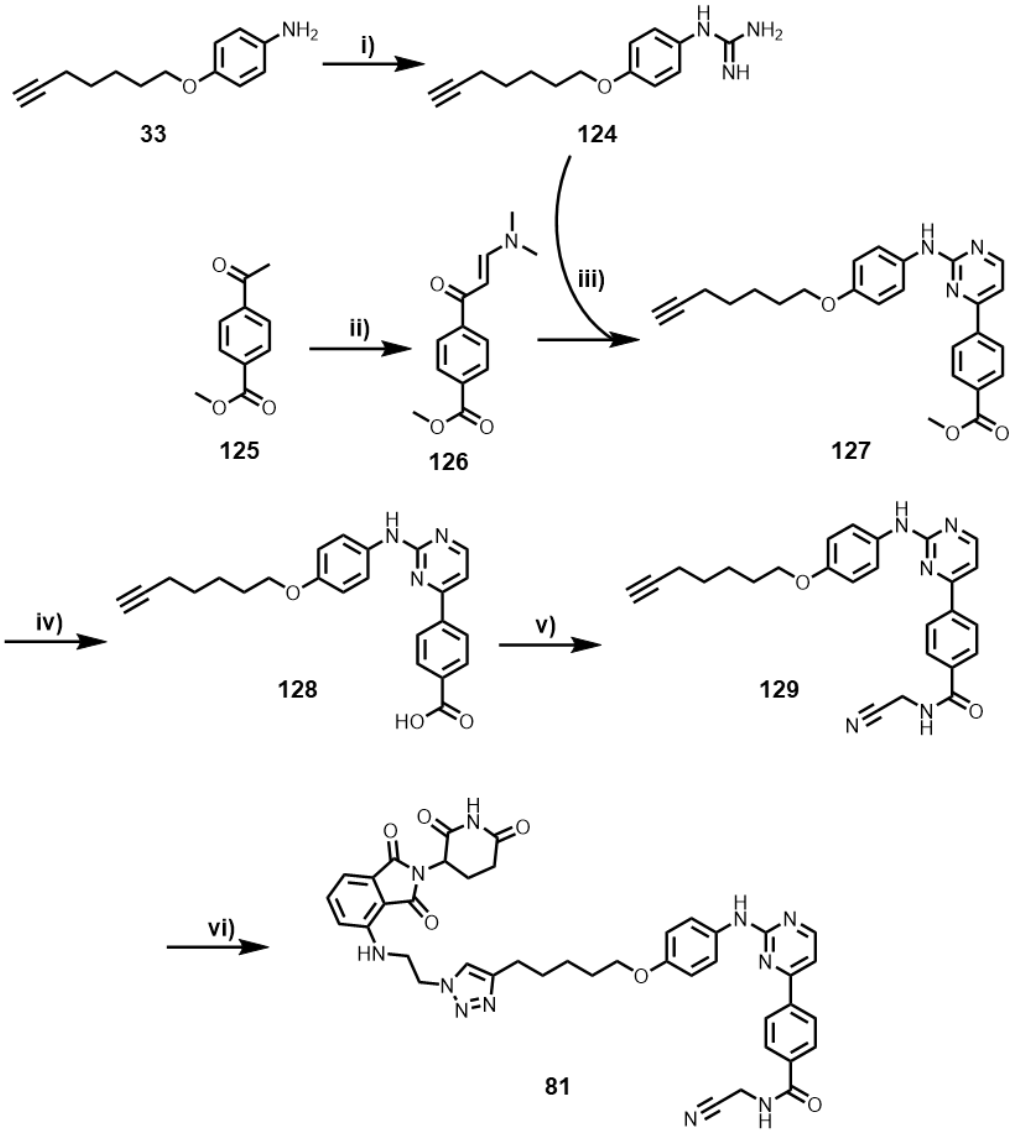

*Scheme 3.11 Synthesis of **81** with a published NEK9 binder. Reagents and conditions: i) Cyanamide, HCl in dioxane MeCN, 100 ˚C overnight. ii) DMF-DMA, toluene, 80 ˚C, overnight, 76%. iii) MeCN 130 ˚C, overnight. iv) NaOH, MeOH, water, 90 ˚C, 2 h. v) triethylamine, DMF, aminoacetonitrile, HOBt, EDC, rt, overnight, 60%. vi) **50**, $CuSO_4$, Sodium ascorbate, THF, water, rt, overnight, 28%.*

Similarly, the commercially available aminothiazole **130** is treated with DMF-DMA in order to subsequently react with the guanidine **124** affording **132**.[118] The alkyne, as before (Chapter 2.3), is subjected to click reaction conditions affording the degrader **83** (Scheme 3.12).

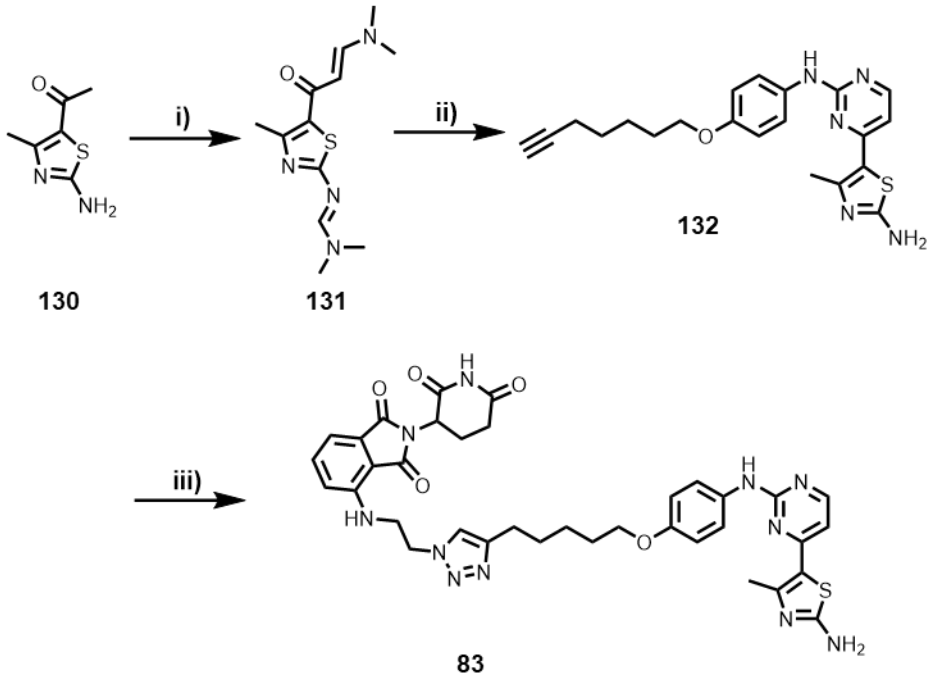

*Scheme 3.12 Synthesis of **83** utilising a published NEK9 binder. Reagents and conditions: i) DMF-DMA, 120 ˚C overnight, 50%. ii) **124**, NaOH, 2-methoxy ethanol, 180 ˚C, 3 h, 33%. iii) **50**, $CuSO_4$, Sodium ascorbate, THF, water, rt, overnight, 17%.*

Finally, the kinobead probe-based degrader **82** was synthesised from the previously described chloropyrimidine **133** (synthesised by Jack Cheung following a previously disclosed route).[119] A S_NAr reaction was performed on **133** using aniline **33** affording the alkyne **134** that was subjected to Click conditions affording **82** (Scheme 3.13).

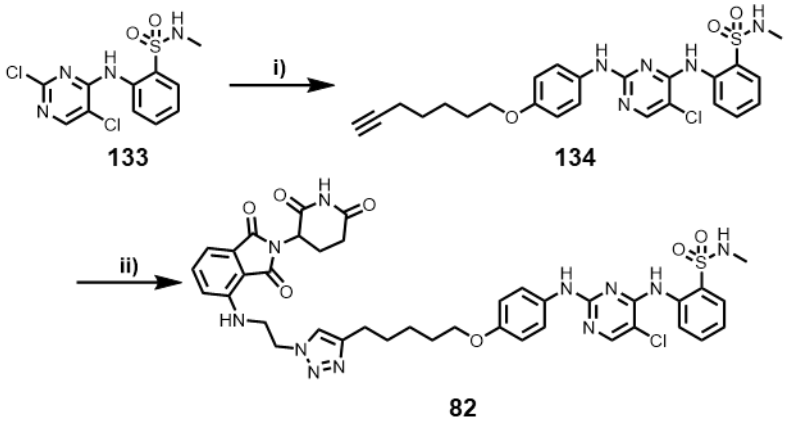

*Scheme 3.13 Synthesis of **82** utilising a warhead known to pull down NEK9 in a kinobead assay. Reagents and conditions: i) **33**, DIPEA, NMP 120 ˚C, overnight, quantitative. ii) **50**, $CuSO_4$, Sodium ascorbate, THF, water, rt, overnight, 21%.*

3.5 Conclusion and Future Work

Although the NEK9 degraders screened go through an unknown degradation mechanism, the proteomics screen did afford a PROTAC suitable for

optimisation, both for warhead and linker modifications. Through validation of **8** as a NEK9 degrader, we discovered stringent linker requirements, including linker length and the position of the triazole. The fact that such specific linker requirements were observed suggests that running more linker lengths, in place of exploring warhead SAR, may be advantageous if the screen were to be repeated. The strict linker requirements could likely be explained through ternary complex structural requirements, however, to confirm this would require either crystallography or cooperativity experiments. Other, less time-consuming, methods to rationalise the degradation potency changes are available in the form of computational models, however, NEK9 has no crystal structure available on the PDB.

We discovered the mechanism of NEK9 degradation with **8** was not CRBN mediated through its lack of dependence on neddylation and maintained degradation in $CRBN^{-/-}$ cells. It was therefore important to synthesise the published NEK9 degrader **DB-0614** and validate its mode of action. Furthering the discovery that **DB-0614** degrades in the canonical PROTAC manner, we wanted to discover if it was the linker or warhead portion of the hit degrader **8** that was causing its change in degradation mechanism. It was discovered that slightly improved degradation could be achieved with the use of the warhead from **DB-0614** (**80**) whilst maintaining the lack of neddylation dependence. This suggests the linker-E3 ligase binder could be causing the altered degradation mechanism.

The discovery of a degrader with an improved D_{max} (**83**) using the ChEMBL chemical probe database was key to further mechanistic studies due to the better contrast in Western blots. The mechanism of NEK9 degradation of **83** requires further experiments in order to elucidate the means by which NEK9 is being ubiquitinated. We currently have no hypothesis for the presence of degradation upon neddylation inhibition or CRBN knockout. To elucidate if another E3 ligase is responsible for the ubiquitination of NEK9, a focussed siRNA or CRISPR screen covering the human ubiquitination system could be conducted. The screen would have to be performed in CRBN knockout cells in order to control for parallel degradation mechanisms taking place. CRBN could initially be causing the degradation and only upon compromising CRBN activity, another mechanism takes place. The fact that the degradation mechanism is

maintained through multiple scaffolds suggests that this is robust and warrants further exploration.

Further SAR exploration is required to gain more understanding of the degradation of NEK9. As methylation of the IMiD can rescue degradation, it would be important to explore more SAR around this region of the degrader, especially considering it contradicts the neddylation and CRBN independence result. Trying alternate CRBN binding scaffolds and other negative control compounds could uncover required functionality of the IMiD ligand, developing on the discovery that the N-H of the glutarimide is required for degradation (Figure 3.14). In addition, the linkage atom can impact degradation and would be interesting to see if this effects activity and recruited IMiD neo-substrate off targets.[120,121]

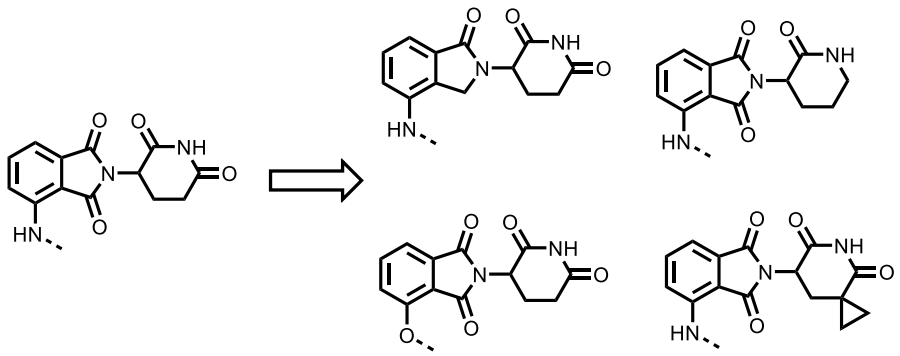

Figure 3.14 Suggested IMiD modifications to explore SAR around the CRBN binder portion of the NEK9 degraders. As methylation is an important piece of SAR, abrogating degradation of NEK9, it is important to find other structural features essential for NEK9 degradation.

As multiple NEK9 binding warheads were tolerated, further exploration of the warhead may yield compounds with improved solubility. As the solubility of **8** is low (1.8 μM) and potentially limiting potency (D_{max}) at higher concentrations, addition of basic centres could improve this, such as a replacement of the morpholine for piperazines (Figure 3.15). The lack of structural information means it is not known if the morpholine position or core pyridopyrimidine on **8** is required for the degradation. The improved NEK9 degrader **83** could therefore be truncated to identify the minimum pharmacophore to cause NEK9 degradation (Figure 3.15).

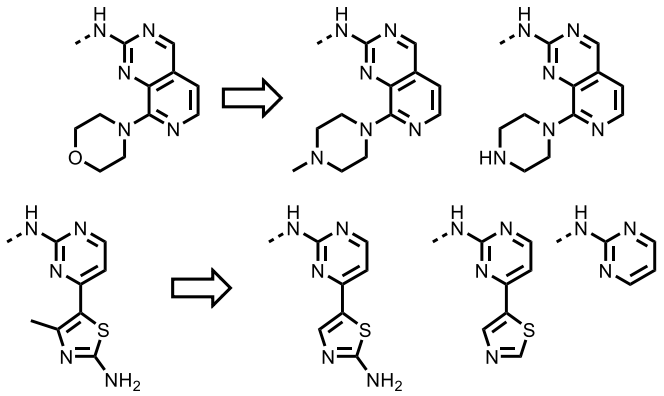

Figure 3.15 Warhead modifications to identify more soluble degraders and the minimum pharmacophore for NEK9 degradation. This will aim to identify necessary structural features essential for NEK9 degradation.

The position of the triazole moiety is important for degradation of NEK9 therefore, it would be interesting to see if a swap to other rigid scaffolds is tolerated (Figure 3.16). Isosteric replacement with an amide, could elucidate if the triazole is forming productive hydrogen bonds within the ternary complex pocket. Triazole replacement with a rigid piperazine moiety could improve the physicochemical properties of the degrader through addition of basic centres. This may improve the solubility of the degraders, potentially improving D_{max} at high concentrations.

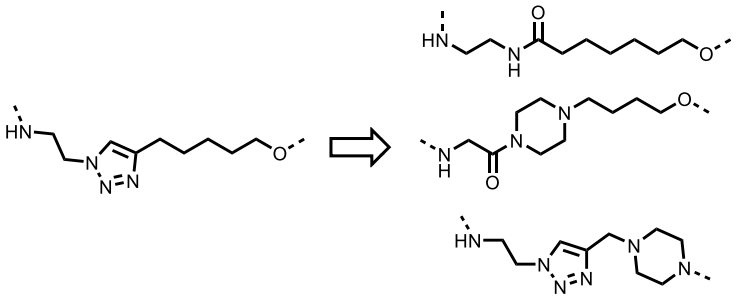

Figure 3.16 Linker modifications to introduce solubilising and rigid groups whilst maintaining a rigid group in the triazole position due to its importance in the degradation of NEK9.

Chapter 4: Validation and Optimisation of Aurora Kinase A PROTACs

4.1 Aurora Kinase A Introduction

Aurora kinase A (AURKA) inhibitors have gained significant interest as potential anticancer treatments.[122–124] Both AURKA and Aurora kinase B (AURKB) have essential roles in mitotic progression and function as oncogenes, promoting tumorigenesis in cancer cell lines.[125,126] Despite multiple clinical candidates, no successful AURKA targeting drug has emerged, potentially a result of other scaffolding functions remaining active, in addition to AURKB off target toxicity.[127,128] PROTACs have the potential to both increase selectivity and remove all scaffolding roles thereby mitigating the pitfalls of AURKA inhibition.

AURKA has a known function in the MDM2-mediated destabilisation of P53. The tumour suppressor P53 is the most commonly mutated protein in cancer and is linked to poor prognosis, a result of inactivation of its 'genome guarding' role.[129] AURKA, through its kinase domain, phosphorylates P53 at serine 315, signalling for its MDM2-mediated ubiquitination and degradation *via* the proteasome. Inhibition of the AURKA kinase domain, or knockout with siRNA, can lead to rescue of P53 and therefore drive cancer cell death.[130]

MYC is a family of three proteins *c-myc*, *l-myc,* and *n-myc* that act as transcription factors and are heavily involved in cancer, in particular, *NMYC* amplification is often associated with poor prognosis in neuroblastoma.[131] Neuroblastoma originates from early nerve cells, commonly starting in either the adrenal gland tissue or spinal cord. Upon formation, neuroblastoma can metastasise, often to the bone and liver. AURKA has a key protective role of *n-myc* through blocking Fbxw7 mediated ubiquitination and degradation, increasing the half-life of *n-myc*.[132] Therefore, abrogation of the protective scaffolding role of AURKA could afford potential therapies for *NMYC* driven cancers.

Current AURKA degraders are based upon **MK5108**, **ribociclib,** and **alisertib**, all of which show low nM activity in multiple cell lines against AURKA (Figure 4.1).[127,133,134] Several key discoveries with degraders of AURKA have emerged,

mainly highlighting the stark phenotypic differences with inhibition. Inhibition of AURKA induces characteristic mitotic spindle defects, causing spindle checkpoint-dependent mitotic arrest. The arrest is not maintained and the cell exits mitosis leading to apoptosis through induction of G2 arrest.[135] In contrast, degradation of AURKA confers a different effect on mitosis to inhibition, being S-phase arrest as opposed to G2.[136,137] AURKA degradation only tends to reach ~80% D_{max} across multiple diverse PROTACs, likely accounting for cytoplasmic and microtubule localised protein. The ~20% remaining is thought to be centrosomally-engaged AURKA and unavailable for degradation. Although Wang *et al.* showed degraders can engage the centrosomally associated AURKA, no degradation was observed.[138] The authors believe this could be a result of a conformational change of AURKA or PROTAC subcellular localisation.

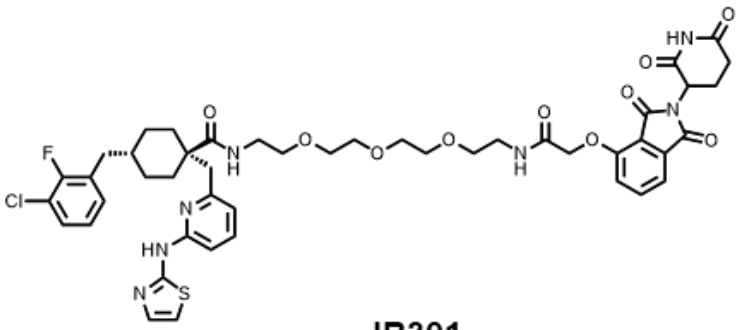

JB301

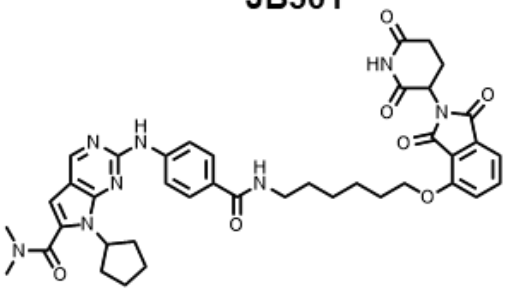

PROTAC 4

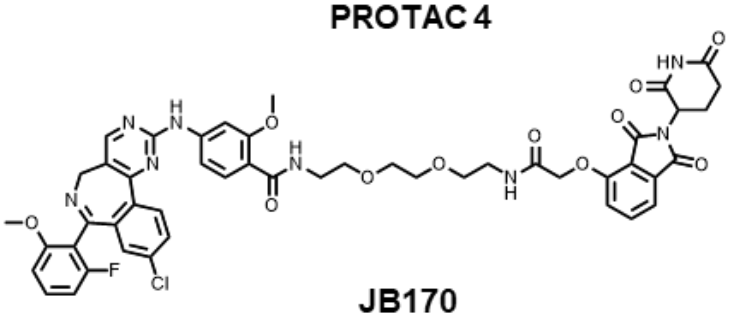

JB170

*Figure 4.1 Structure of three AURKA targetting PROTACs based on **MK5108**, **ribociclib,** and **alisertib**, all utilising a CRBN binder. All of which show potent loss in AURKA but only ~80% D_{max}. To date no other E3 ligase recruiter has been utilised for AURKA degradation.*

To date, only one pre-print publication addresses *n-myc* degradation as a consequence of AURKA PROTAC treatment however, it is likely that most current potent degraders will affect *n-myc* levels.[134] The publication highlights the need to induce >75% AURKA degradation in order to see an effect on *n-myc* levels with small recoveries of AURKA leading to full rescue of *n-myc* degradation.

4.2 Aurora Kinase A Hit Validation

As highlighted previously (Chapter 2.2), a proteomics screen showed degradation of AURKA with two of the 9 screened PROTACs (**3**, **9**), similar to the validation in Chapter 3.2, we sought to validate this through Western blotting (Figure 4.2). The library compounds (**1**-**9**) were treated under identical conditions as the proteomics (HCT116 cells, 6 h, 1 μM) showing degradation of AURKA with the n=5 linker length compounds (**3**, **6**, **9**). This corroborated the degradation of **3** and **9** seen in the screen. However, **6** showed no significant result in the proteomics screen. This result highlights the requirement of screening closely related analogues in proteomics as if only **6** was screened AURKA degradation would have been missed. Degradation was also observed with **2**, **5** and **8**, although at reduced levels, showing a higher toleration of other linker lengths against AURKA as opposed to NEK9 (Chapter 3.2). The proteomics showed no significant degradation of AURKA with **2**, **5** or **8**. Similar to NEK9, flat SAR was observed when changing the amine substituent of the warhead, meaning exploration of this position could afford improved degraders, both in terms of potency and physicochemical properties. **9** was selected for further validations as we had the largest amount of this compound.

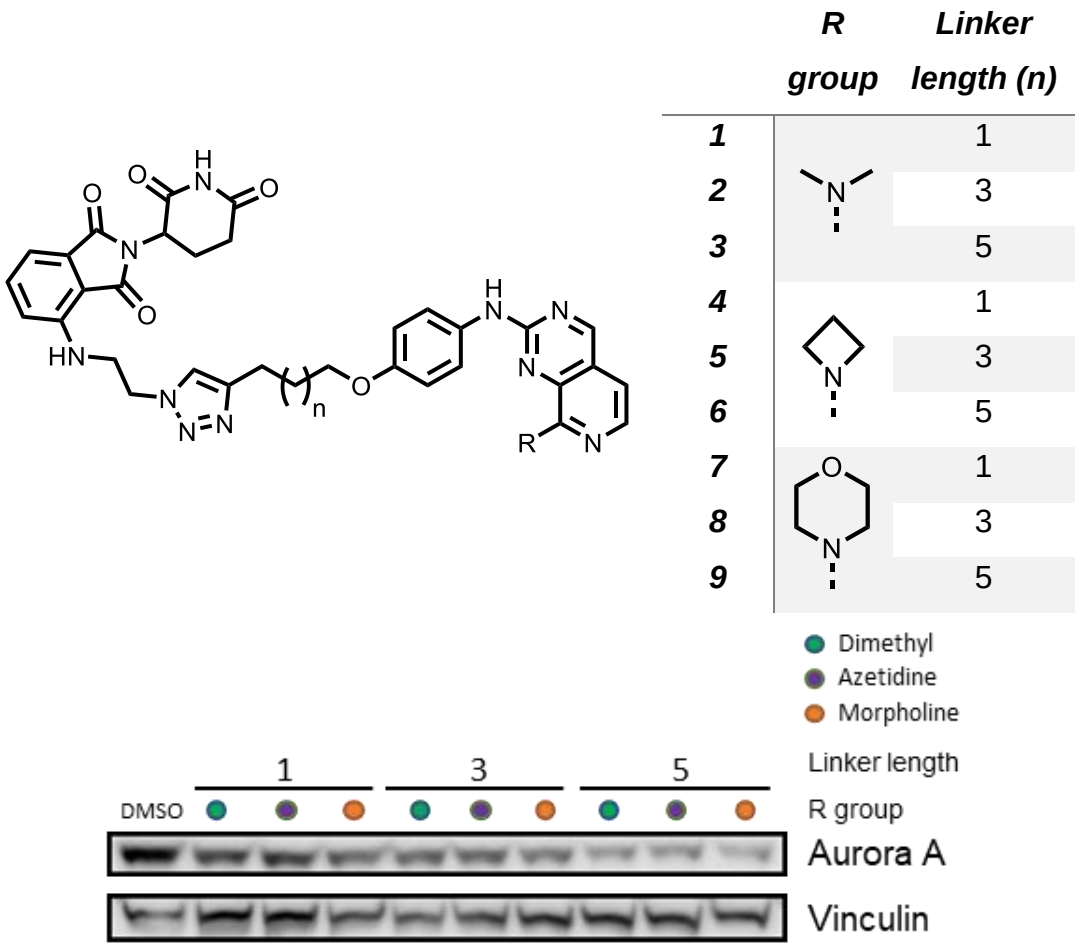

*Figure 4.2 Structure of the screened compounds (**1**-**9**) and the selectivity of AURKA degradation after a 6 h treatment in HCT116 cells at 1 μM. Degradation of **3** and **9** was consistent with proteomics but the Western also shows degradation with **6**. No SAR was seen around warhead changes.*

The dose response of **9** showed activity in the low nM range however, complete degradation was not observed at any concentration at 6 or 24 h (Figure 4.3 A, B). Commonly with AURKA degraders ~80% D_{max} is seen, likely due to centrosomally protected protein.[138] Whether this is a result of conformationally changed AURKA or compartmentally inaccessible protein is unknown. No hook effect was seen with **9**, an observation often associated with a PROTACs mode of action, where rescue in degradation is observed through saturation of both binding partners of the degrader. The lack of an observed hook effect may be a result of several factors including: low solubility, low binary affinity towards AURKA, or strong ternary complex affinity. Despite the excellent degradation potency, solubility was measured to be 0.9 μM for **9**, highlighting an area to optimise to progress these compounds further. **JB170** also shows similarly poor solubility (2.4 μM) whilst maintaining a hook effect at high concentrations. This

suggests the lack of rescue in degradation of **9** at high concentrations is a result of reduced affinity towards AURKA or high ternary complex affinity.

Maximal degradation was achieved at the earliest time point tested (2 h) and was maintained throughout a 72 h treatment, this is improved when compared with **JB170** where AURKA levels recover after 9 h (Figure 4.3 C).[137] Although **JB170** was tested in an alternate cell line, this highlights **9** is a potent and stable PROTAC with long lasting effects. The levels of degradation and selectivity achieved were especially surprising when considering the size and lack of an optimised warhead and linker. **9** is therefore a suitable starting point to optimise further and explore AURKA degradation.

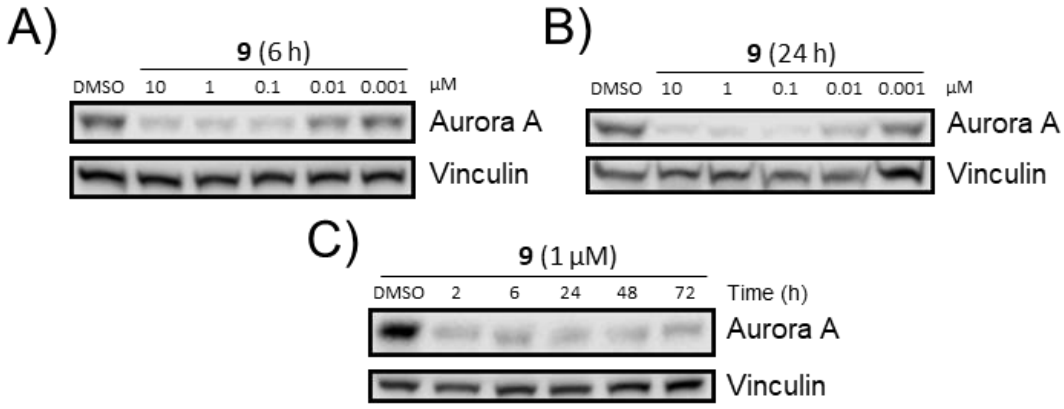

*Figure 4.3 Dose response of **9** after both a 6 (A) and 24 h (B) treatment in HCT116 cells. Both show highly potent degradation of AURKA in the low nM range. Slightly improved DC_{50} was observed at the 24 h time point. C) Time course experiment with 1 uM of **9** in HCT116 cells. Excelent levels of degradation was achieved throughout a 3 day treatment with extremely fast onset.*

The mechanism of action of **9** was determined using a rescue experiment under the same conditions as previously described (Chapter 3.2). Degradation was dependant on the proteasome, neddylation, E1 inhibition, and co-treatment with binders of both CRBN and AURKA (Figure 4.4).

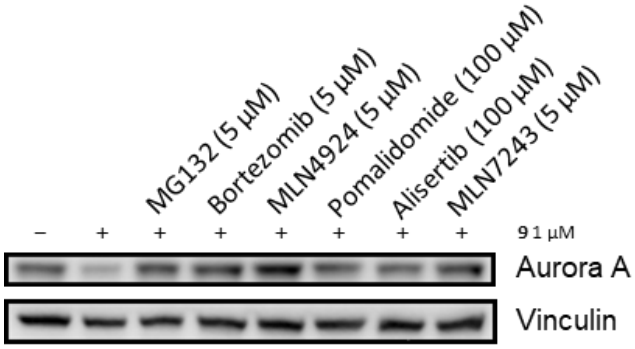

*Figure 4.4 AURKA degradation rescue experiment with 1 μM of **9** after a 6 h treatment in HCT116 cells. degradation was rescued with treatment of proteasome inhibitors, neddylation inhibition, co-treatment with both a CRBN and AURKA inhibitor, and an E1 inhibitor. Results are consistent with a PROTAC mechanism of action.*

A cell growth inhibition assay was performed in HCT116 cells after a 5-day treatment with **alisertib**, **JB170**, **9**, and **10**, the parent warhead precursor to **9** (Table 4.1). HCT116 cells were selected as **alisertib** had been previously tested in this line, showing a GI_{50} of 70 nM after a 3 day treatment.[139] **9** showed comparable potency with **JB170** in the μM range however, **alisertib** showed significantly improved growth inhibition. This may be attributed to the phenotypic differences associated with inhibition vs degradation of AURKA (Chapter 4.1), or a result of off target AURKB activity of **alisertib**.

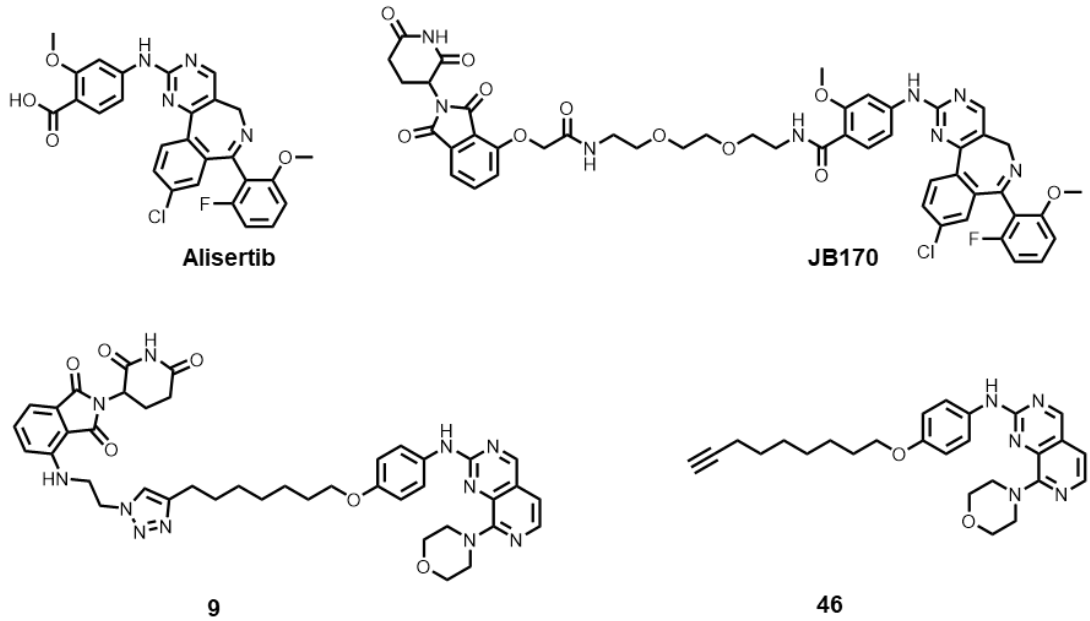

	Alisertib	**JB170**	**9**	**46**
GI_{50}/μM	0.036 ± 0.004	3.3 ± 0.3	5.2 ± 0.9	3.0 ± 0.7

*Table 4.1 Structures of **alisertib**, **JB170**, **9**, and **46** and GI_{50} data from HCT116 cells treated with each compound over 5 days. PROTACs do not cause significant growth inhibition at cellular concentrations*

where AURKA degradation is seen. Likely due to 20% of disease relevant AURKA being present after PROTAC treatment.

A common challenge with AURKA inhibition is AURKB off target activity. AURKB inhibition effects the cells ability to align chromosomes during mitosis, overriding the mitotic spindle checkpoint and allowing polyploidy, failure of cytokinesis and endoreduplication to occur.[128] The proteomics screen showed one significant result for a lack of AURKB degradation with **3** (Log2FC -0.28, -Log10(p-value) 3.71) however for **6** and **9** the results need to be validated through Western blotting. No significant degradation was seen with any of the library compounds (**1**-**9**) suggesting the PROTACs are selective for AURKA (Figure 4.5).

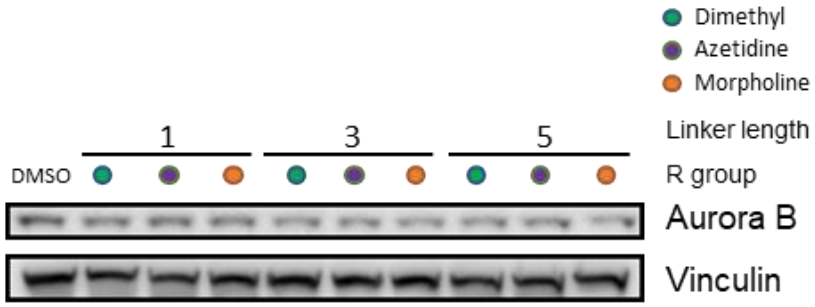

*Figure 4.5 Selectivity of AURKB degradation with **1**-**9** after a 6 h treatment in HCT116 cells at 1 μM. Blot shows no significant degradation of AURKB, a common off-target with AURKA inhibition.*

The kinome wide binding profile of **9** was explored to ensure AURKA degradation selectivity was not the product of a highly selective warhead, and in fact a result of productive ternary complex formation. The scanMAX KINOME*scan*™ profile of **9** at 1 μM showed 36 kinases, spanning a large range of the kinome, were bound over 35% relative to the control, including AURKA (16%, Figure 4.6, Table 4.2). The results highlight that the ternary complex may be responsible for the selective degradation of AURKA and how other linkers and E3 ligases may be able to degrade the other bound kinases if a productive combination can be found. The results also confirm that the changes made to **BOS172722** successfully decreased selectivity whilst still maintaining binding of MPS1 (22%, gene code TTK).

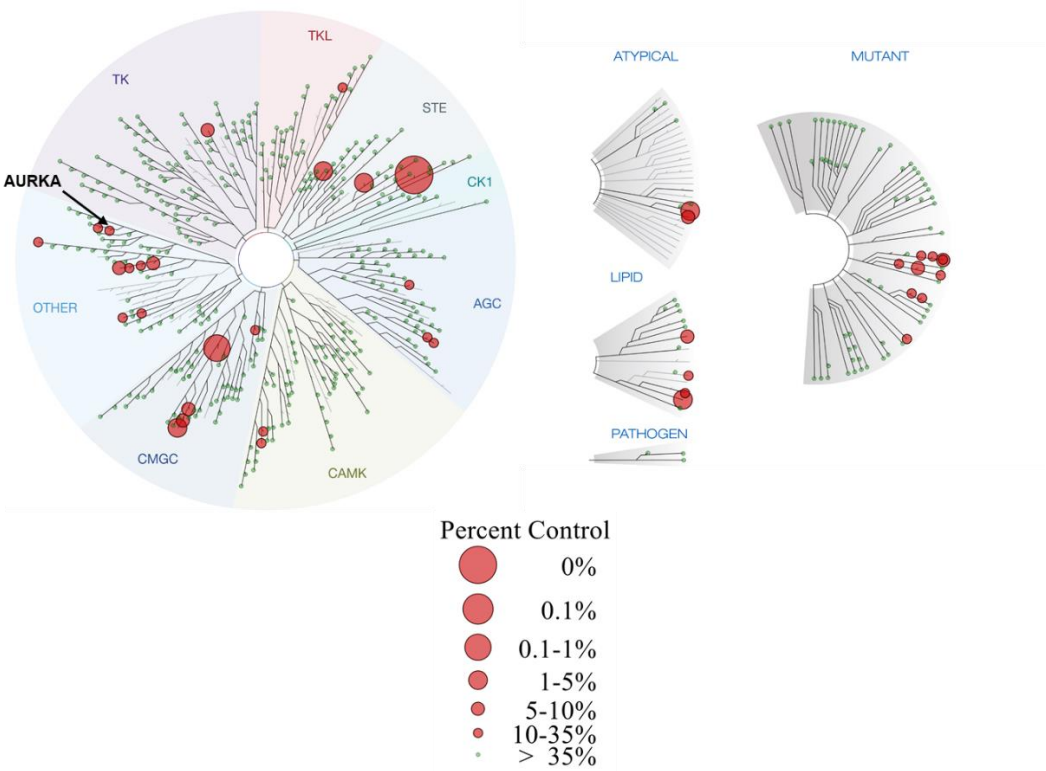

*Figure 4.6 scanMAX KINOMEscan™ profile of **9** at 1 μM showing the large span of the kinome **9** could have potentially degraded with alternate linker lengths or E3 ligase binder selection.*

Selectivity Score	Kinases Hit
S(35)=0.074	FLT3, AURKC, FLT3, AURKA, NUAK2, KIT, PIP5K1A, PIP4K2B, CSNK2A2, FLT3, NUAK1, NEK5, TTK, GRK4, CDKL5, FLT3, FLT3, MAP3K7, LRRK2, SGK1, AAK1, KIT, SGK3, GAK
S(10)=0.035	MAPK10, MAP2K5, PIP4K2C, TAOK1, RIOK3, BMP2K, FLT3, MAPK8, RIOK1, PIK3C3, JAK3, FLT3, MAPK9, STK16
S(1)=0.005	MAP3K19, MAPK15

*Table 4.2 Selectivity scores of **9** including the kinases bond at the specified %. Both AURKA and TTK are not amongst the highest levels of inhibition highlighting the disconnect between inhibition and degradation potency.*

Altogether, the results highlight **9** is an extremely potent AURKA PROTAC with degradation in the nM range and, consistent with other degraders of AURKA, shows ~80% maximal degradation. The degradation was long lasting with rapid onset and active up to, and likely beyond, 3 days. Degradation was also shown to be extremely selective for AURKA in the proteomics screen and therefore is an excellent tool compound to further AURKA biological studies, in addition to being an ideal starting point for medicinal chemistry optimisation. Improving solubility would need to be considered for initial optimisation efforts and could be explored through changes to the linker portion of the degrader, or even warhead alterations from the synthetically tractable site where flat SAR was observed. Although reduced cellular potency was seen when compared to

alisertib, it was similar to both **JB170** and the alkyne-warhead (**46**). With the simplicity of **9**, several options for optimisation are available, suggesting it is an excellent starting point that could be used to further probe AURKAs role and function. As the warhead utilised in **9** is small and unoptimised, we sought to explore further changes to this portion of the degrader to see how this impacted degradation potency. We aimed to elucidate if degradation potency could be maintained by transfer to another AURKA binding scaffold, and what the minimum pharmacophore required for AURKA degradation was.

4.3 Aurora Kinase A Warhead Exploration

4.3.1 Alternate Warhead Attachment

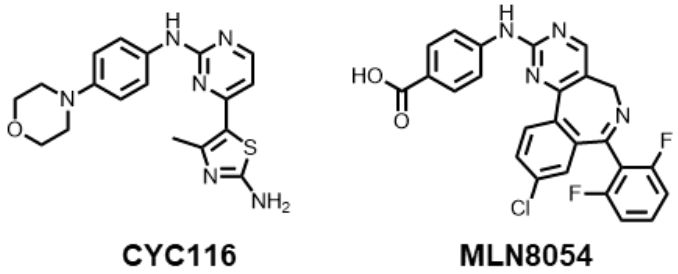

*Figure 4.7 Structure of **CYC116** and **MLN8054**, potent AURKA inhibitors selected to use as warheads to test if the E3 ligase and linker of **9** can be transferred to another AURKA binding scaffold.*

All AURKA degraders to date are based on large molecular weight warheads with a high binding affinity. We wanted to see if some of these scaffolds could be harnessed and if the degradation potency of **9** would translate to a new warhead. To achieve this, we appended known AURKA inhibitors to the linker and E3 ligase binder of **9** (Figure 4.7). It is likely **CYC116** and **MLN8054** will bind in an analogous way to **9**, as all three contain an amino-pyrimidine hinge binding motif, similar to the rational in Chapter 3.3.2 for NEK9.[140,141]

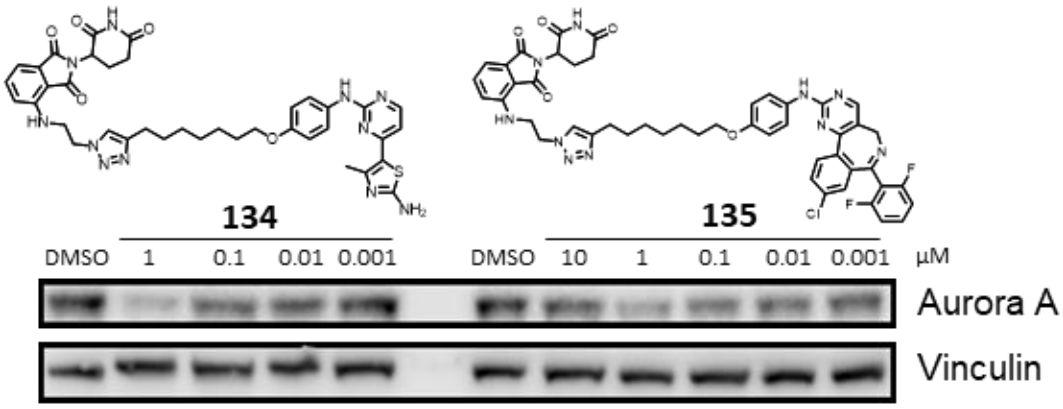

*Figure 4.8 Dose response of **134** and **135** in HCT116 cells after a 6 h treatment. **134** could not achieve DMSO concentrations above 1 mM, therefore 1 µM is the maximum achieved dose. Degradation with **134** shows a hook effect unlike compound **9**. Both degraders are much less potent than **9**.*

	9	***134***	***135***
Molecular weight/gmol^{-1}	759.81	763.87	913.37
tPSA/ Å^2	198.69	212.24	185.69
cLogD	4.1	5.6	8.8
HBD/HBA	3/15	4/15	3/13

*Table 4.3 Table 1.1 Predicted properties of **9**, **134** and **135.** cLogD calculated in MOKA, highlighting the poor chemical space **134** and **135** occupy.*

AURKA degradation with **134** and **135** was over 10-fold lower than **9**, in addition, a hook effect was observed with the **MLN8054**-based PROTAC **135** (Figure 4.8). A maximum concentration of 1 µM could only be achieved with **134** due to solubility issues in DMSO. As the warheads of **134** and **135** are structurally dissimilar to **9,** the physicochemical property differences are large (Table 4.3), especially cLogD, which may be resulting in low intracellular free concentrations and therefore effect potencies. This does not exclude potential slight conformational changes affording this reduced degrader potency but would require further structural information to prove.

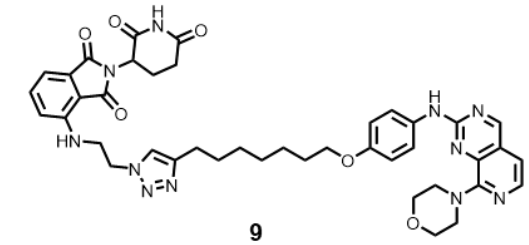

9

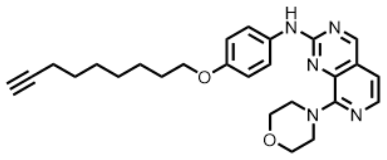

46

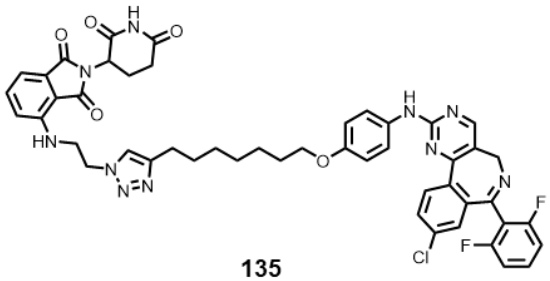

135

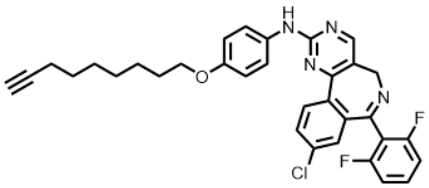

136

	9	***46***	***135***	***136***
Aurora A K_d/μM	0.28 ± 0.05	7.2 ± 0.2	1.0 ± 0.08	6.2 ± 0.9

*Table 4.4 Structure of **9**, **46**, **135**, and **136** and K_d values of each, determined against AURKA using the DiscoverX platform. An increase in affinity towards AURKA was seen with both alkynes when a triazole and IMiD is attached.*

In order to determine if the difference in degradation activities of **9** and **135** was driven through binary affinity towards AURKA, the K_d of each was determined, along with the non-CRBN binding compounds **46** and **136** (Table 4.4). Binding affinity against AURKA was tested using the DiscoverX platform previously described (Chapter 3.3). Commonly in PROTAC design, a solvent exposed region is used to append a linker, as this is unlikely to affect binding affinity towards the target and has been done for other AURKA-based degraders. Previous examples with AURKA degraders show a 2-6 fold drop off with PROTACs vs the corresponding parent inhibitor.[134,138]

Surprisingly, the K_d of the PROTAC **9** was 26-fold more potent than that of the parent alkyne **46** (Table 4.4). As the triazole and E3 ligase binder of **9** are solvent exposed, we expected this to have little impact on monovalent binding affinity. Instead, our results show that these parts of the PROTAC could be forming meaningful interactions with the surface of AURKA. The **MLN8054** based PROTAC **135** showed a 6-fold increase relative to **136** and was 4-fold less potent than **9**. To ensure that the interactions with the IMiD and triazole alone aren't what is driving AURKA potency, **137** was synthesised and tested in a ^{31}P-ATP-based kinase activity assay at Reaction Biology, showing no AURKA activity (Table 4.5). **9** and **46** were also tested in this assay format and showed

a 20 fold higher activity of **9**, consistent with the previous assay. Overall, it is unclear how relevant the binding activity is to degradation potency as the triazole-IMiD moiety of **9** may be engaging AURKA in a binary complex but could be irrelevant when considering where it sits in the ternary complex. Further SAR or structural information would be required to identify the relevance of the triazole-IMiD moiety of **9.**

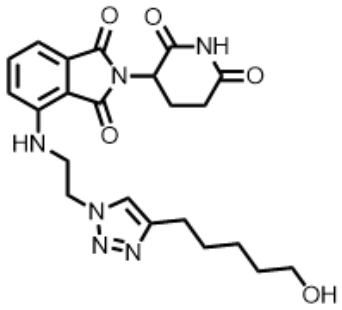

137

	9	***46***	***137***
Aurora A IC_{50}/μM	0.15 ± 0.03	2.95 ± 0.1	Inactive

*Table 4.5 Structure of **137** and K_d values of **9**, **46**, and **137** determined against AURKA using the Reaction Biology ^{31}P kinase activity platform with 1 μM ATP concentration. Results are consistent with assays ran at DiscoverX. **137** shows no measurable potency towards AURKA so it is unknown why **9** shows such high affinity towards AURKA relative to **46**.*

4.3.2 Truncating the warhead

Despite the small warhead utilised in **9**, potent degradation of AURKA was seen. We wanted to identify the minimum warhead pharmacophore required for AURKA degradation, and in addition, investigate if similar gains in binding affinity were maintained for other PROTAC/parent alkyne-warhead pairs (similar to **9** and **46**, Table 4.4). To achieve this, we truncated the scaffold, removing the morpholine (**138**), changing to a quinazoline (**139**) and removed the bottom pyridine ring (**140**), all whilst maintaining the core hinge binder. Remarkably, degradation of AURKA was seen in all three truncated examples however, led to a 10-100 fold drop off in degrader potency whilst maintaining a similar D_{max} when compared to **9** (Figure 4.9). The fact **140** is active with a warhead <100 molecular weight demonstrates AURKA has a high propensity for degradation, as hypothesised previously.[76]

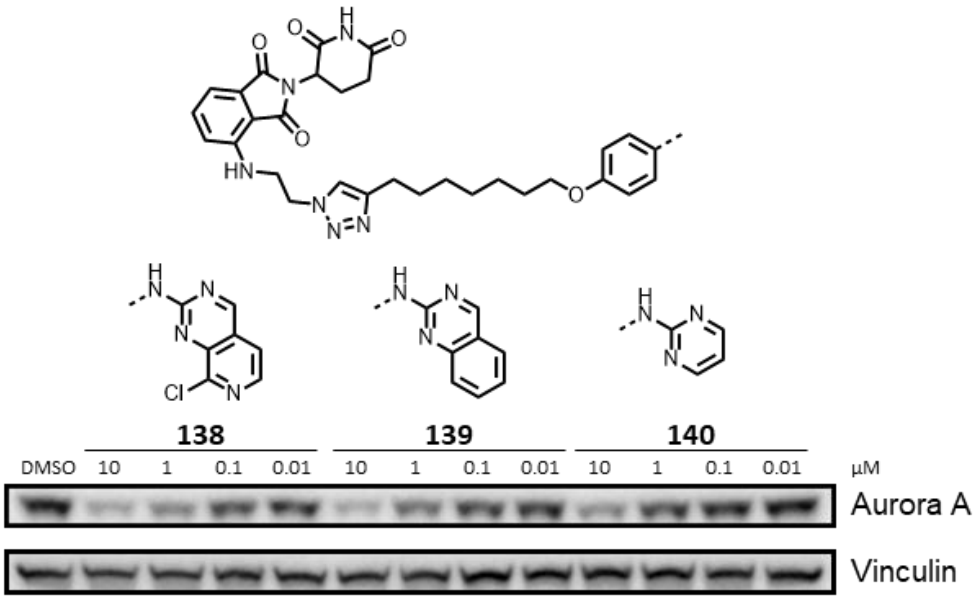

*Figure 4.9 Dose response of **138**, **139**, and **140** in HCT116 cells after a 6 h treatment. Degradation was maintained with all truncated scaffolds despite a lack of binding affinity towards AURKA although significantly less potent than hit compound **9**.*

To discover if binding affinity was also driving degradation with **138**-**140**, the compounds and alkyne pairs were tested against AURKA to determine the K_d. No binding events were observed for any compound up to 10 μM, suggesting a productive ternary complex must be driving the degradation potency of these compounds and not binding affinity. There is a significant difference in binding affinity with **9** and **138**, suggesting the morpholine of **9** is making meaningful interactions within the AURKA pocket, which could be exploited further to improve binding affinity. Our results highlight the need for exploration of the warhead portion of **9** and the fact significantly truncated warheads can confer modest degradation of AURKA.

4.4 Synthesis of Aurora Kinase A Degraders

135 and **136** were synthesised in an analogous way to **81** and **83** (Chapter 3.4.3), whereby a ketone DMF-DMA product (**131**, **142**) is reacted with a guanidine (**141**) to form the pyrimidines **143** and **136** (Scheme 4.1). **142** was synthesised by Jack O'Hanlon following a published route, while the subsequent reactions to make PROTAC **135** were performed by Alice Harnden.[140] Click reaction with azide **50** afforded the two PROTACs **134** and **135**. Control compound **137** was synthesised through utilisation of the Click conditions used for PROTAC synthesis of all the degraders (Scheme 4.2).

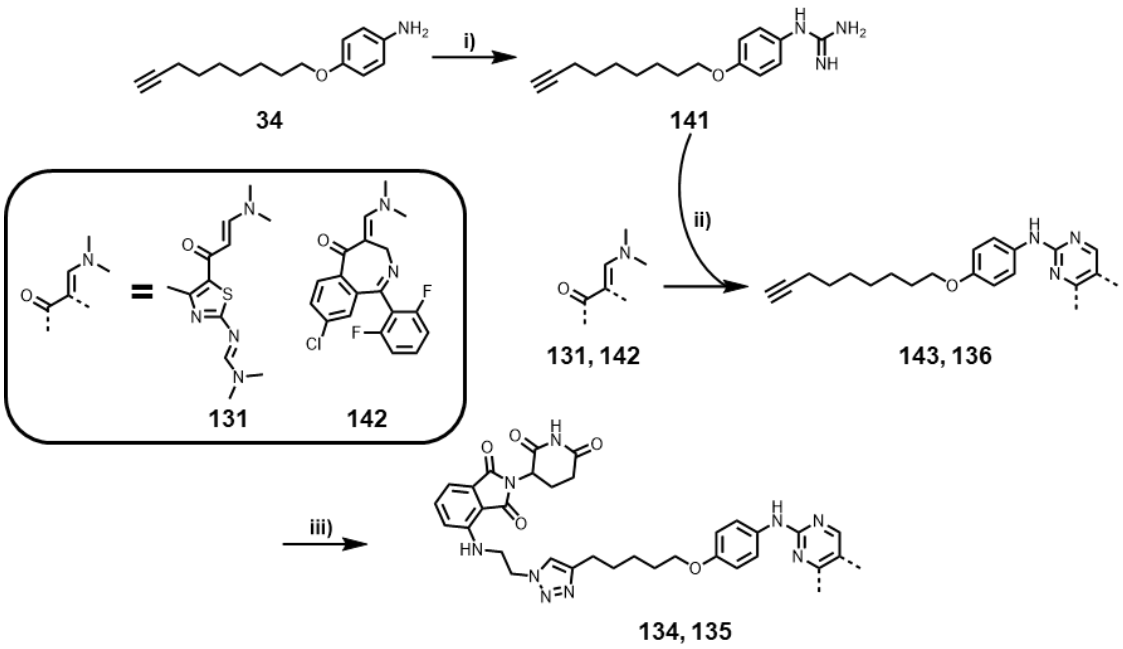

*Scheme 4.1 Synthesis of PROTACs **134** and **135**. Reagents and conditions: i) Cyanamide, MeCN, 100 ˚C, 6 h, quantitative. ii) NaOH, MeCN, 80 ˚C, 65% (**143**), 47% (**136**). iii) **50**, sodium ascorbate, $CuSO_4$, THF, water, rt, 53% (**134**), 61% (**135**).*

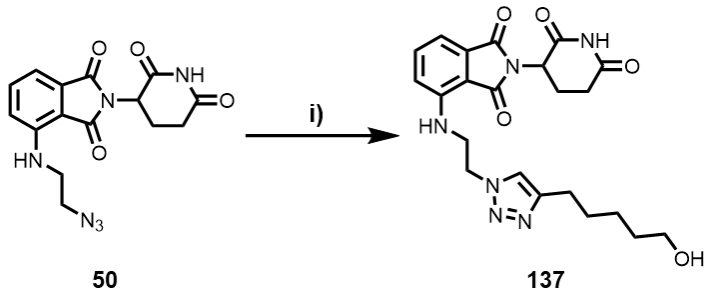

*Scheme 4.2 Synthesis of the control compound **137**. Reagents and conditions: i) $CuSO_4$, sodium ascorbate, THF, water, 75%.*

PROTACs **138** and **140** were synthesised analogously to **9** where the corresponding sulfones (**68** and **145**) were reacted with the formamide **37** to afford alkynes **144** and **146**. **144** and **146** were subsequently reacted with the azide **50** under Click conditions to afford **138** and **140** (Scheme 4.3, Scheme 4.4). Finally, **139** was synthesised using the same Buchwald-Hartwig chemistry applied to the synthesis of **79** (Chapter 3.4.3). After the chloro-quinazoline **147** had been reacted with aniline **34**, a Click reaction was performed, affording **139** (Scheme 4.5)**.**

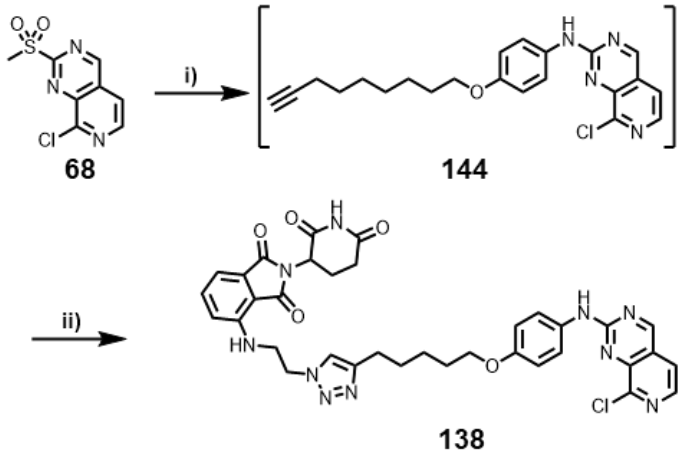

68 144 138

*Scheme 4.3 Synthesis of PROTAC **138**. Reagents and conditions: i) NaH, **37**, THF. ii) **50**, $CuSO_4$, sodium ascorbate, THF, water, 36%.*

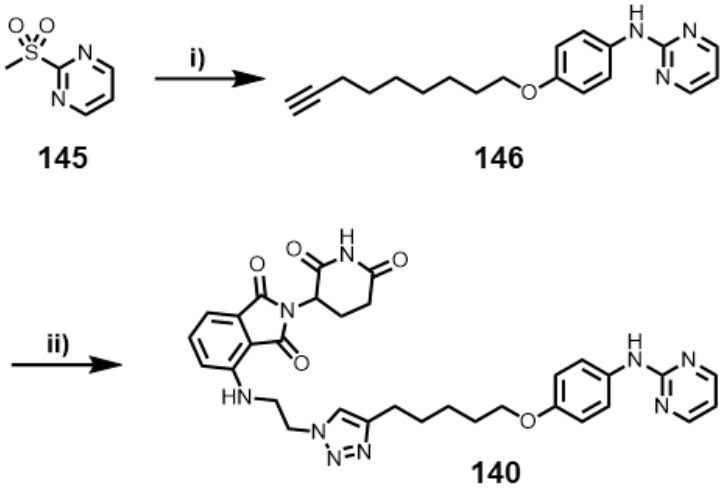

145 146 140

*Scheme 4.4 Synthesis of PROTAC **140**. Reagents and conditions: i) NaH, **37**, THF, 25%. ii) **50**, $CuSO_4$, sodium ascorbate, THF, water, 36%.*

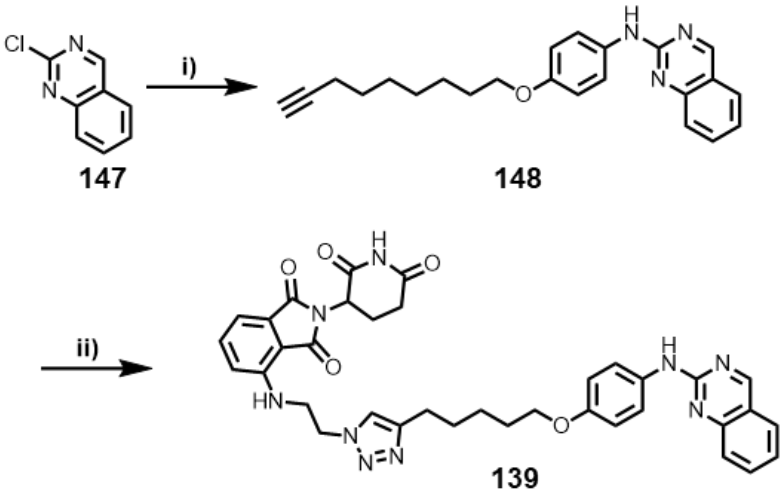

147 148 139

*Scheme 4.5 Synthesis of PROTAC **139**. Reagents and conditions: i) **34**, XPhos, Cs_2CO_3, DMF, $Pd(dba)_3$, 90 ˚C, 30 min. ii) **50**, $CuSO_4$, sodium ascorbate, THF, water, 30%.*

4.5 Conclusion and Future Work

Successful validation of the screened library compounds **1**-**9** confirmed AURKA degradation of 3 of the 9 PROTACs (**3**, **6**, **9**) with a preference towards the n=5 linker length and flat SAR around warhead alterations. Although longer linkers were preferred, we do not know the ideal length for AURKA degradation as we did not explore beyond n=5. Longer linkers would need to be synthesised to identify the ideal length. Then, further optimisation could take place introducing rigidity and solubilising groups to increase both potency and solubility (Figure 4.10). In addition to length and rigidity, we hypothesise the degradation of **9** or **135** could be improved through addition of an amide linkage to the warhead. Commonly an amide is used to append the linker to **alisertib**-based PROTACs and often affords potent binders of AURKA, potentially translating to improved degradation (Figure 4.10).[133,138]

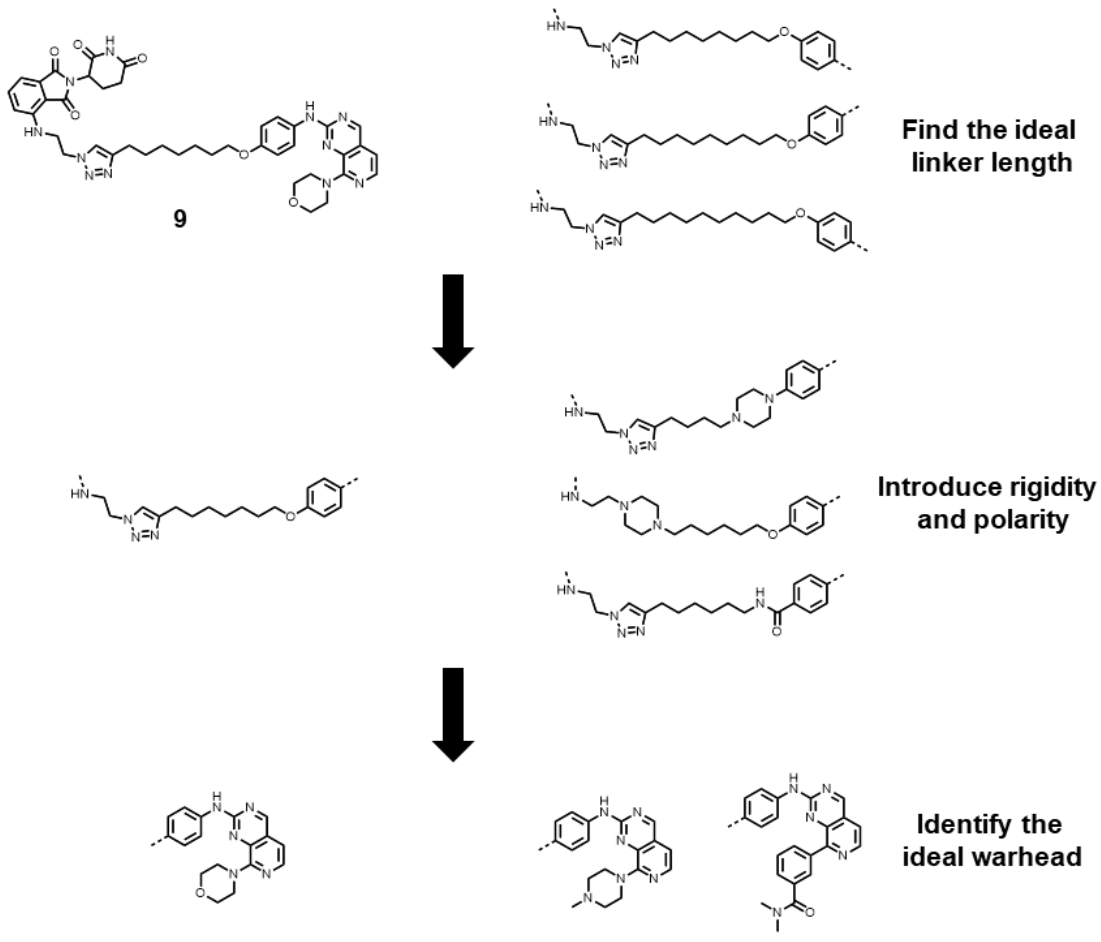

*Figure 4.10 Key steps needed to further optimise **9** to improve degradation potency and solubility. Longer linkers have not been tested for degradation against AURKA and may improve potency of the compounds. Linker modifications should both improve solubility and may lock the PROTAC in its active conformation. Warhead alterations may be able to increase binding affinity towards AURKA and therefore improve degradation potency.*

We tested if the linker and E3 ligase combination used on **9** could be utilised on other AURKA binding scaffolds, discovering that degradation was negatively affected. We believe this may be a result of cLogD changes, influencing intracellular free concentrations. It is currently unclear whether degradation correlated with AURKA binding affinity but could be elucidated through further SAR exploration around the warhead of **9**. Truncation of the warhead identified the necessity of the morpholine functionality in **9** (Figure 4.9) the morpholine, therefore, must be forming meaningful interactions within the AURKA pocket. As this is a synthetically tractable area of the molecule to explore further substitutions, modifications could gain AURKA binding affinity and may translate to degradation potency (Figure 4.10). Despite the use of warheads <100 molecular weight with no notable binding towards AURKA, degradation was still observed, highlighting the high propensity AURKA has for CRBN-mediated degradation. Similar to molecular glues, the truncated compounds show no affinity towards AURKA yet degrade them in the μM range.

An unexpected 26-fold increase in binding affinity of **9** was seen when compared to the alkyne-warhead **46**, suggesting a role of either the triazole or IMiD in binding AURKA (Table 4.4). However, the IMiD-triazole **137** showed no notable affinity towards AURKA (Table 4.5). We believed this area to be solvent exposed and therefore would require either SAR exploration of the triazole and IMiD, or a co-crystal structure to determine the cause of the increased binding affinity.

Chapter 5: Conclusions and Future Work

Although potent PROTACs have been developed for a wide range of target classes, a high affinity and selective binder is required, limiting the scope of PROTAC discovery to targets that have been extensively explored previously. In an attempt to increase the degradable kinome, we implemented a global proteomics screen of small and potentially promiscuous degraders, identifying targets to validate and explore further.

Through utilisation of a truncated **BOS172722** scaffold, a ligand known to bind multiple kinases early in its development and with favourable physicochemical properties, 14 PROTACs (**1**-**9**) were synthesised and triaged through global proteomics. The modular synthesis of multiple PROTACs was achieved through the utilisation of Click chemistry, allowing for a convergent final reaction. Striking linker length selectivity was observed for the two significantly degraded kinases, NEK9 and AURKA, with flat SAR seen with small amine warhead changes. The results suggest an excellent linker length starting point has been identified, along with a warhead that can tolerate small changes. The screening results highlight that small warheads can confer observable and selective degradation in proteomics and highly elaborated ligands may not always be required.

The proteomics was validated through Western blotting, confirming the SAR observed from the screen. Strangely, further NEK9 degradation revealed a lack of neddylation and CRBN dependence for **6**. This was extremely unexpected as rescue of degradation was observed with methylated IMiD control **73**, having reduced affinity for CRBN. We conclude that further mechanistic studies are required to identify the mechanism by which NEK9 is degraded. Elucidation of the mechanism of degradation may either be achieved through identification of structural features of the PROTACs required to maintain degradation, or more directly through an E3 ligase component siRNA screen.

Three AURKA PROTACs (**3**, **6**, **9**) of the same linker length were identified and validated, showing potent and selective degradation. Despite the use of the same exit vector whilst performing warhead alterations, other AURKA binding scaffolds decreased degradation potency. This is likely a result of the decreased binding affinity of the PROTACs towards AURKA. Surprisingly, PROTAC **9**

showed high monovalent affinity for AURKA that was significantly reduced upon removal of the IMiD or triazole moiety. We hypothesise these functionalities are forming interactions on the surface of AURKA, as this exit vector must be solvent exposed. Truncation of the warhead led to decreased degradation potency (μM range), however, no binding towards AURKA was detected. This is further evidence to demonstrate that it is a productive ternary complex driving the degradation of AURKA with these PROTACs. To determine if the selective degradation of AURKA was a result of warhead selectivity a KINOMEscan^{TM} was performed, showing a lack of selectivity of the warhead, and suggests ternary complex productivity is driving selective degradation of AURKA.

The NEK9 and AURKA PROTACs discovered are excellent hit degraders that can be readily optimised from multiple tractable areas. We envision the described proteomics screen being applicable to fragment sized warheads, able to bind proteins outside the kinome. This approach has the potential to drastically increase the degradable kinome and proteome, whilst driving the molecular weight and property space of PROTACs to a more desirable area.

Chapter 6: Experimental

6.1 Proteomics analysis

6.1.1 Sample Preparation for TMT Labelling

Cell pellets were dissolved in 150 µL lysis buffer containing 1% sodium deoxycholate (SDC), 100 mM triethylammonium bicarbonate (TEAB), 10% isopropanol, 50 mM NaCl and Halt protease and phosphatase inhibitor cocktail (100X) (Thermo, #78442) on ice, assisted with pulsed probe sonication for 15 sec. Samples were subsequently boiled at 90 °C for 5 min on a thermomixer and were re-sonicated for 5 sec. Protein concentration was measured with the Quick Start™ Bradford Protein Assay (Bio-Rad) according to manufacturer's instructions. Aliquots containing 30 µg of total protein were prepared for trypsin digestion. Samples were reduced with 5 mM tris-2-carboxyethyl phosphine (TCEP) for 1 h at 60 °C and alkylated with 10 mM Iodoacetamide (IAA) for 30 min in dark. Proteins were then digested by adding 75 ng/µL trypsin (Pierce) to each sample and incubating overnight. The resultant peptides were labelled with the TMTpro-16plex or TMT 11plex reagents (Thermo) according to manufacturer's instructions and were combined in equal amounts to a single tube. The combined sample was SpeedVac dried at 45 ˚C.

6.1.2 Basic Reversed-Phase Peptide Fractionation and LC-MS Analysis

Offline high pH Reversed-Phase (RP) peptide fractionation was performed with the XBridge C18 column (2.1 x 150 mm, 3.5 µm, Waters) on a Dionex Ultimate 3000 HPLC system. Mobile phase A was 0.1% ammonium hydroxide and mobile phase B was acetonitrile, 0.1% ammonium hydroxide. The TMT labelled peptide mixture was reconstituted in 200 mL mobile phase A and was fractionated using a multi-step gradient elution method at 0.2 mL/min as follows: for 5 minutes isocratic at 5% B, for 35 min gradient to 35% B, gradient to 80% B in 5 min, isocratic for 5 minutes and re-equilibration to 5% B. Fractions were collected every 42 sec, vacuum dried and orthogonally pooled into 12 fractions.

LC-MS analysis was performed on the Dionex Ultimate 3000 UHPLC system coupled with the Orbitrap Lumos Mass Spectrometer (Thermo Scientific). Each peptide fraction was reconstituted in 40 µL 0.1% formic acid and 10 µL were

loaded to the Acclaim PepMap 100, 100 µm × 2 cm C18, 5 µm, 100 Å trapping column at 10 µL/min flow rate of 0.1% formic acid loading buffer. The sample was then subjected to a gradient elution on the EASY-Spray C18 capillary column (75 µm × 50 cm, 2 µm) at 50 °C. Mobile phase A was 0.1% formic acid and mobile phase B was 80% acetonitrile, 0.1% formic acid. The gradient separation method at flow rate 300 nL/min was as follows: for 90 min gradient from 5%-38% B, for 10 min up to 95% B, for 5 min isocratic at 95% B, re-equilibration to 5% B in 5 min, for 10 min isocratic at 10% B. Precursors between 375-1,500 HRMS (ESI +ve): were selected with mass resolution of 120 k with the top speed mode in 3 sec and were isolated for HCD fragmentation with quadrupole isolation width 0.7 Th. Collision energy was set at 36%. Targeted precursors were dynamically excluded for further isolation and activation for 45 seconds with 7 ppm mass tolerance.

6.1.3 Database Search and Protein Quantification

The SequestHT search engine was used to analyse the acquired mass spectra in Proteome Discoverer 2.4 (Thermo Scientific) for protein identification and quantification. The precursor mass tolerance was set at 20 ppm and the fragment ion mass tolerance was set at 0.02 Da. Spectra were searched for fully tryptic peptides with maximum 2 miss-cleavages. TMTpro at N-terminus/K and Carbamidomethyl at C were defined as static modifications. Dynamic modifications included oxidation of M and Deamidation of N/Q. Peptide confidence was estimated with the Percolator node. Peptides were filtered for q-value<0.01 based on decoy database search. All spectra were searched against reviewed UniProt human protein entries. The reporter ion quantifier node included a TMTpro quantification method with an integration window tolerance of 15 ppm at the MS2 level. Peptide quantification was corrected for isotopic impurities. Only unique peptides were used for quantification, considering protein groups for peptide uniqueness. Peptides with average reporter signal-to-noise >3 were used for protein quantification. Statistical analysis for differentially regulated proteins was performed in the Perseus platform. Significant hits were filtered for two-sample t-test p-value <0.01 (drug vs DMSO) and log2fold-change<-0.35 as well as for ANOVA FDR<0.05. Volcano plots were plotted in GraphPad Prism 9.

6.2 Western Blotting

All Westerns blots used HCT116, HEK293T, or HEK293T CRBN$^{-/-}$ cells that were incubated at 37 ˚C with 5% CO_2 in Dulbecco's Modified Eagle's medium. 300,000 cells were plated in each well of a 6 well plate in 2 mL media and treated with the indicated compound and doses for the specified time. Cells were washed with ice cold PBS and lysed in D0.4 lysis buffer (20 mM HEPES pH 7.5, 10% Glycerol, 0.4 M KCl, 0.4% Triton X-100, 15 mM EDTA) containing 1X protease inhibitor (cOmplete™, Mini, EDTA-free Protease Inhibitor Cocktail, Sigma, 4693159001, diluted from 30x stock made up in water) + 1X phosphatase inhibitors (PhosSTOP, Sigma, 4906845001, diluted from 30x stock made up in water). Protein quantification was performed using 1 µL of sample in 200 µL 1x Protein Assay Dye Reagent Concentrate (Bio-Rad, #5000006) along with duplicate blank samples in a 96 well plate format in duplicate. Absorbance at 590 nm was measured and compared to a BSA standard curve. NuPAGE LDS Sample buffer (Thermo, NP0008) and NuPAGE Sample Reducing Agent (Thermo, NP0009) were added at 1x final concentration and samples boiled for 5 mins at 90°C. NuPAGE 4-12% Bis-Tris gels, 1.5 mm (15 wells) were used for all Western blots. Gels were clipped into XCell SureLock™ Mini-Cell Electrophoresis System tanks and 1X NuPAGE MOPS running buffer was added. Sample was added to relevant lanes, with 10µl of SeeBlue™ Plus2 Pre-stained Protein Standard (Thermo, LC5925) as a marker. Equal amounts of protein were loaded onto the gel, which was run at 150V for 90 min. A square of Immobilon-P PVDF Membrane (Millipore, IPVH00010) was equilibrated in MeOH and a stack was assembled, equilibrating all components in 1X NuPAGE Transfer Buffer (Thermo, NP00061). A stack contains sponge, two squares of Whatman paper, membrane, gel, two squares of Whatman paper, sponge. Protein was transferred in Mini Trans-Blot® Cell (Bio-Rad, 1703930) at 100V for 90 mins. Antibody was added at desired concentration (1 in 1000 for NEK9 (ThermoFisher Scientific, MA5-26550), 1 in 5000 for GAPDH (Cell Signalling, 97166), 1 in 2000 for Aurora kinase A (Cell Signalling D3E4Q)), in 5% BSA/TBST (1X Tris-Buffered Saline + 0.05% Tween-20), and incubated overnight on a rocker at 4°C. Blots were washed for 3 x 5 mins in TBST, followed addition of HRP-conjugated secondary antibody, at 1:5000 (mouse:BioRad

103005, rabbit:BioRad 5213-2504) in 5% milk/TBST and incubated on a rocker for 1h at room temperature. Blots were washed for 3 x 5 mins in TBST and developed using Pierce™ ECL Western Blotting Substrate (Thermo, 32106) and visualised using LI-COR. Unedited blots containing the marker lane are available on request.

6.3 TaqMan Assay

HCT116 cells were incubated at 37 ˚C with 5% CO_2 in Dulbecco's Modified Eagle's medium. 300,000 cells were plated in each well of a 6 well plate in 2 mL media and treated with the indicated compound and doses for the specified time. Cells were harvested and RNA was extracted using the RNeasy kit (Qiagen). cDNA was generated from 1 µg of RNA (calculated using Nanodrop) using Thermo High Capacity cDNA Reverse Transcription Kit. cDNA was diluted 1:10 and 2 µL of cDNA was added into wells of MicroAmp Optical 384-Well Reaction Plate (Thermo 4309849) in triplicate for each sample. 18 µL of TaqMan Probe mix (20X TaqMan probe (either GAPDH (Hs02758991_g1) or NEK9 (Hs00929598_m1), 2X TaqMan Master Mix, RAase-free water) was added into triplicate wells and mixed. Samples were read on a Viia-7 Real Time PCR System and made relative to both DMSO and the GAPDH control.

6.4 Ubiquitin Pull-Down

HCT116 cells were incubated at 37 ˚C with 5% CO_2 in Dulbecco's Modified Eagle's medium. 1,200,000 cells were plated in 10 ml plates with 8 ml of media and treated with the indicated compound and doses for the specified time. Cells were washed with ice cold PBS and lysed (50mM Tris-HCl, pH 7.5, 0.15M NaCl, 1mM EDTA, 1% NP-40, 10% glycerol) containing 1X protease inhibitor (cOmplete™, Mini, EDTA-free Protease Inhibitor Cocktail, Sigma, 4693159001, diluted from 30x stock made up in water) + 1X phosphatase inhibitors (PhosSTOP, Sigma, 4906845001, diluted from 30x stock made up in water). Equilibrated control agarose was added to the lysate and incubated for 30 min at 4 ˚C. Input sample was removed and ran following (**Western blotting protocol 6.2**). The appropriate amount of cell lysate was added to the Agarose-TUBEs for 1 h at 4 ˚C. Beads were washed with TBS-T and resuspended in

SDS reducing sample buffer. Western blot was ran following **Western blotting protocol 6.2.**

6.5 CellTitre Glo GI50 Determination

200 HCT116 cells were plated in all except one row of a 384 well plate where media alone was plated and incubated at 37 ˚C with 5% CO_2 in Dulbecco's Modified Eagle's medium. After one day cells were treated with the indicated compound and doses for the specified time and a T_0 plate was taken. Addition of 25 µl CellTitre-Glo reagent was followed by 2 mins of mixing before luminescence was measured.

6.6 Chemistry

All anhydrous solvents and reagents were obtained from commercial suppliers (Alfa Aesar, Apollo, Fisher Scientific, Fluorochem, Sigma Aldrich, Thermo Scientific and VWR) and used without further purification. All reactions were carried out under a positive pressure of N_2 and moisture sensitive reagents transferred via syringe. All compounds reported at >95% purity unless otherwise stated.

Analytical thin layer chromatography (TLC) was performed on pre-coated aluminium sheets (60 F245 nm, Merck) and visualised by short-wave UV light or a ninhydrin dip followed by heat. Semi-automated flash column chromatography was carried out using a Biotage purification system, utilising Biotage Sfar duo cartridges (silica solid phase for normal phase and C18 modified silica for reverse phase).

6.6.1 NMR

NMR data was collected on a Bruker Avance NEO 600 spectrometer equipped with a 5 mm TCI-Cryo probe. The 1H and 13C spectra were referenced to the internal deuterated solvent. All NMR data were acquired at the temperature of 298 K. Data was acquired and processed using Bruker Topspin 4.0. NMR data was also collected on a Bruker Avance 500 spectrometer equipped with a 5 mm BBO probe. The ^{1}H and ^{13}C spectra were referenced to the internal deuterated solvent. All NMR data were acquired at the temperature of 295 K. Data was acquired and processed using Bruker Topspin 2.1. The ^{1}H-NMR spectrum was

acquired using a Bruker standard 1D zg30 pulse sequence with 16 scans. The sweep width was 20.5 ppm, and the FID contained 64k time-domain data points. The ^{13}C-NMR spectrum was acquired using a Bruker zgpg30 pulse sequence with 1024 scans and 2 prior dummy scans. The sweep width was 238.9 ppm, and the FID contained 64k time-domain data points. Chemical shifts are quoted to 0.1 ppm. Atom numbering is arbitrary and does not refer to IUPAC nomenclature.

6.6.2 LCMS and HRMS

LCMS and HRMS analyses were performed on both an Agilent 1260 Infinity II series UPLC and diode array detector coupled to a 6530 Quadrupole time of flight mass spectrometer with Agilent Jet Stream ESI source, and a Waters Acquity UPLC and diode array detector coupled to a Waters G2 QToF mass spectrometer fitted with a multimode ESI/APCI source.

Agilent 1260 Infinity II series UPLC:

Positive and negative mode LC/MS and HRMS analysis was performed on an Agilent 1260 Infinity II series UPLC and diode array detector coupled to a 6530 Quadrupole time of flight mass spectrometer with Agilent Jet Stream ESI source. Analytical separation was carried out at 40 ˚C on a Phenomenex Kinetex C18 column (30 x 2.1 mm, 2.6 µm, 100 Å) using a flow rate of 0.6 mL/min in a 2 minute gradient elution with detection at 254, 280 and 214 nm. The mobile phase was a mixture of methanol (solvent A) and water (solvent B), both containing formic acid at 0.1%. Gradient elution was as follows: 10:90 (A/B) to 90:10 (A/B) over 1.25 min, 90:10 (A/B) for 0.5 min, and then reversion back to 10:90 (A/B) over 0.15 min, finally 10:90 (A/B) for 0.1 min.

Waters Acquity UPLC:

Analytical separation was carried out at 30˚C on a Phenomenex Kinetex C18 column (30 x 2.1 mm, 2.6 µm, 100 Å) using a flow rate of 0.3 mL/min in a 4 minute gradient elution with detection at 254 nm. The mobile phase was a mixture of methanol (solvent A) and water (solvent B), both containing formic acid at 0.1%. Gradient elution was as follows: 10:90 (A/B) to 90:10 (A/B) over 3 min, 90:10 (A/B) for 0.5 min, and then reversion back to 10:90 (A/B) over 0.3 min, finally 10:90 (A/B) for 0.2 min.

HRMS references: caffeine $[M+H]^+$ 195.08765; hexakis (2,2difluoroethoxy) phosphazene $[M+H]^+$ 622.02896; and hexakis(1*H*,1*H*,3*H*tetrafluoropnetoxy) phophazene $[M+H]^+$ 922.00980.

General Procedure 1 – Chloride S_NAr

To a solution of aryl chloride (1 eq) in NMP (0.2 M) was added the relevant amine (3 eq). The reaction was heated to 80 °C in a sealed microwave vial for 18 h before being quenched with sat. aq. sodium bicarbonate and extracted with EtOAc (3 times). The organic layers were combined, washed with water, brine, and concentrated under reduced pressure affording the corresponding sulphides.

General Procedure 2 – Sulfone oxidation

Sulfide (1 eq) was dissolved in 1:1 MeOH:H_2O (0.2 M) and stirred at rt. OXONE (2.5 eq) was added and the mixture was stirred for 3 h at rt. The water layer was extracted with EtOAc (3 times), the organic layers were combined, washed with brine, and solvent was removed *in vacuo.* The residue was dissolved in MeOH and passed through an SCX-2 column and washed with MeOH. Product was eluted with 3.5 M ammonia in MeOH and solvent was removed *in vacuo* affording the corresponding sulfone.

General Procedure 3 a-c – Formamide synthesis

To a solution of *p*-nitrophenol (1 eq), alcohol (1 eq) and triphenylphosphine (1.15 eq) in THF (0.3 M) at 0 °C was added DIAD (1.1 eq). The reaction was allowed to warm to rt and stirred for 2 h. Water was added and was extracted with EtOAc (3 times). The organic layers were combined, washed with aq. 1M NaOH, brine, and solvent was removed *in vacuo*. No characterisation is reported for these products as the PPh_3O overpowers all other signals in the spectra. Product was used without further purification.

The corresponding crude nitro compound (1 eq), iron powder (10 eq) and ammonium chloride (10 eq) were dissolved in 1:1 EtOH:water (0.2 M) then heated to 80 °C for 3 h. After cooling, the mixture was filtered through Celite and washed with MeOH. Solvent was removed in *vacuo* and crude product was dissolved in EtOAc. This was washed with water, brine, dried over $MgSO_4$, and solvent was removed *in vacuo*. The residue was dissolved in MeOH and passed

through an SCX-2 column and washed with MeOH. Product was eluted with 3.5 M ammonia in MeOH and solvent was removed *in vacuo* affording the corresponding crude aniline.

The corresponding aniline (1 eq) was dissolved in Formic acid (0.2 M) and heated to 80 °C for 18 h. After cooling to room temperature, the formic acid was removed *in vacuo* and the residue was dissolved in EtOAc. Water was added and was extracted with EtOAc (3 times). The organic layers were combined, washed with brine, dried over $MgSO_4$, and solvent was removed *in vacuo*. Crude product was purified using column chromatography (EtOAc:c-hex 0% - 70%) affording the corresponding formamide.

General Procedure 4 - Sulfone S_NAr

A solution of sulfone (1 eq) and formamide (1.2 eq) in THF (0.1 M) was cooled to 0 °C and sodium hydride (2 eq) was added. The reaction was stirred at rt overnight. Water was added to quench the reaction and was extracted with EtOAc (3 times). The organic layers were combined, washed with brine, dried over $MgSO_4$ and solvent was removed in *vacuo*. Crude product was dissolved in MeOH and 3 drops of formic acid were added. This mixture was passed through an SCX-2 column and washed with MeOH. Product was eluted with 3.5 M ammonia in MeOH and solvent was removed *in vacuo* affording the corresponding alkyne.

General Procedure 5 - Click reaction

Alkyne (1 eq), azide (1 eq), sodium ascorbate (1.2 eq), and copper sulphate (0.1 eq) were dissolved in 1:1 water:THF (0.05 M) and stirred at rt for 18 h. Water was added and was extracted with DCM (3 times). The organic layers were combined, washed with brine, and solvent was removed *in vacuo*. Product was purified using column chromatography (MeOH:DCM 0 - 10% then a 30% flush) to afford the corresponding triazole.

General Procedure 6 a-c – Piperazine synthesis

DMSO (3.5 eq) in DCM (4 M) was added dropwise to a solution of oxalyl chloride (2 eq) in DCM (0.3 M) at –78 °C. The reaction was stirred for 10 minutes and then a solution of alcohol (1 eq) in DCM (2 mL,) was added slowly. After 45 minutes triethylamine (5 eq) was added at –78 °C. After stirring at –78 °C for 30

minutes, the mixture was warmed to rt and stirred for a further 30 minutes. The reaction was quenched with water and the organic phase were separated. The organic layer was washed with 1M aq. HCl, $NaHCO_3$ (sat.) and brine. The organic phase was carefully concentrated under reduced pressure. The crude aldehyde was submitted to the next step without purification assuming 100% yield. Aldehyde presence was determined through identification of a downfield peak in the ^1H NMR spectra.

Crude aldehyde (1 eq), t-Butyl-1-piperazinecarboxylate (1 eq) and sodium triacetoxy borohydride (4 eq) were dissolved in DCM (0.2 M) and stirred at rt overnight. The reaction was quenched with water (10 mL) and extracted with DCM (3 times). The organic layers were combined, washed with brine, dried over $MgSO_4$, and solvent was removed in *vacuo*. Crude product was dissolved in MeOH and 2 drops of formic acid were added. This mixture was then passed through a SCX-2 column and washed with MeOH. Product was eluted with 3.5 M ammonia in MeOH and was used in the next step without further purification assuming 100% yield.

Boc protected amine (1 eq) was dissolved in DCM (0.2 M) to which HCl in dioxane (4 M, 10 eq) was added. The reaction was allowed to stir for 18 h at rt. The reaction was quenched with sat. aq. $NaHCO_3$ (20 mL) and extracted with DCM (3 times). The organic layers were combined and solvent was removed *in vacuo*. Crude product was dissolved in MeOH and 3 drops of formic acid were added. This mixture was passed through an SCX-2 column and washed with MeOH. Product was eluted with 3.5 M ammonia in MeOH and solvent was removed *in vacuo* affording the corresponding alkyne.

Methyl 5-[(*E*)-2-ethoxyvinyl]-2-methylsulfanyl-pyrimidine-4-carboxylate (17)

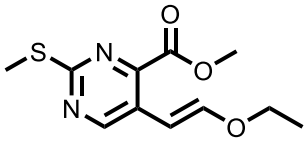

A solution of 2-[(E)-2-ethoxyvinyl]-4,4,5,5-tetramethyl-1,3,2-dioxaborolane (703 mg, 3.55 mmol), methyl-5-bromo-2-(methylsulfanyl)-4-pyrimidinecarboxylate (623 mg, 2.37 mmol), $Pd(dppf)Cl_2 \cdot DCM$ (97 mg, 0.12 mmol) and aq. $NaHCO_3$

(2M) (2 mL) in THF (6 mL) was heated to 65 °C for 18 h. The reaction was quenched with brine and extracted with EtOAc. The organic layers were combined, washed with water and brine, and concentrated under reduced pressure. The residue was purified by flash column chromatography (EtOAc:c-hex 0-10%) to afford the title product (229 mg, 38%, 0.90 mmol)s. ^{1}H NMR (500 MHz, DMSO-d_6) δ 8.99 (s, 1H), 7.39 (d, J = 12.9 Hz, 1H), 6.01 (d, J = 12.9 Hz, 2H), 3.94 (q, J = 7.0 Hz, 2H), 3.89 (s, 3H), 2.52 (s, 3H), 1.26 (t, J = 7.0 Hz, 3H); ^{13}C NMR (126 MHz, DMSO-d_6) δ 167.8, 165.4s , 156.5, 152.4, 151.3, 124.6, 97.6, 66.4, 53.3, 15.1, 14.1; HRMS (ESI +ve): $C_{11}H_{15}N_2O_3S$ $[M+H]^+$: 255.0798 (Found: 255.0801). Characterisation consistent with the literature.[101]

2-methylsulfanyl-7*H*-pyrido[3,4-*d*]pyrimidin-8-one (18)

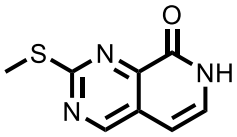

Methyl 5-[(*E*)-2-ethoxyvinyl]-2-methylsulfanyl-pyrimidine-4-carboxylate (229 mg, 0.90 mmol) was treated with ammonia in MeOH (7 M, 5 mL) and heated to 85 °C for 18 h. The reaction was concentrated under reduced pressure, the residue was suspended in toluene (5 mL) and *p* -toluenesulfonic acid monohydrate (17 mg, 0.09 mmol) was added. The reaction was heated to 90 °C for 2 h. The reaction was concentrated under reduced pressure and the residue purified by column chromatography (MeOH:DCM 0–5%) to afford the title product (103 mg, 59%, 0.53 mmol). ^{1}H NMR (500 MHz, DMSO-d_6) δ 11.87 (s, 1H), 9.21 (s, 1H), 7.29 (dd, J = 6.9, 5.3 Hz, 1H), 6.58 (d, J = 6.9 Hz, 1H), 2.60 (s, 3H); ^{13}C NMR (126 MHz, DMSO-d_6) δ 169.1, 159.9, 146.8, 130.8, 126.0, 101.3, 14.2, C=O not observed; HRMS (ESI +ve): $C_8H_8N_3OS$ $[M+H]^+$: 194.0383 (Found: 194.0391). Characterisation consistent with the literature.[101]

8-chloro-2-methylsulfanyl-pyrido[3,4-*d*]pyrimidine (19)

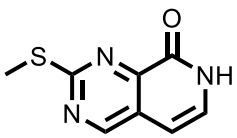

A solution of 2-methylsulfanyl-7*H*-pyrido[3,4-*d*]pyrimidin-8-one (103 mg, 0.53 mmol) in phosphorus oxychloride (5 mL) was heated to 70 °C for 18 h. The reaction was concentrated under reduced pressure and partitioned between EtOAc and sat. aq. $NaHCO_3$. The aqueous layer was extracted with EtOAc and the organic layers were combined, washed with water, brine, and concentrated under reduced pressure. The residue was purified by flash column chromatography (EtOAc:c-hex 0–20%) affording the title product (45 mg, 40%, 0.21 mmol). ^{1}H NMR (500 MHz, DMSO-d_6) δ 9.60 (s, 1H), 8.48 (d, *J*= 5.3 Hz, 1H), 8.02 (d,*J*= 5.3 Hz, 1H), 2.68 (s, 3H); ^{13}C NMR (126 MHz, DMSO-d_6) δ 171.7, 162.09, 149.8, 143.1, 142.4, 126.8, 120.7, 14.4; HRMS (ESI +ve): $C_8H_7ClN_3S$ $[M+H]^+$: 212.0044 (Found: 212.0053). Characterisation consistent with the literature.[101]

_N,N_-dimethyl-2-methylsulfanyl-pyrido[3,4-*d*]pyrimidin-8-amine (20)

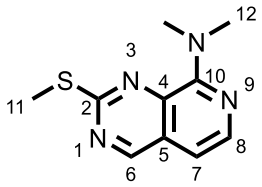

Product was synthesised following **general procedure 1** using 5.6 M dimethylamine in EtOH (0.27 mL, 1.51 mmol) and 8-chloro-2-methylsulfanyl-pyrido[3,4-*d*]pyrimidine, affording 144 mg (92%, 0.65 mmol) of the title product. ^{1}H NMR (500 MHz, DMSO-d_6) δ 9.27 (s, 1H, H6), 8.08 (d, *J* = 5.4 Hz, 1H, H8), 7.07 (d, *J* = 5.4 Hz, 1H, H7), 3.41 (s, 6H, H12), 2.60 (s, 3H, H11); ^{13}C NMR (126 MHz, DMSO-d_6) δ 166.2 (C2), 160.9 (C6), 156.1 (C10), 142,5 (C8), 138.2 (C4), 126.9 (C5), 108.3 (C7), 41.9 (C12), 14.4 (C11); HRMS (ESI +ve): $C_{10}H_{13}N_4S$ $[M+H]^+$: 221.0855 (Found: 221.0855).

8-chloro-2-methylsulfanyl-pyrido[3,4-*d*]pyrimidine (21)

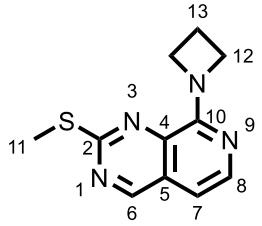

Product was synthesised following **general procedure 1** using azetidine (105 µL, 1.57 mmol) and 8-chloro-2-methylsulfanyl-pyrido[3,4-*d*]pyrimidine, affording

136 mg (97%, 0.59 mmol) of the title product. ^{1}H NMR (500 MHz, DMSO-d_6) δ 9.22 (s, 1H, H6), 7.99 (d, J = 5.5 Hz, 1H, H8), 6.95 (d, J = 5.5 Hz, 1H, H7), 4.44 (br s, 4H, H12), 4.46 (br s, 4H, H12), 2.58 (s, 3H, H11), 2.54-2.60 (m, 2H, H13); ^{13}C NMR (126 MHz, DMSO-d_6) δ 167.1 (C2), 160.2 (C6), 155.4 (C10), 143.2 (C8), 137.8 (C4), 125.9 (C5), 106.9 (C7), 17.8 (C13), 14.4 (C11), C12 not observed; HRMS (ESI +ve): $C_{11}H_{13}N_4S$ $[M+H]^+$: 233.0855 (Found: 233.0863).

8-chloro-2-methylsulfanyl-pyrido[3,4-*d*]pyrimidine (22)

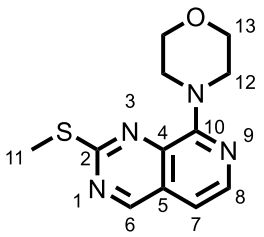

Product was synthesised following **general procedure 1** using morpholine (137 µL, 1.57 mmol) and 8-chloro-2-methylsulfanyl-pyrido[3,4-*d*]pyrimidine, affording 1.13 g (80%, 0.48 mmol) of the title product. ^{1}H NMR (500 MHz, DMSO-d_6) δ 9.35 (s, 1H, H6), 8.15 (d, J = 5.4 Hz, 1H, H8), 7.25 (d, J = 5.4 Hz, 1H, H7), 3.94 - 3.90 (m, 4H, H12), 3.83 – 3.76 (m, 4H, H13), 2.56 (s, 3H, H11); ^{13}C NMR (126 MHz, DMSO-d_6) δ 167.0 (C2), 161.5 (C6), 156.0 (C10), 142.2 (C8), 138.3 (C4), 126.7 (C5), 110.9 (C7), 66.7 (C13), 49.3 (C12), 14.3 (C11); HRMS (ESI +ve): $C_{12}H_{15}N_4OS$ $[M+H]^+$: 263.0961 (Found: 263.0958).

***N,N*-dimethyl-2-methylsulfonyl-pyrido[3,4-d]pyrimidin-8-amine (23)**

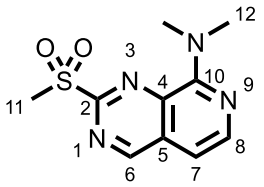

Product was synthesised following **general procedure 2** using *N,N*-dimethyl-2-methylsulfanyl-pyrido[3,4-*d*]pyrimidin-8-amine (128 mg, 0.58 mmol), affording 92 mg (63%, 0.36 mmol) of the title product. ^{1}H NMR (500 MHz, DMSO-d_6) δ 9.68 (s, 1H, C6), 8.33 (d, J = 5.3 Hz, 1H, C8), 7.21 (d, J = 5.3 Hz, 1H, C7), 3.50 (s, 6H, C12), 3.46 (s, 3H, C11). ^{13}C NMR (126 MHz, DMSO-d_6) δ 162.7 (C6), 150.2 (C2), 156.6 (C10), 146.7 (C8), 135.8 (C4), 131.2 (C5), 107.3 (C7), 42.1 (C12), 39.7 (C11); HRMS (ESI +ve): $C_{10}H_{12}N_4O_2S$ $[M+H]^+$: 253.0754 (Found: 253.0754).

8-(azetidin-1-yl)-2-methylsulfonyl-pyrido[3,4-*d*]pyrimidine (24)

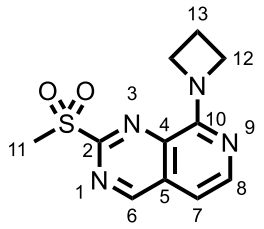

Product was synthesised following **general procedure 2** using 8-chloro-2-methylsulfanyl-pyrido[3,4-*d*]pyrimidine (136 mg, 0.59 mmol), affording 83 mg (54%, 0.31 mmol) of the title product. ^{1}H NMR (600 MHz, MeOD-d_4) δ 9.50 (s, 1H, H6), 8.19 (d, *J* = *5.7* Hz, 1H, H8), 7.07 (d, *J* = 5.7 Hz, 1H, H7), 4.60 (br s, 4H, H12), 3.44 (s, 3H, H11), 2.60-2.54 (m, 2H, H13); ^{13}C NMR (151 MHz, MeOD-d_4) δ 161.1 (C6), 158.2 (C2), 155.3 (C10), 146.4 (C8), 135.7 (C4), 129.1 (C5), 105.0 (C7), 38.3 (C11), 17.1 (C13); HRMS (ESI +ve): $C_{11}H_{13}N_4O_2S$ $[M+H]^+$: 265.0754 (Found: 265.0753)

4-(2-methylsulfonylpyrido[3,4-*d*]pyrimidin-8-yl)morpholine (25)

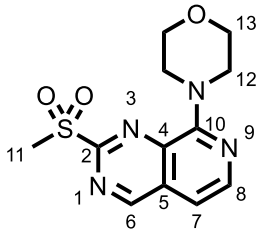

Product was synthesised following **general procedure 2** using 8-chloro-2-methylsulfanyl-pyrido[3,4-*d*]pyrimidine (127 mg, 0.48 mmol) affording 34 mg of the title product (24%, 0.12 mmol). ^{1}H NMR (600 MHz, MeOD-d_4) δ 9.62 (s, 1H, H6), 8.38 (d, *J* = 5.5 Hz, 1H, H8), 7.33 (d, *J* = 5.5 Hz, 1H, H7), 4.22 – 4.19 (m, 4H, H12), 3.93 – 3.90 (m, 4H, H13), 3.45 (s, 3H, H11); ^{13}C NMR (151 MHz, MeOD-d_4) δ 162.6 (C6), 159.5 (C2), 156.0 (C10), 145.6 (C8), 137.2 (C4), 131.0 (C5), 108.9 (C7), 49.3 (C13), 49.0 (C12), 38.3 (C11); HRMS (ESI +ve): $C_{12}H_{15}N_4O_3S$ $[M+H]^+$: 295.0859 (Found: 295.0857).

***N*-(4-pent-4-ynoxyphenyl)formamide (35)**

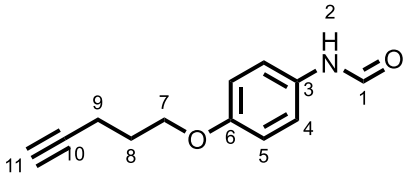

Product was synthesised following **general procedure 3a-c** using pent-4-yn-1-ol. Intermediate aniline **32** was seen by LCMS ([M+H]$^+$: 176.11) with a retention time of 0.37min. The title product (20 mg, 37%, 0.10 mmol) was afforded. Rotamers observed in NMR. ^{1}H NMR (500 MHz, $CDCl_3$) δ 8.52 (d, *J* = 11.5 Hz, 0.5H, H1), 8.34 (d, *J* = 1.85, 0.5H, H1), 7.84 (br d, *J* = 11.52, 0.5H, H2) 7.48 – 7.43 (m, 1H, C4), 7.25 (br s, 0.5H, H2), 7.07 – 7.01 (m, 1H, H4), 6.93 – 6.86 (m, 2H, H5), 4.08-4.05 (m, H7), 2.44-2.40 (m, 2H, H8), 2.06-1.96 (m, 2H, H9, 11); ^{13}C NMR (126 MHz, $CDCl_3$) δ 163.0 (C1), 158.8 (C1), 157.0 (C6), 156.1 (C6), 129.9 (C3), 129.5 (C3), 121.8 (C4), 121.7 (C4), 115.5 (C5), 114.9 (C5), 83.4 (C10), 83.3 (C10), 69.0 (C11), 68.9 (C11), 66.5 (C7), 66.4 (C7), 28.1 (C8), 28.1 (C8), 15.2 (C9), 15.1 (C9); HRMS (ESI +ve): $C_{12}H_{14}NO_2$ [M+H]$^+$: 204.1019 (Found: 204.1034).

***N*-(4-hept-6-ynoxyphenyl)formamide (36)**

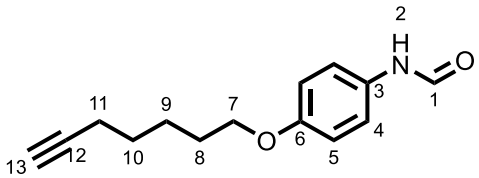

Product was synthesised following **general procedure 3a-c** using hept-6-yn-1-ol. Intermediate aniline **33** was seen by LCMS ([M+H]$^+$: 204.14) with a retention time of 1.05 min. The title product (59 mg, 12%, 0.26 mmol) was afforded. Rotamers observed in NMR. ^{1}H NMR (500 MHz, $CDCl_3$) δ 8.50 (d, *J* = 11.5 Hz, 0.5H, H1), 8.35 (d, *J* = 1.8 Hz, 0.5H, H1'), 7.47 – 7.43 (m, 1.5H, H2, 4), 7.06 – 7.00 (m, 1.5H, H2',4'), 6.93 – 6.85 (m, 2H, H5), 3.96 (td, *J* = 6.5, 1.9 Hz, 2H, H7), 2.25 (tt, *J*= 6.7, 2.6 Hz, 2H, H11), 1.97 (td, *J* = 2.7, 1.3 Hz, 1H, H13), 1.82 (h, *J* = 6.6 Hz, 2H, H8), 1.67 – 1.55 (m, 2H, H9,10); ^{13}C NMR (126 MHz, $CDCl_3$) δ 162.8 (C1), 158.7 (C1), 157.2 (C6), 156.3 (C6), 129.7 (C3), 129.2 (C3), 121.9 (C4), 121.7 (C4), 115.5 (C5), 114.9 (C5), 84.4 (C12), 68.4 (C13), 68.4 (C13), 68.1 (C7), 68.0 (C7), 28.8 (C8), 28.7 (C8), 28.2 (C9 or 10), 28.2 (C9 or 10), 25.2 (C9 or 10), 25.2 (C9 or 10), 18.4s (C11); HRMS (ESI +ve): $C_{14}H_{18}NO_2$ [M+H]$^+$: 232.1332 (Found: 232.1344).

***N*-(4-non-8-ynoxyphenyl)formamide (37)**

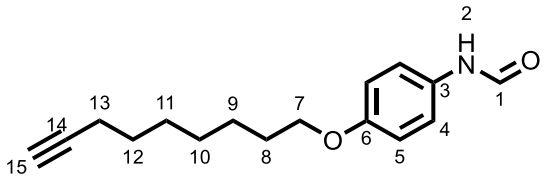

Product was synthesised following **general procedure 3** using non-8-yn-1-ol. Intermediate aniline **34** was seen by LCMS ($[M+H]^+$: 232.18) with a retention time of 1.26 min. The title product (258 mg, 49%, 0.99 mmol) was afforded. Rotamers observed in NMR. ^{1}H NMR (500 MHz, $CDCl_3$) δ 8.51 (d, *J* = 11.6 Hz, 0.5H, H1), 8.35 (d, *J* = 1.9 Hz, 0.5H, H1'), 7.54 (d, *J* = 11.6 Hz, 0.5H, H2), 7.46 – 7.42 (m, 1H, H4), 7.11 (s, 0.5H, H2'), 7.06 – 7.01 (m, 1H, H4'), 6.92 – 6.85 (m, 2H, H5), 3.95 (td, *J* = 6.5, 2.1 Hz, 2H, H7), 2.21 (tdd, *J* = 7.1, 2.7, 1.1 Hz, 2H, H13), 1.96 (td, *J* = 2.6, 0.6 Hz, 2H, H15), 1.84 – 1.74 (m, 2H, H8), 1.60 – 1.34 (m, 8H, H9-12); ^{13}C NMR (126 MHz, $CDCl_3$) δ 162.8 (C1), 158.7 (C1'), 157.3 (C6), 156.3 (C6'), 129.7 (C3), 128.9 (C3'), 121.9 (C4), 121.7 (C4'), 115.5 (C5), 114.9 (C5'), 84.7 (C14), 68.3 (C7), 68.2 (C7'), 68.2 (C15), 68.2 (C15'), 29.2 (C8), 29.2 (C8'), 28.9 (C11), 28.6(C10), 28.48 (C12), 25.9(C9), 18.34 (C13); HRMS (ESI +ve): $C_{16}H_{22}NO_2$ $[M+H]^+$: 260.1645 (Found: 260.1648).

N^8,N^8-dimethyl-N^2-(4-(pent-4-yn-1-yloxy)phenyl)pyrido[3,4-*d*]pyrimidine-2,8-diamine (38)

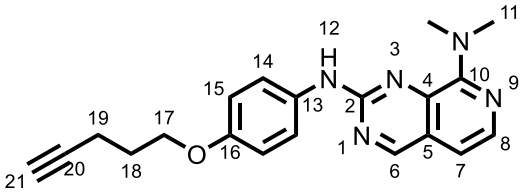

Product was synthesised following **general procedure 4** using *N,N*-dimethyl-2-methylsulfonyl-pyrido[3,4-*d*]pyrimidin-8-amine (20 mg, 0.08 mmol) and *N*-(4-pent-4-ynoxyphenyl)formamide affording 16 mg (58%, 0.05 mmol) of the title product. ^{1}H NMR (600 MHz, DMSO-d_6) δ 9.73 (s, 1H, H12), 9.19 (s, 1H, H6), 7.92 – 7.86 (m, 1H, H8), 7.72 – 7.68 (m, 2H, H14), 7.03 (d, *J* = 5.3 Hz, 1H, H7), 6.96 - 6.93 (m, 2H, H15), 4.03 (td, *J* = 6.2, 2.5 Hz, 2H, H17), 3.29 (s, 6H, H11), 2.83 (t, *J* = 2.6 Hz, 1H, H21), 2.35 (td, *J* = 7.1, 2.7 Hz, 2H, H19), 1.93 – 1.86 (m, 2H, H18); ^{13}C NMR (151 MHz, DMSO-d_6) δ 162.4 (C6), 156.9 (10), 156.3 (C2), 154.3 (C16), 138.8 (C8), 133.7 (C13), 124.0 (C4), 122.1 (C5), 121.5 (C14), 114.9 (C15), 109.8 (C7), 84.2 (C20), 72.1 (C21), 66.6 (C17), 41.8 (C11), 28.3

(C18), 15.0 (C19); HRMS (ESI +ve): $C_{20}H_{22}N_5O$ $[M+H]^+$: 348.1819 (Found: 348.1804).

N^2-(4-(hept-6-yn-1-yloxy)phenyl)-N^8,N^8-dimethylpyrido[3,4-*d*]pyrimidine-2,8-diamine (39)

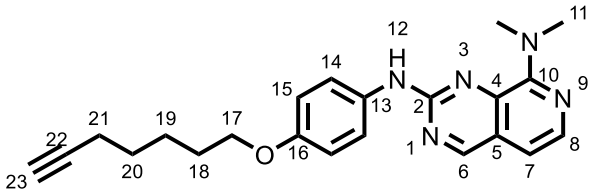

Product was synthesised following **general procedure 4** using *N,N*-dimethyl-2-methylsulfonyl-pyrido[3,4-*d*]pyrimidin-8-amine (19 mg, 0.08 mmol) and *N*-(4-hept-6-ynoxyphenyl)formamide (17 mg, 0.08 mmol), affording 15 mg (53%, 0.04 mmol) of the title product. ^{1}H NMR (600 MHz, $CDCl_3$) δ 8.98 (s, 1H, H6), 7.98 (d, *J* = 5.4 Hz, 1H, H8), 7.60 – 7.55 (m, 2H, H14), 7.19 (s, 1H, H12), 6.97 – 6.92 (m, 2H, H15), 6.88 (d, *J* = 5.4 Hz, 1H, H7), 4.01 (t, *J* = 6.5 Hz, 2H, H17), 3.38 (s, 6H, H11), 2.27 (td, *J* = 6.7, 2.7 Hz, 2H, H22), 1.99 (t, *J* = 2.7 Hz, 1H, H25), 1.88 – 1.81 (m, 2H, H18), 1.69 – 1.58 (m, 4H, H19 and 20); ^{13}C NMR (151 MHz, $CDCl_3$) δ 161.5 (C6), 158.8 (C10), 157.2 (C2), 156.1 (C16), 139.7 (C4), 139.2 (C8), 132.2 (C13), 124.3 (C5), 121.9 (C14), 114.8 (C15), 109.0 (C7), 84.7 (C22), 68.4 (C23), 68.1 (C17), 41.8 (C11), 28.9 (C18), 28.2 (C19), 25.3 (C20), 18.4 (C21). HRMS (ESI +ve): $C_{22}H_{26}N_5O$ $[M+H]^+$: 377.2161 (Found: 377.2176).

N^8,N^8-dimethyl-N^2-(4-(non-8-yn-1-yloxy)phenyl)pyrido[3,4-*d*]pyrimidine-2,8-diamine (40)

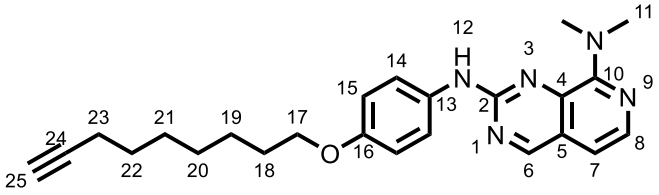

Product was synthesised following **general procedure 4** using *N,N*-dimethyl-2-methylsulfonyl-pyrido[3,4-*d*]pyrimidin-8-amine (15 mg, 0.06 mmol) and *N*-(4-non-8-ynoxyphenyl)formamide (14 mg, 0.06 mmol), affording 14 mg (61%, 0.04 mmol) of the title product. ^{1}H NMR (600 MHz, $CDCl_3$) δ 8.98 (s, 1H, H6), 7.98 (d, *J* = 5.4 Hz, 1H, H8), 7.59 – 7.56 (m, 2H, H14), 7.19 (s, 1H, H12), 6.96 – 6.92 (m, 2H, H15), 6.88 (d, *J* = 5.4 Hz, 1H, H7), 3.99 (t, *J* = 6.5 Hz, 2H, H17), 3.38

(s, H11), 2.22 (td, *J* = 7.1, 2.6 Hz, 2H, H24), 1.99 – 1.96 (m, 1H, H25), 1.86 – 1.79 (m, 2H, H18), 1.61 – 1.39 (m, 8H, H19, 20, 21, 22); ^{13}C NMR (151 MHz, $CDCl_3$) δ 161.5 (C6), 157.3 (C10), 156.1 (C2), 155.4 (C16), 139.8 (C4), 139.2 (C8), 132.2 (C13), 124.3 (C5), 121.9 (C14), 114.8 (C15), 109.0 (C7), 84.7 (C24), 68.3 (C17), 68.2 (C25), 41.8 (C11), 29.3 (C18), 28.9 (either C19, 20, 21, or 22), 28.7 (either C19, 20, 21, or 22), 28.4 (either C19, 20, 21, or 22), 26.0 (either C19, 20, 21, or 22), 18.4 (C23); HRMS (ESI +ve): $C_{24}H_{30}N_5O$ $[M+H]^+$: 404.2421 (Found: 404.2445).

8-(azetidin-1-yl)-*N*-(4-(pent-4-yn-1-yloxy)phenyl)pyrido[3,4-*d*]pyrimidin-2-amine (41)

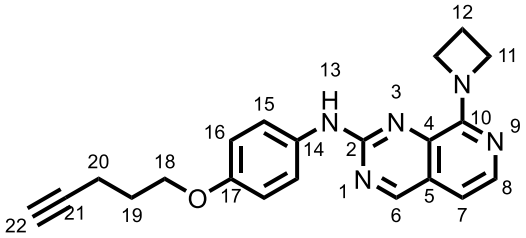

Product was synthesised following **general procedure 4** using 8-(azetidin-1-yl)-2-methylsulfonyl-pyrido[3,4-*d*]pyrimidine (15 mg, 0.06 mmol) and *N*-(4-pent-4-ynoxyphenyl)formamides (11 mg, 0.06 mmol), affording 12 mg (59%, 0.03 mmol) of the title product. ^{1}H NMR (600 MHz, $CDCl_3$) δ 8.93 (s, 1H, H6), 7.91 (d, *J* = 5.5 Hz, 1H, H8), 7.51 – 7.47 (m, 2H, H15), 7.11 (s, 1H, H13), 6.96 – 6.93 (m, 2H, H16), 6.75 (d, *J* = 5.6 Hz, 1H, H7), 4.47 (t, *J* = 7.5 Hz, 4H, H11), 4.13 – 4.09 (m, 2H, H18), 2.48 – 2.39 (m, 4H, H12 and 20), 2.07 – 2.00 (m, 3H, H19 and 22); ^{13}C NMR (151 MHz, $CDCl_3$) δ 160.7 (C6), 156.8 (C10), 155.8 (C2), 155.2 (C17), 139.8 (C4), 138.9 (C8), 132.2 (C14), 123.6 (C5), 122.5 (C15), 114.7 (C16), 106.9 (C7), 83.5 (C21), 68.9 (C22), 66.5 (C18), 53.3 (C11), 28.3 (C19), 17.8 (C12), 15.2 (C20); HRMS (ESI +ve): $C_{21}H_{22}N_5O$ $[M+H]^+$: 360.1819 (Found: 360.1804).

8-(azetidin-1-yl)-*N*-(4-(hept-6-yn-1-yloxy)phenyl)pyrido[3,4-*d*]pyrimidin-2-amine (42)

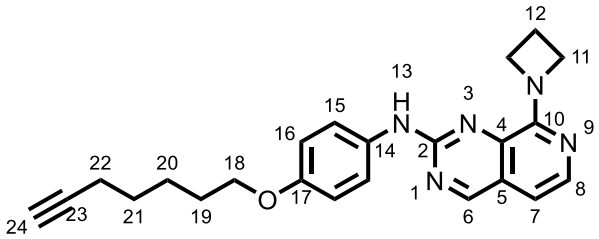

Product was synthesised following **general procedure 4** using 8-(azetidin-1-yl)-2-methylsulfonyl-pyrido[3,4-*d*]pyrimidine (15 mg, 0.06 mmol) and *N*-(4-hept-6-ynoxyphenyl)formamide (13 mg, 0.06 mmol), affording 12 mg (59%, 0.03 mmol) of the title product. ^{1}H NMR (600 MHz, $CDCl_3$) δ 8.93 (s, 1H, H6), 7.90 (d, *J* = 5.6 Hz, 1H, H8), 7.50 – 7.45 (m, 2H, H15), 7.12 (s, 1H, H13), 6.95 – 6.90 (m, 2H, H16), 6.77 – 6.73 (m, 1H, H7), 4.54 – 4.40 (m, 4H, H11), 4.00 (t, *J* = 6.5 Hz, 2H, H18), 2.38 – 2.45 (m, 2H, H12), 2.32 – 2.21 (m, 2H, 22), 1.99 (t, *J* = 2.7 Hz, 1H, H24), 1.84 (apparent p, *J* = 6.7 Hz, 2H, H19), 1.70 – 1.59 (m, 4H, H20 and 21); ^{13}C NMR (151 MHz, $CDCl_3$) δ 160.7 (C6), 156.8 (C10), 155.7 (C2), 155.4 (C17), 139.8 (C4), 139.0 (C8), 132.0 (C14), 122.9 (C5), 122.5 (C15), 114.6 (C16), 106.9 (C7), 84.6 (C23), 68.4 (C24), 68.1 (C18), 52.4 (C11), 28.9 (C19), 28.3 (C20), 25.3 (C21), 18.4 (C22), 17.8 (C12); HRMS (ESI +ve): $C_{23}H_{26}N_5O$ $[M+H]^+$: 389.2161 (Found: 389.2172).

8-(azetidin-1-yl)-*N*-(4-(non-8-yn-1-yloxy)phenyl)pyrido[3,4-*d*]pyrimidin-2-amine (43)

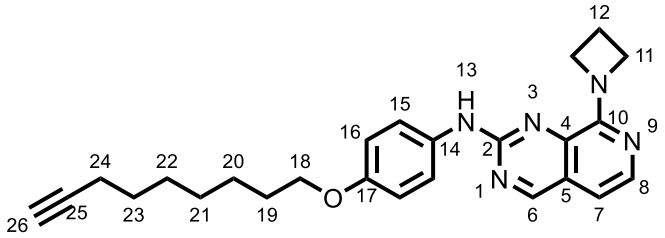

Product was synthesised following **general procedure 4** using 8-(azetidin-1-yl)-2-methylsulfonyl-pyrido[3,4-*d*]pyrimidine (20 mg, 0.08 mmol) and *N*-(4-non-8-ynoxyphenyl)formamide (19 mg, 0.08 mmol), affording 11 mg (35%, 0.03 mmol) of the title product. ^{1}H NMR (600 MHz, $CDCl_3$) δ 8.93 (s, 1H, H6), 7.90 (d, *J* = 5.5 Hz, 1H, H8), 7.50 – 7.45 (m, 2H, H15), 7.11 (s, 1H, H13), 6.95 – 6.90 (m, 2H, H16), 6.75 (d, *J* = 5.6 Hz, H7), 4.46 (t, *J* = 7.4 Hz, 4H, H11), 3.99 (t, *J* = 6.5 Hz, 2H, H18), 2.45-2.38 (m, 2H, H19), 2.22 (td, *J* = 7.1, 2.7 Hz, 2H, H24), 1.97 (t, *J* = 2.6 Hz, 1H, H26), 1.82 (apparent p, *J* = 6.7 Hz, 2H, H19), 1.62 – 1.39 (m,

8H, H20, 21, 22, 23); ^{13}C NMR (151 MHz, $CDCl_3$) δ 160.7 (C6), 158.1 (C10), 156.8 (C2), 155.9 (C17), 139.8 (C4), 139.0 (C8), 131.9 (C14), 123.6 (C5), 122.9 (C15), 114.7 (C16), 106.9 (C7), 84.68 (C25), 68.30 (C18), 68.18 (C26), 51.59 (C11), 29.30 (C19), 28.90 (C20, 21, 22, or 23), 28.66 (C20, 21, 22, or 23), 28.40 (C20, 21, 22, or 23), 25.96 (C20, 21, 22, or 23), 18.40 (C24), 17.83(C12); HRMS (ESI +ve): $C_{25}H_{30}N_5O$ $[M+H]^+$: 416.2445 (Found: 416.2417).

8-morpholino-*N*-(4-(pent-4-yn-1-yloxy)phenyl)pyrido[3,4-*d*]pyrimidin-2-amine (44)

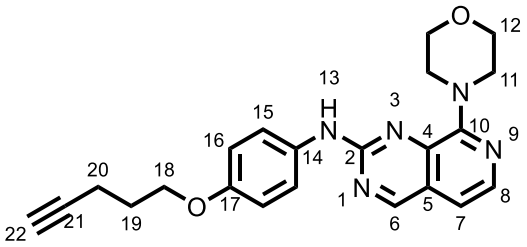

Product was synthesised following **general procedure 4** using 4-(2-methylsulfonylpyrido[3,4-*d*] pyrimidin-8-yl)morpholine (11 mg, 0.04 mmol) and *N*-(4-pent-4-ynoxyphenyl)formamide (7 mg, 0.04 mmol), affording 6 mg (41%, 0.02 mmol) of the title product. ^{1}H NMR (600 MHz, $CDCl_3$) δ 9.03 (s, 1H, H6), 8.04 (d, *J* = 5.4 Hz, 1H, H8), 7.64 – 7.58 (m, 2H, H15), 7.26 (s, 1H, H13), 7.04 (d, *J* = 5.4 Hz, 1H, H7), 6.99 – 6.93 (m, 2H, H16), 4.12 (t, *J* = 6.1 Hz, 3H, H18), 3.98 – 3.95 (m, 4H, H12), 3.91-3.85 (m, 4H, H11), 2.46 (td, *J* = 7.0, 2.6 Hz, 2H, H20), 2.10 – 2.00 (m, 3H, H19 and 22); ^{13}C NMR (151 MHz, $CDCl_3$) δ 162.0 (C7), 156.8 (C10), 156.2 (C2), 155.3 (C17), 139.7 (C4), 139.2 (C8), 132.2 (C14), 124.2 (C5), 121.7 (C16), 114.8 (C15), 111.3 (C7), 83.5 (C21), 69.0 (C22), 67.3 (C12), 66.6 (C18), 49.3 (C11), 28.2 (C19), 15.2 (C20), C17 not observed; HRMS (ESI +ve): $C_{22}H_{24}NO_2$ $[M+H]^+$: 392.1981 (Found: 392.1998).

***N*-(4-(hept-6-yn-1-yloxy)phenyl)-8-morpholinopyrido[3,4-*d*]pyrimidin-2-amine (45)**

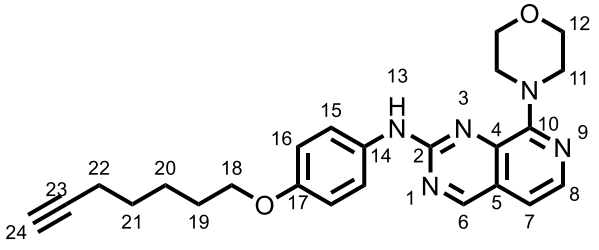

Product was synthesised following **general procedure 4** using 4-(2-methylsulfonylpyrido[3,4-*d*] pyrimidin-8-yl)morpholine (9 mg, 0.03 mmol) and *N*-(4-hept-6-ynoxyphenyl)formamide (7 mg, 0.03 mmol), affording 5 mg (39%, 0.03 mmol) of the title product. ^{1}H NMR (600 MHz, $CDCl_3$) δ 9.03 (s, 1H, H6), 8.04 (d, *J* = 5.0 Hz, 1H, H8), 7.66 – 7.57 (m, 2H, H15), 7.25 (s, 1H, H13), 7.05 (d, J=5.0 Hz, 1H, H7), 6.96-6.92 (m, 2H, H16), 4.01 (t, *J* = 7.5 Hz, 2H, H18), 3.98 – 3.93 (m, 4H, H12), 3.90-3.86 (m, 4H, H11), 2.35 – 2.21 (m, 2H, H22), 2.02 – 1.96 (m, 1H, H24), 1.92 – 1.79 (m, 2H, H19), 1.73 – 1.48 (m, 4H, H21, 22); ^{13}C NMR (151 MHz,) δ 162.0 (C6), 156.8 (C10), 156.3 (C2), 155.4 (C17), 139.8 (C4), 139.1 (C8), 132.2 (C14), 124.3 (C5), 121.7 (C15), 114.7 (C16), 111.3 (C7), 84.4 (C23), 68.4 (C24), 68.2 (C18), 67.3 (C12), 49.3 (C11), 28.9 (C19), 28.2 (C20), 25.3 (C21), 18.4 (C22); HRMS (ESI +ve): $C_{24}H_{28}N_5O_2$ $[M+H]^+$: 418.2238 (Found: 418.2246).

8-morpholino-*N*-(4-(non-8-yn-1-yloxy)phenyl)pyrido[3,4-*d*]pyrimidin-2-amine (46)

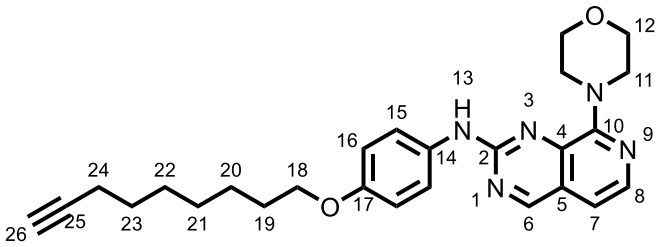

Product was synthesised following **general procedure 4** using 4-(2-methylsulfonylpyrido[3,4-*d*] pyrimidin-8-yl)morpholine (8 mg, 0.03 mmol) and *N*-(4-non-8-ynoxyphenyl)formamide (7 mg, 0.03 mmol), affording 6 mg (50%, 0.01 mmol) of the title product. ^{1}H NMR (600 MHz, $CDCl_3$) δ 9.03 (s, 1H, H6), 8.04 (d, *J* = 5.4 Hz, 1H, H8), 7.62 – 7.57 (m, 2H, H15), 7.26 (s, 1H, H13), 7.03 (d, *J* = 5.4 Hz, 1H, H7), 6.97 – 6.92 (m, 2H, H16), 4.01 (t, *J* = 7.5 Hz, 2H, H18), 3.97 – 3.92 (m, 4H, H12), 3.90-3.87 (m, 4H, H11), 2.23 (td, *J* = 7.1, 2.7 Hz, 2H, H24), 1.97 (t, *J* = 2.6 Hz, 1H H26), 1.83 (dt, *J* = 14.7, 6.7 Hz, 2H H19), 1.62 – 1.38 (m, 8H, H20, 21, 22, 23); ^{13}C NMR (151 MHz, $CDCl_3$) δ 162.0 (C6), 156.8 (C10), 156.3 (C2), 155.5 (C17), 139.9 (C4), 139.1 (C8), 132.0 (C14), 124.1 (C5), 121.7 (C14), 114.7 (C116), 111.3 (C7), 84.6 (C25), 68.4 (C26), 68.2 (C18), 67.3 (C12), 49.5 (C11), 29.3 (C19), 28.9 (C20, 21, 22, or 23), 28.7 (C20, 21, 22, or 23), 28.4

(C20, 21, 22, or 23), 26.0 (C20, 21, 22, or 23), 18.4 (C24); HRMS (ESI +ve): $C_{26}H_{32}N_5O_2$ $[M+H]^+$: 448.2609 (Found: 448.2603).

4-((2-azidoethyl)amino)-2-(2,6-dioxopiperidin-3-yl)isoindoline-1,3-dione (50)

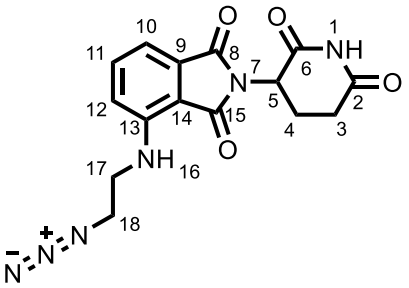

2-Bromoethylammonium bromide (80 mg, 0.39 mmol) and sodium azide (25 mg, 0.39 mmol) were dissolved in DMSO (2 mL) and heated overnight at 75 °C. No SM was observed by TLC after 18 h (DCM-MeOH 5% Rf: 0.5). 2-(2,6-Dioxo-3-piperidyl)-4-fluoro-isoindoline-1,3-dione (107 mg, 0.39 mmol) and DIPEA (204 µl, 1.17 mmol) were added and the reaction was stirred at 75 °C overnight. Water was added to the reaction mixture and was extracted with EtOAc (3 times). The organic layers were combined, washed with brine, dried over $MgSO_4$, and solvent was removed *in vacuo*. The residue was purified using reverse phase column chromatography (water:MeOH (+0.1% formic acid) 30-80%) affording the title product (45 mg, 34%, 0.13 mmol). ^{1}H NMR (600 MHz, $CDCl_3$) δ 8.00 (s, 1H, H1), 7.56 (dd, *J* = 8.5, 7.1 Hz, 1H, H11), 7.21 – 7.17 (m, 1H, H12), 6.96 (d, *J* = 8.5 Hz, 1H, H10), 6.47 (t, *J* = 6.1 Hz, 1H, H16), 4.95 (dd, *J* = 12.5, 5.4 Hz, 1H, H5), 3.60 (t, *J* = 5.6 Hz, 2H, H18), 3.54 (t, *J* = 6.1 Hz, 2H, H17), 2.95 – 2.72 (m, 3H, H3, 4), 2.19 – 2.14 (m, 1H, H4); ^{13}C NMR (151 MHz, $CDCl_3$) δ 170.8 (C2), 169.4 (C15), 168.1 (C6), 167.4 (C8), 146.3 (C13), 136.3 (C11), 132.5 (C9), 116.4 (C12), 112.4 (C10), 110.8 (C14), 50.6 (C18), 49.0 (C5), 41.9 (C17), 31.4 (C3), 22.8 (C4) HRMS (ESI +ve): $C_{15}H_{15}N_6O_4$ $[M+H]^+$: 343.1154 (Found: 343.1166).

4-((2-(4-(3-(4-((8-(dimethylamino)pyrido[3,4-*d*]pyrimidin-2-yl)amino) phenoxy)propyl)-1*H*-1,2,3-triazol-1-yl)ethyl)amino)-2-(2,6-dioxopiperidin-3-yl)isoindoline-1,3-dione (1)

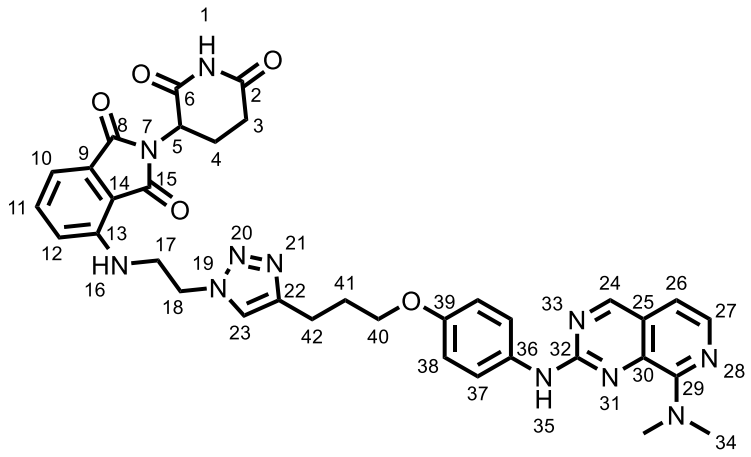

Product was synthesised following **general procedure 5** using N^8,N^8-dimethyl-N^2-(4-(pent-4-yn-1-yloxy)phenyl)pyrido[3,4-*d*]pyrimidine-2,8-diamine (12 mg, 0.03 mmol) and 4-((2-azidoethyl)amino)-2-(2,6-dioxopiperidin-3-yl)isoindoline-1,3-dione, affording 11 mg (44%, 0.02 mmol) of the title product. ^{1}H NMR (600 MHz, $CDCl_3$) δ 8.98 (s, 1H, H24), 7.98 (d, *J* = 5.4 Hz, 1H, H27), 7.61 – 7.56 (m, 2H, H37), 7.53 (s, 1H, H35), 7.47 (dd, *J* = 8.5, 7.1 Hz, 1H, H11), 7.33 (s, 1H, H23), 7.16 – 7.13 (m, 1H, H10), 6.91 – 6.86 (m, 3H, H26, and 38), 6.71 (d, *J* = 8.5 Hz, 1H, H12), 6.45 (t, *J* = 6.6 Hz, 1H, H16), 4.92 (dd, *J* = 12.5, 5.4 Hz, 1H, H5), 4.57 (t, *J* = 5.8 Hz, 2H, H18), 3.98 (t, *J* = 6.3 Hz, 2H, H40), 3.90 – 3.84 (m, 2H, H17), 3.37 (s, 6H, H34), 2.93 – 2.67 (m, 5H, H42 , 3 and 4), 2.18 – 2.09 (m, 3H, H3 and 41), H1 not observed; ^{13}C NMR (151 MHz, $CDCl_3$) δ 171.2 (C2), 169.3 (C15), 168.6 (C6), 167.3 (C8), 161.4 (C24), 157.4 (C29),155.9 (C32), 154.9 (C39), 147.6 (C22), 146.1 (C13), 139.8 (C30), 139.2 (C27), 136.4 (C11), 132.5 (C9), 132.5 (C36), 124.2 (C25), 122.1 (C23), 121.7 (C37), 116.2 (C12), 114.8 (C38), 112.7 (C10), 111.0 (C14), 109.1 (C26), 67.1 (C40), 49.8 (C18), 49.0 (C5), 42.9 (C17), 41.8 (C34), 31.4 (C3), 28.9 (C41), 22.7 (C4), 22.0 (C42); HRMS (ESI +ve): $C_{35}H_{36}N_{11}O_5$ $[M+H]^+$: 690.2895 (Found: 690.2877).

4-((2-(4-(5-(4-((8-(dimethylamino)pyrido[3,4-*d*]pyrimidin-2-yl)amino) phenoxy)pentyl)-1*H*-1,2,3-triazol-1-yl)ethyl)amino)-2-(2,6-dioxopiperidin-3-yl)isoindoline-1,3-dione (2)

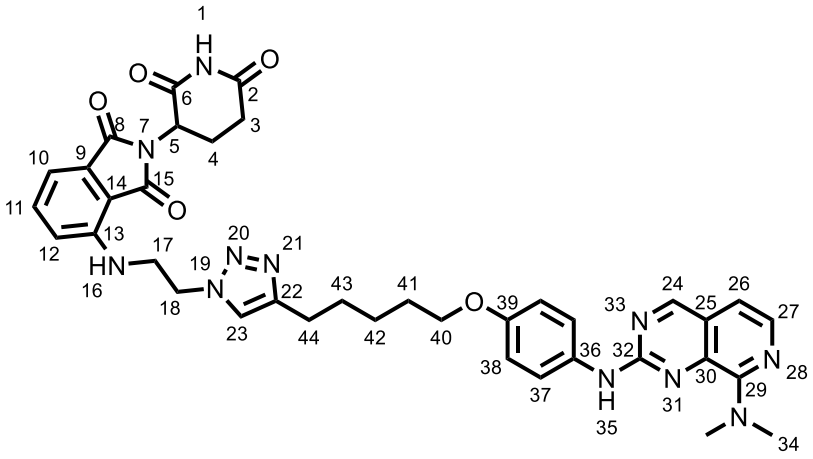

Product was synthesised following **general procedure 5** using N^2-(4-(hept-6-yn-1-yloxy)phenyl)-N^8,N^8-dimethylpyrido[3,4-*d*]pyrimidine-2,8-diamine (15 mg, 0.04 mmol) and 4-((2-azidoethyl)amino)-2-(2,6-dioxopiperidin-3-yl)isoindoline-1,3-dione, affording 12 mg (40%, 0.02 mmol) of the title product. ^{1}H NMR (600 MHz, $CDCl_3$) δ 8.98 (s, 1H, H24), 7.98 (d, *J*= 5.5 Hz, 1H, H27) 7.61 – 7.56 (m, 2H, H37), 7.52 (s, 1H, H35), 7.47 (ddd, *J* = 8.3, 7.0, 1.2 Hz, 1H, H11), 7.31 (s, 1H, H23), 7.15 (dd, *J* = 7.0, 1.1 Hz, 1H, H10), 6.94 – 6.89 (m, 2H, H38), 6.87 (dd, *J* = 5.5, 1.2 Hz, 1H, H26), 6.71 (d, *J* = 8.5 Hz, 1H, H12), 6.46 (t, *J* = 6.6 Hz, 1H, H16), 4.92 (dd, *J* = 12.7, 5.4 Hz, 1H, H5), 4.58 – 4.54 (m, 2H, H18), 3.98 (td, *J* = 6.5, 1.1 Hz, 2H, H40), 3.85 (q, *J* = 6.1 Hz, 2H, H17), 3.37 (d, *J* = 1.2 Hz, 6H, H34), 2.93 – 2.67 (m, 5H, H3, 4 and 44), 2.17 – 2.09 (m, 1H, H3), 1.82 (p, *J* = 6.8 Hz, 2H, H41), 1.76 – 1.67 (m, 2H, H43), 1.48-1.57 (m, 2H, H42), H1 not observed; ^{13}C NMR (151 MHz, $CDCl_3$) δ 171.2 (C2), 169.3 (C15), 168.6 (C6), 167.3 (C8), 161.4 (C24), 157.2 (C29), 156.0 (C32), 155.0 (C39), 148.5 (C22), 146.0 (C13), 139.7 (C30), 139.2 (C27), 136.4 (C11), 132.5 (C9), 132.4 (C36), 124.2 (C25), 121.8 (C23 and 37), 116.1 (C12), 114.8 (C38), 112.6 (C10), 111.0 (C14), 109.1 (C26), 68.0 (C40), 49.8 (C18), 49.0 (C5), 42.9 (C17), 41.8 (C34), 31.4 (C3), 29.0 (C43), 28.9 (C41), 25.5 (C42), 25.4 (C44), 22.8 (C4); HRMS (ESI +ve): $C_{37}H_{40}N_{11}O_5$ $[M+H]^+$: 718.3208 (Found: 718.3192).

4-((2-(4-(7-(4-((8-(dimethylamino)pyrido[3,4-*d*]pyrimidin-2-yl)amino) phenoxy)heptyl)-1*H*-1,2,3-triazol-1-yl)ethyl)amino)-2-(2,6-dioxopiperidin-3-yl)isoindoline-1,3-dione (3)

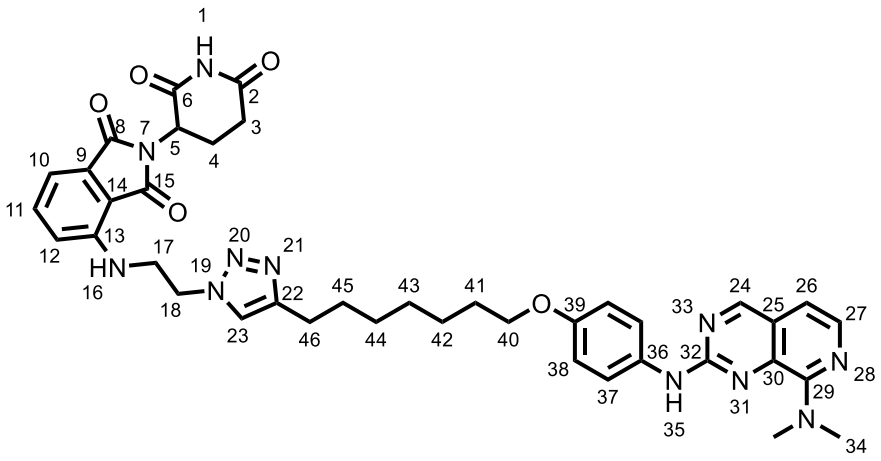

Product was synthesised following **general procedure 5** using N^8,N^8-dimethyl-N^2-(4-(non-8-yn-1-yloxy)phenyl)pyrido[3,4-*d*]pyrimidine-2,8-diamine (13 mg, 0.03 mmol) and 4-((2-azidoethyl)amino)-2-(2,6-dioxopiperidin-3-yl)isoindoline-1,3-dione, affording 12 mg (40%, 0.02 mmol) of the title product. ^{1}H NMR (600 MHz, $CDCl_3$) δ 9.00 (s, 1H, H24), 7.98 (d, *J* = 5.4 Hz, 1H, H27), 7.61 – 7.57 (m, 2H, H37), 7.52 (s, 1H, H35), 7.47 (dd, *J* = 8.5, 7.1 Hz, 1H, H11), 7.29 (s, 1H, H23), 7.15 (d, *J* = 7.1 Hz, 1H, H10), 6.94 – 6.90 (m, 2H, H38), 6.88 (d, *J*= 5.4 Hz, 1H, H26), 6.68 (d, *J* = 8.5 Hz, 1H, H12), 6.48 (t, *J* = 6.6 Hz, 1H, H16), 4.94 (dd, *J* = 12.4, 5.3 Hz, 1H, H5), 4.55 (t, *J* = 5.8 Hz, 2H, H18), 3.98 (t, *J* = 6.5 Hz, 2H. H40), 3.86 (q, *J* = 6.2 Hz, 2H, H17), 3.37 (s, 6H, H34), 2.93 – 2.71 (m, 3H, H3 and 4), 2.69 (t, *J* = 7.7 Hz, 2H, H46), 2.14 (dtd, *J* = 14.3, 4.7, 4.2, 2.2 Hz, 1H, H4), 1.83 – 1.73 (m, 2H, H41), 1.65 (q, *J* = 5.8, 4.1 Hz, 2H, H45), 1.50 – 1.44 (m, 2H, H42), 1.43 – 1.33 (m, 4H, H43, and 44), H1 not observed; ^{13}C NMR (151 MHz, $CDCl_3$) δ 171.2 (C2), 169.4 (C15), 168.6 (C6), 167.3 (C8), 161.4 (C24), 157.2 (C29), 155.9 (C32), 155.4 (C39), 148.9 (C22), 146.1 (C13), 139.8 (C30), 139.2 (C27), 136.4 (C11), 132.5 (C9), 132.4 (C36), 124.2 (C25), 121.8 (C37), 121.7 (C23), 116.1 (C12), 114.8 (C38), 112.6 (C10), 110.9 (C14), 109.1 (C26), 68.3 (C40), 49.9 (C18), 49.0 (C5), 43.0 (C17), 41.8 (C34), 31.4 (C3), 29.3 (C45), 29.2 (C41), 29.0 (C43 or C44), 29.0 (C43 or C44), 25.9 (C42), 25.5 (C46), 22.8 (C4); HRMS (ESI +ve): $C_{39}H_{44}N_{11}O_5$ $[M+H]^+$: 746.3521 (Found: 746.3503).

4-((2-(4-(3-(4-((8-(azetidin-1-yl)pyrido[3,4-*d*]pyrimidin-2-yl)amino)phenoxy) propyl)-1*H*-1,2,3-triazol-1-yl)ethyl)amino)-2-(2,6-dioxopiperidin-3-yl) isoindoline-1,3-dione (4)

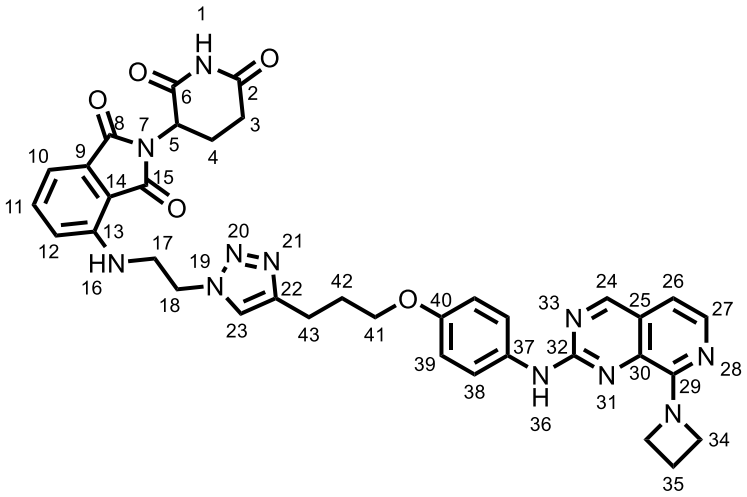

Product was synthesised following **general procedure 5** using 8-(azetidin-1-yl)-*N*-(4-(pent-4-yn-1-yloxy)phenyl)pyrido[3,4-*d*]pyrimidin-2-amine (11 mg, 0.03 mmol) and 4-((2-azidoethyl)amino)-2-(2,6-dioxopiperidin-3-yl)isoindoline-1,3-dione, affording 6 mg (27%, 0.01 mmol) of the title product. ^{1}H NMR (600 MHz, $CDCl_3$) δ 8.93 (s, 1H, H24), 7.89 (d, *J* = 5.6 Hz, 1H, H27), 7.44-7.51 (m, 3H, H38, H11), 7.41 (s, 1H, H36), 7.33 (s, 1H, H23), 7.14 (d, *J* = 7.1 Hz, 1H, H10), 6.90 – 6.85 (m, 2H, H39), 6.74 (d, *J* = 5.6 Hz, 1H, H26), 6.70 (d, *J* = 8.5 Hz, 1H, H12), 6.45 (t, *J* = 6.6 Hz, 1H, H16), 4.92 (dd, *J* = 12.4, 5.4 Hz, 1H, H5), 4.57 (t, *J* = 5.8 Hz, 2H, H18), 4.45 (d, *J* = 7.7 Hz, 4H, H34), 3.98 (t, *J* = 6.3 Hz, 2H, H41), 3.86 (td, *J* = 6.6, 5.1 Hz, 2H, H17), 2.94 – 2.68 (m, 5H, H43, H3, H4), 2.45 – 2.36 (m, 2H, H35), 2.17 – 2.09 (m, 4H, H42, H3), H1 not observed; ^{13}C NMR (151 MHz, $CDCl_3$) δ 171.2 (C2), 169.4 (C15), 168.6 (C6), 167.3 (C8), 160.6 (C24), 156.6 (C32), 155.7 (C29), 155.0 (C40), 147.7 (C22), 146.1 (C13), 139.8 (C26), 138.8 (C30), 136.4 (C11), 132.6 (C9), 132.3 (C37), 123.5 (C25), 122.2 (C38), 122.1 (C23), 116.2 (C12), 114.7 (C39), 112.7 (C10), 111.0 (C14), 107.0 (C26), 67.1 (C41), 53.5 (C34), 49.8 (C18), 49.0 (C5), 42.9 (C17), 31.4 (C3), 28.9 (C42), 22.8 (C4), 22.0 (C42), 17.8 (C35); HRMS (ESI +ve): $C_{36}H_{36}N_{11}O_5$ $[M+H]^+$: 702.2895 (Found: 702.2886).

4-((2-(4-(5-(4-((8-(azetidin-1-yl)pyrido[3,4-*d*]pyrimidin-2-yl)amino)phenoxy)pentyl)-1*H*-1,2,3-triazol-1-yl)ethyl)amino)-2-(2,6-dioxopiperidin-3-yl)isoindoline-1,3-dione (5)

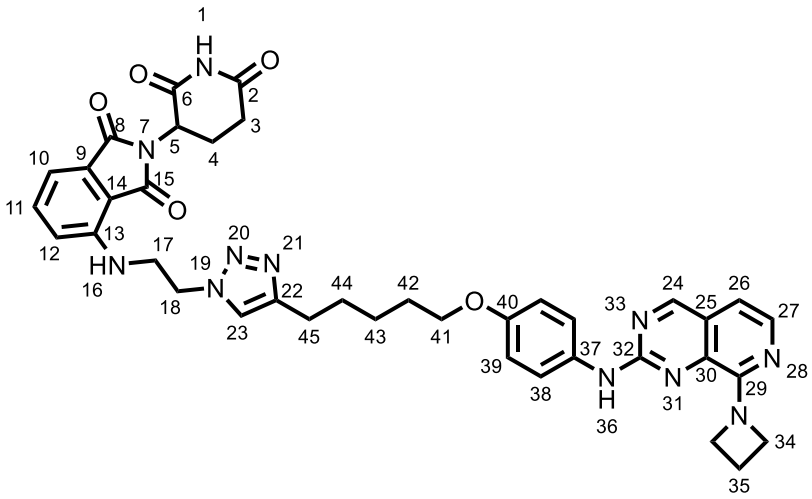

Product was synthesised following **general procedure 5** using 8-(azetidin-1-yl)-*N*-(4-(hept-6-yn-1-yloxy)phenyl)pyrido[3,4-*d*]pyrimidin-2-amine (8 mg, 0.02 mmol) and 4-((2-azidoethyl)amino)-2-(2,6-dioxopiperidin-3-yl)isoindoline-1,3-dione, affording 7 mg (44%, 0.01 mmol) of the title product. ^{1}H NMR (600 MHz, $CDCl_3$) δ 8.92 (s, 1H, H24), 7.82 (d, *J* = 5.9 Hz, 1H, H27), 7.61 (s, 1H, H38), 7.48 (dd, *J* = 8.5, 7.1 Hz, 1H, H11), 7.46 – 7.41 (m, 2H, H36), 7.31 (s, 1H, H23), 7.17 – 7.12 (m, 1H, H10), 6.93 – 6.88 (m, 2H, H39), 6.74 (d, *J* = 5.9 Hz, 1H, H26), 6.71 (d, *J* = 8.5 Hz, 1H, H12), 6.47 (t, *J* = 6.6 Hz, 1H, H16), 4.92 (dd, *J* = 12.5, 5.4 Hz, 1H, H5), 4.55 (dt, *J* = 19.8, 7.0 Hz, 6H, H18, H34), 3.98 (t, *J* = 6.5 Hz, 2H, H41), 3.86 (q, *J* = 6.1 Hz, 2H, H17), 2.93 – 2.69 (m, 6H, H3, H4, H45), 2.43 (tt, *J* = 8.8, 7.0 Hz, 2H, H35), 2.17 – 2.10 (m, 1H, H3), 1.82 (p, *J* = 6.7 Hz, 2H, H42), 1.71 (p, *J* = 7.7 Hz, 2H, H44), 1.57 – 1.48 (m, 2H, H43), H1 not observed; ^{13}C NMR (151 MHz, $CDCl_3$) δ 171.2 (C2), 169.4 (C15), 168.6 (C6), 167.3 (C8), 160.5 (C24), 157.1 (C32), 155.6 (C29), 153.8 (C40), 148.5 (C22), 146.0 (C13), 139.9 (C30), 136.5 (C27), 136.4 (C11), 132.5 (C9), 131.6 (C37), 123.3 (C25), 122.9 (C38), 121.8 (C23), 116.1 (C12), 114.7 (C39), 112.6 (C10), 110.9 (C14), 106.9 (C26), 68.0 (C41), 49.8 (C18), 49.0 (C5), 42.9 (C17), 31.4 (C3), 29.1 (C44), 28.9 (C42), 25.5 (C43), 25.4 (C45), 22.8 (C4), 17.8 (C35), C34 not observed; HRMS (ESI +ve): $C_{38}H_{40}N_{11}O_5$ $[M+H]^+$: 730.3208 (Found: 730.3197).

4-((2-(4-(7-(4-((8-(azetidin-1-yl)pyrido[3,4-*d*]pyrimidin-2-yl)amino)phenoxy)heptyl)-1*H*-1,2,3-triazol-1-yl)ethyl)amino)-2-(2,6-dioxopiperidin-3-yl)isoindoline-1,3-dione (6)

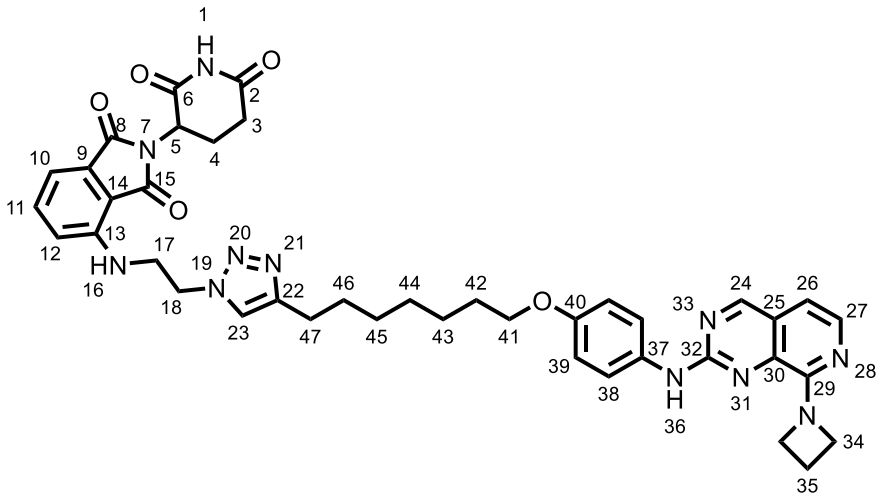

Product was synthesised following **general procedure 5** using 8-(azetidin-1-yl)-*N*-(4-(non-8-yn-1-yloxy)phenyl)pyrido[3,4-*d*]pyrimidin-2-amine (8 mg, 0.02 mmol) and 4-((2-azidoethyl)amino)-2-(2,6-dioxopiperidin-3-yl)isoindoline-1,3-dione, affording 7 mg (44%, 0.01 mmol) of the title product. ^{1}H NMR (600 MHz, $CDCl_3$) δ 8.95 (s, 1H, H24), 7.90 (d, *J* = 5.6 Hz, 1H, H27), 7.51 – 7.44 (m, 3H, H11, H38), 7.40 (s, 1H, H36), 7.29 (s, 1H, H23), 7.15 (d, *J* = 7.1 Hz, 1H, H10), 6.94 – 6.89 (m, 2H, H39), 6.75 (d, *J* = 5.6 Hz, 1H, H26), 6.68 (d, *J* = 8.5 Hz, 1H, H12), 6.48 (t, *J* = 6.6 Hz, 1H, H16), 4.94 (dd, *J* = 12.5, 5.4 Hz, 1H, H5), 4.56 (t, *J* = 5.8 Hz, 2H, H18), 4.46 (t, *J* = 7.7 Hz, 4H, H34), 3.98 (t, *J* = 6.5 Hz, 2H, 41), 3.86 (q, *J* = 6.1 Hz, 2H, H17), 2.95 – 2.65 (m, 5H, H47, H3, H4), 2.45 – 2.37 (m, 2H, H35), 2.18 – 2.11 (m, 1H, H4), 1.79 (p, *J* = 6.6 Hz, 2H, H42), 1.73 – 1.56 (m, 2H, H46), 1.51 – 1.43 (m, 2H, H43), 1.43 – 1.32 (m, 4H, H44 H45), H1 not observed; ^{13}C NMR (151 MHz, $CDCl_3$) δ 171.1 (C2), 169.3 (C15), 168.7 (C6), 166.3 (C8), 160.6 (C24), 156.7 (C32), 155.7 (C29), 155.4 (C40), 148.8 (C22), 146.1 (C13), 139.8 (C27), 139.0 (C30), 136.4 (C11), 132.5 (C9), 132.0 (C37), 123.5 (C25), 122.5 (C38), 121.7 (C23), 116.1 (C12), 114.7 (C39), 112.6 (C10), 110.9 (C14), 107.0 (C26), 68.3 (C41), 53.3 (C34), 49.9 (C18), 49.0 (C5), 43.0 (C17), 31.4 (C3), 29.3 (C46), 29.2 (C42), 29.0 (C44 or 45), 29.0 (C44 or 45), 25.9 (C43), 25.5 (C47), 22.8 (C4), 17.8 (C35); HRMS (ESI +ve): $C_{40}H_{44}N_{11}O_5$ $[M+H]^+$: 758.3521 (Found: 758.3494).

2-(2,6-dioxopiperidin-3-yl)-4-((2-(4-(3-(4-((8-morpholinopyrido[3,4-*d*] pyrimidin-2-yl)amino) phenoxy)propyl)-1*H*-1,2,3-triazol-1-yl)ethyl)amino) isoindoline-1,3-dione (7)

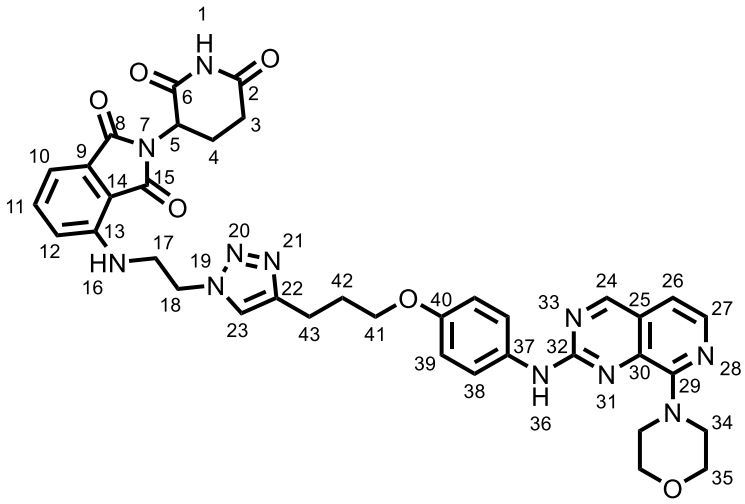

Product was synthesised following **general procedure 5** using 8-morpholino-*N*-(4-(pent-4-yn-1-yloxy)phenyl)pyrido[3,4-*d*]pyrimidin-2-amine (8 mg, 0.02 mmol) and 4-((2-azidoethyl)amino)-2-(2,6-dioxopiperidin-3-yl)isoindoline-1,3-dione, affording 5 mg (26%, 0.01 mmol) of the title product. ^{1}H NMR (600 MHz, $CDCl_3$) δ 9.03 (s, 1H, H24), 8.03 (d, *J* = 5.6 Hz, 1H, H27), 7.61 – 7.56 (m, 3H, H11 and 38), 7.52 (s, 1H, H36), 7.48 (dd, *J* = 8.5, 7.1 Hz, 1H, H10), 7.34 (s, 1H, H23), 7.15 (d, *J* = 7.1 Hz, 1H, H10), 7.02 (d, *J* = 5.6 Hz, 1H, H26), 6.92 – 6.87 (m, 2H, H39), 6.72 (d, *J* = 8.5 Hz, 1H, H12), 6.45 (t, *J* = 6.6 Hz, 1H, H16), 4.92 (dd, *J* = 12.5, 5.4 Hz, 1H, H5), 4.58 (td, *J* = 5.5, 1.3 Hz, 2H, H18), 3.99 (td, *J* = 6.2 Hz, 2H, H41), 3.97 – 3.93 (m, 4H, H35), 2.94 – 2.69 (m, 5H, H43, H4, H3), 2.18 – 2.10 (m, 2H, H42), H1 not observed; ^{13}C NMR (151 MHz, $CDCl_3$) δ 171.1 (C2), 169.3 (C15), 168.5 (C6), 167.3 (C8), 161.9 (C24), 156.7 (C32), 156.1 (C29), 155.1 (C40), 147.6 (C22), 146.1 (C13), 139.8 (C27), 139.1 (C30), 136.4 (C11), 132.5 (C9), 132.3 (C37), 124.1 (C25), 122.1 (C38), 121.7 (C23), 116.2 (C12), 114.8 (C39), 112.7 (C10), 111.4 (C26), 111.0 (C14), 67.2 (C35), 67.1 (C41), 49.8 (C18), 49.2 (C34), 49.0 (C5), 42.9 (C17), 31.4 (C3), 28.9 (C42), 22.7 (C4), 22.0 (C43); HRMS (ESI +ve): $C_{37}H_{38}N_{11}O_6$ 733.3029 (Found: 733.3011).

2-(2,6-dioxopiperidin-3-yl)-4-((2-(4-(5-(4-((8-morpholinopyrido[3,4-*d*] pyrimidin-2-yl)amino) phenoxy)pentyl)-1*H*-1,2,3-triazol-1-yl)ethyl)amino) isoindoline-1,3-dione (8)

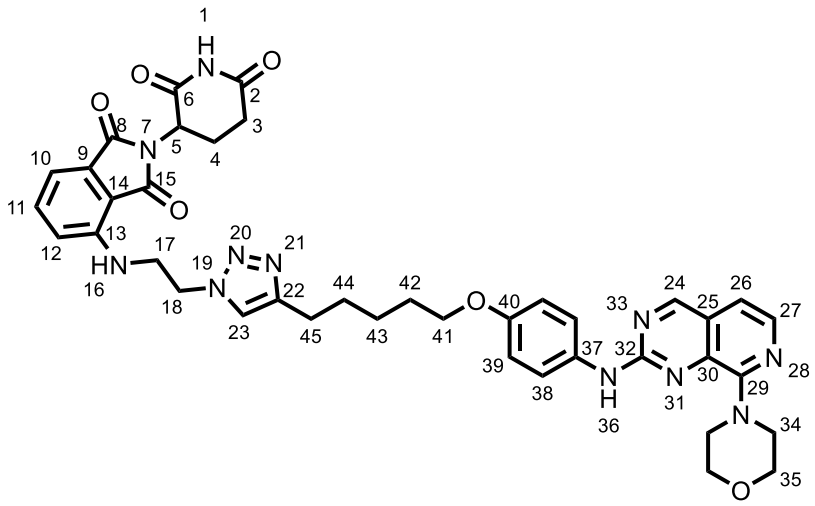

Product was synthesised following **general procedure 5** using *N*-(4-(hept-6-yn-1-yloxy)phenyl)-8-morpholinopyrido[3,4-*d*]pyrimidin-2-amine (5 mg, 0.01 mmol) and 4-((2-azidoethyl)amino)-2-(2,6-dioxopiperidin-3-yl)isoindoline-1,3-dione, affording 2 mg (21%, 0.001 mmol) of the title product. ^{1}H NMR (600 MHz, $CDCl_3$) δ 9.03 (s, 1H, H24), 8.03 (d, *J* = 5.4 Hz, 1H, H27), 7.64 – 7.57 (m, 2H, H36), 7.55 – 7.47 (m, 2H, H11, H36), 7.32 (s, 1H, H23), 7.16 (d, *J* = 7.2 Hz, 1H, H10), 7.02 (d, *J* = 5.4 Hz, 1H, H26), 6.95 – 6.89 (m, 2H, H39), 6.73 (d, *J* = 8.5 Hz, 1H, H12), 6.47 (t, *J* = 6.6 Hz, 1H, H16), 4.93 (dd, *J* = 12.6, 5.4 Hz, 1H, H5), 4.57 (t, *J* = 5.8 Hz, 2H, H18), 4.01 – 3.94 (m, 6H, H35, H41), 3.87 (t, *J* = 5.3 Hz, 6H, H34), 2.94 – 2.70 (m, 5H, H3, H4, H45), 2.18 – 2.11 (m, 1H, H3), 1.83 (p, *J* = 6.7 Hz, 2H, H42), 1.72 (p, *J* = 7.6 Hz, 2H, H44), 1.53 (tt, *J* = 9.6, 6.5 Hz, 2H, H43), H1 not observed; ^{13}C NMR (151 MHz, $CDCl_3$) δ 171.1 (C2), 169.4 (C15), 168.6 (C6), 167.3 (C8), 161.9 (C24), 156.8 (C29), 156.1 (C32), 155.2 (C40), 148.6 (C22) 146.1 (C13), 139.7 (C30), 139.1 (C27), 136.4 (C11), 132.5 (C9), 132.2 (C37), 124.0 (C25), 121.8 (C23), 121.6 (C38), 116.2 (C12), 114.8 (C39), 112.7 (C10), 111.4 (C14), 111.0 (C26), 68.1 (C41), 67.2 (C35), 49.8 (C18), 49.3 (C34), 49.0 (C5), 42.9 (C17), 31.4 (C3), 29.0 (C44), 28.9 (C42), 25.5 (C43), 25.4 (C45), 22.8 (C4); HRMS (ESI +ve): $C_{39}H_{42}N_{11}O_6$ $[M+H]^+$: 760.3314 (Found: 760.3299).

2-(2,6-dioxopiperidin-3-yl)-4-((2-(4-(7-(4-((8-morpholinopyrido[3,4-d] pyrimidin-2-yl)amino)phenoxy)heptyl)-1H-1,2,3-triazol-1-yl)ethyl)amino) isoindoline-1,3-dione (9)

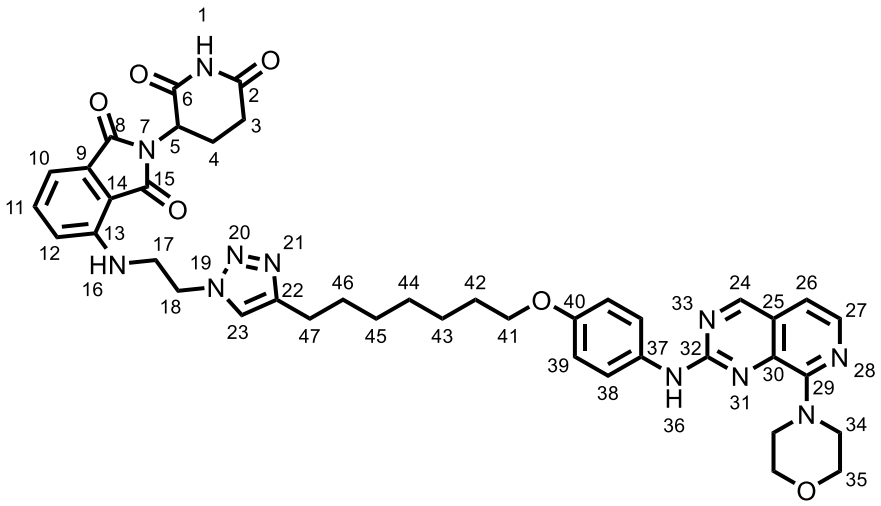

Product was synthesised following **general procedure 5** using 8-morpholino-*N*-(4-(non-8-yn-1-yloxy)phenyl)pyrido[3,4-*d*]pyrimidin-2-amine (6 mg, 0.01 mmol) and 4-((2-azidoethyl)amino)-2-(2,6-dioxopiperidin-3-yl)isoindoline-1,3-dione, affording 4 mg (36%, 0.01 mmol) of the title product; ^{1}H NMR (600 MHz, $CDCl_3$) δ 9.05 (s, 1H, H24), 8.04 (d, *J* = 5.4 Hz, 1H, H27), 7.62 – 7.59 (m, 2H, H38), 7.55 (s, 1H, H36), 7.47 (dd, *J* = 8.5, 7.2 Hz, 1H, H11), 7.30 (s, 1H, H23), 7.16 (d, *J* = 7.1 Hz, 1H, H10), 7.04 (d, *J* = 5.4 Hz, 1H, H26), 6.95 – 6.90 (m, 2H, H39), 6.68 (d, *J* = 8.5 Hz, 1H, H12), 6.48 (t, *J* = 6.6 Hz, 1H, H16), 4.94 (dd, *J* = 12.4, 5.4 Hz, 1H, H5), 4.56 (t, *J* = 5.8 Hz, 2H, H18), 4.01 – 3.94 (m, 6H, H41, H35), 3.89 – 3.84 (m, 6H, H34, H17), 2.95 – 2.72 (m, 3H, H3, H4), 2.69 (t, *J* = 7.7 Hz, 1H, H47), 2.18-2.12 (m, 1H, H4), 1.83 – 1.75 (m, 2H, H42), 1.68 – 1.59 (m, 2H, H46), 1.52 – 1.43 (m, 2H, H43), 1.43 – 1.33 (m, 4H, H45, H46), H1 not observed; ^{13}C NMR (151 MHz, $CDCl_3$) δ 171.1 (C2), 169.4 (C15), 168.6 (C6), 167.4 (C8), 161.9 (C24), 156.8 (C29), 156.1 (C32), 155.4 (C40), 148.8 (C22), 146.1 (C13), 139.7 (C30), 139.1 (C27), 136.4 (C11), 132.6 (C9), 132.1 (C37), 124.1 (C25), 121.7 (C23), 121.6 (C38), 116.1 (C12), 114.8 (C39), 112.6 (C10), 111.4 (C14), 110.9 (C26), 68.4 (C41), 67.2 (C35), 49.9 (C18), 49.3 (C34), 49.0 (C5), 43.0 (C17), 31.4 (C3), 29.3 (C46), 29.1 (C42), 29.0 (C44 or 45), 28.9 (C44 or 45), 25.9 (C43), 25.5 (C47), 22.8 (C4); HRMS (ESI +ve): $C_{41}H_{46}N_{11}O_6$ $[M+H]^+$: 788.3627 (Found: 788.3591).

1-(pent-4-yn-1-yl)piperazine (57)

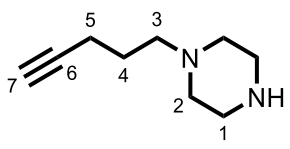

Product was synthesised following **general procedure 6a-c** using 4-pentyn-1-ol (0.25 mL, 2.67 mmol). Aldehyde ^{1}H NMR shift at 9.82 ppm in $CDCl_3$. The Boc-protected amine mass ($[M+H]^+$ 253.20) was seen by LCMS with a retention time of 0.37 min. This afforded the title compound (130 mg, 72%, 0.85 mmol). ^{1}H NMR (500 MHz, DMSO-d6) δ 3.01 (t, J = 5.2 Hz, 4H, H1), 2.76 (t, J = 2.7 Hz, 1H, H7), 2.56 (d, J = 5.2 Hz, 4H, H2), 2.38 (t, J = 7.1 Hz, 2H, H3), 2.16 (td, J = 7.1, 2.7 Hz, 2H, H5), 1.57 (p, J = 7.1 Hz, 2H, H4); ^{13}C NMR (126 MHz, DMSO-d6) δ 84.7 (C6), 71.8 (C7), 56.6 (C3), 49.6 (C2), 43.1 (C1), 25.5 (C4), 16.0 (C5); HRMS (ESI +ve): $C_9H_{17}N_2$ $[M+H]^+$: 153.1391 (Found: 153.1389).

1-(hept-6-yn-1-yl)piperazine (58)

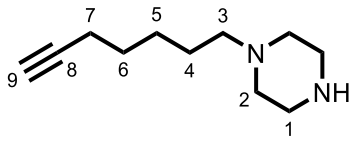

Product was synthesised following **general procedure 6a-c** using hept-6-yn-1-ol (0.34 mL, 2.67 mmol). Aldehyde ^{1}H NMR shift at 9.79 ppm in $CDCl_3$. The boc protected amine mass ($[M+H]^+$ 281.23) was seen by LCMS with a retention time of 1.06 min. This afforded the title compound (22 mg, 37%, 0.12 mmol).^{1}H NMR (500 MHz, $CDCl_3$) δ 2.92 (t, J = 4.9 Hz, 4H, H2), 2.43 (s, 4H, H3), 2.37 – 2.30 (m, 2H, H4), 2.21 (td, J = 7.1, 2.7 Hz, 2H, H8a), 1.95 (t, J = 2.7 Hz, 1H, H10), 1.65 – 1.38 (m, 6H, H5, 6 and 7); ^{13}C NMR (126 MHz, $CDCl_3$) δ 84.5 (C9), 68.2 (C10), 59.2 (C4), 54.5 (C3), 46.0 (C2), 28.4 (C5), 26.7 (C6), 26.1 (C7), 18.4 (C8); HRMS (ESI +ve): $C_{11}H_{21}N_2$ $[M+H]^+$: 181.1699 (Found: 181.1724).

1-(non-8-yn-1-yl)piperazine (59)

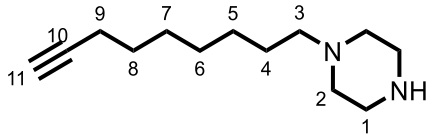

Product was synthesised following **general procedure 6a-c** using non-8-yn-1-ol (310 mg, 2.21 mmol). Aldehyde ^{1}H NMR shift at 9.78 ppm in $CDCl_3$. The boc protected amine mass ($[M+H]^+$ 309.26) was seen by LCMS with a retention time of 1.27 min. This afforded the title compound.^{1}H NMR (600 MHz, MeOH-d4) δ 3.76 – 3.59 (m, 4H, H1 or 2), 3.30 – 3.26 (m, 2H, H3), 2.22 – 2.18 (m, 3H, H11 and 9), 1.87 – 1.81 (m, 2H, H4), 1.58 – 1.52 (m, 2H, H8), 1.52 – 1.40 (m, 6H,

H5-7); ^{13}C NMR (151 MHz, MeOH-d4) δ 83.4 (C10), 68.1 (C11), 56.9 (C3), 40.6 (C1 or 2), 28.2 (C5-8), 28.1 (C5-8), 28.0 (C5-8), 26.0 (C5-8), 23.4 (C4), 17.5 (C9); HRMS (ESI +ve): $C_{13}H_{25}N_2$ $[M+H]^+$: 209.2012 (Found: 209.2034).

2-(methylthio)-8-(4-(pent-4-yn-1-yl)piperazin-1-yl)pyrido[3,4-*d*]pyrimidine (60)

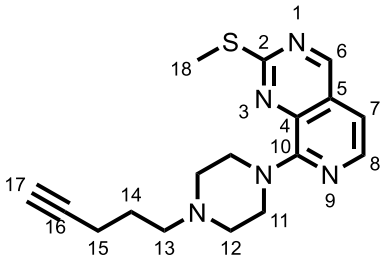

Product was synthesised following **general procedure 1** using 1-(pent-4-yn-1-yl)piperazine (162 mg, 1.06 mmol) and 8-chloro-2-methylsulfanyl-pyrido[3,4-*d*]pyrimidine, affording the title product (81 mg, 35%, 0.25 mmol). ^{1}H NMR (600 MHz, $CDCl_3$) δ 9.11 (s, 1H, H6), 8.17 (d, *J* = 5.4 Hz, 1H, H8), 7.09 (d, *J* = 5.4 Hz, 1H, H7), 4.27 (s, 4H, H12), 3.09 (t, *J* = 5.2 Hz, 4H, H13), 2.93 – 2.88 (m, 2H, H14), 2.64 (s, 3H, H11), 2.34 (td, *J* = 6.9, 2.7 Hz, 2H, H16), 2.02 (t, *J* = 2.6 Hz, 1H, H18), 2.01 – 1.92 (m, 2H, H15); ^{13}C NMR (151 MHz, $CDCl_3$) δ 167.9 (C2), 160.2 (C6), 155.6 (C10), 141.9 (C8), 138.8 (C4), 126.4 (C5), 110.7 (C7), 82.7 (C16), 69.6 (C17), 56.6 (C13), 52.2 (C12), 46.8 (C11), 23.6 (C14), 16.3 (C15), 14.5 (C18); HRMS (ESI +ve): $C_{17}H_{22}N_5S$ $[M+H]^+$: 328.1596 (Found: 328.1594).

8-(4-(hept-6-yn-1-yl)piperazin-1-yl)-2-(methylthio)pyrido[3,4-*d*]pyrimidine (61)

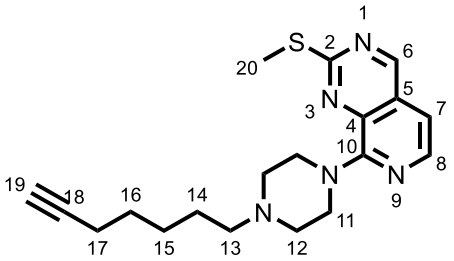

Product was synthesised following **general procedure 1** using 1-(hept-6-yn-1-yl)piperazine (10 mg, 0.06 mmol) and 8-chloro-2-methylsulfanyl-pyrido[3,4-*d*]pyrimidine, affording the title product (9 mg, 54%, 0.03 mmol). ^{1}H NMR (600 MHz, $CDCl_3$) δ 9.11 (s, 1H, H6), 8.17 (d, *J* = 5.4 Hz, 1H, H8), 7.09 (d, *J* = 5.4

Hz, 1H, H7), 4.29 (s, 4H, H11), 3.11 (t, *J* = 5.1 Hz, 4H, H12), 2.86 – 2.79 (m, 3H, H13), 2.64 (d, *J* = 9.5 Hz, 3H, H20), 2.23 (td, *J* = 6.9, 2.7 Hz, 2H, H17), 1.97 (t, *J* = 2.6 Hz, 1H, H19), 1.80 – 1.73 (m, 2H, H14), 1.59 (dq, *J* = 8.8, 6.7 Hz, 3H, H16), 1.53 – 1.46 (m, 2H, H15); ^{13}C NMR (151 MHz, $CDCl_3$) δ 168.0 (C2), 160.2 (C6), 155.5 (C10),141.9 (C8), 138.8 (C4), 126.4 (C5), 110.8 (C7), 84.0 (C18), 68.7 (C19), 57.4 (C13), 51.9 (C12), 46.6 (C11), 27.9 (C16), 26.1 (C15), 24.1 (C14), 18.2 (C17), 14.5 (C20); HRMS (ESI +ve): $C_{19}H_{26}N_5S$ $[M+H]^+$: 356.1903 (Found: 356.192).

8-(4-(hept-6-yn-1-yl)piperazin-1-yl)-2-(methylsulfonyl)pyrido[3,4-*d*] pyrimidine (62)

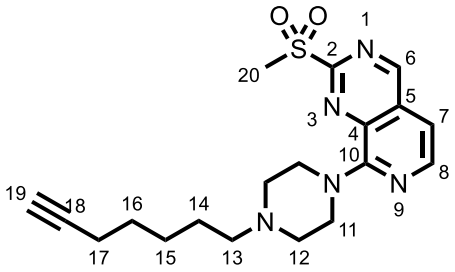

Product was synthesised following **general procedure 2** using 8-(4-(hept-6-yn-1-yl)piperazin-1-yl)-2-(methylthio)pyrido[3,4-*d*]pyrimidine (169 mg, 0.48 mmol) affording the title product (37 mg, 20%, 0.10 mmol). ^{1}H NMR (600 MHz, $CDCl_3$) δ 9.40 (s, 1H, H6), 8.37 (d, *J* = 5.4 Hz, 1H, H8), 7.07 (d, *J* = 5.4 Hz, 1H, H7), 4.26 (t, *J* = 5.2 Hz, 4H, H11), 3.41 (s, 3H, H20), 2.68 (t, *J* = 5.0 Hz, 4H, H12), 2.50 – 2.40 (m, 2H, H13), 2.23 (td, *J* = 7.1, 2.7 Hz, 2H, H17), 1.97 (t, *J* = 2.7 Hz, 1H, H19), 1.59 (qd, *J* = 7.6, 3.5 Hz, 4H, H15, H16), 1.48 (qd, *J* = 7.3, 3.1 Hz, 2H, H14);^{13}C NMR (151 MHz, $CDCl_3$) δ 161.7 (C6), 159.1 (C2), 156.6 (C10), 146.8 (C8), 136.6 (C4), 131.0 (C5), 107.7 (C7), 84.5 (C18), 68.3 (C19), 58.5 (C13), 53.4 (C12), 48.5 (C11), 39.5 (C20), 28.4 (C16), 26.7 (C15), 26.3 (C14), 18.4 (C17); HRMS (ESI +ve): $C_{19}H_{26}N_5O_2S$ $[M+H]^+$: 388.1807 (Found: 388.1809).

8-(4-(hept-6-yn-1-yl)piperazin-1-yl)-*N*-(tetrahydro-2*H*-pyran-4-yl)pyrido [3,4-*d*]pyrimidin-2-amine (66)

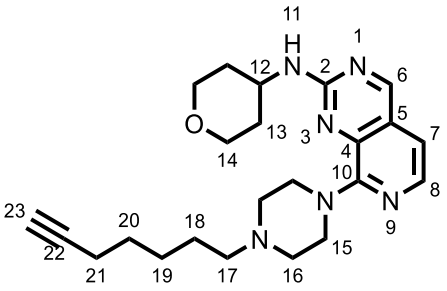

8-(4-(hept-6-yn-1-yl)piperazin-1-yl)-2-(methylsulfonyl)pyrido[3,4-*d*]pyrimidine (37 mg, 0.10 mmol) and 4-aminotetrahydropyran (98 µL, 0.10 mmol) were dissolved in NMP (0.30 mL) and heated to 120 °C for 18 h. Water was added (10 mL) and extracted with DCM (3 times). The DCM layers were combined and concentrated *in vacuo*. The residue was dissolved in MeOH and 3 drops of formic acid was added. This was passed through an SCX-2 column, washing with MeOH. 3.5 M ammonia in MeOH was used to elute product which was then removed *in vacuo* to afford the title product (38 mg, 97%, 0.09 mmol). ^{1}H NMR (600 MHz, $CDCl_3$) δ 8.92 (s, 1H, H6), 7.96 (d, *J* = 5.4 Hz, 1H, H8), 6.95 (d, *J* = 5.5 Hz, 1H, H7), 4.07 (dt, *J* = 11.8, 3.6 Hz, 4H, H14, H12), 3.94 (s, 5H, H15), 3.57 (td, *J* = 11.5, 2.2 Hz, 3H, H14), 2.69 (t, *J* = 5.0 Hz, 5H, H16), 2.49 – 2.42 (m, 3H, H17), 2.23 (dt, *J* = 7.1, 3.6 Hz, 3H, H21), 2.16 – 2.09 (m, 3H, H13), 1.97 (t, *J* = 2.6 Hz, 1H, H23), 1.72 – 1.43 (m, 13H, H18, H19, H20); ^{13}C NMR (151 MHz, $CDCl_3$) δ 162.1 (C6), 157.7 (C2), 156.6 (C10), 139.7 (C4), 138.4 (C8), 123.4 (C5), 111.0 (C7), 84.5 (C22), 68.3 (C23), 66.9 (C14), 58.8 (C17), 53.5 (C16), 48.7 (C15), 48.0 (C12), 33.0 (C13), 28.4 (C20), 26.8 (C19), 26.4 (C18), 18.4 (C21); HRMS (ESI +ve): $C_{23}H_{33}N_6O$ $[M+H]^+$: 409.2716 (Found: 409.2713).

8-(4-(non-8-yn-1-yl)piperazin-1-yl)-*N*-(tetrahydro-2H-pyran-4-yl)pyrido[3,4-*d*]pyrimidin-2-amine (67)

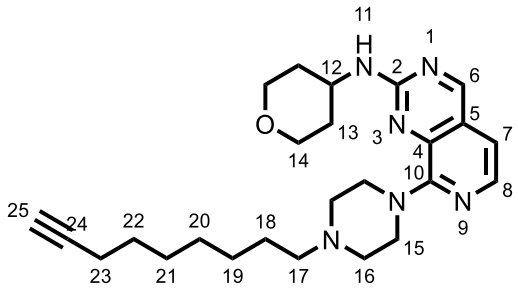

To a solution of 1-(non-8-yn-1-yl)piperazine (217 mg, 0.89 mmol) in NMP (2 mL) was added 8-chloro-2-methylsulfanyl-pyrido[3,4-*d*]pyrimidine (75 mg, 0.35

mmol). The reaction was heated to 80 °C for 20 h before being quenched with sat. aq. $NaHCO_3$ and extracted with EtOAc (3 times). The organic layer was combined, washed with water and brine, dried and concentrated under reduced pressure. The crude product was used in the next step without further purification assuming 100% yield. LCMS of the reaction showed the correct mass of product ($[M+H]^+$ 384.22) with a retention time of 1.04 min. Crude 2-(methylthio)-8-(4-(non-8-yn-1-yl)piperazin-1-yl)pyrido[3,4-*d*]pyrimidine (135 mg, 0.35 mmol) was dissolved in MeOH (1.2 mL) and stirred at rt. A solution of OXONE (270 mg, 0.88 mmol) in water (1.2 mL) was added and the mixture was stirred for 18 h at rt. Water (15 mL) was added and extracted with EtOAc (3 times). The organic layers were combined, washed with brine, and solvent was removed *in vacuo* to afford crude title product that was used in the next step assuming 100% yield. LCMS of the reaction showed the correct mass of product ($[M+H]^+$ 416.21) with a retention time of 0.84 min. 2-(methylsulfonyl)-8-(4-(non-8-yn-1-yl)piperazin-1-yl)pyrido[3,4-*d*]pyrimidine (140 mg, 0.34 mmol) and 4-aminotetrahydropyran (347 µL, 3.37 mmol) were dissolved in NMP (1 mL) and heated to 120 °C for 18 h. Water was added and was extracted using DCM. The DCM layers were combined, washed with brine, dried over $MgSO_4$, and solvent was removed in *vacuo*. Crude product was purified using reverse phase column chromatography (water:MeOH (+0.1% formic acid) 5-80%) to afford the title product (50 mg, 34%, 0.11 mmol). ^{1}H NMR (600 MHz, $CDCl_3$) δ 8.95 (s, 1H, H6), 7.96 (d, *J* = 5.4 Hz, 1H, H8), 7.01 (d, *J* = 5.4 Hz, 1H, H7), 4.16 (s, 4H, H15), 4.06 (dt, *J* = 11.8, 3.7 Hz, 3H, H12, 14), 3.57 (td, *J* = 11.5, 2.3 Hz, 2H, H14), 3.10 (s, 4H, H16), 2.84 – 2.76 (m, 2H, H17), 2.20 (td, *J* = 7.1, 2.7 Hz, 3H, H23), 2.09 (dt, *J* = 12.3, 2.5 Hz, 2H, H13), 1.96 (t, *J* = 2.7 Hz, 1H, H25), 1.76 – 1.61 (m, 4H, H13, 18), 1.54 (p, *J* = 7.2 Hz, 2H, H22), 1.47 – 1.40 (m, 2H, H21), 1.40 – 1.35 (m, 4H, H19, 20); ^{13}C NMR (151 MHz, $CDCl_3$) δ 162.23 (C6), 161.05 (C10), 157.71 (C2), 155.39 (C4), 138.22 (C8), 123.42 (C5), 111.92 (C7), 84.53 (C24), 68.27 (C25), 66.76 (C14), 57.55 (C17), 51.72 (C16), 47.84 (C12), 46.55 (C15), 32.82 (C13), 28.69 (C18 or 19), 28.47 (C21), 28.27 (C22), 26.91 (C18 or 19), 24.45 (C18), 18.33 (C23); HRMS (ESI +ve): $C_{25}H_{36}N_6O$ $[M+H]^+$: 437.3028 (Found: 437.3019).

8-chloro-2-(methylsulfonyl)pyrido[3,4-*d*]pyrimidine (68)

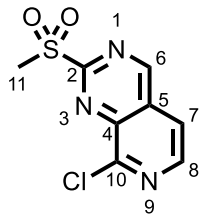

A cooled (0 °C) suspension of 8-chloro-2-methylsulfanyl-pyrido[3,4-*d*]pyrimidine (130mg, 0.61 mmol) in DCM (4.5 mL) was treated with 77% w/w *m*CPBA (303 mg, 1.35 mmol) and stirred for 18 h, whilst slowly warming to rt. The reaction was quenched with water and extracted with DCM (3 times). The organic layers were combined, washed with water, dried and concentrated under reduced pressure. The residue was purified by flash column chromatography (EtOAc:c-hex 0-80%) affording the title product (85 mg, 57%, 0.35 mmol). ^{1}H NMR (600 MHz, $CDCl_3$) δ 9.76 (s, 1H, H6), 8.77 (d, *J* = 5.5 Hz, 1H, H8), 7.90 (d, *J* = 5.5 Hz, 1H, H7), 3.59 (s, 3H, H11); ^{13}C NMR (151 MHz, $CDCl_3$) δ 164.1 (C2), 163.3 (C6), 154.0 (C10), 146.6 (C8), 141.7 (C5), 129.6 (C4), 118.2 (C7), 39.1, (C11); HRMS (ESI +ve): $C_8H_7ClN_3O_2S$ $[M+H]^+$:243.9942 (Found: 244.0012).

8-chloro-*N*-phenylpyrido[3,4-*d*]pyrimidin-2-amine (69)

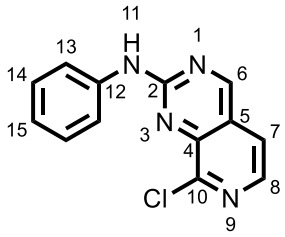

Product was synthesised following **general procedure 4** using *N*-phenylformamide (20 mg, 0.16 mmol) and 8-chloro-2-(methylsulfonyl)pyrido [3,4-*d*]pyrimidine (40 mg, 0.16 mmol) affording the title product (43 mg, quantitative, 0.16 mmol). ^{1}H NMR (600 MHz, $CDCl_3$) δ 9.19 (s, 1H, H6), 8.28 (d, *J* = 5.3 Hz, 1H, H8), 7.97 (d, *J* = 7.9 Hz, 2H, H13), 7.61 (s, 1H, H11), 7.54 (d, *J* = 5.3 Hz, 1H, H7), 7.49 – 7.43 (m, 2H, H14), 7.17 (td, *J* = 7.4, 1.1 Hz, 1H, H15); ^{13}C NMR (151 MHz, $CDCl_3$) δ 161.8 (C6), 157.5 (C2), 150.5 (C10), 144.0 (C5), 140.2 (C8), 138.6 (C12), 129.2 (C14), 124.4 (C4), 123.5 (C15), 119.1 (C13), 118.5 (C7); HRMS (ESI +ve): $C_{13}H_{10}ClN_4$ $[M+H]$+:257.0589 (Found: 257.0555).

8-(4-(pent-4-yn-1-yl)piperazin-1-yl)-*N*-phenylpyrido[3,4-*d*]pyrimidin-2-amine (70)

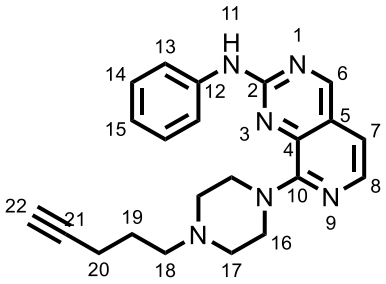

Product was synthesised following **general procedure 1** using 1-(pent-4-yn-1-yl)piperazine (25 mg, 0.13 mmol) and 8-chloro-*N*-phenylpyrido[3,4-*d*]pyrimidin-2-amine**,** affording the title product (6 mg, 24%, 0.02 mmol). ^{1}H NMR (600 MHz, $CDCl_3$) δ 9.05 (s, 1H, H6), 8.07 (d, *J* = 5.4 Hz, 1H, H8), 7.81 – 7.73 (m, 2H, H13), 7.45 – 7.37 (m, 3H, H11, H14), 7.13 (t, *J* = 7.3 Hz, 1H, H15), 7.03 (d, *J* = 5.4 Hz, 1H, H7), 3.95 (s, 4H, H16), 2.75 (t, *J* = 5.0 Hz, 4H, H17), 2.63 – 2.56 (m, 2H, H18), 2.33 (td, *J* = 7.1, 2.7 Hz, 2H, 20), 2.01 (t, J = 2.6 Hz, 1H, H22), 1.84 (h, *J* = 7.3 Hz, 2H, H19); ^{13}C NMR (151 MHz, $CDCl_3$) δ 161.9 (C6), 157.1 (C10), 155.6 (C2), 139.6 (C8), 139.2 (C12), 128.9 (C14), 124.4 (C4 or 5), 122.9 (C15), 119.2 (C13), 110.9 (C7), 84.2 (C21), 68.5 (C22), 57.6 (C18), 53.6 (C17), 48.8 (C16), 25.8 (C19), 16.5 (C20); HRMS (ESI +ve): $C_{22}H_{25}N_6$ $[M+H]^+$: 373.2135 (Found: 373.2137).

8-(4-(hept-6-yn-1-yl)piperazin-1-yl)-*N*-phenylpyrido[3,4-*d*]pyrimidin-2-amine (71)

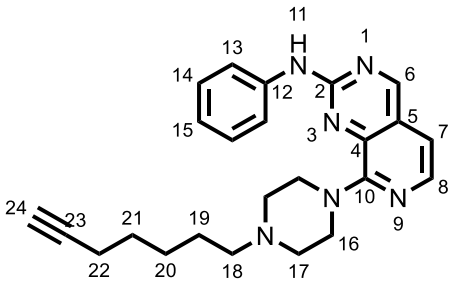

Product was synthesised following **general procedure 1** using 1-(hept-6-yn-1-yl)piperazine (7 mg, 0.04 mmol) and 8-chloro-*N*-phenylpyrido[3,4-*d*]pyrimidin-2-amine, affording the title product (6 mg, 55%, 0.02 mmol). ^{1}H NMR (600 MHz, $CDCl_3$) δ 9.05 (s, 1H), 8.07 (d, *J* = 5.4 Hz, 1H), 7.79 – 7.75 (m, 2H), 7.43 – 7.38 (m, 3H), 7.14 (t, *J* = 7.4 Hz, 1H), 7.03 (d, *J* = 5.4 Hz, 1H), 4.00 – 3.95 (m, 4H), 2.78 (s, 4H), 2.53 (d, *J* = 6.8 Hz, 2H), 2.25 (td, *J* = 7.1, 2.7 Hz, 2H), 1.98 (t, *J* = 2.6 Hz, 1H), 1.70 - 1.60 (m, 4H), 1.56 – 1.48 (m, 2H); ^{13}C NMR (151 MHz, $CDCl_3$) δ 162.0 (C6), 155.8 (C10), 155.8 (C2), 139.6 (C4,8), 139.2 (C12), 128.9 (C14),

124.8 (C5), 124.4 (C15), 119.3 (C13), 110.9 (C7), 84.9 (C23), 68.3 (C24), 58.7 (C18), 53.4 (C16), 48.4 (C17), 28.4 (C19 or 21), 26.7 (C20), 25.9 (C19 or 21), 18.4 (C22); HRMS: $C_{24}H_{29}N_6$ $[M+H]^+$: 401.2448 (Found: 401.2462).

8-(4-(non-8-yn-1-yl)piperazin-1-yl)-*N*-phenylpyrido[3,4-*d*]pyrimidin-2-amine (72)

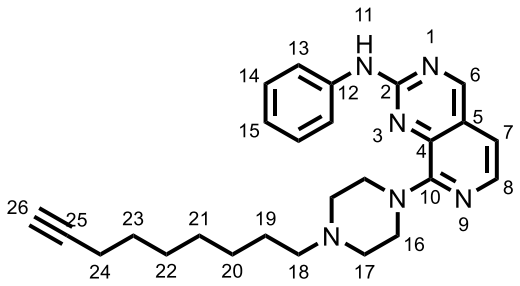

Product was synthesised following **general procedure 1** using 1-(non-8-yn-1-yl)piperazine (34 mg, 0.14 mmol) and 8-chloro-*N*-phenylpyrido[3,4-*d*]pyrimidin-2-amine, affording the title product (10 mg, 33%, 0.02 mmol). ^{1}H NMR (600 MHz, $CDCl_3$) δ 9.07 (s, 1H, H6), 8.06 (d, *J* = 5.4 Hz, 1H, H8), 7.74 – 7.68 (m, 2H, H13), 7.51 (s, 1H, H11), 7.44 – 7.37 (m, 2H, H14), 7.16 (tt, *J* = 7.3, 1.2 Hz, 1H, H15), 7.08 (d, *J* = 5.4 Hz, 1H, H7), 4.16 (s, 4H, H16), 3.12 (s, 4H, H17), 2.85 – 2.80 (m, 2H, H18), 2.22 (td, *J* = 7.0, 2.6 Hz, 2H, H24), 1.97 (t, *J*= 2.7 Hz, 1H, H26), 1.79 – 1.71 (m, 2H, H19), 1.58 – 1.51 (m, 2H, H23), 1.48 – 1.42 (m, 2H, H22), 1.45 – 1.37 (m, 2H, H20); ^{13}C NMR (151 MHz, $CDCl_3$) δ 162.1 (C6), 155.9 (C10), 155.9 (C2), 140.8 (C4), 139.4 (C8), 138.9 (C12), 129.0 (C14), 124.3 (C5), 123.5 (C15), 119.8 (C13), 111.7 (C7), 84.8 (C25), 68.3 (C26), 57.5 (C18), 51.9 (C17), 46.6 (C16), 28.7 (C20, 21, 22, 23), 28.5 (C20, 21, 22, 23), 28.3 (C20, 21, 22, 23), 27.0 (C20, 21, 22, 23), 24.5 (C19), 18.4 (C24); HRMS (ESI +ve): $C_{26}H_{33}N_6$ $[M+H]^+$: 429.2767 (Found: 429.2764).

2-(2,6-dioxopiperidin-3-yl)-4-((3-(4-(5-(4-(2-((tetrahydro-2*H*-pyran-4-yl) amino)pyrido[3,4-*d*]pyrimidin-8-yl)piperazin-1-yl)pentyl)-1*H*-1,2,3-triazol-1-yl)propyl)amino)isoindoline-1,3-dione (11)

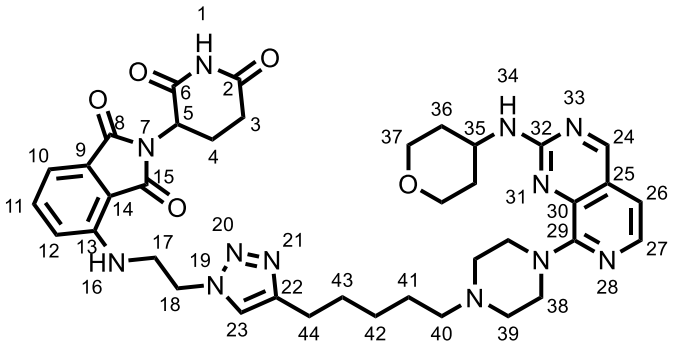

Product was synthesised following **general procedure 5** using 8-(4-(hept-6-yn-1-yl)piperazin-1-yl)-*N*-(tetrahydro-2*H*-pyran-4-yl)pyrido[3,4-*d*]pyrimidin-2-amine (28 mg, 0.07 mmol) and 4-((2-azidoethyl)amino)-2-(2,6-dioxopiperidin-3-yl)isoindoline-1,3-dione, affording the title compound (7 mg, 13%, 0.01 mmol). ^{1}H NMR (600 MHz, $CDCl_3$) δ 8.93 (s, 1H, H24), 7.96 (d, *J* = 5.4 Hz, 1H, H27), 7.52 (dd, *J* = 8.5, 7.1 Hz, 1H, H11), 7.37 (s, 1H, H23), 7.18 (d, *J* = 7.1 Hz, 1H, H12), 6.96 (d, *J* = 5.4 Hz, 1H, H26), 6.84 (d, *J* = 8.5 Hz, 1H, H10), 6.34 (t, *J* = 6.4 Hz, 1H, H16), 4.91 (dd, *J* = 12.5, 5.4 Hz, 1H, H5), 4.63 – 4.49 (m, 2H, H18), 4.13 – 4.04 (m, 2H, H35, H37), 4.00 – 3.72 (m, 5H, H38, H17), 3.57 (ddd, *J* = 12.2, 10.8, 1.3 Hz, 2H, H37), 2.91 – 2.63 (m, 9H, H3, H4, H39, H44), 2.59 – 2.39 (m, 3H, H40), 2.12 (dddd, *J* = 15.8, 13.5, 5.1, 2.9 Hz, 3H, H4, 36), 1.76 – 1.58 (m, 3H, H36, H42, H43), 1.44 – 1.35 (m, 1H, H41); ^{13}C NMR (151 MHz, $CDCl_3$) δ 171.8 (C2), 169.4 (C15), 169.1 (C6), 167.4 (C8), 162.1 (C24), 157.7 (C32), 156.6 (C29), 148.9 (C22), 145.7 (C13), 140.4 (C30), 138.4 (C27), 136.4 (C11), 132.7 (C9), 123.4 (C25), 121.8 (C23), 116.1 (C10), 112.7 (C12), 111.3 (C14), 111.2 (C26), 66.9 (C37), 58.2 (C40), 52.9 (C39), 49.6 (C18), 49.2 (C5), 48.2 (C35), 47.9 (C38), 42.7 (C17), 32.9 (C36), 31.7 (C3), 29.2 (C42 or 43), 27.0 (C41), 25.9 (C42, C43), 25.6 (C44), 22.8 (C4); HRMS (ESI +ve): $C_{38}H_{47}N_{12}O_5$ $[M+H]^+$: 751.3716 (Found: 751.3776).

2-(2,6-dioxopiperidin-3-yl)-4-((3-(4-(7-(4-(2-((tetrahydro-2H-pyran-4-yl) amino)pyrido[3,4-d]pyrimidin-8-yl)piperazin-1-yl)heptyl)-1H-1,2,3-triazol-1-yl)propyl)amino)isoindoline-1,3-dione (12)

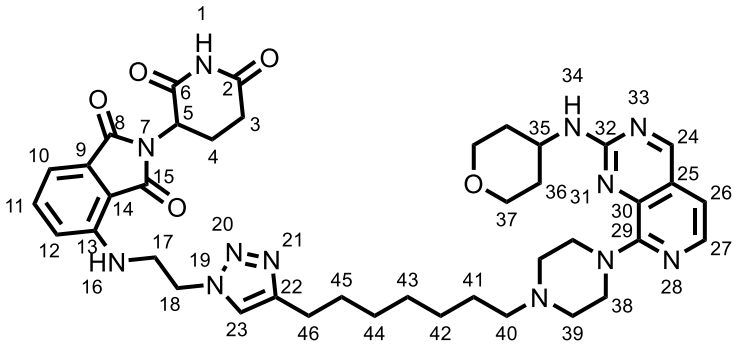

Product was synthesised following **general procedure 5** using 8-(4-(non-8-yn-1-yl)piperazin-1-yl)-*N*-(tetrahydro-2H-pyran-4-yl)pyrido[3,4-*d*]pyrimidin-2-amine (30 mg, 0.07 mmol) and 4-((2-azidoethyl) amino)-2-(2,6-dioxopiperidin-3-yl)isoindoline-1,3-dione, affording the title compound (8 mg, 14%, 0.01 mmol). ^{1}H NMR (600 MHz, $CDCl_3$) δ 8.96 (s, 1H, H24), 7.96 (d, *J* = 5.4 Hz, 1H, H27), 7.46 (dd, *J* = 8.5, 7.1 Hz, 1H, H11), 7.32 (s, 1H, H23), 7.13 (d, *J* = 7.1 Hz, 1H, H12), 7.02 (d, *J* = 5.4 Hz, 1H, H26), 6.69 (d, *J* = 8.5 Hz, 1H, H10), 6.45 (t, *J* = 6.6 Hz, 1H, H16), 4.92 (dd, *J* = 12.4, 5.3 Hz, 1H, H5), 4.63 – 4.53 (m, 2H, H18), 4.21 (s, 4H, H38), 4.06 (dt, *J* = 11.8, 3.8 Hz, 3H, H35, H37), 3.90 – 3.83 (m, 2H, H17), 3.58 (td, *J* = 11.5, 2.3 Hz, 2H, H37), 3.19 (s, 4H, H39), 2.96 – 2.72 (m, 5H, H3, H4, H40), 2.69 – 2.65 (m, 2H, H46), 2.17 – 2.12 (m, 1H, H4), 2.11 – 2.06 (m, 2H, H36), 1.73 (dd, *J* = 10.3, 6.0 Hz, 2H, H41), 1.69 – 1.62 (m, 2H, H36), 1.56 (p, *J* = 7.5 Hz, 2H, H45), 1.33 – 1.27 (m, 7H, H42, H43, H44); ^{13}C NMR (151 MHz, $CDCl_3$) δ 171.5 (C2), 169.4 (C15), 168.7 (C6), 167.4 (C8), 162.2 (C24), 157.8 (C32), 155.2 (C29), 148.6 (C22), 146.0 (C13), 140.0 (C30), 138.2 (C27), 136.4 (C11), 132.5 (C9), 123.4 (C25), 122.0 (C23), 116.1 (C10), 112.5 (C12), 112.1 (C26), 110.9 (C14), 66.7 (C37), 57.2 (C40), 51.5 (C39), 49.9 (C18), 49.1 (C5), 47.8 (C35), 46.2 (C38), 42.8 (C17), 32.8 (C36), 31.6 (C3), 29.1 (C45), 28.7 (C44 , C43), 28.6 (C44, C43), 26.7 (C42), 25.3 (C46), 24.0 (C41), 22.8 (C4); HRMS (ESI +ve): $C_{40}H_{51}N_{12}O_5$ $[M+H]^+$: 779.4105 (Found: 779.4012).

2-(2,6-dioxopiperidin-3-yl)-4-((3-(4-(3-(4-(2-(phenylamino)pyrido[3,4-*d*]pyrimidin-8-yl)piperazin-1-yl)propyl)-1*H*-1,2,3-triazol-1-yl)propyl) amino)isoindoline-1,3-dione (13)

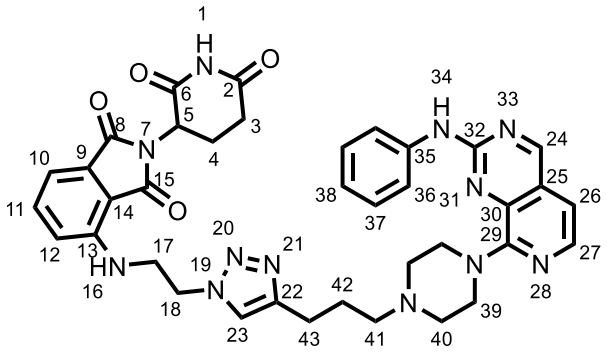

Product was synthesised following **general procedure 5** using 8-(4-(pent-4-yn-1-yl)piperazin-1-yl)-*N*-phenylpyrido[3,4-*d*]pyrimidin-2-amine (6 mg, 0.20 mmol) and 4-((2-azidoethyl)amino)-2-(2,6-dioxopiperidin-3-yl)isoindoline-1,3-dione, affording the title compound (6 mg, 50%, 0.01 mmol). ^{1}H NMR (600 MHz, $CDCl_3$) δ 9.03 (s, 1H, H24), 8.04 (d, *J* = 5.4 Hz, 1H, H27), 7.77 – 7.72 (m, 2H, H36), 7.58 – 7.52 (m, 2H, H34, 11), 7.43 – 7.36 (m, 3H, H37, 23), 7.20 (d, *J* = 7.1 Hz, 1H, H10), 7.16 – 7.11 (m, 1H, H38), 7.01 (d, J = 5.4 Hz, 1H, H26), 6.90 (d, *J* = 8.5 Hz, 1H, H12), 6.32 (t, *J* = 6.5 Hz, 1H, H16), 4.88 – 4.83 (m, 1H, H5), 4.67- 4.47 (m, 2H, H18), 4.06 – 3.72 (m, 6H, H40, H17), 3.04 – 2.47 (m, 10H, H39, H41, H42, H43, H3, H4), 2.20 – 2.11 (m, 1H, H4), 2.07 – 1.89 (m, 2H, H41, H42, H43); ^{13}C NMR (151 MHz, $CDCl_3$) δ 172.1 (C2), 169.7 (C15), 169.5 (C6), 167.4 (C8), 161.9 (C24), 156.9 (C29), 155.7 (C32), 148.1 (C22), 145.7 (C9), 139.6 (C25), 139.4 (C27), 139.1 (C35), 136.4 (C11), 132.9 (C15), 129.0 (C37), 124.3 (C30), 123.1 (C38), 122.2 (C23), 119.3 (C36), 116.4 (C12), 112.9 (C10), 111.6 (C13), 111.2 (C26), 58.3 (C41, 42, 43), 53.2 (C39), 49.4 (C18), 49.1 (C5), 48.0 (C17), 42.7 (C17), 31.4, (C3) 25.5 (C41, 42, 43), 23.8 (C41, 42, 43), 23.0 (C4); HRMS (ESI +ve): $C_{37}H_{39}N_{12}O_4$ $[M+H]^+$: 715.3212 (Found: 715.3197).

2-(2,6-dioxopiperidin-3-yl)-4-((3-(4-(5-(4-(2-(phenylamino)pyrido[3,4-*d*] pyrimidin-8-yl)piperazin-1-yl)pentyl)-1*H*-1,2,3-triazol-1-yl)propyl)amino) isoindoline-1,3-dione (14)

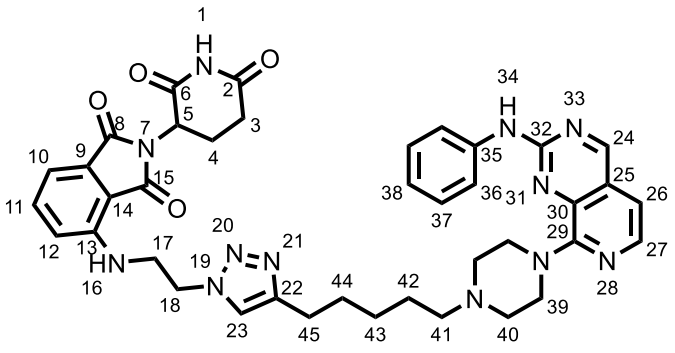

Product was synthesised following **general procedure 5** using 8-(4-(hept-6-yn-1-yl)piperazin-1-yl)-*N*-phenylpyrido[3,4-*d*]pyrimidin-2-amine (10 mg, 0.03 mmol) and 4-((2-azidoethyl)amino)-2-(2,6-dioxopiperidin-3-yl)isoindoline-1,3-dione, affording the title compound (12 mg, 61%, 0.02 mmol). ^{1}H NMR (600 MHz, $CDCl_3$) δ 9.05 (s, 1H, H24), 8.04 (d, *J* = 5.4 Hz, 1H, H27), 7.76 – 7.71 (m, 2H, H36), 7.65 (s, 1H, H34), 7.50 (dd, *J* = 8.5, 7.1 Hz, 1H, H11), 7.42 – 7.34 (m, 3H, H37, H23), 7.15 (d, *J* = 7.1 Hz, 1H, H10), 7.12 (tt, *J* = 7.3, 1.2 Hz, 1H, H38), 7.02 (d, *J* = 5.4 Hz, 1H, H26), 6.80 (d, *J* = 8.5 Hz, 1H, H12), 6.37 (t, *J* = 6.5 Hz, 1H, H16), 4.90 (dd, *J* = 12.4, 5.4 Hz, 1H, H5), 4.64-4.54 (m, 2H, H18), 411-3.93 (s, 4H, H40), 3.89-3.77 (m,, 2H, H17), 2.98 – 2.52 (m, 7H, H39, H3, H4), 2.15-2.08 (m, 1H, H4), 1.69 (p, *J* = 7.6 Hz, 6H, H41, H42, H43, H44, H45), 1.45 – 1.35 (m, 4H, H41, H42, H43, H44, H45); ^{13}C NMR (151 MHz, $CDCl_3$) δ 171.8 (C2), 169.4 (C15), 169.0 (C6), 167.4 (C8), 161.9 (C24), 156.7 (C29), 155.7 (C32), 148.5 (C22), 145.8 (C9), 139.5 (C25) 139.4 (C27), 139.1 (C35), 136.3 (C11), 132.6 (C14), 129.1 (C37),124.3 (C30), 123.1 (C38), 122.0 (C23), 119.4 (C36), 116.2 (C12), 112.6 (C10), 111.3 (C26), 111.1 (C13), 58.1 (C41), 52.9 (C39), 49.6 (C18), 49.1 (C5), 47.7 (C40), 42.7 (C17), 31.6 (C3), 29.0 (C45), 26.7 (C42, C43, C44), 25.4 (C42, C43, C44), 22.8 (C4); HRMS (ESI +ve): $C_{39}H_{43}N_{12}O_4$ $[M+H]^+$: 743.3525 (Found: 743.3508).

2-(2,6-dioxopiperidin-3-yl)-4-((3-(4-(7-(4-(2-(phenylamino)pyrido[3,4-d]pyrimidin-8-yl)piperazin-1-yl)heptyl)-1H-1,2,3-triazol-1-yl)propyl) amino)isoindoline-1,3-dione (15)

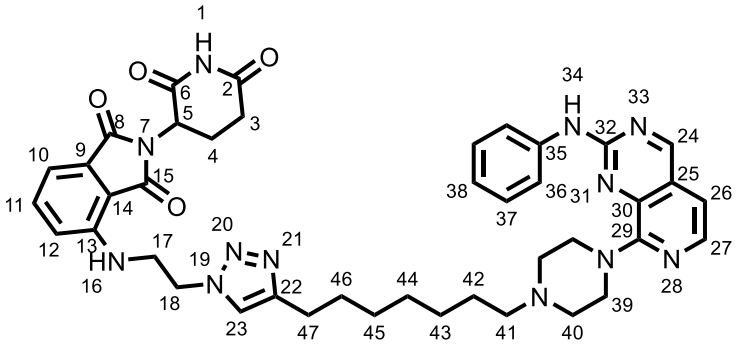

Product was synthesised following **general procedure 5** using 8-(4-(non-8-yn-1-yl)piperazin-1-yl)-*N*-phenylpyrido[3,4-*d*]pyrimidin-2-amine (10 mg, 0.02 mmol) and 4-((2-azidoethyl)amino)-2-(2,6-dioxopiperidin-3-yl)isoindoline-1,3-dione, affording the title compound (6 mg, 32%, 0.01 mmol). ^{1}H NMR (600 MHz, $CDCl_3$) δ 9.08 (s, 1H, H24), 8.05 (d, *J* = 5.4 Hz, 1H, H27), 7.71 (d, *J* = 7.9 Hz,

2H, H36), 7.52 (s, 1H, H34), 7.47 (dd, *J* = 8.5, 7.1 Hz, 1H, H11), 7.43 – 7.38 (m, 2H, H37), 7.36 (s, 1H, H23), 7.16 – 7.12 (m, 2H, H38, H10), 7.07 (d, *J* = 5.4 Hz, 1H, H26), 6.72 (d, *J* = 8.5 Hz, 1H, H12), 6.45 (t, *J* = 6.6 Hz, 1H, H16), 4.96 – 4.89 (m, 1H, H5), 4.62 – 4.54 (m, 2H, H18), 4.18 (s, 4H, H40), 3.90-3.83 (m, 2H, H17), 3.06 (s, 4H, H39), 2.92 – 2.67 (m, 5H, H3, H4, H41, H42, H43, H44, H45, H46, H47), 2.17 – 2.01 (m, 1H, H4), 1.61 (p, J = 7.3 Hz, 2H, H41, H42, H43, H44, H45, H46, H47), 1.41 – 1.22 (m, 10H, H41, H42, H43, H44, H45, H46, H47); ^{13}C NMR (151 MHz, $CDCl_3$) δ 171.2 (C2), 169.3 (C15), 168.5 (C6), 167.4 (C8), 162.1, (C24) 155.9 (C29), 154.4 (C32), 148.6 (C22), 146.1 (C9), 139.4 (C27), 139.3 (C25), 139.0 (C35), 136.4 (C11), 132.5 (C14), 129.0 (C37), 124.3 (C30), 123.4 (C38), 121.9 (C23), 119.7 (C36), 116.2 (C12), 112.5 (C10), 111.7 (C13), 110.9 (26), 57.9 (C41, C42, C43, C44, C45, C46, 47), 52.4 (C39), 49.8 (C18), 49.0 (C5), 46.8 (C40), 42.9 (C17), 31.5 (C3), 29.7 (C41, C42, C43, C44, C45,C 46, C47), 29.0 (C41, C42, C43, C44, C45,C 46, C47), 28.7 (C41, C42, C43, C44, C45,C 46, C47), 26.8 (C41, C42, C43, C44, C45,C 46, C47), 25.4 (C41, C42, C43, C44, C45,C 46, C47), 22.8 (C4), 22.7 (C41, C42, C43, C44, C45,C 46, C47); HRMS (ESI +ve): $C_{41}H_{47}N_{12}O_4$ $[M+H]^+$: 771.3837 (Found: 771.3835).

4-((2-azidoethyl)amino)-2-(1-methyl-2,6-dioxopiperidin-3-yl)isoindoline-1,3-dione (86)

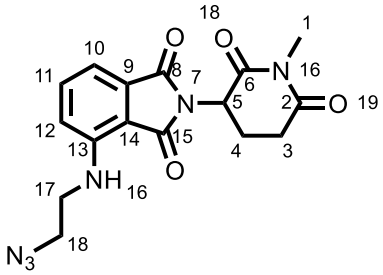

Sodium azide (63 mg, 0.98 mmol) was dissolved DMSO (5 mL) and 2-Bromoethylamine hydrobromide (200 mg, 0.98 mmol) was added. This was heated overnight at 75 °C. No SM was observed by TLC after 18 h (DCM-MeOH 5% RF: 0.5). 4-fluoro-2-(1-methyl-2,6-dioxopiperidin-3-yl)isoindoline-1,3-dione (150 mg, 0.52 mmol) and DIPEA (204 µL, 1.17 mmol) were added and the reaction was stirred at 75 °C overnight. Water was added to the reaction mixture and was extracted with EtOAc (3 times). The organic layers were combined, washed with brine, and solvent was removed *in vacuo*. The residue was purified

using reverse phase column chromatography (water:MeOH (+0.1% formic acid) 30-80%) affording the title product (38 mg, 11%, 0.11 mmol). ^{1}H NMR (600 MHz, $CDCl_3$) δ 7.55 (dd, *J* = 8.5, 7.1 Hz, 1H, H11), 7.18 (d, *J* = 7.2, Hz, 1H, H10), 6.96 (d, *J* = 8.5 Hz, 1H, H12), 6.46 (t, *J* = 6.2 Hz, 1H, H16), 4.97 – 4.90 (m, 1H, H5), 3.61-3.57 (m, 2H, H18), 3.56 – 3.48 (m, 2H, H17), 3.24 (s, 3H, H1), 3.05 – 2.94 (m, 1H, H3), 2.85 – 2.73 (m, 2H, H3, H4), 2.17 – 2.07 (m, 1H, H4); ^{13}C NMR (151 MHz, $CDCl_3$) δ 171.2 (C2), 169.6 (C8), 168.9 (C6), 167.7 (C15), 146.3 (C13), 136.2 (C11), 132.7 (C9), 116.3 (C12), 112.3 (C10), 111.0 (C14), 50.6 (C18), 49.7 (C5), 41.9 (C17), 31.9 (C3), 27.3 (C1), 22.1 (C4); HRMS (ESI +ve): $C_{16}H_{17}N_6O_4$ $[M+H]^+$: 357.1306 (Found: 357.1327).

2-(1-methyl-2,6-dioxopiperidin-3-yl)-4-((2-(4-(5-(4-((8-morpholinopyrido [3,4-*d*]pyrimidin-2-yl)amino)phenoxy)pentyl)-1*H*-1,2,3-triazol-1-yl)ethyl) amino)isoindoline-1,3-dione (73)

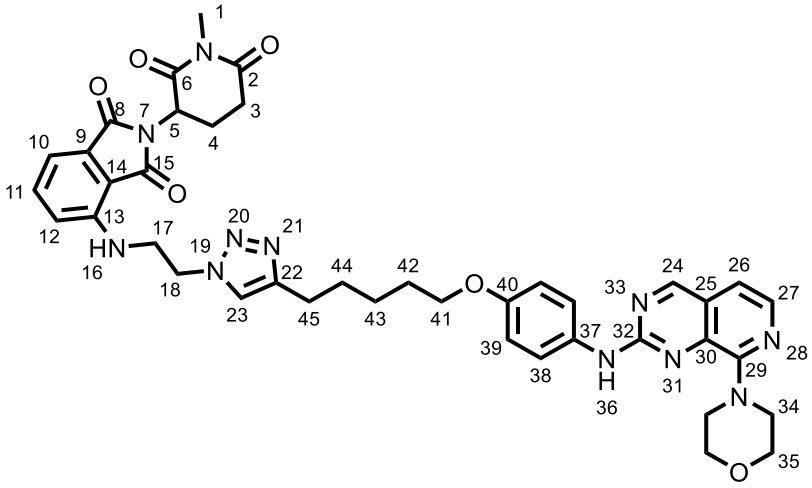

Product was synthesised following **general procedure 5** using *N*-(4-(hept-6-yn-1-yloxy)phenyl)-8-morpholinopyrido[3,4-*d*]pyrimidin-2-amine (13 mg, 0.03 mmol) and 4-((2-azidoethyl)amino)-2-(1-methyl-2,6-dioxopiperidin-3-yl) isoindoline-1,3-dione, affording the title compound (10 mg, 39%, 0.0123 mmol). ^{1}H NMR (600 MHz, $CDCl_3$) δ 9.02 (s, 1H, H24), 8.04 (d, *J* = 5.4 Hz, 1H, H27), 7.62 – 7.57 (m, 2H, H36), 7.48 (dd, *J* = 8.5, 7.1 Hz, 1H, H11), 7.39 (s, 1H, H36), 7.32 (s, 1H, H23), 7.15 (d, *J* = 7.1 Hz, 1H, H10), 7.03 (d, *J* = 5.4 Hz, 1H, H26), 6.94 – 6.90 (m, 2H, H39), 6.72 (d, *J* = 8.5 Hz, 1H, H12), 6.48 (t, *J* = 6.6 Hz, 1H, H16), 4.95 – 4.90 (m, 1H, H5), 4.57 (t, *J* = 6.0 Hz, 2H, H18), 4.00 – 3.93 (m, 6H, H35, H41), 3.90 – 3.84 (m, 4H, H34, H17), 3.23 (s, 3H, H1), 2.98 (ddd, *J* = 16.7, 6.9, 3.8 Hz, 1H, H3), 2.81 – 2.71 (m, 4H, H3, H4, H45), 2.15 – 2.07 (m, 5H, H4),

1.83 (p, *J* = 6.7 Hz, 2H, H42), 1.73 (p, *J* = 7.6 Hz, 3H, H44), 1.59 – 1.50 (m, 2H, H43); ^{13}C NMR (151 MHz, $CDCl_3$) δ 171.2 (C2), 169.5 (C15), 168.9 (C6), 167.4 (C8), 161.9 (C24), 156.8 (C29), 156.2 (C32), 155.4 (C40), 148.5 (C22), 146.0 (C13), 139.8 (C30), 139.1 (C27), 136.4 (C11), 132.6 (C9), 132.1 (C37), 124.1 (C25), 121.7 (C23), 121.7 (C38), 116.0 (C12), 114.7 (C39), 112.6 (C10), 111.3 (C14), 111.1 (C26), 68.1 (C41), 67.3 (C35), 49.8 (C18, C5), 49.3 (C34), 42.9 (C17), 31.9 (C3), 29.2 (C44), 29.0 (C42), 27.3 (C1), 25.6 (C43), 25.5 (C45), 22.1 (C4); HRMS (ESI +ve): $C_{40}H_{44}N_{11}O_6$ $[M+H]^+$:774.3476 (Found: 774.3459).

_N_-(4-(hex-5-yn-1-yloxy)phenyl)formamide (93)

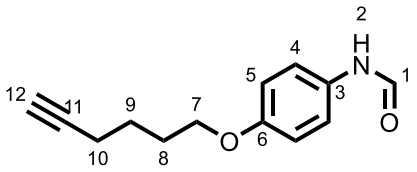

Product was synthesised following **general procedure 3a-c** using hex-5-yn-1-ol (568 µL, 5.09 mmol). Intermediate aniline was seen by LCMS ($[M+H]^+$: 190.12) with a retention time of 0.85 min. The title product (313 mg, 29%, 1.65 mmol) was afforded. Rotamers observed in NMR. ^{1}H NMR (500 MHz, $CDCl_3$) δ 8.51 (d, *J* = 11.6 Hz, 0.5H, H1), 8.34 (d, *J* = 1.8 Hz, 0.5H, H1), 7.59 (d, *J* = 11.5 Hz, 0.5H, H2), 7.51 – 7.39 (m, 1H, H4), 7.15 (s, 0.5H, H2), 7.07 – 6.99 (m, 1H, H4), 6.94 – 6.81 (m, 2H, H5), 3.99 (td, *J* = 6.3, 2.7 Hz, 2H, H2), 2.29 (tt, *J* = 7.1, 3.0 Hz, 2H, H7), 1.99 (q, *J* = 2.6 Hz, 1H, H12), 1.97 – 1.87 (m, 2H, H9), 1.80 – 1.66 (m, 2H, H8); ^{13}C NMR (126 MHz, $CDCl_3$) δ 162.8 (C1), 158.7 (C1), 157.1 (C6), 156.2 (C6), 129.8 (C3), 129.3 (C3), 121.8 (C4), 121.7 (C4), 115.5 (C5), 114.9 (C5), 84.1 (C11), 84.0 (C11), 68.7 (C12), 68.7 (C12), 67.7 (C7), 67.6 (C7), 28.3 (C9), 28.2 (C9), 25.0 (C8), 25.0 (C8), 18.2 (C10); HRMS (ESI +ve): $C_{13}H_{16}NO_2$ $[M+H]^+$: 218.1175 (Found: 218.1180).

_N_-(4-(oct-7-yn-1-yloxy)phenyl)formamide (94)

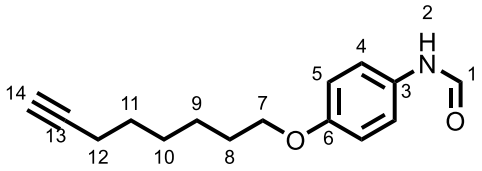

Product was synthesised following **general procedure 3a-c** using oct-7-yn-1-ol (524 mg, 4.15 mmol). Intermediate aniline was seen by LCMS ($[M+H]^+$: 218.15)

with a retention time of 1.13 min. The title product (212 mg, 52%, 0.86 mmol) was afforded. Rotamers observed in NMR. ^{1}H NMR (500 MHz, $CDCl_3$) δ 8.51 (d, *J* = 11.6 Hz, 0.5H, H1), 8.34 (d, *J* = 1.8 Hz, 0.5H, H1), 7.54 (d, *J* = 11.4 Hz, 0.5H, H2), 7.47 – 7.41 (m, 1H, H4), 7.13 (s, 0.5H, H4), 7.06 – 6.99 (m, 1H, H4), 6.94 – 6.84 (m, 2H, H5), 3.95 (td, *J* = 6.5, 2.3 Hz, 2H, H7), 2.32 – 2.18 (m, 2H, H12), 2.04 – 1.94 (m, 1H, H14), 1.90 – 1.73 (m, 2H, H8), 1.69 – 1.54 (m, 2H, H11), 1.50 (dt, *J* = 7.6, 3.6 Hz, 4H, H9, H10); ^{13}C NMR (126 MHz, $CDCl_3$) δ 162.8 (C1), 158.7 (C1), 157.2 (C6), 156.3 (C6), 129.7 (C3), 129.2 (C3), 121.9 (C4), 121.7 (C14), 115.5 (C5), 114.9 (C5), 84.6 (C13), 84.5 (C13), 68.3 (C14), 68.3 (C14), 68.2 (C7) 68.1 (C7), 29.1 (C8), 29.1 (C8), 28.5 (C9 or 10), 28.4 (C9, C10), 28.4 (C11), 28.3 (C11), 25.6 (C9, C10) 18.3 (C12); HRMS (ESI +ve): $C_{15}H_{20}NO_2$ $[M+H]^+$: 246.1488 (Found: 246.1489).

2-(2,6-dioxopiperidin-3-yl)-4-((2-(4-(4-(4-((8-morpholinopyrido[3,4-*d*] pyrimidin-2-yl)amino)phenoxy)butyl)-1*H*-1,2,3-triazol-1-yl)ethyl)amino) isoindoline-1,3-dione (74)

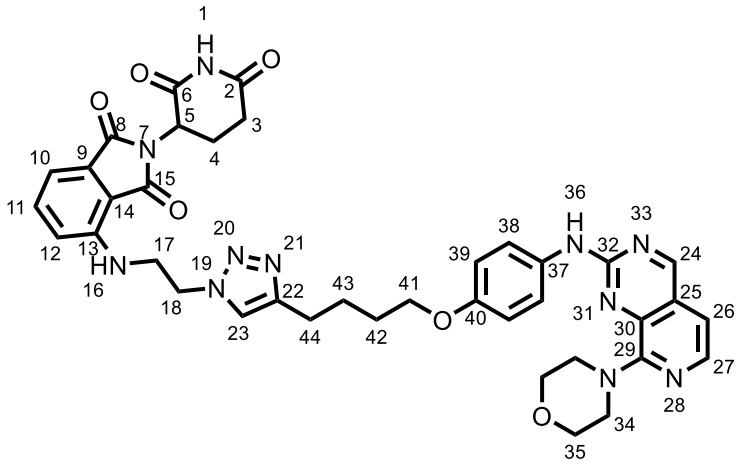

The alkyne intermediate **93** was synthesised following **general procedure 4** using *N*-(4-hex-5-ynoxyphenyl)formamide (25 mg, 0.12 mmol) and 4-(2-methylsulfonylpyrido[3,4-*d*]pyrimidin-8-yl)morpholine (16 mg, 0.08 mmol). Use of the general procedure only afforded crude title product that was used in the next step without further purification. Mass of product was observed ($[M+H]^+$ 404.21) with a retention time of 1.36 min. Title product was synthesised following **general procedure 5** using crude *N*-(4-(hex-5-yn-1-yloxy)phenyl)-8-morpholinopyrido[3,4-*d*]pyrimidin-2-amine, affording the product (4 mg, 17%, 0.01 mmol). ^{1}H NMR (600 MHz, $CDCl_3$) δ 9.03 (s, 1H, H24), 8.03 (d, *J* = 5.4 Hz,

1H, H27), 7.59 (d, *J* = 8.9 Hz, 2H, H38), 7.52 – 7.44 (m, 2H, H11, H36), 7.33 (s, 1H, H23), 7.14 (d, *J* = 7.1 Hz, 1H, H10), 7.03 (d, *J* = 5.4 Hz, 1H, H26), 6.91 (d, *J* = 8.9 Hz, 2H, H39), 6.71 (d, *J* = 8.5 Hz, 1H, H12), 6.47 (t, *J* = 6.5 Hz, 1H, H16), 4.92 (dd, *J* = 12.6, 5.4 Hz, 1H, H5), 4.57 (t, *J* = 5.8 Hz, 3H, H18), 4.03 – 3.93 (m, 8H, H35, H41), 3.88 (dd, *J* = 5.9, 2.8 Hz, 6H, H17, H34), 2.95 – 2.61 (m, 6H, H3, H4, H44), 2.19 - 2.09 (m, 1H, H4), 1.87 – 1.79 (m, 4H, H42, H43), H1 not observed; ^{13}C NMR (151 MHz, $CDCl_3$) δ 171.1 (C2), 169.4 (C15), 168.4 (C6), 167.3 (C8), 161.9 (C24), 156.7 (C29), 156.1 (C32), 155.2 (C40), 148.3 (C22), 146.1 (C13), 139.8 (C29), 139.1 (C27), 136.4 (C10), 132.5 (C9), 132.2 (C37), 124.1 (C25), 121.9 (C23), 121.7 (C28), 116.1 (C12), 114.8 (C39), 112.6 (C11), 111.4 (C26), 110.9 (C14), 67.9 (C41), 67.2 (C35), 49.8 (C44), 49.3 (C34), 49.0 (C5), 42.9 (C17), 31.4 (C3), 28.7 (C42, C43), 25.9 (C42, C43), 25.3 (C44), 22.7 (C4); HRMS (ESI +ve): $C_{38}H_{39}N_{11}O_6$ $[M+H]^+$: 746.3158 (Found: 746.3158178).

2-(2,6-dioxopiperidin-3-yl)-4-((2-(4-(6-(4-((8-morpholinopyrido[3,4-*d*] pyrimidin-2-yl)amino) phenoxy)hexyl)-1*H*-1,2,3-triazol-1-yl)ethyl)amino) isoindoline-1,3-dione (75)

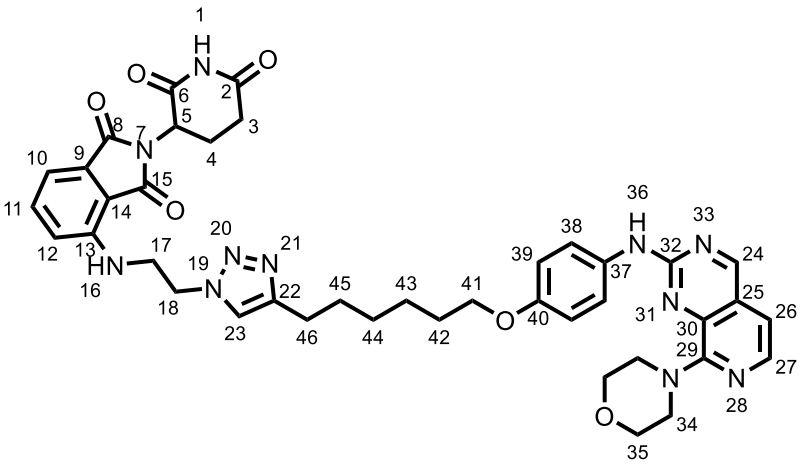

The alkyne intermediate **94** was synthesised following **general procedure 4** using *N*-(4-oct-7-ynoxyphenyl)formamide (34 mg, 0.14 mmol) and 4-(2-methylsulfonylpyrido[3,4-*d*]pyrimidin-8-yl)morpholine (16 mg, 0.08 mmol). Use of the general procedure only afforded crude title product that was used in the next step without further purification. Mass of product was observed ($[M+H]^+$ 432.24) with a retention time of 1.50 min. Product was synthesised following **general procedure 5** using crude 8-morpholino-*N*-(4-(oct-7-yn-1-yloxy)

phenyl)pyrido[3,4-*d*]pyrimidin-2-amine affording the title product (7 mg, 26%, 0.01 mmol). ^{1}H NMR (600 MHz, $CDCl_3$) δ 9.04 (s, 1H, H24), 8.03 (d, *J* = 5.4 Hz, 1H, H27), 7.60 (d, *J* = 8.6 Hz, 3H, H38), 7.47 (t, *J* = 7.8 Hz, 2H, H11), 7.30 (s, 1H, H23), 7.15 (d, *J* = 7.1 Hz, 2H, H10), 7.03 (d, *J* = 5.4 Hz, 1H, H26), 6.92 (d, *J* = 8.7 Hz, 2H, H39), 6.69 (d, *J* = 8.5 Hz, 1H, H12), 6.47 (t, *J* = 6.6 Hz, 2H, H16), 4.94 (dd, *J* = 12.4, 5.4 Hz, 1H, H5), 4.54 (t, *J* = 5.9 Hz, 3H, H18), 3.97 (dt, *J* = 9.5, 5.4 Hz, 9H, H35, H41), 3.89 – 3.80 (m, 8H, H17, H34), 2.95 – 2.66 (m, 6H, H4, H5, H46), 2.21 – 2.12 (m, 2H, H4), 1.78 (p, *J* = 6.6 Hz, 4H, H42), 1.66 (p, *J* = 7.6 Hz, 3H, H45), 1.50 (p, *J* = 7.4 Hz, 3H, H43), 1.40 (td, *J* = 8.4, 3.9 Hz, 3H, H44), H1 not observed; ^{13}C NMR (151 MHz, $CDCl_3$) δ 171.1 (C2), 169.4 (C16), 168.6 (C6), 167.3 (C8), 161.9 (C26), 156.7 (C29), 156.1 (C32), 155.3 (C40), 148.6 (C22), 146.6 (C13), 146.1 (C13), 139.8 (C30), 139.1 (C27), 136.4 (C11), 132.5 (C9), 132.2 (C37), 124.1 (C25), 121.7 (C23), 121.7 (C38), 116.1 (C12), 114.8 (C39), 112.6 (C10), 111.4 (C26), 110.9 (C14), 68.2 (C41), 67.2 (C35), 49.82 (C18), 49.29 (C34), 48.99 (C5), 42.94 (C17), 31.44 (C3), 29.22 (C45), 29.06 (C42), 28.65 (C41), 25.6 (C43), 25.4 (C46), 22.8 (C4); HRMS (ESI +ve): $C_{40}H_{44}N_{11}O_6$ $[M+H]^+$: 774.3471 (Found: 774.3474).

4-((3-azidopropyl)amino)-2-(2,6-dioxopiperidin-3-yl)isoindoline-1,3-dione (99)

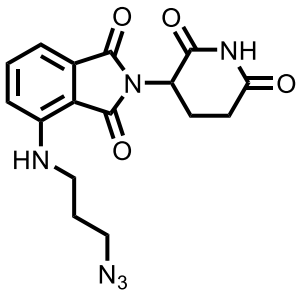

3-Bromopropylamine hydrobromide (79 mg, 0.36 mmol) was dissolved DMSO (5 mL) and sodium azide (24 mg, 0.36 mmol) was added. This was heated overnight at 75 °C. No SM was observed by TLC after 18 h (DCM-MeOH 5% RF: 0.5). 2-(2,6-dioxo-3-piperidyl)-4-fluoro-isoindoline-1,3-dione (100 mg, 0.36 mmol) and DIPEA (0.19 mL, 1.09 mmol) were added, and the reaction was stirred at 75 °C overnight. Water was added to the reaction mixture and was extracted with EtOAc (3 times). The organic layers were combined, washed with brine, and solvent was removed *in vacuo*. The residue was purified using

column chromatography (DCM:MeOH 0-10%) affording title product (57 mg, 44%, 0.16 mmol). ^{1}H NMR (600 MHz, $CDCl_3$) δ 7.56 – 7.51 (m, 1H), 7.13 (dd, *J* = 7.1, 0.6 Hz, 1H), 6.93 (d, *J* = 8.5 Hz, 1H), 6.32 (t, *J* = 6.0 Hz, 1H), 4.93 (dd, *J* = 12.5, 5.4 Hz, 1H), 3.48 (t, *J* = 6.4 Hz, 2H), 3.42 (q, *J* = 6.6 Hz, 2H), 2.93 – 2.67 (m, 3H), 2.18 – 2.11 (m, 1H), 1.97 – 1.93 (m, 2H); ^{13}C NMR (151 MHz, $CDCl_3$) δ 171.2, 169.5, 168.4, 167.5, 146.7, 136.3, 132.5, 116.5, 111.9, 110.3, 48.9, 48.9, 39.8, 31.4, 28.6, 22.8; HRMS (ESI +ve): $C_{16}H_{17}N_6O_4$ $[M+H]^+$: 379.1131 (Found: 379.1122). Characterisation consistent with literature.[116]

2-(2,6-dioxopiperidin-3-yl)-4-((3-(4-(4-(4-((8-morpholinopyrido[3,4-*d*] pyrimidin-2-yl)amino)phenoxy)butyl)-1*H*-1,2,3-triazol-1-yl)propyl) amino)isoindoline-1,3-dione (76)

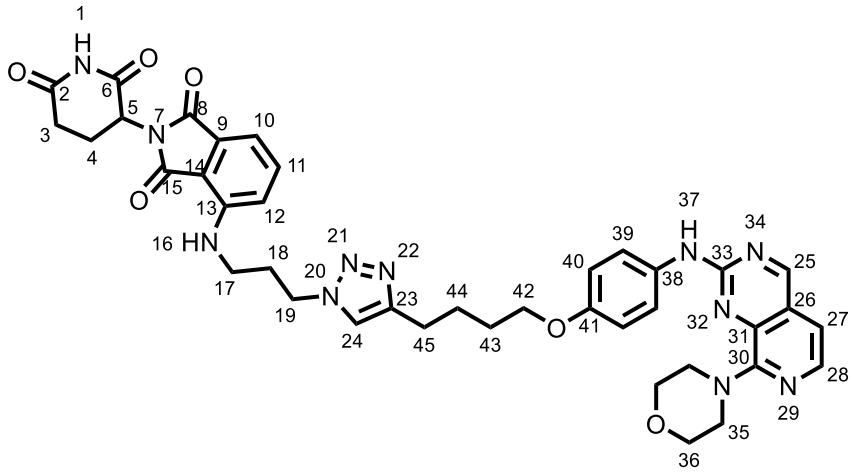

Product was synthesised following **general procedure 5** using *N*-(4-hex-5-ynoxyphenyl)-8-morpholino-pyrido[3,4-*d*]pyrimidin-2-amine (12 mg, 0.03 mmol), and 4-(3-azidopropylamino)-2-(2,6-dioxo-3-piperidyl)isoindoline-1,3-dione (11 mg, 0.03 mmol), affording the title compound (10 mg, 42%, 0.01 mmol). ^{1}H NMR (600 MHz, $CDCl_3$) δ 9.04 (s, 1H, H25), 8.04 (d, *J* = 5.4 Hz, 1H, H28), 7.61 (dd, *J* = 8.1, 5.8 Hz, 3H, H37, H39), 7.55 – 7.50 (m, 1H, H11), 7.35 (s, 1H, H24), 7.14 (d, *J* = 7.1 Hz, 1H, H12), 7.03 (d, *J* = 5.4 Hz, 1H, H27), 6.90 (d, *J* = 8.9 Hz, 2H, H40), 6.86 (d, *J* = 8.5 Hz, 1H, H10), 6.30 (t, *J* = 6.0 Hz, 1H, H16), 4.95 (dd, *J* = 12.3, 5.4 Hz, 1H, H5), 4.47 (t, *J* = 6.9 Hz, 2H, H19), 4.01 (t, *J* = 5.8 Hz, 2H, H42), 3.96 (t, *J* = 4.7 Hz, 4H, H36), 3.87 (t, *J* = 4.7 Hz, 4H, H35), 3.35 (q, *J* = 6.6 Hz, 2H, H17), 2.91 – 2.72 (m, 4H, H3, H4, H45), 2.28 (t, *J* = 6.8 Hz, 2H, H18), 2.17 (ddt, *J* = 10.5, 5.5, 2.6 Hz, 1H, H3), 1.90 (dt, *J* = 12.1, 4.4 Hz, 4H, H43, H44); ^{13}C NMR (151 MHz, $CDCl_3$) δ 171.2 (C2), 169.5 (C15), 168.7

(C6), 167.5 (C8), 161.9 (C25), 156.8 (C30), 156.1 (C33), 155.2 (C41), 148.2 (C23), 146.5 (C13), 139.8 (C31), 139.1 (C28), 136.4 (C11), 132.5 (C9), 132.3 (C38), 124.1 (C26), 121.6 (C39), 121.0 (C24), 116.6 (C10), 114.7 (C40), 112.1 (C12), 111.4 (C27), 110.6 (C14), 67.9 (C42), 67.2 (C36), 49.3 (C35), 49.0 (C5), 47.3 (C19), 39.5 (C17), 31.5 (C3), 29.8 (C18), 28.8 (C43, C44), 25.9 (C43, C44), 25.4 (C45), 22.9 (C4); HRMS (ESI +ve): $C_{39}H_{42}N_{11}O_6$ $[M+H]^+$: 760.3320 (Found: 760.3312).

Tert-butyl (4-((2-(2,6-dioxopiperidin-3-yl)-1,3-dioxoisoindolin-4-yl)amino) butyl)carbamate (105)

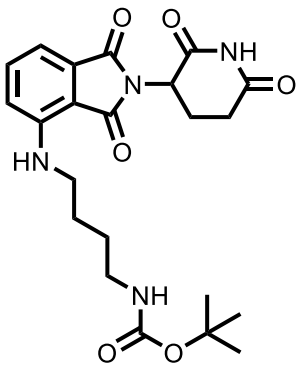

Tert-butyl *N*-(4-aminobutyl)carbamate (265 mg, 1.18 mmol), 2-(2,6-dioxopiperidin-3-yl)-4-fluoroisoindoline-1,3-dione (163 mg, 0.59 mmol) and DIPEA (0.3 mL, 1.77 mmol) were dissolved in DMSO (3 mL) and stirred at 75 °C overnight. Water was added to the reaction and was extracted with DCM (3 times). The DCM was removed *in vacuo* affording the title product. ^{1}H NMR (600 MHz, $CDCl_3$) δ 8.34 (s, 1H), 7.50 (dd, *J* = 8.5, 7.1 Hz, 1H), 7.10 (d, *J* = 7.0 Hz, 1H), 6.90 (d, *J* = 8.5 Hz, 1H), 6.26 (t, *J* = 5.8 Hz, 1H), 4.93 (dd, *J* = 12.4, 5.4 Hz, 1H), 3.31 (q, *J* = 6.6 Hz, 2H), 3.18 (t, *J* = 6.7 Hz, 2H), 2.95 – 2.71 (m, 3H), 2.19 – 2.11 (m, 1H), 1.76 – 1.68 (m, 2H), 1.67 – 1.58 (m, 2H), 1.46 (s, 9H); ^{13}C NMR (151 MHz, $CDCl_3$) δ 171.2, 169.5, 168.4, 167.6, 156.0, 146.9, 136.2, 132.5, 116.7, 111.5, 110.0, 79.3, 48.9, 42.3, 40.1, 31.4, 28.4, 27.6, 26.5, 22.8; HRMS (ESI +ve): $C_{22}H_{28}N_4O_6Na$ $[M+Na]^+$: 467.1878 (Found: 467.1907). Characterisation consistent with literature.[116]

Tert-butyl (5-((2-(2,6-dioxopiperidin-3-yl)-1,3-dioxoisoindolin-4-yl)amino) pentyl)carbamate (106)

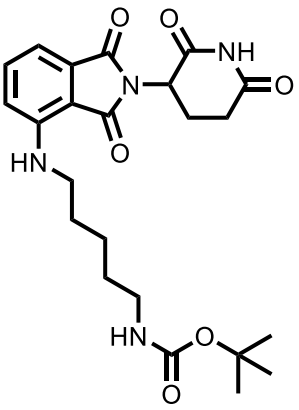

Tert-butyl *N*-(5-aminopentyl)carbamate (293 mg, 1.45 mmol)), 2-(2,6-dioxopiperidin-3-yl)-4-fluoroisoindoline-1,3-dione and DIPEA (0.4 mL, 2.17 mmol) were dissolved in DMSO (2 mL) and stirred at 75 °C overnight. Water was added to the reaction and was extracted with DCM (3 times). The DCM was removed *in vacuo* affording the title product (65 mg, 18%, 0.1418 mmol). ^{1}H NMR (600 MHz, $CDCl_3$) δ 8.18 (s, 1H), 7.51 (dd, *J* = 8.5, 7.1 Hz, 1H), 7.11 (d, *J* = 7.1 Hz, 1H), 6.90 (d, *J* = 8.5 Hz, 1H), 6.25 (t, *J* = 5.7 Hz, 1H), 4.93 (dd, *J* = 12.4, 5.3 Hz, 1H), 3.29 (td, *J* = 7.1, 5.6 Hz, 2H), 3.15 (q, *J* = 6.7 Hz, 2H), 2.96 – 2.72 (m, 3H), 2.21 – 2.11 (m, 1H), 1.76 – 1.68 (m, 2H), 1.55 (q, *J* = 7.3 Hz, 2H), 1.46 (s, 11H); ^{13}C NMR (151 MHz, $CDCl_3$) δ 171.0, 169.5, 168.3, 167.6, 156.0, 147.0, 136.2, 132.5, 116.6, 111.5, 110.0, 79.3, 48.9, 42.3, 40.1, 31.4, 28.9, 28.9, 28.4, 24.2, 22.8; HRMS (ESI +ve): $C_{23}H_{30}N_4O_6Na$ $[M+Na]^+$: 481.2063 (Found: 481.2043). Characterisation consistent with literature.[116]

4-((4-aminobutyl)amino)-2-(2,6-dioxopiperidin-3-yl)isoindoline-1,3-dione (107)

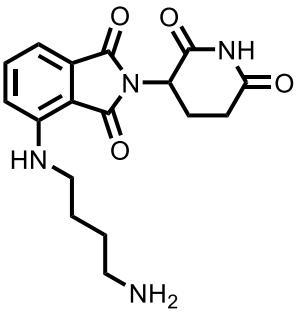

Product was synthesised following **general procedure 6c** using *tert*-butyl (4-((2-(2,6-dioxopiperidin-3-yl)-1,3-dioxoisoindolin-4-yl)amino)butyl)carbamate (60 mg, 0.14 mmol), affording the title product (59 mg, 100%, 0.14 mmol). ^{1}H NMR (500 MHz, MeOH-d_4) δ 10.76 (s, 1H), 7.55 (dd, *J* = 8.5, 7.1 Hz, 1H), 7.07 (d, *J*

= 8.6 Hz, 1H), 7.05 (d, *J* = 7.1 Hz, 1H), 5.07 (dd, *J* = 12.7, 5.5 Hz, 1H), 3.40 (t, *J* = 6.4 Hz, 2H), 3.00 (t, *J* = 7.1 Hz, 2H), 2.92 – 2.65 (m, 3H), 2.16 – 2.08 (m, 1H), 1.78 (tdd, *J* = 15.3, 7.0, 3.6 Hz, 4H); ^{13}C NMR (126 MHz, MeOH-d_4) δ 173.29, 170.27, 169.35, 167.88, 146.65, 135.95, 132.51, 116.68, 110.60, 109.79, 48.82, 41.38, 39.17, 30.85, 25.90, 24.63, 22.41; HRMS (ESI +ve): $C_{17}H_{21}N_4O_4$ $[M+H]^+$: 345.1562 (Found: 345.1479). Characterisation consistent with literature.[116]

4-((5-aminopentyl)amino)-2-(2,6-dioxopiperidin-3-yl)isoindoline-1,3-dione (108)

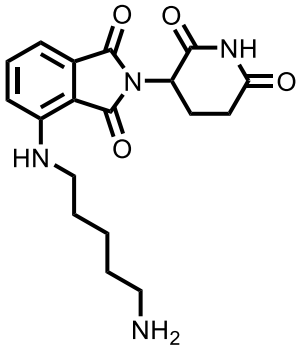

Product was synthesised following **general procedure 6c** using *tert*-butyl (4-((2-(2,6-dioxopiperidin-3-yl)-1,3-dioxoisoindolin-4-yl)amino)butyl)carbamate (126 mg, 0.27 mmol), affording the title product (37 mg, 86%, 0.09 mmol). ^{1}H NMR (600 MHz, MeOH-d_4) δ 7.57 (dd, *J* = 8.6, 7.1 Hz, 1H), 7.07 (t, *J* = 7.8 Hz, 2H), 5.07 (dd, *J* = 12.8, 5.5 Hz, 1H), 3.38 (t, *J* = 6.9 Hz, 2H), 2.97 (t, *J* = 7.7 Hz, 2H), 2.91 – 2.66 (m, 3H), 2.16 – 2.09 (m, 1H), 1.74 (p, *J* = 7.5 Hz, 4H), 1.60 – 1.50 (m, 2H); ^{13}C NMR (151 MHz, MeOH-d4) δ 173.25, 170.29, 169.42, 167.88, 146.79, 135.91, 132.54, 116.61, 110.47, 109.71, 48.80, 41.70, 39.26, 30.82, 28.41, 26.95, 23.42, 22.41; HRMS (ESI +ve): $C_{18}H_{23}N_4O_4$ $[M+H]^+$: 359.1719 (Found: 359.1730). Characterisation consistent with literature.[116]

Sulfurazidic fluoride (110)

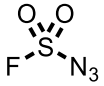

An aqueous NaN_3 solution (0.50 M in 3.1 ml water, containing sodium azide (46 mg, 0.71 mmol)) and methyl *tert*-butyl ether (MTBE, 3.1 ml) were stirred at 0 ˚C. 3-methylimidazol-3-ium-1-sulfonyl fluoride;trifluoromethanesulfonate (267 mg,

0.85 mmol) was dissolved in MeCN (0.5 ml), and the resultant solution was added rapidly to the stirred NaN_3/water/MTBE mixture. This was followed by a rinse of the vial used with additional MeCN (0.5 ml), which was also added to the reaction mixture. The reaction mixture was stirred in an ice-water bath for 10 min then was poured into a separating funnel. The organic phase was separated from the aqueous phase, and this organic phase was kept in a loosely sealed vial at room temperature for 12 h. The colourless organic phase was used as a solution in MTBE without further purification assuming 100% yield as in the literature.[116]

4-((4-azidobutyl)amino)-2-(2,6-dioxopiperidin-3-yl)isoindoline-1,3-dione (111)

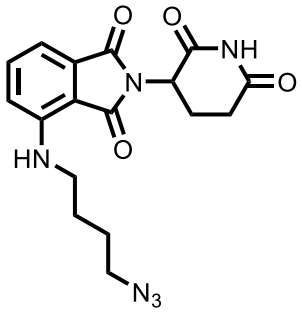

To a stirred solution of 4-((4-aminobutyl)amino)-2-(2,6-dioxopiperidin-3-yl)isoindoline-1,3-dione (12 mg, 0.03 mmol) in DMF (0.25 mL) was added sulfurazidic fluoride in MTBE (0.27 mL, ~0.25 M, 0.07 mmol). After 10 minutes, water was added and was extracted with EtOAc. The EtOAc layers were combined and solvent was removed in *vacuo*. Product was purified using column chromatography (DCM:MeOH 0-10%) affording the title product (11 mg, 43%, 0.03 mmol). ^{1}H NMR (500 MHz, $CDCl_3$) δ 7.52 (dd, *J* = 8.5, 7.1 Hz, 1H), 7.15 – 7.10 (m, 1H), 6.90 (d, *J* = 8.5 Hz, 1H), 6.27 (t, *J* = 5.8 Hz, 1H), 4.93 (dd, *J* = 12.4, 5.4 Hz, 1H), 3.35 (dt, *J* = 19.4, 6.5 Hz, 4H), 2.94 – 2.68 (m, 3H), 2.19 – 2.08 (m, 1H), 1.83 – 1.69 (m, 4H); ^{13}C NMR (126 MHz, $CDCl_3$) δ 170.91, 169.50, 168.25, 167.54, 146.79, 136.21, 132.54, 116.52, 111.68, 110.17, 51.09, 48.91, 42.14, 31.41, 26.56, 26.36, 22.80; HRMS (ESI +ve): $C_{17}H_{19}N_6O_4$ $[M+H]^+$: 371.1468 (Found: 371.1469). Characterisation was consistent with the literature.[116]

4-((5-azidopentyl)amino)-2-(2,6-dioxopiperidin-3-yl)isoindoline-1,3-dione(112)

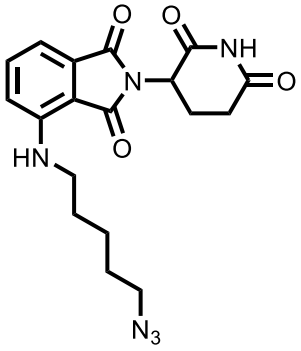

To a stirred solution of 4-((5-aminopentyl)amino)-2-(2,6-dioxopiperidin-3-yl)isoindoline-1,3-dione (15 mg, 0.04 mmol) in DMF (0.25 mL) sulfurazidic fluoride in MTBE (152 µl, ~0.25 M, 0.04 mmol) was added. After 10 minutes, water was added and was extracted with EtOAc. The EtOAc layers were combined and solvent was removed *in vacuo*. Product was purified using column chromatography (DCM:MeOH 0-10%) affording the title product (11 mg, 75%, 0.03 mmol). ^{1}H NMR (500 MHz, $CDCl_3$) δ 7.47 (dd, *J* = 8.5, 7.2 Hz, 1H), 7.08 (d, *J* = 6.9 Hz, 1H), 6.86 (d, *J* = 8.5 Hz, 1H), 6.28 (t, *J* = 5.8 Hz, 1H), 3.63 (t, *J* = 7.2 Hz, 2H), 3.39 – 3.18 (m, 3H), 1.79 – 1.60 (m, 6H), 1.59 – 1.51 (m, 2H), 1.49 – 1.38 (m, 2H); ^{13}C NMR (126 MHz, $CDCl_3$) δ 170.86, 168.74, 146.46, 135.62, 132.98, 116.05, 110.97, 110.55, 51.26, 42.46, 37.18, 28.91, 28.64, 28.42, 28.22, 24.19, 23.98; HRMS (ESI +ve): $C_{18}H_{21}N_6O_4$ $[M+H]^+$: 385.1624 (Found: 385.2091). Characterisation was consistent with the literature.[116]

2-(2,6-dioxopiperidin-3-yl)-4-((4-(4-(3-(4-((8-morpholinopyrido[3,4-d] pyrimidin-2-yl)amino)phenoxy)propyl)-1H-1,2,3-triazol-1-yl)butyl)amino) isoindoline-1,3-dione (77)

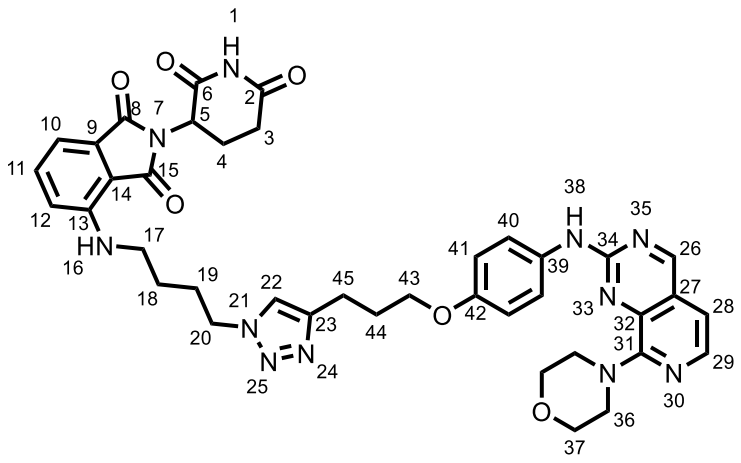

Product was synthesised following **general procedure 5** using 8-morpholino-*N*-(4-(pent-4-yn-1-yloxy)phenyl)pyrido[3,4-*d*]pyrimidin-2-amine (13 mg, 0.03 mmol) and 4-((4-azidobutyl)amino)-2-(2,6-dioxopiperidin-3-yl)isoindoline-1,3-dione (16 mg, 0.04 mmol), affording 9 mg (29%, 0.0118 mmol) of the title product. ^{1}H NMR (500 MHz, $CDCl_3$) δ 9.04 (s, 1H, H26), 8.03 (d, *J* = 5.5 Hz, 1H, H29), 7.74 (s, 1H, H38), 7.62 – 7.55 (m, 2H, H40), 7.50 (dd, *J* = 8.5, 7.1 Hz, 1H, H11), 7.32 (s, 1H, H22), 7.11 (d, *J* = 7.0 Hz, 1H, H12), 7.02 (d, *J* = 5.5 Hz, 1H, H28), 6.87 (t, *J* = 8.7 Hz, 3H, H10, H41), 6.22 (t, *J* = 5.8 Hz, 1H, H16), 4.95 (dd, *J* = 12.4, 5.4 Hz, 1H, H5), 4.39 (td, *J* = 6.9, 4.3 Hz, 2H, H20), 4.00 (td, *J* = 6.2, 1.4 Hz, 2H, H43), 3.98 – 3.92 (m, 4H, H37), 3.86 (dd, *J* = 5.7, 3.4 Hz, 4H, H36), 3.30 (q, *J* = 6.7 Hz, 2H, H17), 2.95 (t, *J* = 7.4 Hz, 2H, H45), 2.91 – 2.68 (m, 3H, H3, H4), 2.23 – 2.12 (m, 3H, H3, H44), 2.08 – 1.99 (m, 2H, H19), 1.68 (p, *J* = 7.2 Hz, 2H, H18) H1 not observed; ^{13}C NMR (126 MHz, $CDCl_3$) δ 171.24 (C2), 169.55 (C15), 169.03 (C6), 167.54 (C8), 161.84 (C26), 156.73 (C31), 156.03 (C34), 155.07 (C42), 147.34 (C23), 146.67 (C13), 139.78 (C32), 139.12 (C29), 136.24 (C11), 132.54 (C9), 132.39 (C39), 124.02 (C27), 121.54 (C40), 121.02 (C22), 116.51 (C10), 114.72 (C41), 111.78 (C12), 111.38 (C28), 110.22 (C14), 67.22 (C37), 67.08 (C43), 49.68 (C20), 49.30 (C36), 48.97 (C5), 41.90 (C17), 31.46 (C3), 28.71 (C44), 27.66 (C19), 26.33 (C18), 22.86 (C4), 22.05 (C45); HRMS (ESI +ve): $C_{39}H_{42}N_{11}O_6$ $[M+H]^+$: 760.3320 (Found: 760.3245).

N-(4-(but-3-yn-1-yloxy)phenyl)-8-morpholinopyrido[3,4-d]pyrimidin-2-amine (104)

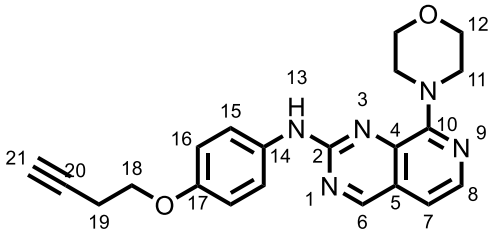

Product was synthesised following **general procedure 3a-c** using 3-Butyn-1-ol (359 µL, 4.74 mmol). Intermediate aniline was seen by LCMS ($[M+H]^+$: 162.09) with a retention time of 0.47 min. Intermediate crude formamide was seen by NMR. Rotamers observed in crude NMR. ^{1}H NMR (500 MHz, $CDCl_3$) δ 8.52 (d, *J* = 11.5 Hz, 0.5H), 8.34 (d, *J* = 1.9 Hz, 0.5H), 7.69 (s, 0.5H), 7.52 – 7.44 (m, 1H), 7.33 (s, 0.5H), 7.04 (d, *J* = 8.9 Hz, 1H), 6.91 (dd, *J* = 16.0, 8.9 Hz, 2H), 4.10 (td, *J* = 6.9, 3.0 Hz, 2H), 2.69 (qd, *J* = 6.9, 2.7 Hz, 1H), 2.06 (dt, *J* = 4.3,

2.7 Hz, 1H). The title product was synthesised following **general procedure 4** using 4-(2-methylsulfonylpyrido[3,4-*d*] pyrimidin-8-yl)morpholine (56 mg, 0.19 mmol) and crude *N*-(4-pent-4-ynoxyphenyl)formamide (36 mg, 0.19 mmol), affording 23 mg (32%, 0.06 mmol) of the title product. ^{1}H NMR (500 MHz, Chloroform-d) δ 9.02 (s, 1H, H6), 8.03 (d, *J* = 5.4 Hz, 1H, H8), 7.60 (d, *J* = 8.9 Hz, 2H, H15), 7.02 (d, *J* = 5.5 Hz, 1H, H7), 6.95 (d, *J* = 9.0 Hz, 2H, H16), 4.13 (t, *J* = 7.0 Hz, 2H, H18), 3.97 – 3.93 (m, 4H, H12), 3.87 (dd, *J* = 5.8, 3.5 Hz, 4H, H11), 2.71 (td, *J* = 7.0, 2.6 Hz, 2H, H19), 2.08 (t, *J* = 2.7 Hz, 1H, H21); ^{13}C NMR (126 MHz, Chloroform-d) δ 162.0 (C6), 156.8 (C10), 156.2 (C2), 154.7 (C17), 139.7 (C4), 139.2 (C8), 132.6 (C14), 124.2 (C5), 121.6 (C15), 115.0 (C16), 111.3 (C7), 80.4 (C20), 70.0 (C21), 67.2 (C12), 66.5 (C18), 49.3 (C11), 19.6 (C19); HRMS (ESI +ve): $C_{21}H_{22}N_5O_2$ $[M+H]^+$: 376.1773 (Found: 376.1744)

2-(2,6-dioxopiperidin-3-yl)-4-((5-(4-(2-(4-((8-morpholinopyrido[3,4-d] pyrimidin-2-yl)amino)phenoxy)ethyl)-1H-1,2,3-triazol-1-yl)pentyl)amino) isoindoline-1,3-dione (78)

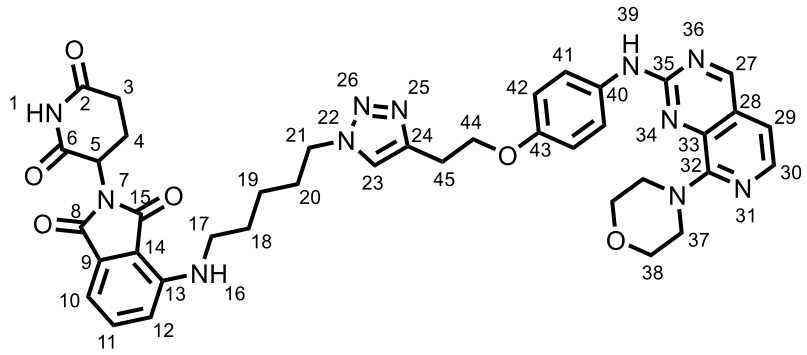

Product was synthesised following **general procedure 5** using N-(4-(but-3-yn-1-yloxy)phenyl)-8-morpholinopyrido[3,4-d]pyrimidin-2-amine (10 mg, 0.03 mmol) and 4-((5-azidopentyl)amino)-2-(2,6-dioxopiperidin-3-yl)isoindoline-1,3-dione (11 mg, 0.03 mmol), affording 7 mg (43%, 0.01 mmol) of the title product. ^{1}H NMR (600 MHz, $CDCl_3$) δ 9.04 (s, 1H, H27), 8.03 (d, *J* = 5.4 Hz, 1H, H30), 7.70 (s, 1H, H39), 7.62 (d, *J* = 8.9 Hz, 2H, H41), 7.50 (dd, *J* = 8.5, 7.1 Hz, 1H, H11), 7.47 (s, 1H, H23), 7.11 (d, *J* = 7.1 Hz, 1H, H10), 7.02 (d, *J* = 5.4 Hz, 1H, H29), 6.92 (d, *J* = 8.9 Hz, 2H, H42), 6.87 (d, *J* = 8.5 Hz, 1H, H12), 6.21 (t, *J* = 5.7 Hz, 1H, H16), 4.94 (dd, *J* = 12.4, 5.4 Hz, 1H, H5), 4.39 (t, *J* = 7.0 Hz, 2H, H21), 4.29 (t, *J* = 6.3 Hz, 2H, H44), 3.96 (t, *J* = 4.7 Hz, 4H, H38), 3.87 (dd, *J* = 5.9, 3.6 Hz, 4H, H37), 3.25 (t, *J* = 6.2 Hz, 4H, H45, H17), 2.94 – 2.59 (m, 3H,

H3, H4), 2.15 (dtd, *J* = 11.9, 4.7, 2.0 Hz, 1H, H4), 1.99 (p, *J* = 6.9 Hz, 2H, H20), 1.71 (dt, *J* = 14.1, 6.5 Hz, 2H, H18), 1.50 – 1.41 (m, 2H, H19); ^{13}C NMR (151 MHz, $CDCl_3$) δ 171.3 (C2), 169.6 (C15), 168.9 (C6), 167.6 (C8), 161.9 (C27), 156.8 (C32), 156.0 (C35), 154.8 (C43), 146.8 (C9), 144.8 (C24), 139.7 (C33), 139.2 (C30), 136.2 (C11), 132.7 (C40), 132.5 (C14), 124.0 (C28), 121.9 (C23), 121.5 (C41), 116.6 (C12), 114.8 (C42), 111.6 (C10), 111.4 (C29), 110.1 (C13), 67.2 (C44), 67.2 (C38), 49.9 (C21), 49.3 (C37), 48.9 (C5), 42.4 (C17), 31.5 (C4), 30.0 (C20), 28.6 (C18), 26.3 (C45), 23.8 (C19), 22.9 (C3); HRMS (ESI +ve): $C_{39}H_{42}N_{11}O_6$ $[M+H]^+$: 760.3320 (Found: 760.3310).

Pentane-1,5-diyl bis(4-methylbenzenesulfonate) (113)

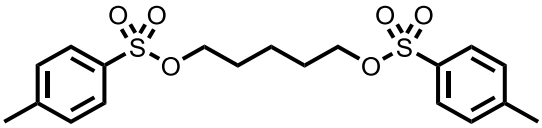

pentane-1,5-diol (0.3 mL, 2.88 mmol) was dissolved in pyridine (0.5 mL) and cooled to 0 °C. *p*-toluene-sulfonyl-chloride (1.65 g, 8.64 mmol) was dissolved in pyridine (1.9 mL) and added dropwise. This was stirred for 2 h at rt. The mixture was poured into water (10 mL) under vigorous stirring and the resulting white precipitate was vacuum filtered and recrystallized in hot MeOH to yield the title product (962 mg, 81%, 2.33 mmol). ^{1}H NMR (500 MHz, $CDCl_3$) δ 7.78 (d, *J* = 8.4 Hz, 2H), 7.37 (d, *J* = 8.0 Hz, 2H), 3.99 (t, *J* = 6.3 Hz, 4H), 2.47 (s, 6H), 1.74 – 1.53 (m, 4H), 1.47 – 1.26 (m, 2H); ^{13}C NMR (126 MHz, $CDCl_3$) δ 144.9, 133.0, 129.9, 127.9, 70.0, 28.2, 21.6, 21.5; HRMS (ESI +ve): $C_{19}H_{25}O_6S_2$ $[M+H]^+$ 413.1041 (Found: 413.1092). Characterisation consistent with literature.[76]

5-((2-(2,6-dioxopiperidin-3-yl)-1,3-dioxoisoindolin-4-yl)oxy)pentyl4-methyl benzenesulfonate (114)

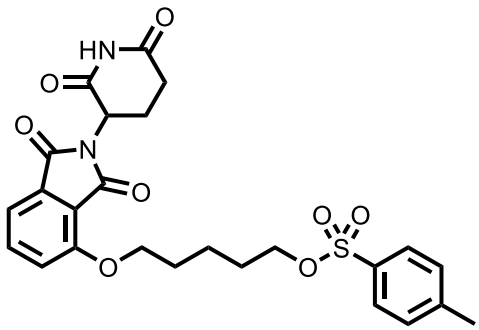

5-(p-tolylsulfonyloxy)pentyl 4-methylbenzenesulfonate (451 mg, 1.09 mmol), 2-(2,6-dioxopiperidin-3-yl)-4-hydroxyisoindoline-1,3-dione (100 mg, 0.36 mmol) , and DIPEA (0.19 mL, 1.09 mmol) were dissolved in DMF (7.3 mL) and heated to 80 °C for 3 h. Water was added and extracted with DCM. The organic layers were combined, washed with brine, dried over $MgSO_4$, and solvent was removed in *vacuo*. residue was purified using column chromatography (EtOAc:c-hex 0-100%) affording the title product (113 mg, 60%, 0.2196 mmol). ^{1}H NMR (600 MHz, $CDCl_3$) δ 8.44 (s, 1H), 7.79 (d, *J* = 8.3 Hz, 2H), 7.67 (dd, *J* = 8.5, 7.2 Hz, 1H), 7.45 (d, *J* = 7.3 Hz, 1H), 7.36 – 7.32 (m, 2H), 7.19 (d, *J* = 8.5 Hz, 1H), 4.96 (dd, *J* = 12.3, 5.3 Hz, 1H), 4.14 (t, *J* = 6.3 Hz, 2H), 4.06 (t, *J* = 6.4 Hz, 2H), 2.91 – 2.71 (m, 3H), 2.43 (s, 3H), 2.17 – 2.11 (m, 1H), 1.88 – 1.82 (m, 2H), 1.80 – 1.74 (m, 2H), 1.61 – 1.56 (m, 2H); HRMS (ESI +ve): $C_{19}H_{25}O_6S_2$ $[M+H]^+$ 515.1354 (Found: 515.1488). Characterisation consistent with literature.[76]

2-chloro-7-iodothieno[3,2-*d*]pyrimidine (116)

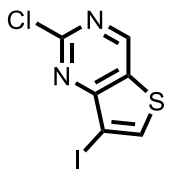

2-chlorothieno[3,2-*d*]pyrimidine (150 mg, 0.88 mmol) and 1-iodopyrrolidine-2,5-dione (593 mg, 2.64 mmol) were dissolved in Acetic acid (4 mL) and heated to 80 °C overnight. Water was added and extracted with EtOAc. The organic layers were combined and purified using column chromatography (EtOAc:c-hex 0-10%) affording 2-chloro-7-iodo-thieno[3,2-d]pyrimidine (87 mg, 33%, 0.29 mmol). ^{1}H NMR (600 MHz, $CDCl_3$) δ 9.13 (s, 1H), 8.26 (s, 1H); ^{13}C NMR (151 MHz, $CDCl_3$) δ 175.9, 162.5, 153.9, 140.1, 128.8, 80.0; HRMS (ESI +ve): $C_6H_2ClIN_2S$ $[M+H]^+$: 296.8750 (Found: 296.8640). Characterisation was consistent with the literature.[142]

***N*-(3-(2-chlorothieno[3,2-*d*]pyrimidin-7-yl)phenyl)methanesulfonamide (117)**

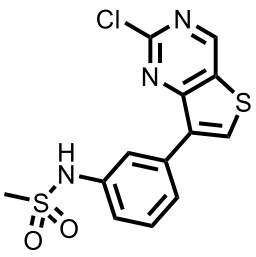

2-chloro-7-iodo-thieno[3,2-*d*]pyrimidine (51 mg, 0.17 mmol), [3-(methane sulfonamido)phenyl] boronic acid (40 mg, 0.19 mmol) and K_2CO_3 (71 mg, 0.52 mmol) were dissolved in 1,4 dioxane (0.8 mL) and water (0.2 mL) and degassed. Pd(dppf)Cl_2 DCM (14 mg, 0.02 mmol) was added and degassed again. The reaction was heated to 90 °C under microwave irradiation for 6 h. Product was concentrated and purified using column chromatography (EtOAc:c-hex 0-100%) affording the title product (18 mg, 31%, 0.05 mmol). ^{1}H NMR (600 MHz, $CDCl_3$) δ 9.22 (s, 1H), 8.25 (s, 1H), 7.98 (t, *J* = 2.0 Hz, 2H), 7.74 – 7.71 (m, 1H), 7.52 (t, *J* = 7.9 Hz, 2H), 7.26 (ddd, *J* = 8.1, 2.3, 0.9 Hz, 2H), 3.20 (s, 5H); ^{13}C NMR (151 MHz, $CDCl_3$) δ 154.1, 135.0, 130.3, 124.8, 120.3, 120.03, 39.8 (Quaternary carbons not seen); HRMS (ESI +ve): $C_{13}H_{11}ClN_3S_2$ $[M+Na]^+$ 361.9800 (Found: 361.9701). Characterisation was consistent with the literature.[143]

_N_-(3-(2-((4-(piperazin-1-yl)phenyl)amino)thieno[3,2-*d*]pyrimidin-7-yl) phenyl)methanesulfonamide (119)

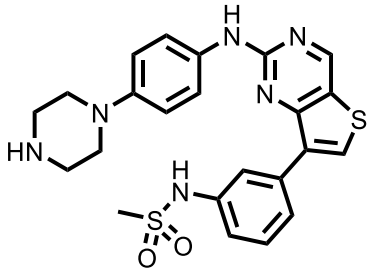

4-(4-Aminophenyl)piperazine-1-carboxylic acid *tert*-butyl ester (21 mg, 0.08 mmol), *N*-[3-(2-chlorothieno [3,2-*d*]pyrimidin-7-yl)phenyl]methanesulfonamide (20 mg, 0.06 mmol), XPhos (3 mg, 0.01 mmol) and Cs_2CO_3 (57 mg, 0.18 mmol) were dissolved in DMF (0.6 mL) . The solution was degassed and $Pd_2(DBA)_3$ (3 mg, 0.003 mmol) was added following further degassing. The reaction was placed under nitrogen and heated to 90 °C under microwave irradiation for 30 mins. The mixture was purified using column chromatography (EtOAc:c-hex 0-

100%). The residue was dissolved in DCM (0.2 mL) and HCl in dioxane (4M, 86 µL, 0.34 mmol) was added. The reaction was stirred for 2 h at rt. Solvent was removed in *vacuo*, affording title product (18 mg, 58%, 0.03 mmol). ^{1}H NMR (600 MHz, DMSO-d_6) δ 9.94 (s, 0H), 9.59 (d, *J* = 9.2 Hz, 1H), 9.24 (s, 1H), 8.53 (s, 1H), 7.87 – 7.78 (m, 2H), 7.49 (t, *J* = 7.9 Hz, 1H), 7.33 – 7.29 (m, 1H), 7.17 (d, *J* = 8.6 Hz, 1H), 3.48 (t, *J* = 5.2 Hz, 2H), 3.32 (s, 1H), 3.04 (s, 2H); ^{13}C NMR (151 MHz, DMSO-d_6) δ 159.0, 157.7, 154.1, 150.0, 139.1, 135.9, 134.9, 134.1, 129.8, 124.5, 124.3, 123.2, 120.5, 119.8, 118.3, 47.8, 42.5; HRMS (ESI +ve): $C_{23}H_{24}N_6O_2S_2$ $[M+H]^+$ 481.1480 (Found: 481.1383). Characterisation consistent with literature.[76]

_N_-(3-(2-((4-(4-(5-((2-(2,6-dioxopiperidin-3-yl)-1,3-dioxoisoindolin-4-yl)oxy) pentyl)piperazin-1-yl)phenyl)amino)thieno[3,2-*d*]pyrimidin-7-yl)phenyl) methanesulfonamide (DB-0614)

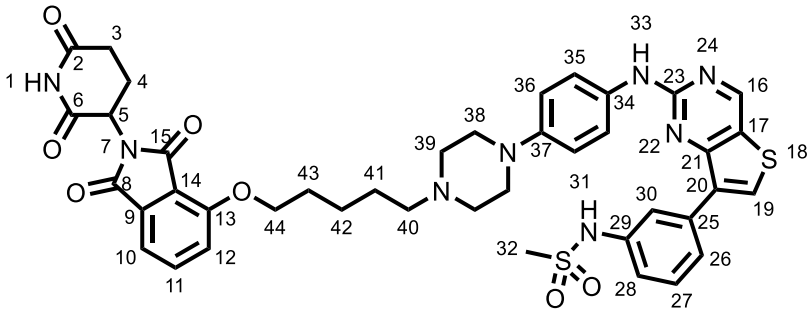

N-[3-[2-(4-piperazin-1-ylanilino)thieno[3,2-*d*]pyrimidin-7-yl]phenyl] methane sulfonamide (18 mg, 0.03 mmol), 5-[2-(2,6-dioxo-3-piperidyl)-1,3-dioxo-isoindolin-4-yl]oxypentyl 4-methyl benzene sulfonate (21 mg, 0.04 mmol) and DIPEA (0.02 mL, 0.10 mmol) were dissolved in DMF (0.2 mL) and heated to 60 °C overnight. Water was added and washed 3 times with DCM. The organic layers were combined, washed with brine, and solvent was removed in *vacuo*. The residue was purified using column chromatography (DCM:MeOH 0-10%) affording the title product (5 mg, 17%, 0.01 mmol). ^{1}H NMR (600 MHz, $CDCl_3$) δ 8.92 (s, 1H, H16), 8.10 (t, *J* = 1.9 Hz, 1H, H30), 8.02 (s, 1H, H19), 7.82 – 7.77 (m, 1H, H26), 7.74 – 7.66 (m, 1H, H11), 7.62 – 7.56 (m, 2H, H35), 7.46 (dd, *J* = 9.8, 7.5 Hz, 2H, H27, H12), 7.40 – 7.35 (m, 1H, H28), 7.23 (d, *J* = 8.5 Hz, 1H, H10), 6.94 (d, *J* = 8.7 Hz, 2H, H36), 4.96 (dd, *J* = 12.5, 5.5 Hz, 1H, H5), 4.21 (tt, *J* = 6.4, 3.3 Hz, 2H, H40), 3.99 (t, *J* = 6.3 Hz, 1H, H44), 3.21 (t, *J* = 5.0 Hz, 4H, H38), 3.01 (s, 3H, H32), 2.90 – 2.78 (m, 2H, H3), 2.66 (d, *J* = 5.2 Hz, 4H, H39),

2.16 – 2.08 (m, 1H, H4), 1.94 (p, *J* = 6.5 Hz, 2H, H41), 1.67 (q, *J* = 7.4, 5.6 Hz, 2H, H42), 1.65 – 1.56 (m, 2H, H43); ^{13}C NMR (151 MHz, $CDCl_3$) δ 171.71 (C2), 168.42 (C6), 167.14 (C15), 165.68 (C8), 159.09 (C20), 157.94 (C23), 156.68 (C13), 153.06 (C16), 147.32 (C37), 137.17 (C29), 136.50 (C11), 135.11 (C17), 133.85 (C25), 133.80 (C41), 132.98 (C19), 132.12 (C34), 129.90 (C27), 127.88 (C26), 123.18 (C21), 121.02 (C35), 120.51 (C30), 119.51 (C28), 118.89 (C10), 117.10 (C9), 116.49 (C36), 115.74 (C12), 69.98 (C44), 69.38 (C40), 53.12 (C39), 49.55 (C38), 49.11 (C5), 39.42 (C32), 31.39 (C3), 28.74 (C41), 28.20 (C42 or 43), 26.35 (C42 or 43), 22.68 (C4); HRMS (ESI +ve): $C_{41}H_{43}N_8O_7S_7$ $[M+H]^+$ 823.2696 (Found: 823.2537).

8-morpholino-*N*-(4-(piperazin-1-yl)phenyl)pyrido[3,4-*d*]pyrimidin-2-amine (122)

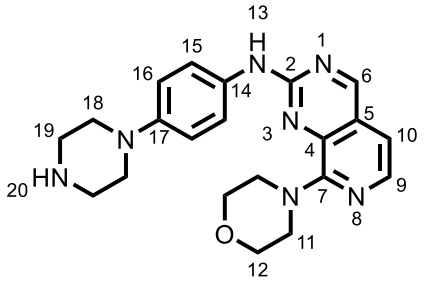

A solution of sodium hydride (4 mg, 0.10 mmol) and *tert*-butyl 4-(4-formamidophenyl)piperazine-1-carboxylate (31 mg, 0.10 mmol) in THF (0.3 mL) was cooled to 0 °C. 4-(2-methylsulfonylpyrido[3,4-d]pyrimidin-8-yl) morpholine (30 mg, 0.10 mmol) was added and the reaction was allowed to warm to rt. The reaction was stirred at rt overnight. Water was added to quench the reaction and was extracted with EtOAc (3 times). The organic layers were combined, washed with brine, dried over $MgSO_4$, and solvent was removed in *vacuo* to afford crude *tert*-butyl 4-[4-[(8-morpholinopyrido[3,4-d]pyrimidin-2-yl)amino]phenyl]piperazine-1-carboxylate (51 mg, 100%, 0.10 mmol). Intermediate Boc-protected piperazine was seen by LCMS ($[M+H]^+$: 492.26) with a retention time of 1.54 min. *tert*-butyl 4-[4-[(8-morpholinopyrido[3,4-*d*]pyrimidin-2-yl)amino]phenyl] piperazine-1-carboxylate (51 mg, 0.10 mmol) was dissolved in DCM (2 mL) and HCl in dioxane (0.3 mL, 1.04 mmol) was added. The reaction was stirred for 1 h at rt then solvent was removed in *vacuo*. Product was dissolved in MeOH and 3 drops of formic acid was added. This was passed through an SCX-2 column washing with MeOH. 3.5 M ammonia in

MeOH was used to elute product which was then removed in vacuo to afford the title product (11 mg, 27%, 0.03 mmol. ^{1}H NMR (600 MHz, $CDCl_3$) δ 9.01 (s, 1H, H6), 8.03 (d, *J* = 5.4 Hz, 1H, H9), 7.59 (d, *J* = 8.6 Hz, 2H, H15), 7.37 (s, 1H, H13), 7.02 (d, *J* = 5.4 Hz, 1H, H10), 6.97 (d, *J* = 8.6 Hz, 2H, H16), 4.01 – 3.80 (m, 8H, H11, H12), 3.19 – 2.99 (m, 8H, H18, H19); ^{13}C NMR (151 MHz, $CDCl_3$) δ 161.9 (C6), 156.8 (C7), 156.2 (C2), 148.2 (C17), 139.8 (C4), 139.0 (C9), 131.7 (C14), 124.0 (C5), 121.2 (C15), 116.7 (C16), 111.3 (C10), 67.3 (C11, C12), 51.0 (C18, C19), 49.3 (C11, C12), 46.0 (C18, C19); HRMS (ESI +ve): $C_{21}H_{26}N_7O$ $[M+H]^+$ 392.2199 (Found: 392.2119).

2-(2,6-dioxopiperidin-3-yl)-4-((5-(4-(4-((8-morpholinopyrido[3,4-*d*] pyrimidin-2-yl)amino)phenyl) piperazin-1-yl)pentyl)oxy)isoindoline-1,3-dione (79)

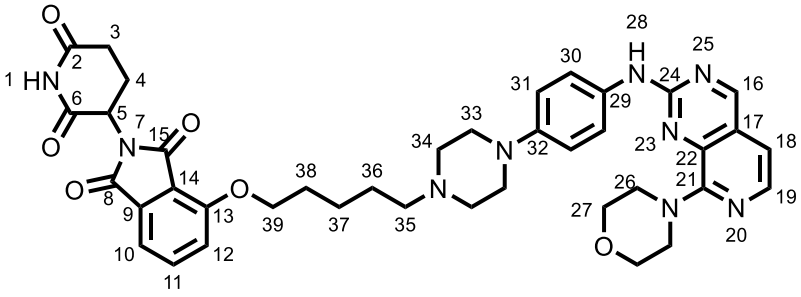

8-morpholino-*N*-(4-piperazin-1-ylphenyl)pyrido[3,4-*d*]pyrimidin-2-amine (11 mg, 0.03 mmol), 5-[2-(2,6-dioxo-3-piperidyl)-1,3-dioxo-isoindolin-4-yl]oxypentyl 4-methylbenzenesulfonate (22 mg, 0.04 mmol) and DIPEA (15 µL, 0.08 mmol) were dissolved in DMF (0.2 mL) and heated to 60 °C overnight. Water was added and washed 3 times with DCM. The organic layers were combined, washed with brine, and solvent was removed in vacuo. The residue was purified using column chromatography (DCM:MeOH 0-10%) affording the title product (8 mg, 39%, 0.01 mmol). ^{1}H NMR (600 MHz, DMSO) δ 11.10 (s, 1H, H1), 9.80 (s, 1H, H28), 9.23 (s, 1H, H16), 7.95 (d, *J* = 5.3 Hz, 1H, H19), 7.85 – 7.79 (m, 1H, H11), 7.67 (d, *J* = 8.7 Hz, 2H, H30), 7.53 (d, *J* = 8.5 Hz, 1H, H10), 7.45 (d, *J* = 7.2 Hz, 1H, H12), 7.19 (d, *J* = 5.3 Hz, 1H, H18), 6.94 (d, *J* = 9.0 Hz, 2H, H31), 5.08 (dd, *J* = 12.8, 5.5 Hz, 1H, H23), 4.23 (t, *J* = 6.4 Hz, 2H, H39), 3.83 (t, *J* = 4.7 Hz, 4H, H27), 3.75 (t, *J* = 4.6 Hz, 4H, H26), 3.09 (t, *J* = 5.0 Hz, 4H, H34), 2.88 (ddd, *J* = 17.0, 13.8, 5.5 Hz, 1H, H3), 2.60 (dd, *J* = 4.4, 2.5 Hz, 1H, H3, H4), 2.52 (q, *J* = 5.7, 5.0 Hz, 4H, H33), 2.35 (t, *J* = 7.1 Hz, 2H, H35), 2.02 (dtd,

J = 13.2, 5.4, 2.3 Hz, 1H, H4), 1.81 (p, *J* = 6.8 Hz, 2H, H38), 1.60 – 1.46 (m, 4H, H36, H37); ^{13}C NMR (151 MHz, DMSO) δ 173.25 (C2), 170.43 (C6), 167.33 (C8), 165.79 (C15), 162.78 (C16), 156.43 (C13), 156.39 (C24), 147.19 (C32), 139.37 (C21), 138.56 (C19), 137.51 (C11), 133.72 (C9), 132.41 (C29), 123.83 (C17), 120.87 (C30), 120.29 (C10), 116.69 (C14), 116.10 (C31), 115.60 (C12), 112.16 (C18), 69.27 (C39), 66.82 (C27), 58.27 (C35), 53.29 (C33), 49.30 (C34), 49.20 (C26), 49.35 (C5), 31.42 (C3), 28.80 (C38), 26.42 (C36, C37), 23.71 (C36, 37), 22.48 (C4); HRMS (ESI +ve): $C_{39}H_{44}N_9O_6$ $[M+H]^+$ 734.3415 (Found: 734.3404).

_N_-(3-(2-((4-(hept-6-yn-1-yloxy)phenyl)amino)thieno[3,2-*d*]pyrimidin-7-yl) phenyl)methane sulfonamide (123)

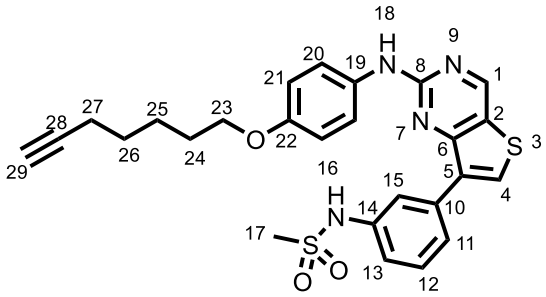

4-hept-6-ynoxyaniline (13 mg, 0.07 mmol), N-[3-(2-chlorothieno[3,2-*d*]pyrimidin-7-yl)phenyl] methane sulfonamide (17 mg, 0.05 mmol), XPhos (2 mg, 0.01 mmol), Cs_2CO_3 (49 mg, 0.15 mmol) were dissolved in DMF (0.6 mL) and degassed. $Pd_2(dba)_3$ (2 mg, 0.003 mmol) was added and degassed again. The solution was placed under nitrogen and heated to 90 °C under microwave irradiation for 30 mins. The mixture was purified using column chromatography (EtOAc:c-hex 0-100%) affording the title product (10 mg, 39%, 0.02 mmol). ^{1}H NMR (500 MHz, $CDCl_3$) δ 8.92 (s, 1H, H1), 8.03 (s, 1H, H4), 8.02 (t, *J* = 2.0 Hz, 1H, H15), 7.79 (dt, *J* = 8.0, 1.2 Hz, 1H, H11), 7.57 (d, *J* = 9.0 Hz, 2H, H20), 7.47 (t, *J* = 7.9 Hz, 1H, H12), 7.35 – 7.31 (m, 1H, H13), 6.93 – 6.89 (m, 2H, H21), 3.99 (t, *J* = 6.5 Hz, 2H, H23), 3.04 (s, 3H, H17), 2.26 (td, *J* = 6.8, 2.7 Hz, 2H, H28), 1.99 (t, *J* = 2.7 Hz, 1H, H29), 1.82 (p, *J* = 6.7 Hz, 2H, H24), 1.66 – 1.58 (m, 4H, H25, H26); ^{13}C NMR (126 MHz, $CDCl_3$) δ 159.1 (C8), 158.1 (C6), 155.1 (C22), 153.2 (C1), 137.1 (C14), 135.1 (C5), 133.9 (C10), 133.1 (C4), 132.7 (C19), 129.8 (C21), 124.7 (C11), 123.3 (C2), 121.6 (C20), 120.4 (C15), 119.6 (C13), 114.7 (C121), 84.5 (C28), 68.4 (C29), 68.1 (C23), 39.5 (C17), 28.9 (C24),

28.3 (C25, C26), 25.3 (C25, C26), 18.4 (C27); HRMS (ESI +ve): $C_{26}H_{27}N_4O_3S_2$ $[M+H]^+$: 507.1485 (Found: 507.1525).

N-(3-(2-((4-((5-(1-(2-((2-(2,6-dioxopiperidin-3-yl)-1,3-dioxoisoindolin-4-yl) amino)ethyl)-1*H*-1,2,3-triazol-4-yl)pentyl)oxy)phenyl)amino)thieno[3,2-*d*]pyrimidin-7-yl)phenyl)methanesulfonamide (80)

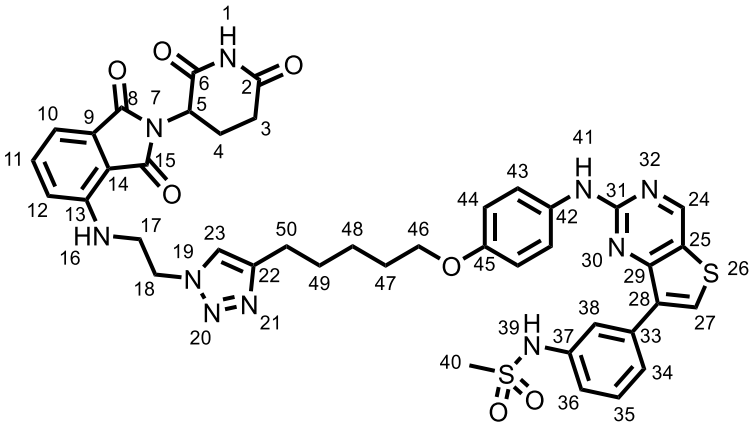

Product was synthesised following **general procedure 5** using N-[3-[2-(4-hept-6-ynoxyanilino)thieno[3,2-d]pyrimidin-7-yl]phenyl]methane sulfonamide (10 mg, 0.02 mmol) and 4-(2-azidoethylamino)-2-(2,6-dioxo-3-piperidyl) isoindoline-1,3-dione, affording 6 mg (36%, 0.0071 mmol) of the title product. ^{1}H NMR (600 MHz, DMSO-d_6) δ 11.10 (s, 1H, H1), 9.51 (s, 1H, H41), 9.19 (s, 1H, H24), 8.47 (s, 1H, H27), 7.88 (s, 1H, H23), 7.82 – 7.78 (m, 2H, H36, H38), 7.74 (d, *J* = 8.9 Hz, 2H, H43), 7.53 (dd, *J* = 8.5, 7.1 Hz, 1H, H11), 7.48 (t, *J* = 7.8 Hz, 1H, H35), 7.28 – 7.26 (m, 1H, H34), 7.03 (d, *J* = 7.1 Hz, 1H, H10), 6.99 (d, *J* = 8.6 Hz, 1H, H12), 6.89 (d, *J* = 9.0 Hz, 1H, H44), 6.76 (t, *J* = 6.4 Hz, 1H, H16), 5.05 (dd, *J* = 12.8, 5.4 Hz, 1H, H5), 4.54 (t, *J* = 6.1 Hz, 2H, H18), 3.92 (t, *J* = 6.5 Hz, 2H, H46), 3.79 (q, *J* = 6.2 Hz, 2H, H17), 2.87 (ddd, *J* = 17.2, 13.9, 5.4 Hz, 1H, H3), 2.55 (s, 3H, H3, H4), 2.52 – 2.49 (m, 3H, H40), 2.01 (dtd, *J* = 9.9, 4.9, 4.3, 2.2 Hz, 1H, H4), 1.72 (p, *J* = 6.7 Hz, 2H, H47), 1.61 (p, *J* = 7.5 Hz, 2H, H49), 1.43 (qd, *J* = 9.4, 8.8, 6.0 Hz, 2H, H48); ^{13}C NMR (151 MHz, DMSO-d_6) δ 173.3 (C2), 170.5 (C6), 169.1 (C15), 167.7 (C8), 158.8 (C29), 158.4 (C31), 154.5 (C24), 154.0 (C45), 147.4 (C22), 146.4 (C13), 139.2 (C33), 136.7 (C11), 135.0 (C27), 134.9 (C37), 134.2 (C28), 134.1 (C42), 132.6 (C9), 129.8 (C35), 124.2 (C36), 122.8 (C25), 122.8 (C23), 120.9 (C43), 120.4 (C38), 119.6 (C34), 117.5 (C12), 114.8 (C44), 111.4 (C10), 110.0 (C14), 67.9 (C46), 49.2 (C18), 49.0 (C5), 42.6 (C17), 40.9 (C40), 31.4 (C3), 29.2 (C49), 29.0 (C47), 25.6 (C48), 25.4 (C50),

22.6 (C4); HRMS (ESI +ve): $C_{41}H_{41}N_{10}O_7S_2$ $[M+H]^+$ 849.2601 (Found: 849.2437).

1-(4-(hept-6-yn-1-yloxy)phenyl)guanidine (124)

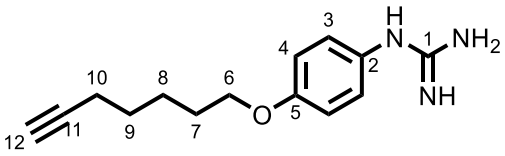

4-(hept-6-yn-1-yloxy)aniline (150 mg, 0.74 mmol), Cyanamide (33 mg, 0.77 mmol), and 4M HCl in dioxane (0.18 mL, 0.74 mmol) were dissolved in MeCN (1 mL) and heated to 100 °C in a sealed microwave vial overnight. The reaction was concentrated under reduced pressure and 1M aq. NaOH was added. The reaction was concentrated in *vacuo* and purified using reverse phase column chromatography (water:MeOH (+0.1% formic acid) 5-50%) affording 1-(4-hept-6-ynoxyphenyl) guanidine (163 mg, 90%, 0.66 mmol).^{1}H NMR (500 MHz, $CDCl_3$) δ 7.13 (d, *J* = 8.4 Hz, 2H, H3), 6.91 (d, *J* = 8.6 Hz, 2H, H4), 3.96 (t, *J* = 6.4 Hz, 2H, H6), 2.24 (td, *J* = 6.7, 2.6 Hz, 2H, H10), 1.97 (t, *J* = 2.6 Hz, 1H, H12), 1.82 (p, *J* = 6.7 Hz, 2H, H7), 1.68 – 1.54 (m, 4H, H8, H9); ^{13}C NMR (126 MHz, $CDCl_3$) δ 158.6 (C1), 157.5 (C1), 127.5 (C3), 126.8 (C2), 115.8 (C4), 84.3 (C11), 68.5 (C12), 68.1 (C6), 28.7 (C7), 28.1 (C8, C9), 25.2 (C8, C9), 18.3 (C10); HRMS (ESI +ve): $C_{14}H_{20}N_3O$ $[M+H]^+$: 246.1606 (Found: 246.1505).

Methyl (*E*)-4-(3-(dimethylamino)acryloyl)benzoate (125)

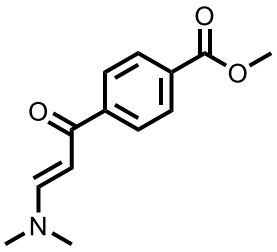

Methyl 4-acetylbenzoate (0.65 g, 3.6 mmol) and DMF-DMA (1 mL, 7.30 mmol) were dissolved in Toluene (5 mL) and heated to 80 ºC overnight. The mixture was allowed to cool to rt and the solid was filtered. The solid was washed with toluene, affording the title product (650 mg, 76%, 2.79 mmol). ^{1}H NMR (500 MHz, $CDCl_3$) δ 8.21 – 8.02 (m, 1H), 7.93 (d, *J* = 8.6 Hz, 1H), 7.83 (d, *J* = 12.3 Hz, 1H), 5.71 (d, *J* = 12.3 Hz, 1H), 3.94 (s, 3H), 3.06 (d, *J* = 111.3 Hz, 6H). ^{13}C NMR (126 MHz, $CDCl_3$) δ 187.7, 166.7, 154.7, 144.5, 131.9, 129.5,

127.4, 92.3, 52.2, 45.2. HRMS (ESI +ve): $C_{13}H_{16}NO_3$ $[M+H]^+$: 234.1130 (Found: 234.1054). Characterisation consistent with literature.[117]

Methyl 4-(2-((4-(hept-6-yn-1-yloxy)phenyl)amino)pyrimidin-4-yl)benzoate (126)

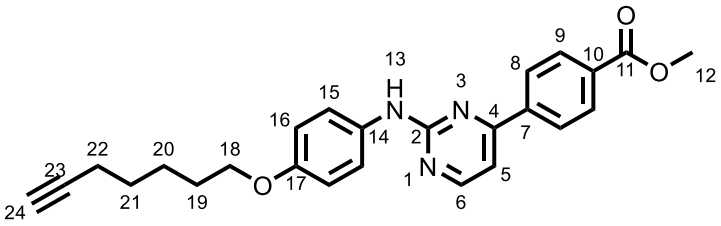

Methyl 4-[(E)-3-(dimethylamino)prop-2-enoyl]benzoate (169 mg, 0.72 mmol) and 1-(4-hept-6-ynoxyphenyl)guanidine (177 mg, 0.72 mmol) were dissolved in MeCN (2.5 mL) and heated to 130 ºC in the microwave for 12 h. MeCN was removed *in vacuo* and the residue was dissolved in DCM. Water was added and extracted with DCM and the organic layers were combined, washed with brine, dried over $MgSO_4$, and solvent was removed *in vacuo*, affording the title product (64 mg, 21%, 0.15 mmol). ^{1}H NMR (600 MHz, $CDCl_3$) δ 8.49 (d, *J* = 5.1 Hz, 1H, H6), 8.17 (d, *J* = 8.5 Hz, 2H, H8), 8.13 (d, *J* = 8.5 Hz, 2H, H9), 7.59 – 7.54 (m, 2H, H15), 7.29 (s, 1H, H13), 7.16 (d, *J* = 5.2 Hz, 1H, H5), 6.96 – 6.91 (m, 2H, H16), 4.00 (t, *J* = 6.5 Hz, 2H, H18), 3.98 (s, 3H, H12), 2.26 (td, *J* = 6.7, 2.6 Hz, 2H, H22), 1.99 (t, *J* = 2.6 Hz, 1H, H24), 1.83 (q, *J* = 6.7 Hz, 2H, H19), 1.64 (tdt, *J* = 9.0, 7.0, 3.1 Hz, 4H, H27, 28); ^{13}C NMR (151 MHz, $CDCl_3$) δ 166.6 (C11), 163.8 (C4), 160.7 (C2), 159.0 (C6), 155.1 (C17), 141.4 (C7), 132.4 (C14), 131.9 (C10), 130.0 (C9), 127.1 (C8), 121.8 (C16), 114.9 (C15), 108.3 (C5), 84.4 (C23), 68.4 (C24), 68.1 (C18), 52.3 (C12), 28.9 (C19), 28.3 (C20, C21), 25.3 (C20, C21), 18.4 (C21); HRMS (ESI +ve): $C_{25}H_{26}N_3O_3$ $[M+H]^+$: 416.1974 (Found: 416.1989).

***N*-(cyanomethyl)-4-(2-((4-(hept-6-yn-1-yloxy)phenyl)amino)pyrimidin-4-yl) benzamide (128)**

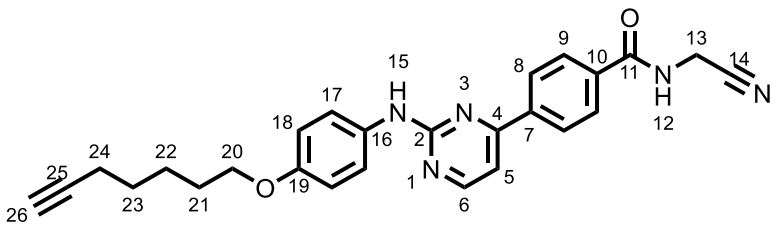

4-[2-(4-hept-6-ynoxyanilino)pyrimidin-4-yl]benzoic acid (52mg, 0.13 mmol) and triethylamine (0.1 mL, 0.34 mmol) were dissolved in DMF (0.7 mL) then aminoacetonitrile (17 µL, 0.28 mmol) , 1-hydroxybenzotriazole (28 mg, 0.20 mmol), and 1-(3-dimethylaminopropyl)-3-ethylcarbodiimide hydrochloride (40 mg, 0.21 mmol) were added. The mixture was stirred at rt overnight. Water was added and extracted with DCM. The organic layers were combined, washed with brine, dried over $MgSO_4$, and solvent was removed in *vacuo*. The residue was purified using column chromatography (DCM:MeOH 0-10%) the title product (34 mg, 60%, 0.08 mmol). ^{1}H NMR (600 MHz, $CDCl_3$) δ 8.49 (d, *J* = 5.1 Hz, 1H, H6), 8.16 (d, *J* = 7.9 Hz, 2H, H8), 7.91 (d, *J* = 7.9 Hz, 2H, H9), 7.56 (d, *J* = 8.3 Hz, 2H, H17), 7.16 – 7.11 (m, 2H, H15, H5), 6.94 (d, *J* = 8.3 Hz, 2H, H18), 6.64 (d, *J* = 5.8 Hz, 1H, H12), 4.44 (d, *J* = 5.7 Hz, 2H, H13), 4.00 (t, *J* = 6.5 Hz, 2H, H20), 2.26 (t, *J* = 6.3 Hz, 2H, H24), 1.98 (s, 1H, H26), 1.85 (dt, *J* = 22.3, 5.6 Hz, 2H, H21), 1.65 – 1.60 (m, 4H, H22, H23); ^{13}C NMR (151 MHz, $CDCl_3$) δ 166.7 (C11), 163.4 (C4), 160.7 (C2), 159.1 (C6), 155.2 (C19), 141.1 (C10), 134.1 (C7), 132.3 (C16), 127.7 (C8), 127.5 (C9), 121.8 (C17), 115.9 (C14), 114.9 (C18), 108.2 (C5), 84.4 (C25), 68.4 (C26), 68.0 (C20), 28.9 (C21), 28.2 (C22), 28.1 (C13), 25.3 (C23), 18.4 (C24); HRMS (ESI +ve): $C_{26}H_{26}N_5O_2$ $[M+H]^+$: 440.2086 (Found: 440.1996).

_N_-(cyanomethyl)-4-(2-((4-((7-(1-(2-((2-(2,6-dioxopiperidin-3-yl)-1,3-dioxoisoindolin-4-yl)amino)ethyl)-1_H_-1,2,3-triazol-4-yl)heptyl)oxy)phenyl)amino)pyrimidin-4-yl)benzamide (81)

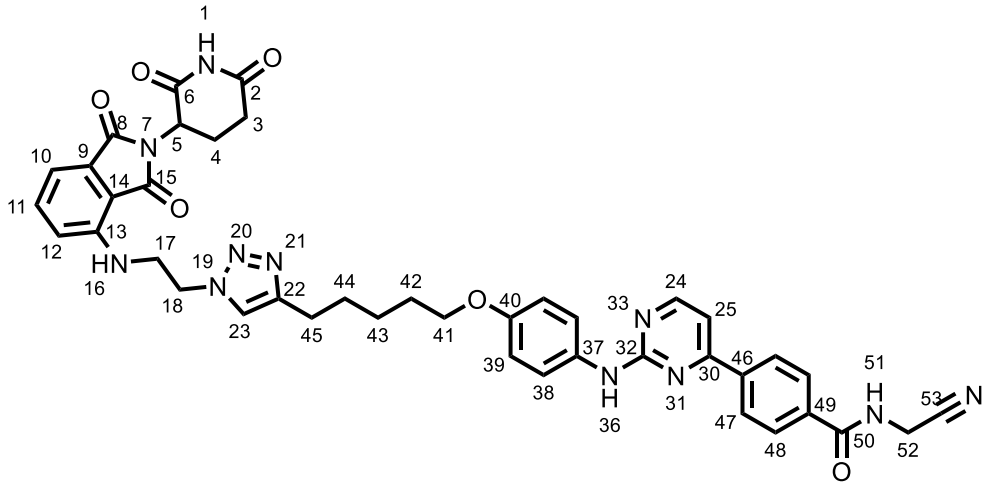

Product was synthesised following **general procedure 5** using *N*-(cyanomethyl)-4-[2-(4-hept-6-ynoxyanilino)pyrimidin-4-yl]benzamide (20 mg,

0.05 mmol) and 4-(2-azidoethylamino)-2-(2,6-dioxo-3-piperidyl)isoindoline-1,3-dione (16 mg, 0.05 mmol), affording 10 mg (28%, 0.02 mmol) of the title product. ^{1}H NMR (600 MHz, DMSO) δ 11.10 (s, 1H, H1), 9.54 (s, 1H, H36), 9.35 (t, *J* = 5.5 Hz, 1H, H51), 8.57 – 8.52 (m, 1H, H24), 8.27 (d, *J* = 8.1 Hz, 2H, H48), 8.06 – 8.01 (m, 2H, H47), 7.88 (s, 1H, H23), 7.70 (dd, *J* = 9.0, 4.0 Hz, 2H, H38), 7.52 (dd, *J* = 8.6, 7.1 Hz, 1H, H11), 7.42 (dd, *J* = 5.2, 1.3 Hz, 1H, H25), 7.03 (d, *J* = 7.0 Hz, 1H, H10), 6.99 (d, *J* = 8.6 Hz, 1H, H12), 6.92 – 6.87 (m, 2H, H39), 6.76 (t, *J* = 6.4 Hz, 1H, H13), 5.05 (dd, *J* = 12.8, 5.4 Hz, 1H, H5), 4.55 (t, *J* = 6.1 Hz, 2H, H18), 4.36 (d, *J* = 2.4 Hz, 2H, H52), *3*.93 (s, 1H, H41), 3.80 (t, *J* = 6.11, 2H, H17), 2.88 (ddd, *J* = 17.1, 13.8, 5.5 Hz, 1H, H3), 2.61 (t, *J* = 7.5 Hz, 2H, H45), 2.57 – 2.42 (m, 2H, H3, H4), 2.02 (dtd, *J* = 13.2, 5.5, 2.5 Hz, 1H, H4), 1.72 (p, *J* = 6.7 Hz, 2H, H42), 1.61 (p, *J* = 7.6 Hz, 2H, H44), 1.43-1.45 (m, 2H, H43); ^{13}C NMR (151 MHz, DMSO) δ 173.2 (C2), 170.4 (C6), 169.1 (C15), 167.7 (C8), 166.5 (C50), 163.0 (C30), 160.7 (C32), 159.8 (C24), 154.2 (C40), 147.3 (C22), 146.3 (C13), 140.4 (C46), 136.7 (C11), 135.0 (C49), 133.9 (C37), 132.6 (C9), 128.4 (C47), 127.5 (C58), 122.8 (C23), 121.1 (C38), 118.1 (C53), 117.4 (C12), 114.8 (C39), 111.4 (C10), 110.0 (C14), 108.3 (C25), 68.0 (C41), 49.2 (C18), 49.0 (C5), 42.5 (C17), 31.4 (C3), 29.2 (C44), 29.0 (C42), 28.2 (C52), 25.6 (C43), 25.4 (C45), 22.6 (C4); HRMS (ESI +ve): $C_{41}H_{40}N_{11}O_6$ $[M+H]^+$: 782.3163 (Found: 782.2955).

(*E*)-*N*'-(5-((*E*)-3-(dimethylamino)acryloyl)-4-methylthiazol-2-yl)-*N,N*-dimethylformimidamide (130)

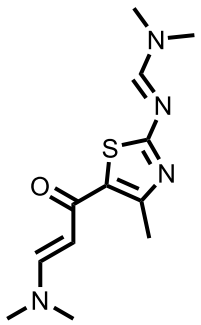

2-amino-4-methyl-5-acetylthiazole (1.50 g, 9.58 mmol) was dissolved in *N,N*-dimethylformamide dimethylacetal (0.65 mL, 4.79 mmol) and heated to 120 °C overnight. The DMF-DMA was removed in *vacuo* affording crude product. The residue was purified using column chromatography (EtOAc:c-hex 0-50%) affording the title product (654 mg, 51%, 2.46 mmol). ^{1}H NMR (500 MHz, $CDCl_3$)

δ 8.21 (s, 1H), 7.65 (d, *J* = 12.3 Hz, 1H), 5.33 (d, *J* = 12.2 Hz, 1H), 3.09 (s, 6H), 3.06 (d, *J* = 0.6 Hz, 6H), 2.62 (s, 3H); ^{13}C NMR (126 MHz, $CDCl_3$) δ 181.56, 173.62, 155.85, 154.05, 152.86, 126.68, 95.16, 40.84, 34.98, 18.25; HRMS (ESI +ve): $C_{12}H_{19}N_4OS$ $[M+H]^+$: 267.1279 (Found: 267.1213). Characterisation was consistent with the literature.[141]

5-(2-((4-(hept-6-yn-1-yloxy)phenyl)amino)pyrimidin-4-yl)-4-methylthiazol-2-amine (131)

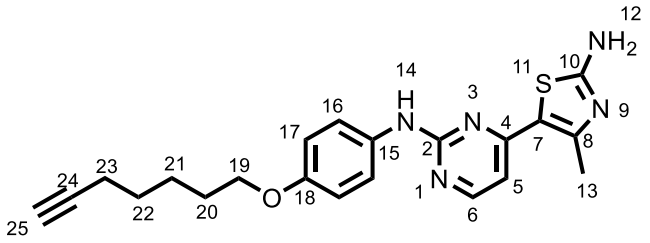

(E)-N'-(5-((E)-3-(dimethylamino)acryloyl)-4-methylthiazol-2-yl)-N,N-dimethyl formimidamide (85 mg, 0.32 mmol), 1-(4-hept-6-ynoxyphenyl) guanidine (102 mg, 0.41 mmol), and NaOH (26 mg, 0.64 mmol) were dissolved in 2-methoxyethanol (0.5 mL) and heated to 180 °C under microwave irradiation for 3 h. Water was added and was extracted with DCM. The DCM layers were combined and concentrated *in vacuo*. Crude product was purified using column chromatography (DCM:MeOH 0-10%) affording the title product (41 mg, 33%, 0.10 mmol). ^{1}H NMR (600 MHz, DMSO-d_6) δ 9.22 (s, 1H, H14), 8.28 (d, *J* = 5.4 Hz, 1H, H6), 7.66 – 7.60 (m, 1H, H16), 7.47 (s, 1H, H12), 6.87 – 6.80 (m, 2H, H17), 3.93 (t, *J* = 6.4 Hz, 2H, H19), 2.77 (t, *J* = 2.7 Hz, 1H, H25), 2.43 (s, 3H, H13), 2.22 – 2.17 (m, 2H, H23), 1.75 – 1.68 (m, 2H, H20), 1.47-1.57 (m, 4H, 21 22); ^{13}C NMR (151 MHz, DMSO-d_6) δ 169.2 (C10), 160.1 (C2), 159.1 (C4), 158.1 (C6), 153.9 (C18), 152.3 (C8), 134.2 (C15), 121.0 (C16), 118.6 (C7), 114.7 (C17), 106.9 (C5), 85.0 (C24), 71.7 (C25), 68.0 (C19), 28.8, (C20), 28.2 (C21, C22), 25.31 (C21, C22), 18.9 (C13), 18.2 (C23); HRMS (ESI +ve): $C_{21}H_{24}N_5OS$ $[M+H]^+$: 394.1696 (Found: 394.1661).

4-((2-(4-(7-(4-((4-(2-amino-4-methylthiazol-5-yl)pyrimidin-2-yl)amino) phenoxy)heptyl)-1*H*-1,2,3-triazol-1-yl)ethyl)amino)-2-(2,6-dioxopiperidin-3-yl)isoindoline-1,3-dione (83)

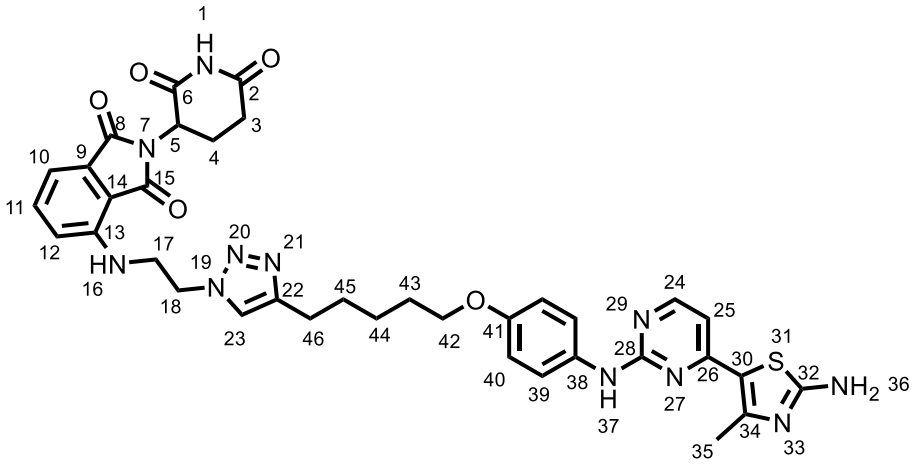

Product was synthesised following **general procedure 5** using 5-[2-(4-hept-6-ynoxyanilino)pyrimidin-5-yl]-4-methyl-thiazol-2-amine (25 mg, 0.06 mmol) and 4-(2-azidoethylamino)-2-(2,6-dioxo-3-piperidyl)isoindoline-1,3-dione (22 mg, 0.06 mmol), affording 8 mg (17%, 0.01 mmol) of the title product. ^{1}H NMR (600 MHz, DMSO-d_6) δ 11.10 (s, 1H, H1), 9.22 (s, 1H, H36), 8.30 (s, 1H, H24), 7.88 (s, 1H, H23), 7.63 (d, *J* = 9.0 Hz, 2H, H40), 7.53 (dd, *J* = 8.6, 7.1 Hz, 1H, H11), 7.47 (s, 2H, H37), 7.03 (d, *J* = 7.0 Hz, 1H, H10), 6.99 (d, *J* = 8.6 Hz, 1H, H12), 6.85 – 6.81 (m, 3H, H39, H25), 6.76 (t, *J* = 6.4 Hz, 1H, H16), 5.05 (dd, *J* = 12.9, 5.5 Hz, 1H, H5), 4.54 (t, *J* = 6.0 Hz, 2H, H18), 3.90 (t, *J* = 6.5 Hz, 2H, H42), 3.80 (q, *J* = 6.2 Hz, 2H, H17), 2.93 – 2.85 (m, 1H, H3), 2.61 (t, *J* = 7.5 Hz, 2H, H46), 2.58 – 2.49 (m, 2H, H3, H4), 2.43 (s, 3H, H35), 1.71 (p, *J* = 6.7 Hz, 2H, H43), 1.65 – 1.57 (m, 5H, H44, H45), 1.46 – 1.39 (m, 2H, H44); ^{13}C NMR (151 MHz, DMSO-d_6) δ 173.3 (C2), 170.5 (C6), 169.1 (C15), 167.7 (C8), 160.1 (C28), 159.1 (C32), 158.0 (C24), 153.9 (C41), 152.3 (C34), 147.4 (C22), 146.4 (C13), 136.7 (C11), 134.2 (C38), 132.6 (C9), 122.8 (C23), 121.0 (C40), 117.5 (C12), 114.7 (C39), 111.4 (C10), 110.0 (C14), 106.9 (C25), 68.0 (C42), 49.2 (C5), 49.0 (C18), 42.6 (C17), 31.4 (C3), 29.2 (C43), 29.0 (C44, C45), 25.6 (C44, C45), 25.4 (C46), 22.6 (C4), 18.9 (C35); HRMS (ESI +ve): $C_{36}H_{38}N_{11}O_5S$ $[M+H]^+$: 736.2778 (Found: 736.2740).

2-((5-chloro-2-((4-(hept-6-yn-1-yloxy)phenyl)amino)pyrimidin-4-yl)amino)-*N*-methylbenzene sulfonamide (134)

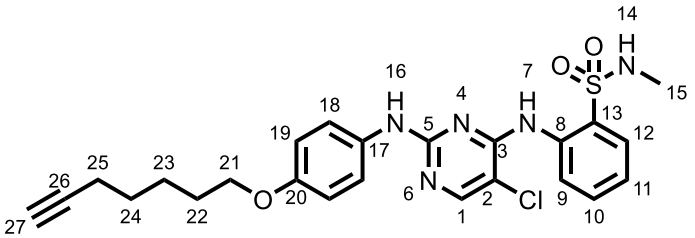

Crude 4-hept-6-ynoxyaniline (71 mg, 0.35 mmol), 2-[(2,5-dichloropyrimidin-4-yl)amino]-*N*-methyl-benzene sulfonamide (90 mg, 0.27 mmol), and DIPEA (0.14 mL, 0.81 mmol) were dissolved in NMP (0.5 mL) and heated to 120 °C overnight. Water was added and extracted with DCM (3 times). The organic layers were combined, and solvent was removed *in vacuo*. The residue was purified using column chromatography (DCM:MeOH 0-10%) affording the title compound (142 mg, quantitative 0.27 mmol). ^{1}H NMR (500 MHz, $CDCl_3$) δ 9.21 (s, 1H, H7), 8.50 (d, *J* = 8.3 Hz, 1H, H12), 8.00 (s, 1H, H1), 7.94 (dd, *J* = 8.0, 1.6 Hz, 1H, H9), 7.61 – 7.46 (m, 1H, H11), 7.39 (d, *J* = 9.0 Hz, 1H, H18), 7.29 – 7.18 (m, 1H, H10), 6.97 (s, 1H, H16), 6.90 – 6.82 (m, 2H, H19), 5.32 (s, 1H, H14), 3.97 (t, *J* = 6.4 Hz, 2H, H21), 2.64 (s, 3H, H15), 2.25 (h, *J* = 2.3 Hz, 2H, H25), 1.97 (t, *J* = 2.7 Hz, 1H, H27), 1.82 (p, *J* = 6.7 Hz, 2H, H22), 1.69 – 1.59 (m, 4H, H23, 24); ^{13}C NMR (126 MHz, $CDCl_3$) δ 158.1 (C3), 155.5 (C17), 155.4 (C5), 154.9 (C1), 136.5 (C8), 133.4 (C11), 132.1 (C20), 129.8 (C9), 126.8 (C13), 123.7 (C12), 123.1 (C10), 122.5 (C18), 105.7 (C19), 84.4 (C26), 68.4 (C27), 68.1 (C21), 29.2 (C15), 28.9 (C22), 28.2 (C23, C24), 25.3 (C23, C24), 18.4 (C25); HRMS (ESI +ve): $C_{24}H_{27}ClN_5O_3S$ $[M+H]^+$: 501.1523 (Found: 501.1521).

2-((5-chloro-2-((4-((5-(1-(2-((2-(2,6-dioxopiperidin-3-yl)-1,3-dioxoisoindolin-4-yl)amino)ethyl)-1*H*-1,2,3-triazol-4-yl)pentyl)oxy)phenyl)amino)pyrimidin-4-yl)amino)-*N*-methylbenzenesulfonamide (82)

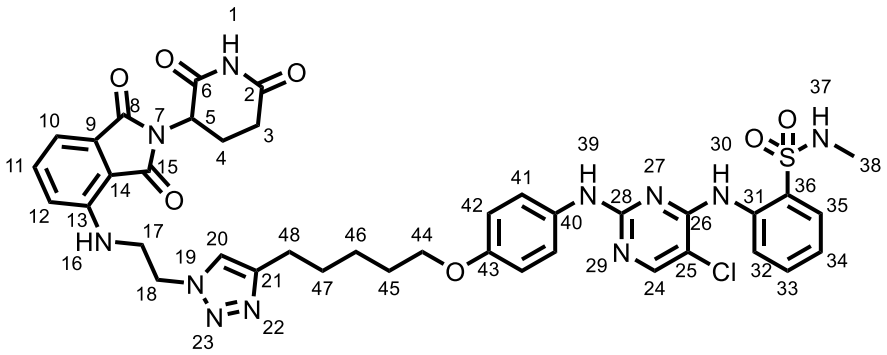

Product was synthesised following **general procedure 5** using 2-[[5-chloro-2-(4-hept-6-ynoxyanilino)pyrimidin-4-yl]amino]-*N*-methyl-benzenesulfonamide (25 mg, 0.05 mmol) and 4-(2-azidoethylamino)-2-(2,6-dioxo-3-piperidyl) isoindoline-1,3-dione (18 mg, 0.05 mmol), affording 9 mg (21%, 0.01 mmol) of the title product. ^{1}H NMR (600 MHz, $CDCl_3$) δ 9.19 (s, 1H, H30), 8.51 (d, *J* = 8.4 Hz, 1H, H35), 8.13 (s, 1H, H24), 7.96 (dd, *J* = 7.9, 1.6 Hz, 1H, H32), 7.56 (t, *J* = 7.9 Hz, 1H, H34), 7.48 (dd, *J* = 8.5, 7.2 Hz, 1H, H11), 7.43 – 7.37 (m, 2H, H41), 7.29 (d, *J* = 8.3 Hz, 1H, H20), 7.24 (t, *J* = 7.8 Hz, 1H, H33), 7.15 (d, *J* = 7.1 Hz, 1H, H10), 6.84 (d, *J* = 8.9 Hz, 2H, H42), 6.72 (d, *J* = 8.5 Hz, 1H, H12), 6.45 (t, *J* = 6.6 Hz, 1H, H16), 4.91 (dd, *J* = 12.6, 5.4 Hz, 1H, H5), 4.62 – 4.53 (m, 2H, H18), 3.97 (t, *J* = 6.4 Hz, 2H, H44), 3.86 (q, *J* = 6.1 Hz, 2H, H17), 2.83 – 2.73 (m, 5H, H3, H4, H48), 2.13 (ddd, *J* = 7.5, 5.3, 2.8 Hz, 1H, H4), 1.81 (p, *J* = 6.6 Hz, 2H, H45), 1.71 (p, *J* = 7.8 Hz, 2H, H47), 1.52 (p, *J* = 7.8 Hz, 2H, H46); ^{13}C NMR (151 MHz, $CDCl_3$) δ 170.95 (C2), 169.34 (C15), 168.58 (C6), 167.58 (C8), 158.7 (C26), 158.3 (C28), 156.7(C40), 148.5 (C21), 146.0 (C9), 136.6 (C31), 136.4 (C11), 133.7 (C25), 133.6 (C34), 132.3 (C14), 132.1 (C43), 129.9 (C32), 129.8 (C24), 127.2 (C36), 124.0 (C35), 123.2 (C33), 122.4 (C41), 121.6 (C20), 116.2 (C12), 114.8 (C42), 112.7 (C10), 110.9 (C13), 68.0 (C44), 49.8 (C18), 49.0 (C5), 42.9 (C17), 31.4 (C3), 29.7 (C38), 29.2 (C45, C47), 29.0 (C45, C47), 25.5 (C46), 25.4 (C48), 22.7 (C4); HRMS (ESI +ve): $C_{39}H_{41}ClN_{11}O_7S$ $[M+H]^+$: 842.2599 (Found: 842.2482).

4-((2-(4-(5-(4-((4-(2-amino-4-methylthiazol-5-yl)pyrimidin-2-yl)amino) phenoxy)pentyl)-1*H*-1,2,3-triazol-1-yl)ethyl)amino)-2-(1-methyl-2,6-dioxopiperidin-3-yl)isoindoline-1,3-dione (84)

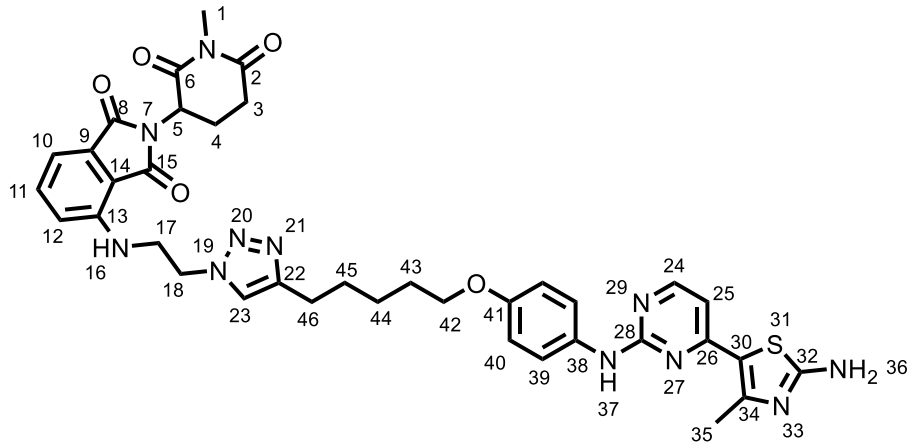

Product was synthesised following **general procedure 5** using 5-[2-(4-hept-6-ynoxyanilino)pyrimidin-4-yl]-4-methyl-thiazol-2-amine (15 mg, 0.04 mmol) and 4-(2-azidoethylamino)-2-(1-methyl-2,6-dioxo-3-piperidyl)isoindoline-1,3-dione (14 mg, 0.04 mmol), affording 3 mg (0.004 mmol, 29%) of the title product. ^{1}H NMR (600 MHz, DMSO) δ 9.22 (s, 1H, H36), 8.30 (s, 1H, H24), 7.88 (s, 1H, H23), 7.63 (d, *J* = 8.6 Hz, 2H, H40), 7.53 (t, *J* = 7.8 Hz, 1H, H11), 7.03 (d, *J* = 7.0 Hz, 1H, H10), 7.00 (d, *J* = 8.6 Hz, 1H, H12), 6.86-6.81 (m, 3H, H39, H25), 6.75 (d, *J* = 6.5 Hz, 1H, H16), 5.11 (dd, *J* = 13.1, 5.5 Hz, 1H, H5), 4.54 (t, *J* = 6.1 Hz, 2H, H18), 3.89 (t, *J* = 6.4 2H, H42), 3.79 (d, *J* = 7.4 Hz, 2H, H17), 3.01 (s, 3H, H1), 2.95 – 2.89 (m, 1H, H3), 2.75 (d, *J* = 16.5 Hz, 1H, H46), 2.60 (t, *J* = 7.4 Hz, 2H, H3, H4), 2.43 (s, 1H, H35), 2.03 (d, *J* = 12.2 Hz, 1H, H4), 1.71 (t, *J* = 7.4 Hz, 2H, H43), 1.60 (t, *J* = 7.7 Hz, 5H, H44, H45), 1.42 (q, *J* = 7.7 Hz, 2H, H44). ^{3}C NMR was attempted but there was too little compound to produce significant signals coupled with poor DMSO solubility of the compound. HRMS (ESI +ve): $C_{37}H_{40}N_{11}O_5S$ $[M+H]^+$: 750.2935 (Found: 750.2940).

1-(4-(non-8-yn-1-yloxy)phenyl)guanidine (141)

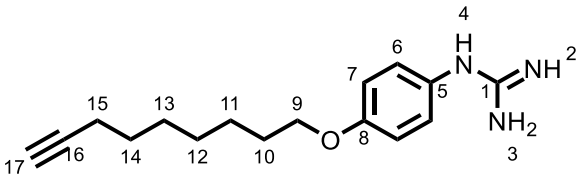

4-non-8-ynoxyaniline (148 mg, 0.64 mmol), cyanamide (81 mg, 1.92 mmol), and HCl in dioxane (0.16 mL, 0.64 mmol) were dissolved in MeCN (1 mL) and heated to 100 °C in the microwave for 6 h. The reaction was concentrated and purified by reverse phase column chromatography (water:MeOH (+0.1% formic acid) 30-80%). The solvent was removed under reduced pressure to yield the title product (300 mg, quantitative, 0.94 mmol). ^{1}H NMR (600 MHz, MeOD) δ 7.21 (d, *J* = 8.9 Hz, 2H, H6), 7.02 (d, *J* = 8.9 Hz, 2H, H7), 4.02 (t, *J* = 6.4 Hz, 2H, H9), 2.25 – 2.10 (m, 3H, H10, H17), 1.86 – 1.73 (m, 2H, H15), 1.61 – 1.34 (m, 8H, H11, H12, H13, H14); ^{13}C NMR (151 MHz, MeOD) δ 160.18 (C1), 158.50 (C8), 128.73 (C5), 128.08 (C6), 116.70 (C7), 85.04 (C16), 69.47 (C17), 69.26 (C9), 30.21 (C12), 29.88 (C13), 29.66 (C14), 29.58 (C10), 26.99 (C11), 18.97 (C15); HRMS (ESI +ve): $C_{16}H_{24}N_3O$ $[M+H]^+$: 274.1914 Found: 274.1909.

9-chloro-7-(2,6-difluorophenyl)-*N*-(4-(non-8-yn-1-yloxy)phenyl)-5*H*-benzo [*c*]pyrimido[4,5-*e*]azepin-2-amine (136)

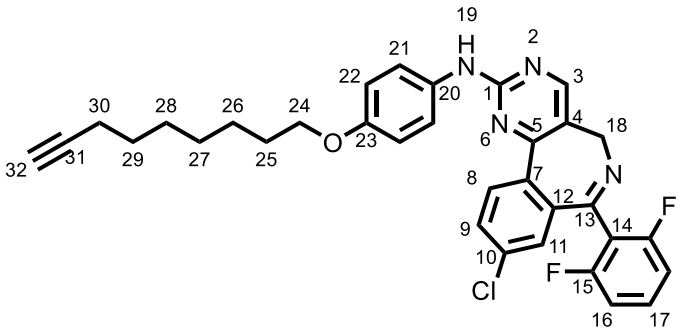

(4*E*)-8-chloro-1-(2,6-difluorophenyl)-4-(dimethylaminomethylene)-3*H*-2-benzazepin-5-one (50 mg, 0.14 mmol) and 1-(4-non-8-ynoxyphenyl)guanidine (50 mg, 0.16 mmol) in MeCN (3 mL) was stirred at 82 °C overnight. NaOH (11 mg, 0.28 mmol) was added and stirred for a further 4 h at 80 °C. The solvent was removed under reduced pressure and the residue was purified by column chromatography (DCM:MeOH 0-10%) to yield the title product (52 mg, 65%, 0.09 mmol). ^{1}H NMR (600 MHz, DMSO) δ 9.66 (s, 1H, H19), 8.60 (s, 1H, H3), 8.25 (d, *J* = 8.5 Hz, 1H, H8), 7.84 (dd, *J* = 8.5, 2.2 Hz, 1H, H9), 7.68 (d, *J* = 9.0 Hz, 2H, H21), 7.54 (tt, *J* = 8.5, 6.5 Hz, 1H, H17), 7.31 (d, *J* = 2.2 Hz, 1H, H11), 7.16 (t, *J* = 8.7 Hz, 2H, H16), 6.89 (d, *J* = 9.1 Hz, 2H, H22), 3.92 (t, *J* = 6.5 Hz, 2H, H24), 2.79 – 2.69 (m, 1H, H32), 2.15 (td, *J* = 7.0, 2.7 Hz, 2H, H30), 1.70 (p, *J* = 6.7 Hz, 2H, H25), 1.51 – 1.26 (m, 8H, H26, H27, H28, H29); ^{13}C NMR (151 MHz, DMSO) δ 160.66 (C5), 159.99 (C1), 159.59 (dd, *J* = 249.0, 6.7 Hz, C15), 157.82 (C13), 157.14 (C3), 153.79 (C23), 136.81 (C10), 135.46 (C7), 134.70 (C12), 133.30 (C20), 131.94 (t, *J* = 10.4 Hz, C17), 131.10 (C8), 130.77 (C9), 127.66 (C11), 122.00 (C4), 120.72 (C21), 117.60 (t, *J* = 19.0 Hz, C14), 114.37 (C22), 112.14 (d, *J* = 21.4 Hz, C16), 84.54 (C31), 71.11 (C32), 67.52 (C24), 49.68 (C18), 28.74 (C25), 28.23 (C27, C28, C29), 28.08 (C27, C28, C29), 27.90 (C27, C28, C29), 25.46 (C26), 17.65 (C30); HRMS (ESI +ve): $C_{33}H_{29}ClF_2N_4O$ $[M+H]^+$: 571.2076 Found: 571.2080.

4-((2-(4-(7-(4-((9-chloro-7-(2,6-difluorophenyl)-5*H*-benzo[c]pyrimido[4,5-*e*]azepin-2-yl)amino) phenoxy)heptyl)-1*H*-1,2,3-triazol-1-yl)ethyl)amino)-2-(2,6-dioxopiperidin-3-yl)isoindoline-1,3-dione (135)

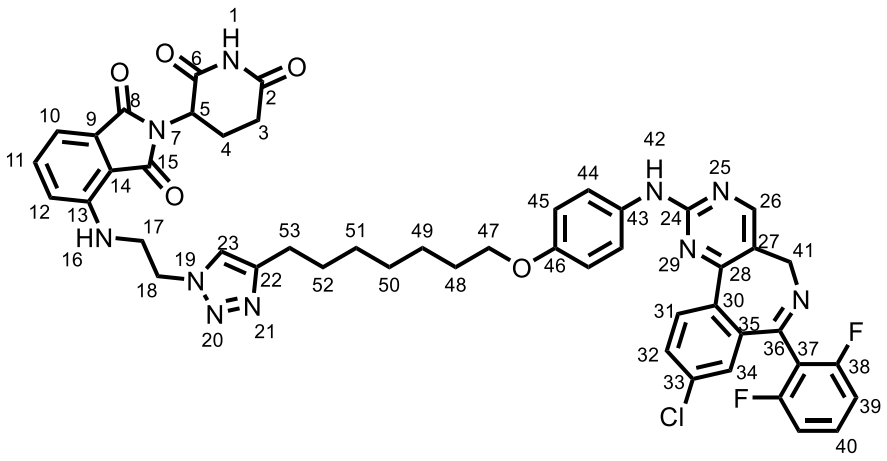

Product was synthesised following **general procedure 5** using 9-chloro -7-(2,6-difluorophenyl)-*N*-(4-non-8-ynoxyphenyl)-5*H*-pyrimido[5,4-*d*][2]benzazepin-2-amine (27 mg, 0.05 mmol) and 4-(2-azidoethylamino)-2-(2,6-dioxo-3-piperidyl) isoindoline-1,3-dione, affording 27 mg (61%, 0.03 mmol) of the title product. ^{1}H NMR (600 MHz, $CDCl_3$) δ 9.31 (s, 1H, H), 8.47 (s, 1H, H26), 8.24 (d, *J* = 8.5 Hz, 1H, H31), 7.61 (d, *J* = 9.0 Hz, 1H, H32), 7.58 (d, *J* = 8.3 Hz, 2H, H44), 7.44 (t, *J* = 8.0 Hz, 1H, H11), 7.35 (t, *J* = 7.5 Hz, 1H, H40), 7.31 – 7.27 (m, 2H, H23, 34), 7.12 (d, *J* = 7.0 Hz, 1H, H12), 6.93 (s, 2H, H39), 6.89 (d, *J* = 8.6 Hz, 2H, H45), 6.67 (d, *J* = 8.9 Hz, 1H, H10), 6.48 (t, *J* = 6.7 Hz, 1H, H16), 4.93 (dd, *J* = 12.2, 5.0 Hz, 1H, H5), 4.53 (t, *J* = 5.2 Hz, 2H, H18), 3.99 – 3.92 (m, 2H, H47), 3.88 – 3.76 (m, 2H, H17), 2.94 – 2.71 (m, 3H, H3, H4), 2.67 (t, *J* = 7.8 Hz, 2H, H53), 2.12 (dd, *J* = 12.0, 5.9 Hz, 1H, H4), 1.76 (t, *J* = 7.2 Hz, 2H, H48), 1.65 – 1.57 (m, 2H, H52), 1.44 (t, *J* = 7.4 Hz, 2H, H49), 1.42 – 1.31 (m, 4H, H50, H51); ^{13}C NMR (151 MHz, $CDCl_3$) δ 171.61 (C2), 169.47 (C8), 168.92 (C6), 167.46 (C15), 161.89 (C28), 160.47 (dd, *J* = 251.7, 6.5 Hz, C38), 160.18 (C24), 159.42 (C36), 156.84 (C26), 155.10 (C46), 148.82 (C22), 146.18 (C13), 137.12 (C35), 136.48 (C11), 136.04 (C33), 135.65 (C30), 132.61 (C9), 132.58 (C43), 131.25 (t, *J* = 10.1 Hz, C40), 131.05 (C31), 130.86 (C32), 128.61 (C34), 122.37 (C27), 121.84 (C23), 121.55 (C44), 118.15 (t, *J* = 18.6 Hz, C37), 116.22 (C10), 115.00 (C45), 112.63 (C12), 111.99 (dd, *J* = 21.6, 3.5 Hz, C39), 110.92 (C14), 68.36 (C47), 49.87 (C18), 49.08 (C5), 43.01 (C17), 31.53 (C3), 29.38 (C52), 29.27 (C48), 29.08 (C50), 29.06 (C51), 25.96 (C50), 25.57 (C53), 22.87 (C4), C and H 41 not observed; HRMS (ESI +ve): $C_{48}H_{43}ClF_2N_{10}O_5$ $[M+H]^+$: 913.3152 Found: 913.3126.

4-methyl-5-(2-((4-(non-8-yn-1-yloxy)phenyl)amino)pyrimidin-4-yl)thiazol-2-amine (143)

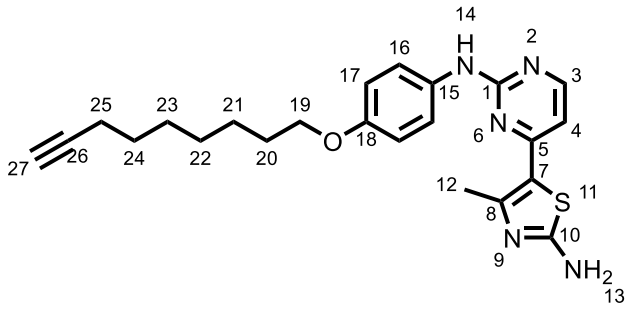

N'-[5-[(*E*)-3-(dimethylamino)prop-2-enoyl]-4-methyl-thiazol-2-yl]-*N*,*N*-dimethyl-formamidine (55 mg, 0.21 mmol), 1-(4-non-8-ynoxyphenyl)guanidine (80 mg, 0.25 mmol) and NaOH (16 mg, 0.41 mmol) were dissolved in 2-methoxyethanol (1.5 mL) and heated to 180 °C under microwave irradiation for 3 h. solvent was removed in vacuo and crude product was purified using column chromatography (DCM:MeOH 0-10%) affording the title compound (41 mg, 47%, 0.1 mmol). ^{1}H NMR (600 MHz, DMSO) δ 9.22 (s, 1H, H14), 8.28 (d, *J* = 5.4 Hz, 1H, 3), 7.66 – 7.60 (m, 2H, H16), 7.47 (s, 2H, H13), 6.87 – 6.79 (m, 3H, H4, H17), 3.92 (t, *J* = 6.5 Hz, 2H, H19), 2.74 (t, *J* = 2.6 Hz, 1H, H27), 2.43 (s, 3H, H12), 2.16 (td, *J* = 7.0, 2.7 Hz, 2H, H25), 1.70 (p, *J* = 6.7 Hz, 2H, H20), 1.50 – 1.30 (m, 6H, H21, H22, H23); ^{13}C NMR (151 MHz, DMSO) δ 169.19 (C10), 160.06 (C1), 159.11 (C5), 158.05 (C3), 153.91 (C18), 152.24 (C8), 134.16 (C15), 120.94 (C16), 118.61 (C7), 114.66 (C17), 106.85 (C4), 85.03 (C26), 71.62 (C27), 67.99 (C19), 29.23 (C20), 28.70 (C21, C22, C23, C24), 28.55 (C21, C22, C23, C24), 28.37 (C21, C22, C23, C24), 25.93 (C21, C22, C23, C24), 18.88 (C12), 18.11 (C25); HRMS (ESI +ve): $C_{23}H_{28}N_5OS$ $[M+H]^+$: 422.2009 Found: 422.2012.

4-((2-(4-(7-(4-((4-(2-amino-4-methylthiazol-5-yl)pyrimidin-2-yl)amino) phenoxy)heptyl)-1*H*-1,2,3-triazol-1-yl)ethyl)amino)-2-(2,6-dioxopiperidin-3-yl)isoindoline-1,3-dione (134)

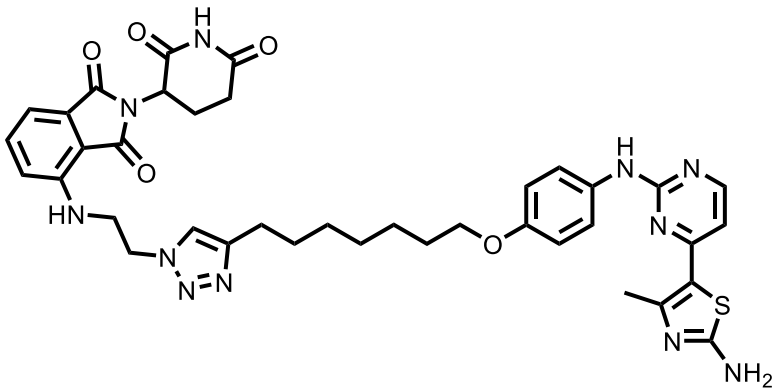

Product was synthesised following **general procedure 5** using 4-methyl-5-[2-(4-non-8-ynoxyanilino)pyrimidin-4-yl]thiazol-2-amine (21 mg, 0.05 mmol) and 4-(2-azidoethylamino)-2-(2,6-dioxo-3-piperidyl) isoindoline-1,3-dione, affording 20 mg (53%, 0.03 mmol) of the title product. Product insoluble in DMSO so NMR was not taken. HRMS (ESI +ve): $C_{38}H_{42}N_{11}O_5S$ $[M+H]^+$: 764.3091 Found: 764.3097.

2-(2,6-dioxopiperidin-3-yl)-4-((2-(4-(5-hydroxypentyl)-1H-1,2,3-triazol-1-yl) ethyl)amino)isoindoline-1,3-dione (137)

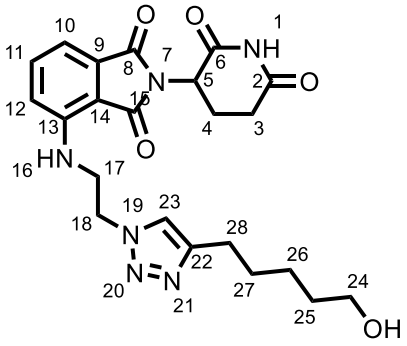

A solution of 4-((2-azidoethyl)amino)-2-(2,6-dioxopiperidin-3-yl)isoindoline-1,3-dione (6 mg, 0.02 mmol), hept-6-yn-1-ol (2 uL, 0.02 mmol) , TBTA (0.9 mg, 0.002 mmol), $CuSO_4$ (0.4 mg, 0.0018 mmol) and sodium ascorbate (3 mg, 0.02 mmol) in water (0.3 mL) and THF (0.434 mL) was stirred at rt. Water (5 mL) was added and was extracted with DCM (3 times). The organic layers were combined, washed with brine, dried, and solvent was removed in *vacuo*. Crude product was purified by reverse phase chromatography (MeOH:water 5-70%) to afford the title product (6 mg, 75%, 0.01 mmol). ^{1}H NMR (600 MHz, $CDCl_3$) δ 8.60 (s, 1H, H1), 7.48 (t, *J* = 7.8 Hz, 1H, H1, H11), 7.32 (s, 1H, H23), 7.15 (d, *J*

= 7.1 Hz, 1H, H10), 6.73 (d, *J* = 8.5 Hz, 1H, H12), 6.43 (t, *J* = 6.6 Hz, 1H, H16), 4.94 (dd, *J* = 12.2, 5.4 Hz, 1H, H5), 4.57 (q, *J* = 5.2 Hz, 2H, H18), 3.86 (h, *J* = 6.5, 5.8 Hz, 2H, H17), 3.64 (t, *J* = 6.5 Hz, 2H, H28), 2.95 – 2.66 (m, 4H, H4, 24), 2.12, 2.18(m, 1H, H4), 1.79 – 1.32 (m, 6H, H25, 26, 27); ^{13}C NMR (151 MHz, $CDCl_3$) δ 171.20 (C2), 169.37 (C15), 168.50 (C6), 167.36 (C8), 148.19 (C22), 145.95 (C9), 136.42 (C11), 132.55 (C14), 122.38 (C23), 116.13 (C12), 112.62 (C10), 110.69 (C13), 68.34 (C28), 49.67 (C18), 49.01 (C5), 42.80 (C17), 31.44 (C3), 28.92 (C25), 25.38 (C24), 25.06 (C27), 22.76 (C4), 19.16 (C26); m/z $C_{22}H_{27}N_6O_5$ $[M+H]^+$: 455.2037 (Found: 455.2058)

4-((2-(4-(7-(4-((8-chloropyrido[3,4-*d*]pyrimidin-2-yl)amino)phenoxy) heptyl)-1*H*-1,2,3-triazol-1-yl)ethyl)amino)-2-(2,6-dioxopiperidin-3-yl) isoindoline-1,3-dione (138)

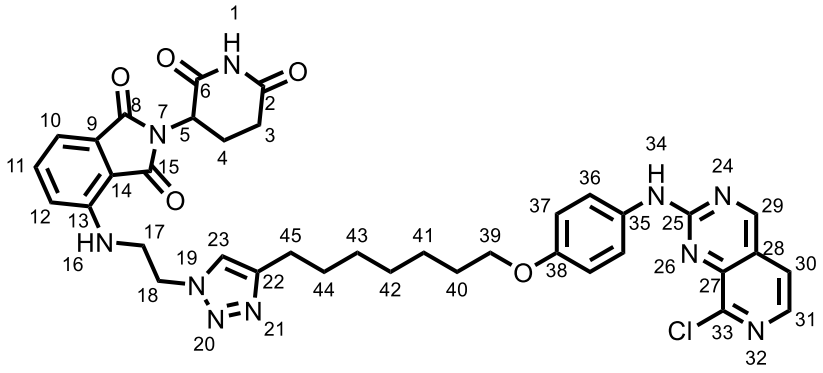

A solution of 8-chloro-2-methylsulfonyl-pyrido[3,4-*d*]pyrimidine (14 mg, 0.06 mmol) and sodium hydride (2 mg, 0.06 mmol) in THF (0.5 mL) was cooled to 0 °C. *N*-(4-non-8-ynoxyphenyl)formamide (15 mg, 0.06 mmol) was added and the reaction was allowed to warm to rt. The reaction was stirred at rt overnight. The reaction was quenched with water (15 mL) and was extracted with DCM. The organic layers were combined, washed with brine, and solvent was removed in *vacuo*. Crude product was dissolved in MeOH and 3 drops of formic acid were added. This was passed through an SCX-2 cartridge and washed with MeOH. Product was eluted with 3.5 M ammonia in MeOH and solvent was removed in *vacuo* to afford crude title product that was used in the next step without further purification. Mass of product was observed ($[M+H]^+$ 395.15) with a retention time of 1.65 min. Product was synthesised following **general procedure 5** using crude 8-chloro-*N*-(4-non-8-ynoxyphenyl)pyrido[3,4-*d*]pyrimidin-2-amine (12.50 mg, 0.0317 mmol) and 4-(2-azidoethylamino)-2-(2,6-dioxo-3-piperidyl)

isoindoline-1,3-dione, affording 8.5 mg (36%, 0.0115 mmol) of the title product. ^{1}H NMR (600 MHz, DMSO) δ 11.10 (s, 1H, H1), 10.32 (s, 1H, H34), 9.44 (s, 1H, H29), 8.21 (d, *J* = 5.2 Hz, 1H, H30), 8.01 (s, 2H, H36), 7.86 (s, 1H, H23), 7.83 (d, *J* = 5.2 Hz, 1H, H31), 7.52 (dd, *J* = 8.6, 7.1 Hz, 1H, H11), 7.03 (d, *J* = 7.0 Hz, 1H, H10), 6.98 (d, *J* = 8.6 Hz, 1H, H12), 6.95 (d, *J* = 9.1 Hz, 2H, H37), 6.76 (t, *J* = 6.4 Hz, 1H, H16), 5.05 (dd, *J* = 12.9, 5.4 Hz, 1H, H5), 4.54 (t, *J* = 6.0 Hz, 2H, H18), 3.95 (t, *J* = 6.5 Hz, 2H, H39), 3.79 (q, *J* = 6.2 Hz, 2H, H17), 2.88 (ddd, *J* = 17.1, 13.9, 5.5 Hz, 1H, H3), 2.64 – 2.55 (m, 4H, H3, 4), 2.53 (s, 2H, H45), 2.02 (dtd, *J* = 12.7, 5.2, 2.2 Hz, 1H, H4), 1.75 – 1.65 (m, 2H, H40), 1.54 (p, *J* = 7.5 Hz, 2H, H44), 1.46 – 1.21 (m, 6H, H41, 42, 43); ^{13}C NMR (151 MHz, DMSO) δ 172.78 (C2), 170.03 (C6), 168.65 (C15), 167.21 (C8), 162.68 (C29), 157.67 (C25), 154.27 (C38), 148.02 (C33), 146.96 (C22), 145.94 (C13), 143.14 (C27), 139.42 (C31), 136.17 (C11), 132.76 (C35), 132.14 (C9), 124.15 (C28), 122.28 (C23), 120.55 (C36), 120.04 (C30), 116.98 (C12), 114.43 (C37), 110.92 (C10), 109.49 (C14), 67.57 (C39), 48.73 (C18), 48.55 (C5), 42.12 (C17), 30.97 (C3), 28.92 (C44), 28.76 (C40), 28.53 (C43), 28.47 (C42), 25.47 (C41), 24.93 (C45), 22.14 (C4); HRMS (ESI +ve): $C_{37}H_3ClN_{10}O_5$ $[M+H]^+$: 737.2715 Found: 737.2725.

N-(4-(non-8-yn-1-yloxy)phenyl)quinazolin-2-amine (148)

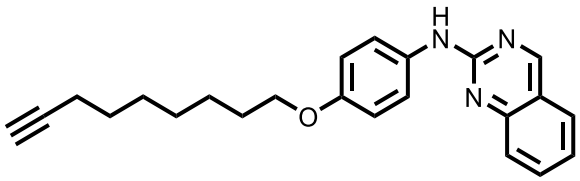

4-non-8-ynoxyaniline (210 mg, 0.91 mmol), 2-chloroquinazoline (115 mg, 0.70 mmol), XPhos (33 mg, 0.07 mmol) , Cs_2CO_3 (683 mg, 2.10 mmol) were dissolved in DMF (1.6 mL) and degassed. $Pd_2(DBA)_3$ (32 mg, 0.03 mmol) was added and degassed again. The solution was placed under nitrogen and heated to 90 °C under microwave irradiation for 30 mins. The mixture was purified using column chromatography (EtOAc:c-hex 0-100%) affording crude title that was used without further purification. Mass of product was observed ($[M+H]^+$ 360.21) with a retention time of 1.61 min.

2-(2,6-dioxopiperidin-3-yl)-4-((2-(4-(7-(4-(quinazolin-2-ylamino)phenoxy) heptyl)-1*H*-1,2,3-triazol-1-yl)ethyl)amino)isoindoline-1,3-dione (139)

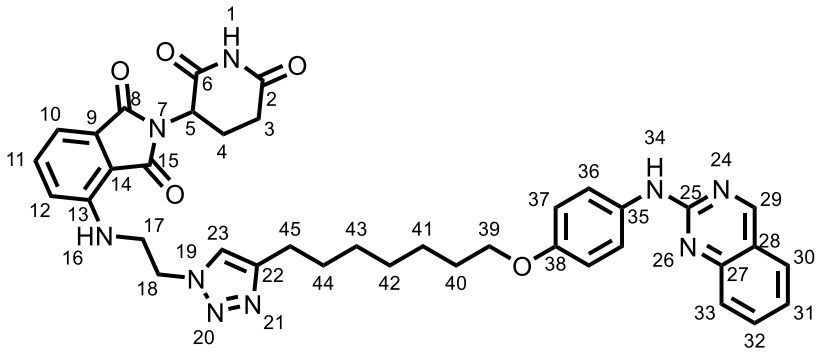

Product was synthesised following **general procedure 5** using N-(4-non-8-ynoxyphenyl)quinazolin-2-amine (17 mg, 0.05 mmol) and 4-(2-azidoethylamino)-2-(2,6-dioxo-3-piperidyl) isoindoline-1,3-dione, affording 10 mg (30%, 0.01 mmol) of the title product. ^{1}H NMR (600 MHz, DMSO) δ 9.67 (s, 1H, H34), 9.26 (s, 1H, H29), 7.90 – 7.81 (m, 4H, H23, H33, H37), 7.77 (ddd, *J* = 8.3, 6.8, 1.4 Hz, 1H, H31), 7.60 (d, *J* = 8.5 Hz, 1H, H30), 7.56 – 7.44 (m, 1H, H11), 7.34 (t, *J* = 7.5 Hz, 1H, H32), 7.11 – 7.01 (m, 1H, H10), 6.98 (d, *J* = 8.6 Hz, 1H, H12), 6.95 – 6.88 (m, 2H, H36), 6.75 (t, *J* = 6.5 Hz, 1H, H16), 5.05 (dd, *J* = 12.9, 5.5 Hz, 1H, H5), 4.54 (t, *J* = 6.0 Hz, 2H, H18), 3.98 – 3.87 (m, 2H, H39), 3.79 (q, *J* = 6.2 Hz, 2H, H17), 2.88 (ddd, *J* = 17.0, 13.6, 5.5 Hz, 1H, H3), 2.60 – 2.45 (m, 4H, H3, H4, H45), 2.01 (ddd, *J* = 10.1, 5.7, 3.0 Hz, 1H, H4), 1.69 (p, *J* = 6.7 Hz, 2H, H40), 1.41 – 1.27 (m, 8H, H41, H42, H43, H44); ^{13}C NMR (151 MHz, DMSO) δ 173.26 (C2), 170.50 (C6), 169.12 (C8), 167.69 (C15), 162.53 (C29), 157.51 (C25), 154.16 (C38), 151.37 (C27), 146.41 (C13), 145.73 (C22), 136.65 (C11), 134.86 (C31), 134.08 (C35), 132.61 (C9), 128.38 (C33), 125.76 (C30), 123.51 (C32), 122.76 (C23), 120.82 (C37), 117.45 (C12), 114.82 (C36), 111.41 (C10), 109.95 (C14), 68.02 (C39), 49.20 (C5), 49.06 (C18), 42.58 (C17), 31.43 (C3), 29.39 (C40, C41, C42, C43, C44), 29.25 (C40, C41, C42, C43, C44), 29.01 (C40, C41, C42, C43, C44), 28.93 (C40, C41, C42, C43, C44), 25.95 (C40, C41, C42, C43, C44), 25.39 (C45), 22.61 (C4); HRMS (ESI +ve): $C_{38}H_{40}N_9O_5$ $[M+H]^+$: 702.3152 Found: 702.2938.

N-(4-(non-8-yn-1-yloxy)phenyl)pyrimidin-2-amine (146)

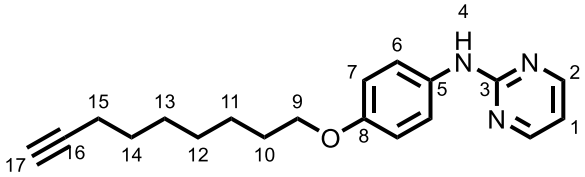

A solution of 2-(methylsulphonyl)pyrimidine (16 mg, 0.10 mmol) and sodium hydride (4 mg, 0.10 mmol) in THF (0.9 mL) was cooled to 0 °C. *N*-(4-non-8-ynoxyphenyl)formamide (26 mg, 0.10 mmol) was added and the reaction was allowed to warm to rt. The reaction was stirred at rt overnight. The reaction was quenched with water and was extracted with DCM. The organic layers were combined, washed with brine, and solvent was removed in *vacuo*. Crude product was dissolved in MeOH and 3 drops of formic acid were added. This was passed through an SCX-2 cartridge and washed with MeOH. Product was eluted with 3.5 M ammonia in MeOH and solvent was removed in vacuo to afford the title product (8 mg, 26%, 0.03 mmol). ^{1}H NMR (600 MHz, $CDCl_3$) δ 8.41 – 8.37 (m, 2H, H2), 7.50 – 7.45 (m, 2H, H6), 7.06 (s, 1H, H4), 6.94 – 6.89 (m, 2H, H7), 6.68 (t, *J* = 4.8 Hz, 1H, H1), 3.97 (td, *J* = 6.6, 1.6 Hz, 2H, H9), 2.22 (tt, *J* = 7.1, 2.1 Hz, 2H, H15), 1.96 (t, *J* = 2.6 Hz, 1H, H17), 1.84 – 1.75 (m, 2H, H10), 1.56 (dd, *J* = 8.3, 6.6 Hz, 2H, H14), 1.52 – 1.36 (m, 6H, H11, H12, H13); ^{13}C NMR (151 MHz, $CDCl_3$) δ 160.65 (C3), 158.07 (C2), 155.37 (C8), 132.10 (C5), 122.22 (C6), 114.93 (C7), 112.04 (C1), 84.70 (C16), 68.27 (C17), 68.16 (C9), 29.26 (C10), 28.87 (C11, C12, C13), 28.66(C11, C12, C13), 28.40 (C14), 25.94(C11, C12, C13), 18.39 (C15); HRMS (ESI +ve): $C_{19}H_{24}N_3O$ $[M+H]^+$: 310.1919 Found: 310.1915.

2-(2,6-dioxopiperidin-3-yl)-4-((2-(4-(7-(4-(pyrimidin-2-ylamino)phenoxy) heptyl)-1*H*-1,2,3-triazol-1-yl)ethyl)amino)isoindoline-1,3-dione (140)

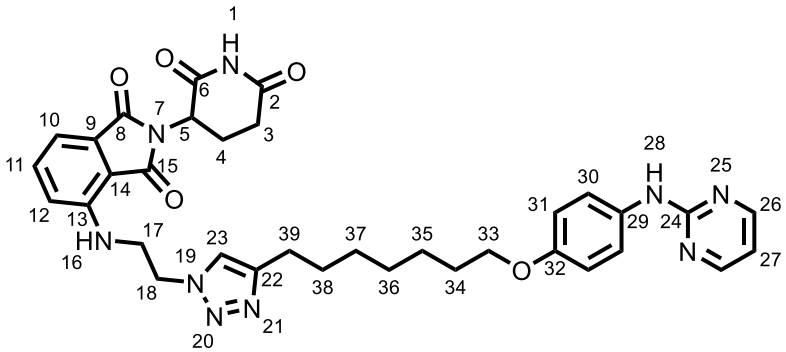

Product was synthesised following **general procedure 5** using *N*-(4-non-8-ynoxyphenyl)pyrimidin-2-amine (8 mg, 0.03 mmol) and 4-(2-azidoethylamino)-2-(2,6-dioxo-3-piperidyl) isoindoline-1,3-dione, affording 6 mg (36%, 0.01 mmol) of the title product. ^{1}H NMR (600 MHz, DMSO) δ 11.10 (s, 1H, H1), 9.38 (s, 1H, H28), 8.41 (d, *J* = 4.8 Hz, 2H, H26), 7.86 (s, 1H, H23), 7.63 – 7.57 (m, 2H, H30),

7.52 (dd, *J* = 8.6, 7.1 Hz, 1H, H11), 7.03 (d, *J* = 7.0 Hz, 1H, H10), 6.98 (d, *J* = 8.6 Hz, 1H, H12), 6.88 – 6.82 (m, 2H, H31), 6.76 (t, *J* = 4.8 Hz, 1H, H27), 5.05 (dd, *J* = 12.9, 5.5 Hz, 1H, H5), 4.53 (t, *J* = 6.0 Hz, 2H, H18), 3.90 (t, *J* = 6.5 Hz, 2H, H33), 3.79 (q, *J* = 6.2, 5.8 Hz, 2H, H17), 2.92 – 2.83 (m, 1H, H3), 2.59 – 2.46 (m, 4H, H3, H4, H39), 2.02 (dtd, *J* = 13.0, 5.4, 2.3 Hz, 1H, H4), 1.72 – 1.61 (m, 2H, H34), 1.54 (p, *J* = 7.4 Hz, 2H, H38), 1.39 – 1.26 (m, 6H, H17, H18, H19); ^{13}C NMR (151 MHz, DMSO) δ 173.26 (C2), 170.50 (C6), 169.12 (C15), 167.69 (C8), 160.64 (C24), 158.40 (C26), 154.10 (C32), 147.43 (C22), 146.31 (C13), 136.65 (C9), 133.91 (C29), 132.61 (C11), 122.75 (C23), 121.12 (C30), 117.45 (C12), 114.74 (C31), 112.22 (C27), 111.40 (C10), 109.94 (C14), 68.00 (C33), 49.20 (C5), 49.01 (C18), 42.54 (C17), 31.43 (C3), 29.39 (C34, C35, C36, C37, C38), 29.24 (C34, C35, C36, C37, C38), 29.01 (C34, C35, C36, C37, C38), 28.92 (C34, C35, C36, C37, C38), 25.94 (C34, C35, C36, C37, C38), 25.39 (C39), 22.61 (C4); HRMS (ESI +ve): $C_{34}H_{38}N_9O_5$ $[M+H]^+$: 652.2996 Found: 652.2767.

Chapter 7: References

1 A. C. Lai and C. M. Crews, *Nat. Rev. Drug Discov.*, 2017, 16, 101.

2 R. Chopra, A. Sadok and I. Collins, *Drug Discov. Today Technol.*, 2019, **31**, 5.

3 D. P. Bondeson, A. Mares, I. E. D. Smith, E. Ko, S. Campos, A. H. Miah, K. E. Mulholland, N. Routly, D. L. Buckley, J. L. Gustafson, N. Zinn, P. Grandi, S. Shimamura, G. Bergamini, M. Faelth-Savitski, M. Bantscheff, C. Cox, D. A. Gordon, R. R. Willard, J. J. Flanagan, L. N. Casillas, B. J. Votta, W. den Besten, K. Famm, L. Kruidenier, P. S. Carter, J. D. Harling, I. Churcher and C. M. Crews, *Nat. Chem. Biol.*, 2015, **11**, 611.

4 S. An and L. Fu, *EBioMedicine*, 2018, 36, 553.

5 S. H. Lecker, A. L. Goldberg and W. E. Mitch, *J Am Soc Nephrol*, 2006, **17**, 1807.

6 X. Huang, S. Wei, S. Ni, Y. Huang and Q. Qin, *Front. Microbiol.*, 2018, **9**, 2798.

7 M. A. Mansour, *Int. J. Biochem. Cell Biol.*, 2018, 80.

8 S. Vijay-kumar, C. E. Bugg and W. J. Cook, *J. Mol. Biol.*, 1987, **194**, 531.

9 L. Buetow and D. T. Huang, *Nat. Rev. Mol. Cell Biol.*, 2016, **17**, 626.

10 E. S. Fischer, K. Böhm, J. R. Lydeard, H. Yang, M. B. Stadler, S. Cavadini, J. Nagel, F. Serluca, V. Acker, G. M. Lingaraju, R. B. Tichkule, M. Schebesta, W. C. Forrester, M. Schirle, U. Hassiepen, J. Ottl, M. Hild, R. E. J. J. Beckwith, J. W. Harper, J. L. Jenkins and N. H. Thomä, 2014, **512**, 49.

11 G. Xu, X. Jiang and S. R. Jaffrey, *J. Biol. Chem.*, 2013, **288**, 29573.

12 T. Van Nguyen, J. Li, C.-C. (Jean) Lu, J. L. Mamrosh, G. Lu, B. E. Cathers and R. J. Deshaies, *Proc. Natl. Acad. Sci.*, 2017, **114**, 3565.

13 Y.-A. Chen, Y.-J. Peng, M.-C. Hu, J.-J. Huang, Y.-C. Chien, J.-T. Wu, T.-Y. Chen and C.-Y. Tang, *Sci. Rep.*, 2015, **5**, 10667.

14 Q. Yang, J. Zhao, D. Chen and Y. Wang, *Mol. Biomed. 2021 21*, 2021, **2**,

1.

15 S. Coomar and D. Gillingham, *bioRxiv*, 2019, 542506.

16 X. Zhang, V. M. Crowley, T. G. Wucherpfennig, M. M. Dix and B. F. Cravatt, *Nat. Chem. Biol.*, 2019, **15**, 737.

17 C. C. Ward, J. I. Kleinman, S. M. Brittain, P. S. Lee, C. Y. S. Chung, K. Kim, Y. Petri, J. R. Thomas, J. A. Tallarico, J. M. McKenna, M. Schirle and D. K. Nomura, *ACS Chem. Biol.*, 2019, **14**, 2430.

18 K. M. Sakamoto, K. B. Kim, R. Verma, A. Ransick, B. Stein, C. M. Crews and R. J. Deshaies, *Mol. Cell. Proteomics*, 2003, **2**, 1350.

19 M. Schapira, M. F. Calabrese, A. N. Bullock and C. M. Crews, *Nat. Rev. Drug Discov.*, 2019, **18**, 949.

20 G. Rabut and M. Peter, *EMBO Rep.*, 2008, 9, 969.

21 D. M. Duda, L. A. Borg, D. C. Scott, H. W. Hunt, M. Hammel and B. A. Schulman, *Cell*, 2008, **134**, 995.

22 N. W. Pierce, J. E. Lee, X. Liu, M. J. Sweredoski, R. L. J. Graham, E. A. Larimore, M. Rome, N. Zheng, B. E. Clurman, S. Hess, S. Shan and R. J. Deshaies, *Cell*, 2013, **153**, 206.

23 J. Merlet, J. Burger, J.-E. Gomes and L. Pintard, *Cell. Mol. Life Sci.*, 2009, **66**, 1924.

24 E. D. Emberley, R. Mosadeghi and R. J. Deshaies, *J. Biol. Chem.*, 2012, **287**, 29679.

25 R. Mosadeghi, K. M. Reichermeier, M. Winkler, A. Schreiber, J. M. Reitsma, Y. Zhang, F. Stengel, J. Cao, M. Kim, M. J. Sweredoski, S. Hess, A. Leitner, R. Aebersold, M. Peter, R. J. Deshaies and R. I. Enchev, *Elife*, , DOI:10.7554/eLife.12102.

26 S. Cavadini, E. S. Fischer, R. D. Bunker, A. Potenza, G. M. Lingaraju, K. N. Goldie, W. I. Mohamed, M. Faty, G. Petzold, R. E. J. Beckwith, R. B. Tichkule, U. Hassiepen, W. Abdulrahman, R. S. Pantelic, S. Matsumoto, K. Sugasawa, H. Stahlberg and N. H. Thomä, *Nature*, 2016, **531**, 598.

27 A. Matouschek, M. Iwakura, S. Prakash, C. Lee and M. P. Schwartz, *Mol. Cell*, 2004, **7**, 627.

28 R. van der Lee, B. Lang, K. Kruse, J. Gsponer, N. S. de Groot, M. A. Huynen, A. Matouschek, M. Fuxreiter and M. M. Babu, *Cell Rep.*, 2014, **8**, 1832.

29 M. R. Q. Deveraux, V. Ustrell, C. Pickart, *J. Biol. Chem.*, 1994, **269**, 7059.

30 X.-B. Qiu, S.-Y. Ouyang, C.-J. Li, S. Miao, L. Wang and A. L. Goldberg, *EMBO J.*, 2006, **25**, 5742.

31 K. Husnjak, S. Elsasser, N. Zhang, X. Chen, L. Randles, Y. Shi, K. Hofmann, K. J. Walters, D. Finley and I. Dikic, *Nature*, 2008, **453**, 481.

32 Y. Shi, X. Chen, S. Elsasser, B. B. Stocks, G. Tian, B. H. Lee, Y. Shi, N. Zhang, S. A. H. De Poot, F. Tuebing, S. Sun, J. Vannoy, S. G. Tarasov, J. R. Engen, D. Finley and K. J. Walters, *Science (80-.).*, 2016, **351**, 831.

33 K. Paraskevopoulos, F. Kriegenburg, M. H. Tatham, H. I. Rösner, B. Medina, I. B. Larsen, R. Brandstrup, K. G. Hardwick, R. T. Hay, B. B. Kragelund, R. Hartmann-Petersen and C. Gordon, *Mol. Cell*, 2014, **56**, 453.

34 A. Peth, T. Uchiki and A. L. Goldberg, *Mol. Cell*, 2010, **40**, 671.

35 R. Verma, L. Aravind, R. Oania, W. H. McDonald, J. R. Yates, E. V Koonin and R. J. Deshaies, *Science (80-.).*, 2002, **298**, 611.

36 A. Borodovsky, B. M. Kessler, R. Casagrande, H. S. Overkleeft, K. D. Wilkinson and H. L. Ploegh, *EMBO J.*, 2001, **20**, 5187.

37 M. Stone, R. Hartmann-Petersen, M. Seeger, D. Bech-Otschir, M. Wallace and C. Gordon, *J. Mol. Biol.*, 2004, **344**, 697.

38 N. V. Dimova, N. A. Hathaway, B. H. Lee, D. S. Kirkpatrick, M. L. Berkowitz, S. P. Gygi, D. Finley and R. W. King, *Nat. Cell Biol.*, 2012, **14**, 168.

39 O. Braten, I. Livneh, T. Ziv, A. Admon, I. Kehat, L. H. Caspi, H. Gonen, B. Bercovich, A. Godzik, S. Jahandideh, L. Jaroszewski, T. Sommer, Y. T. Kwon, M. Guharoy, P. Tompa and A. Ciechanover, *Proc. Natl. Acad. Sci.*,

2016, **113**, 4639.

40 K. M. Sakamoto, K. B. Kim, A. Kumagai, F. Mercurio, C. M. Crews and R. J. Deshaies, *Proc. Natl. Acad. Sci.*, 2001, **98**, 8554.

41 W. C. Hon, M. I. Wilson, K. Harlos, T. D. W. Claridge, C. J. Schofield, C. W. Pugh, P. H. Maxwell, P. J. Ratcliffe, D. I. Stuart and E. Y. Jones, *Nature*, 2002, **417**, 975.

42 C. E. Stebbins, W. G. Kaelin and N. P. Pavletich, *Science (80-.).*, 1999, **284**, 455.

43 J. S. Schneekloth, F. N. Fonseca, M. Koldobskiy, A. Mandal, R. Deshaies, K. Sakamoto and C. M. Crews, *J. Am. Chem. Soc.*, 2004, **126**, 3748.

44 D. Zhang, S. H. Baek, A. Ho and K. Kim, *Bioorganic Med. Chem. Lett.*, 2004, **14**, 645.

45 H. Lee, D. Puppala, E.-Y. Choi, H. Swanson and K.-B. Kim, *ChemBioChem*, 2007, **8**, 2058.

46 A. Rodriguez-Gonzalez, K. Cyrus, M. Salcius, K. Kim, C. M. Crews, R. J. Deshaies and K. M. Sakamoto, *Oncogene*, 2008, **27**, 7201.

47 K. Cyrus, M. Wehenkel, E. Y. Choi, H. Lee, H. Swanson and K. B. Kim, *ChemMedChem*, 2010, **5**, 979.

48 J. Hines, J. D. Gough, T. W. Corson and C. M. Crews, *Proc. Natl. Acad. Sci. U. S. A.*, 2013, **110**, 8942.

49 L. Zhang, B. Riley-Gillis, P. Vijay and Y. Shen, *Mol. Cancer Ther.*, 2019, **18**, 1302–1311.

50 T. Ito, H. Ando, T. Suzuki, T. Ogura, K. Hotta, Y. Imamura, Y. Yamaguchi and H. Handa, *Science (80-.).*, 2010, **327**, 1345.

51 D. L. Buckley, I. Van Molle, P. C. Gareiss, H. S. Tae, J. Michel, D. J. Noblin, W. L. Jorgensen, A. Ciulli and C. M. Crews, *J. Am. Chem. Soc.*, 2012, **134**, 4465.

52 N. Blaquiere, E. Villemure and S. T. Staben, *J. Med. Chem.*, 2020, 63, 7957.

53 L. T. Vassilev, B. T. Vu, B. Graves, D. Carvajal, F. Podlaski, Z. Filipovic, N. Kong, U. Kammlott, C. Lukacs, C. Klein, N. Fotouhi and E. A. Liu, *Science (80-.).*, 2004, **303**, 844.

54 A. R. Smith, M. Pucheault, H. S. Tae and C. M. Crews, *Bioorganic Med. Chem. Lett.*, 2008, **18**, 5904.

55 J. Hines, S. Lartigue, H. Dong, Y. Qian and C. M. Crews, *Cancer Res.*, 2019, **79**, 251.

56 Y. Li, J. Yang, A. Aguilar, D. McEachern, S. Przybranowski, L. Liu, C. Y. Yang, M. Wang, X. Han and S. Wang, *J. Med. Chem.*, 2019, **62**, 448.

57 C. Galdeano, M. S. Gadd, P. Soares, S. Scaffidi, I. Van Molle, I. Birced, S. Hewitt, D. M. Dias and A. Ciulli, *J. Med. Chem.*, 2014, **57**, 8657.

58 M. S. Gadd, A. Testa, X. Lucas, K.-H. Chan, W. Chen, D. J. Lamont, M. Zengerle and A. Ciulli, *Nat. Chem. Biol.*, 2017, **13**, 514.

59 M. Zengerle, K.-H. Chan and A. Ciulli, *ACS Chem. Biol*, 2015, **10**, 1770.

60 L. N. Gechijian, D. L. Buckley, M. A. Lawlor, J. M. Reyes, J. Paulk, C. J. Ott, G. E. Winter, M. A. Erb, T. G. Scott, M. Xu, H. S. Seo, S. Dhe-Paganon, N. P. Kwiatkowski, J. A. Perry, J. Qi, N. S. Gray and J. E. Bradner, *Nat. Chem. Biol.*, 2018, **14**, 405.

61 G. M. Burslem, B. E. Smith, A. C. Lai, S. Jaime-Figueroa, D. C. McQuaid, D. P. Bondeson, M. Toure, H. Dong, Y. Qian, J. Wang, A. P. Crew, J. Hines and C. M. Crews, *Cell Chem. Biol.*, 2018, **25**, 67.

62 J. A. Engelman, K. Zejnullahu, T. Mitsudomi, Y. Song, C. Hyland, O. P. Joon, N. Lindeman, C. M. Gale, X. Zhao, J. Christensen, T. Kosaka, A. J. Holmes, A. M. Rogers, F. Cappuzzo, T. Mok, C. Lee, B. E. Johnson, L. C. Cantley and P. A. Jänne, *Science (80-.).*, 2007, **316**, 1039.

63 B. E. Smith, S. L. Wang, S. Jaime-Figueroa, A. Harbin, J. Wang, B. D. Hamman and C. M. Crews, *Nat. Commun.*, , DOI:10.1038/s41467-018-08027-7.

64 R. P. Nowak, S. L. Deangelo, D. Buckley, Z. He, K. A. Donovan, J. An, N. Safaee, M. P. Jedrychowski, C. M. Ponthier, M. Ishoey, T. Zhang, J. D.

Mancias, N. S. Gray, J. E. Bradner and E. S. Fischer, *Nat. Chem. Biol.*, 2018, **14**, 706.

65 X. Han, L. Zhao, W. Xiang, C. Qin, B. Miao, T. Xu, M. Wang, C. Y. Yang, K. Chinnaswamy, J. Stuckey and S. Wang, *J. Med. Chem.*, 2019, **62**, 11218.

66 K. Sekine, K. Takubo, R. Kikuchi, M. Nishimoto, M. Kitagawa, F. Abe, K. Nishikawa, T. Tsuruo and M. Naito, *J. Biol. Chem.*, 2008, **283**, 8961.

67 Y. Itoh, R. Kitaguchi, M. Ishikawa, M. Naito and Y. Hashimoto, *Bioorg. Med. Chem.*, 2011, **19**, 6768.

68 A. Mares, A. H. Miah, I. E. D. Smith, M. Rackham, A. R. Thawani, J. Cryan, P. A. Haile, B. J. Votta, A. M. Beal, C. Capriotti, M. A. Reilly, D. T. Fisher, N. Zinn, M. Bantscheff, T. T. MacDonald, A. Vossenkamper, P. Dace, I. Churcher, A. B. Benowitz, G. Watt, J. Denyer, P. Scott-Stevens and J. D. Harling, *Commun. Biol.*, , DOI:10.1038/s42003-020-0868-6.

69 A. C. Lai, M. Toure, D. Hellerschmied, J. Salami, S. Jaime-Figueroa, E. Ko, J. Hines and C. M. Crews, *Angew. Chemie Int. Ed.*, 2016, **55**, 807.

70 D. P. Bondeson, B. E. Smith, G. M. Burslem, A. D. Buhimschi, J. Hines, S. Jaime-Figueroa, J. Wang, B. D. Hamman, A. Ishchenko and C. M. Crews, *Cell Chem. Biol.*, 2018, **25**, 78.

71 E. S. Fischer, A. Scrima, K. Böhm, S. Matsumoto, G. M. Lingaraju, M. Faty, T. Yasuda, S. Cavadini, M. Wakasugi, F. Hanaoka, S. Iwai, H. Gut, K. Sugasawa and N. H. Thomä, *Cell*, 2011, **147**, 1024.

72 J. Yang, Y. Li, A. Aguilar, Z. Liu, C. Y. Yang and S. Wang, *J. Med. Chem.*, 2019, **62**, 9471.

73 X. Zhang, P. Zhang, G. Zheng, D. Thummuri, Y. He, X. Liu and D. Zhou, *Chem. Commun.*, 2019, **55**, 14765.

74 W. McCoull, T. Cheung, E. Anderson, P. Barton, J. Burgess, K. Byth, Q. Cao, M. P. Castaldi, H. Chen, E. Chiarparin, R. J. Carbajo, E. Code, S. Cowan, P. R. Davey, A. D. Ferguson, S. Fillery, N. O. Fuller, N. Gao, D. Hargreaves, M. R. Howard, J. Hu, A. Kawatkar, P. D. Kemmitt, E. Leo, D.

M. Molina, N. O'Connell, P. Petteruti, T. Rasmusson, P. Raubo, P. B. Rawlins, P. Ricchiuto, G. R. Robb, M. Schenone, M. J. Waring, M. Zinda, S. Fawell and D. M. Wilson, *ACS Chem. Biol.*, 2018, **13**, 3131.

75 D. E. Scott, T. P. C. Rooney, E. D. Bayle, T. Mirza, H. M. G. Willems, J. H. Clarke, S. P. Andrews and J. Skidmore, *ACS Med. Chem. Lett.*, 2020, **11**, 1539.

76 K. A. Donovan, F. M. Ferguson, J. W. Bushman, N. A. Eleuteri, D. Bhunia, S. S. Ryu, L. Tan, K. Shi, H. Yue, X. Liu, D. Dobrovolsky, B. Jiang, J. Wang, M. Hao, I. You, M. Teng, Y. Liang, J. Hatcher, Z. Li, T. D. Manz, B. Groendyke, W. Hu, Y. Nam, S. Sengupta, H. Cho, I. Shin, M. P. Agius, I. M. Ghobrial, M. W. Ma, J. Che, S. J. Buhrlage, T. Sim, N. S. Gray and E. S. Fischer, *Cell*, 2020, **183**, 1714-1731.e10.

77 J. Popow, H. Arnhof, G. Bader, H. Berger, A. Ciulli, D. Covini, C. Dank, T. Gmaschitz, P. Greb, J. Karolyi-Özguer, M. Koegl, D. B. McConnell, M. Pearson, M. Rieger, J. Rinnenthal, V. Roessler, A. Schrenk, M. Spina, S. Steurer, N. Trainor, E. Traxler, C. Wieshofer, A. Zoephel and P. Ettmayer, *J. Med. Chem.*, 2019, **62**, 2508.

78 C. E. Powell, Y. Gao, L. Tan, K. A. Donovan, R. P. Nowak, A. Loehr, M. Bahcall, E. S. Fischer, P. A. Jänne, R. E. George and N. S. Gray, *J. Med. Chem.*, 2018, **61**, 4249.

79 H. Lebraud, D. J. Wright, C. N. Johnson and T. D. Heightman, *ACS Cent. Sci.*, 2016, **2**, 927–934.

80 G. Xue, K. Wang, D. Zhou, H. Zhong and Z. Pan, *J. Am. Chem. Soc.*, 2019, **141**, 18370.

81 M. Cheng, X. Yu, K. Lu, L. Xie, L. Wang, F. Meng, X. Han, X. Chen, J. Liu, Y. Xiong and J. Jin, *Cite This J. Med. Chem*, 2020, **63**, 1216.

82 J. Liu, H. Chen, L. Ma, Z. He, D. Wang, Y. Liu, Q. Lin, T. Zhang, N. Gray, H. Ü. Kaniskan, J. Jin and W. Wei, *Sci. Adv.*, 2020, **6**, eaay5154.

83 Y. Naro, K. Darrah and A. Deiters, *J. Am. Chem. Soc.*, 2020, **142**, 2193.

84 C. S. Kounde, M. M. Shchepinova, C. N. Saunders, M. Muelbaier, M. D.

Rackham, J. D. Harling and E. W. Tate, *Chem. Commun.*, 2020, **56**, 5532.

85 M. Reynders and D. Trauner, in *Methods in Molecular Biology*, 2021, vol. 2365, pp. 315.

86 Y.-H. Jin, M.-C. Lu, Y. Wang, W.-X. Shan, X.-Y. Wang, Q.-D. You and Z.-Y. Jiang, *J. Med. Chem.*, , DOI:10.1021/acs.jmedchem.9b02058.

87 H. Yokoo, N. Shibata, A. Endo, T. Ito, Y. Yanase, Y. Murakami, K. Fujii, K. Hamamura, Y. Saeki, M. Naito, K. Aritake and Y. Demizu, *Cite This J. Med. Chem*, 2021, **64**, 15868.

88 H. Yokoo, N. Shibata, M. Naganuma, Y. Murakami, K. Fujii, T. Ito, K. Aritake, M. Naito and Y. Demizu, *Cite This ACS Med. Chem. Lett. 2021*, 2021, **12**, 241.

89 W. Xiang, L. Zhao, X. Han, C. Qin, B. Miao, D. Mceachern, Y. Wang, H. Metwally, P. D. Kirchhoff, L. Wang, A. Matvekas, M. He, B. Wen, D. Sun and S. Wang, *J. Med. Chem.*, 2021, **64**, 13487.

90 C. Guo, A. Linton, S. Kephart, M. Ornelas, M. Pairish, J. Gonzalez, S. Greasley, A. Nagata, B. J. Burke, M. Edwards, N. Hosea, P. Kang, W. Hu, J. Engebretsen, D. Briere, M. Shi, H. Gukasyan, P. Richardson, K. Dack, T. Underwood, P. Johnson, A. Morell, R. Felstead, H. Kuruma, H. Matsimoto, A. Zoubeidi, M. Gleave, G. Los and A. N. Fanjul, *J. Med. Chem.*, 2011, **54**, 7693.

91 S. Ryu, G. E. Gadbois, A. J. Tao, B. J. Fram, J. Jiang, B. Boyle, K. A. Donovan, N. M. Krupnick, B. C. Berry, D. Bhunia, I. Shin, E. S. Fischer, N. S. Gray, T. Sim and F. M. Ferguson, *Curr. Res. Chem. Biol.*, 2021, **1**, 100008.

92 G. E. Winter, D. L. Buckley, J. Paulk, J. M. Roberts, A. Souza, S. Dhe-Paganon and J. E. Bradner, *Science*, 2015, **348**, 1376.

93 J. V. Olsen, S. E. Ong and M. Mann, *Mol. Cell. Proteomics*, 2004, **3**, 608.

94 N. Pappireddi, L. Martin and M. Wühr, *ChemBioChem*, 2019, 20, 1210.

95 X. Chen, S. Wei, Y. Ji, X. Guo and F. Yang, *Proteomics*, 2015, 15, 3175.

96 F. J. Sialana, T. I. Roumeliotis, H. Bouguenina, L. Chan Wah Hak, H.

Wang, J. Caldwell, I. Collins, R. Chopra and J. S. Choudhary, *J. Proteome Res.*, 2022, **21**, 1842.

97 M. Brand, B. Jiang, S. Bauer, K. A. Donovan, Y. Liang, E. S. Wang, R. P. Nowak, J. C. Yuan, T. Zhang, N. Kwiatkowski, A. C. Müller, E. S. Fischer, N. S. Gray and G. E. Winter, *Cell Chem. Biol.*, , DOI:10.1016/j.chembiol.2018.11.006.

98 L. Xing, J. Klug-Mcleod, B. Rai and E. A. Lunney, *Bioorganic Med. Chem.*, 2015, **23**, 6520.

99 N. Moret, C. Liu, B. M. Gyori, J. A. Bachman, A. Steppi, R. Taujale, L. C. Huang, C. Hug, M. Berginski, S. Gomez, N. Kannan and P. K. Sorger, *bioRxiv*, 2020, DOI:2020.04.02.022277.

100 H. L. Woodward, P. Innocenti, K. M. J. Cheung, A. Hayes, J. Roberts, A. T. Henley, A. Faisal, G. W. Y. Mak, G. Box, I. M. Westwood, N. Cronin, M. Carter, M. Valenti, A. De Haven Brandon, L. O'Fee, H. Saville, J. Schmitt, R. Burke, F. Broccatelli, R. L. M. Van Montfort, F. I. Raynaud, S. A. Eccles, S. Linardopoulos, J. Blagg and S. Hoelder, *J. Med. Chem.*, 2018, **61**, 8226.

101 P. Innocenti, H. L. Woodward, S. Solanki, S. Naud, I. M. Westwood, N. Cronin, A. Hayes, J. Roberts, A. T. Henley, R. Baker, A. Faisal, G. W. Y. Mak, G. Box, M. Valenti, A. De Haven Brandon, L. O'Fee, H. Saville, J. Schmitt, B. Matijssen, R. Burke, R. L. M. Van Montfort, F. I. Raynaud, S. A. Eccles, S. Linardopoulos, J. Blagg and S. Hoelder, *J. Med. Chem.*, 2016, **59**, 3671.

102 M. Ishoey, S. Chorn, N. Singh, M. G. Jaeger, M. Brand, J. Paulk, S. Bauer, M. A. Erb, K. Parapatics, A. A. Mü, K. L. Bennett, G. F. Ecker, J. E. Bradner and G. E. Winter, *ACS Chem. Biol*, 2018, **13**, 41.

103 T. I. Roumeliotis, S. P. Williams, E. Gonçalves, C. Alsinet, M. Del Castillo Velasco-Herrera, N. Aben, F. Z. Ghavidel, M. Michaut, M. Schubert, S. Price, J. C. Wright, L. Yu, M. Yang, R. Dienstmann, J. Guinney, P. Beltrao, A. Brazma, M. Pardo, O. Stegle, D. J. Adams, L. Wessels, J. Saez-Rodriguez, U. McDermott and J. S. Choudhary, *Cell Rep.*, 2017, **20**, 2201.

104 P. Innocenti, H. Woodward, L. O'Fee and S. Hoelder, *Org. Biomol. Chem.*, 2015, **13**, 893.

105 M. E. Berginski, N. Moret, C. Liu, D. Goldfarb, P. K. Sorger and S. M. Gomez, *Nucleic Acids Res.*, 2021, **49**, 529.

106 M. T. Bertran, S. Sdelci, L. Regué, J. Avruch, C. Caelles and J. Roig, *EMBO J.*, 2011, **30**, 2634.

107 S. Sdelci, M. T. Bertran and J. Roig, *Cell Cycle*, 2011, 10, 3816.

108 F. Milletti, L. Storchi, G. Sforna and G. Cruciani, *J. Chem. Inf. Model.*, 2007, **47**, 2172.

109 L. Zhou, Y. Jiang, Q. Luo, L. Li and L. Jia, *Mol. Cancer*, 2019, 18, 1.

110 R. I. Troup, C. Fallan and M. G. J. Baud, *Explor. Target. Anti-tumor Ther.*, 2020, 1, 273.

111 M. J. Roy, S. Winkler, S. J. Hughes, C. Whitworth, M. Galant, W. Farnaby, K. Rumpel and A. Ciulli, *ACS Chem. Biol.*, 2019, **14**, 361.

112 G. M. Burslem and C. M. Crews, *Chem. Rev.*, 2017, 117, 11269.

113 X. Han, C. Wang, C. Qin, W. Xiang, E. Fernandez-Salas, C. Y. Yang, M. Wang, L. Zhao, T. Xu, K. Chinnaswamy, J. Delproposto, J. Stuckey and S. Wang, *J. Med. Chem.*, 2019, **62**, 941.

114 A. Testa, S. J. Hughes, X. Lucas, J. E. Wright and A. Ciulli, *Angew. Chemie Int. Ed.*, 2020, **59**, 1727.

115 S. Klaeger, S. Heinzlmeir, M. Wilhelm, H. Polzer, B. Vick, P. A. Koenig, M. Reinecke, B. Ruprecht, S. Petzoldt, C. Meng, J. Zecha, K. Reiter, H. Qiao, D. Helm, H. Koch, M. Schoof, G. Canevari, E. Casale, S. Re Depaolini, A. Feuchtinger, Z. Wu, T. Schmidt, L. Rueckert, W. Becker, J. Huenges, A. K. Garz, B. O. Gohlke, D. P. Zolg, G. Kayser, T. Vooder, R. Preissner, H. Hahne, N. Tõnisson, K. Kramer, K. Götze, F. Bassermann, J. Schlegl, H. C. Ehrlich, S. Aiche, A. Walch, P. A. Greif, S. Schneider, E. R. Felder, J. Ruland, G. Médard, I. Jeremias, K. Spiekermann and B. Kuster, *Science (80-.).*, 2017, **358**, 6367.

116 H. Liu, R. Sun, C. Ren, X. Qiu, X. Yang and B. Jiang, *Org. Biomol. Chem.*,

2021, **19**, 166.

117 T. Sun, J. Xu, M. Ji and P. Wang, *J. Chem. Res.*, 2016, **40**, 511.

118 S. Wang, C. A. Midgley, F. Scaërou, J. B. Grabarek, G. Griffiths, W. Jackson, G. Kontopidis, S. J. McClue, C. McInnes, C. Meades, M. Mezna, A. Plater, I. Stuart, M. P. Thomas, G. Wood, R. G. Clarke, D. G. Blake, D. I. Zheleva, D. P. Lane, R. C. Jackson, D. M. Glover and P. M. Fischer, *J. Med. Chem.*, 2010, **53**, 4367.

119 F. M. Deane, A. J. S. Lin, P. G. Hains, S. L. Pilgrim, P. J. Robinson and A. McCluskey, *ACS Omega*, 2017, **2**, 3828.

120 D. Dobrovolsky, E. S. Wang, S. Morrow, C. Leahy, T. Faust, R. P. Nowak, K. A. Donovan, G. Yang, Z. Li, E. S. Fischer, S. P. Treon, D. M. Weinstock and N. S. Gray, *Blood*, 2019, **133**, 952.

121 A. D. Takwale, S. H. Jo, Y. U. Jeon, H. S. Kim, C. H. Shin, H. K. Lee, S. Ahn, C. O. Lee, J. Du Ha, J. H. Kim and J. Y. Hwang, *Eur. J. Med. Chem.*, , DOI:10.1016/j.ejmech.2020.112769.

122 X. Gong, J. Du, S. H. Parsons, F. F. Merzoug, Y. Webster, P. W. Iversen, L. C. Chio, R. D. Van Horn, X. Lin, W. Blosser, B. Han, S. Jin, S. Yao, H. Bian, C. Ficklin, L. Fan, A. Kapoor, S. Antonysamy, A. M. McNulty, K. Froning, D. Manglicmot, A. Pustilnik, K. Weichert, S. R. Wasserman, M. Dowless, C. Marugán, C. Baquero, M. J. Lallena, S. W. Eastman, Y. H. Hui, M. Z. Dieter, T. Doman, S. Chu, H. R. Qian, X. S. Ye, D. A. Barda, G. D. Plowman, C. Reinhard, R. M. Campbell, J. R. Henry and S. G. Buchanan, *Cancer Discov.*, 2019, **9**, 248.

123 C. Wu, J. Lyu, E. J. Yang, Y. Liu, B. Zhang and J. S. Shim, *Nat. Commun.*, , DOI:10.1038/s41467-018-05694-4.

124 G. Mollaoglu, M. R. Guthrie, S. Böhm, J. Brägelmann, I. Can, P. M. Ballieu, A. Marx, J. George, C. Heinen, M. D. Chalishazar, H. Cheng, A. S. Ireland, K. E. Denning, A. Mukhopadhyay, J. M. Vahrenkamp, K. C. Berrett, T. L. Mosbruger, J. Wang, J. L. Kohan, M. E. Salama, B. L. Witt, M. Peifer, R. K. Thomas, J. Gertz, J. E. Johnson, A. F. Gazdar, R. J. Wechsler-Reya, M. L. Sos and T. G. Oliver, *Cancer Cell*, 2017, **31**, 270.

125 T. Marumoto, D. Zhang and H. Saya, *Nat. Rev. Cancer 2004 51*, 2005, **5**, 42.

126 J. R. Bischoff, L. Anderson, Y. Zhu, K. Mossie, L. Ng, B. Souza, B. Schryver, P. Flanagan, F. Clairvoyant, C. Ginther, C. S. M. Chan, M. Novotny, D. J. Slamon and G. D. Plowman, 1998, **17**, 3052.

127 J. Bozilovic, L. Eing, B.-T. Berger, B. Adhikari, J. Weckesser, N. B. Berner, S. Wilhelm, B. Kuster, E. Wolf and S. Knapp, *Curr. Res. Chem. Biol.*, 2022, **2**, 100032.

128 V. Bavetsias and S. Linardopoulos, *Front. Oncol.*, 2015, 5, 278.

129 E. R. Kastenhuber and S. W. Lowe, *Cell*, 2017, 170, 1062.

130 H. Katayama, K. Sasai, H. Kawai, Z. M. Yuan, J. Bondaruk, F. Suzuki, S. Fujii, R. B. Arlinghaus, B. A. Czerniak and S. Sen, *Nat. Genet. 2004 361*, 2003, **36**, 55.

131 E. Bell, L. Chen, T. Liu, G. M. Marshall, J. Lunec and D. A. Tweddle, *Cancer Lett.*, 2010, 293, 144.

132 T. Otto, S. Horn, M. Brockmann, U. Eilers, L. Schüttrumpf, N. Popov, A. M. Kenney, J. H. Schulte, R. Beijersbergen, H. Christiansen, B. Berwanger and M. Eilers, *Cancer Cell*, 2009, **15**, 67.

133 B. Adhikari, J. Bozilovic, M. Diebold, J. Denise Schwarz, J. Hofstetter, M. Schröder, M. Wanior, A. Narain, M. Vogt, N. Dudvarski Stankovic, A. Baluapuri, L. Schönemann, L. Eing, P. Bhandare, B. Kuster, A. Schlosser, S. Heinzlmeir, C. Sotriffer, S. Knapp, E. Wolf, J. D. Schwarz, J. Hofstetter, M. Schröder, M. Wanior, A. Narain, M. Vogt, N. Dudvarski Stankovic, A. Baluapuri, L. Schönemann, L. Eing, P. Bhandare, B. Kuster, A. Schlosser, S. Heinzlmeir, C. Sotriffer, S. Knapp, E. Wolf, J. Denise Schwarz, J. Hofstetter, M. Schröder, M. Wanior, A. Narain, M. Vogt, N. Dudvarski Stankovic, A. Baluapuri, L. Schönemann, L. Eing, P. Bhandare, B. Kuster, A. Schlosser, S. Heinzlmeir, C. Sotriffer, S. Knapp, E. Wolf, J. D. Schwarz, J. Hofstetter, M. Schröder, M. Wanior, A. Narain, M. Vogt, N. Dudvarski Stankovic, A. Baluapuri, L. Schönemann, L. Eing, P. Bhandare, B. Kuster, A. Schlosser, S. Heinzlmeir, C. Sotriffer, S. Knapp and E. Wolf, *Nat.*

Chem. Biol., 2020, **16**, 1179.

134 J. Tang, R. Moorthy, O. Demir, Z. D. Baker, J. A. Naumann, K. F. Jones, M. J. Grillo, E. Haefner, K. Shi, M. J. Levy, H. Aihara, R. S. Harris, R. E. Amaro, N. M. Levinson and D. A. Harki, *Cancer Res.*, 2022, **82**, 2135.

135 P. Kaestner, A. Stolz and H. Bastians, *Mol. Cancer Ther.*, 2009, **8**, 2046.

136 W. C. Gustafson, J. G. Meyerowitz, E. A. Nekritz, J. Chen, C. Benes, E. Charron, E. F. Simonds, R. Seeger, K. K. Matthay, N. T. Hertz, M. Eilers, K. M. Shokat and W. A. Weiss, *Cancer Cell*, 2014, **26**, 414.

137 B. Adhikari, J. Bozilovic, M. Diebold, J. D. Schwarz, J. Hofstetter, M. Schröder, M. Wanior, A. Narain, M. Vogt, N. Dudvarski Stankovic, A. Baluapuri, L. Schönemann, L. Eing, P. Bhandare, B. Kuster, A. Schlosser, S. Heinzlmeir, C. Sotriffer, S. Knapp, E. Wolf, J. Denise Schwarz, J. Hofstetter, M. Schröder, M. Wanior, A. Narain, M. Vogt, N. Dudvarski Stankovic, A. Baluapuri, L. Schönemann, L. Eing, P. Bhandare, B. Kuster, A. Schlosser, S. Heinzlmeir, C. Sotriffer, S. Knapp, E. Wolf, J. D. Schwarz, J. Hofstetter, M. Schröder, M. Wanior, A. Narain, M. Vogt, N. Dudvarski Stankovic, A. Baluapuri, L. Schönemann, L. Eing, P. Bhandare, B. Kuster, A. Schlosser, S. Heinzlmeir, C. Sotriffer, S. Knapp and E. Wolf, *Nat. Chem. Biol.*, 2020, **16**, 1179.

138 R. Wang, C. Ascanelli, A. Abdelbaki, A. Fung, T. Rasmusson, I. Michaelides, K. Roberts and C. Lindon, *Commun. Biol.*, 2021, **4**, 1.

139 M. Furqan, A. Fayyaz, F. Firdous, H. Raza, A. Bilal, R. S. Z. Saleem, S. Shahzad-ul-Hussan, D. Wang, F. S. Youssef, N. M. Al Musayeib, M. L. Ashour, H. Hussain and A. Faisal, *J. Nat. Prod.*, 2022, **85**, 1503.

140 T. B. Sells, R. Chau, J. A. Ecsedy, R. E. Gershman, K. Hoar, J. Huck, D. A. Janowick, V. J. Kadambi, P. J. Leroy, M. Stirling, S. G. Stroud, T. J. Vos, G. S. Weatherhead, D. R. Wysong, M. Zhang, S. K. Balani, J. B. Bolen, M. G. Manfredi and C. F. Claiborne, *ACS Med. Chem. Lett.*, 2015, **6**, 630.

141 S. Wang, C. A. Midgley, F. Scaërou, J. B. Grabarek, G. Griffiths, W. Jackson, G. Kontopidis, S. J. McClue, C. McInnes, C. Meades, M. Mezna,

A. Plater, I. Stuart, M. P. Thomas, G. Wood, R. G. Clarke, D. G. Blake, D. I. Zheleva, D. P. Lane, R. C. Jackson, D. M. Glover, P. M. Fischer, F. Sca€, J. B. Grabarek, G. Griffiths, W. Jackson, G. Kontopidis, S. J. McClue, C. McInnes, C. Meades, M. Mezna, A. Plater, I. Stuart, M. P. Thomas, G. Wood, R. G. Clarke, D. G. Blake, D. I. Zheleva, D. P. Lane, R. C. Jackson, D. M. Glover and P. M. Fischer, *J. Med. Chem.*, 2010, **53**, 4367.

142 R. Wang, S. Yu, X. Zhao, Y. Chen, B. Yang, T. Wu, C. Hao, D. Zhao and M. Cheng, *Eur. J. Med. Chem.*, 2020, **188**, 112024.

143 H. Cho, I. Shin, H. Yoon, E. Jeon, J. Lee, Y. Kim, S. Ryu, C. Song, N. H. Kwon, Y. Moon, S. Kim, N. D. Kim, H. G. Choi and T. Sim, *J. Med. Chem.*, 2021, **64**, 11934.